

RADIATION AS RISK FACTOR, EARLY DIAGNOSIS, THERAPY, AND FOLLOW-UP OF DIFFERENTIATED THYROID CANCER

EDITED BY: Valentina Drozd and Christoph Reiners
PUBLISHED IN: Frontiers in Endocrinology





frontiers

Frontiers eBook Copyright Statement

The copyright in the text of individual articles in this eBook is the property of their respective authors or their respective institutions or funders. The copyright in graphics and images within each article may be subject to copyright of other parties. In both cases this is subject to a license granted to Frontiers.

The compilation of articles constituting this eBook is the property of Frontiers.

Each article within this eBook, and the eBook itself, are published under the most recent version of the Creative Commons CC-BY licence.

The version current at the date of publication of this eBook is CC-BY 4.0. If the CC-BY licence is updated, the licence granted by Frontiers is automatically updated to the new version.

When exercising any right under the CC-BY licence, Frontiers must be attributed as the original publisher of the article or eBook, as applicable.

Authors have the responsibility of ensuring that any graphics or other materials which are the property of others may be included in the CC-BY licence, but this should be checked before relying on the CC-BY licence to reproduce those materials. Any copyright notices relating to those materials must be complied with.

Copyright and source acknowledgement notices may not be removed and must be displayed in any copy, derivative work or partial copy which includes the elements in question.

All copyright, and all rights therein, are protected by national and international copyright laws. The above represents a summary only. For further information please read Frontiers' Conditions for Website Use and Copyright Statement, and the applicable CC-BY licence.

ISSN 1664-8714

ISBN 978-2-88974-231-8

DOI 10.3389/978-2-88974-231-8

About Frontiers

Frontiers is more than just an open-access publisher of scholarly articles: it is a pioneering approach to the world of academia, radically improving the way scholarly research is managed. The grand vision of Frontiers is a world where all people have an equal opportunity to seek, share and generate knowledge. Frontiers provides immediate and permanent online open access to all its publications, but this alone is not enough to realize our grand goals.

Frontiers Journal Series

The Frontiers Journal Series is a multi-tier and interdisciplinary set of open-access, online journals, promising a paradigm shift from the current review, selection and dissemination processes in academic publishing. All Frontiers journals are driven by researchers for researchers; therefore, they constitute a service to the scholarly community. At the same time, the Frontiers Journal Series operates on a revolutionary invention, the tiered publishing system, initially addressing specific communities of scholars, and gradually climbing up to broader public understanding, thus serving the interests of the lay society, too.

Dedication to Quality

Each Frontiers article is a landmark of the highest quality, thanks to genuinely collaborative interactions between authors and review editors, who include some of the world's best academicians. Research must be certified by peers before entering a stream of knowledge that may eventually reach the public - and shape society; therefore, Frontiers only applies the most rigorous and unbiased reviews.

Frontiers revolutionizes research publishing by freely delivering the most outstanding research, evaluated with no bias from both the academic and social point of view. By applying the most advanced information technologies, Frontiers is catapulting scholarly publishing into a new generation.

What are Frontiers Research Topics?

Frontiers Research Topics are very popular trademarks of the Frontiers Journals Series: they are collections of at least ten articles, all centered on a particular subject. With their unique mix of varied contributions from Original Research to Review Articles, Frontiers Research Topics unify the most influential researchers, the latest key findings and historical advances in a hot research area! Find out more on how to host your own Frontiers Research Topic or contribute to one as an author by contacting the Frontiers Editorial Office: frontiersin.org/about/contact

RADIATION AS RISK FACTOR, EARLY DIAGNOSIS, THERAPY, AND FOLLOW-UP OF DIFFERENTIATED THYROID CANCER

Topic Editors:

Valentina Drozd, Other, Belarus

Christoph Reiners, University Hospital Würzburg, Germany

Citation: Drozd, V., Reiners, C., eds. (2022). Radiation as Risk Factor, Early Diagnosis, Therapy, and Follow-up of Differentiated Thyroid Cancer. Lausanne: Frontiers Media SA. doi: 10.3389/978-2-88974-231-8

Table of Contents

- 05 Editorial: Radiation as Risk Factor, Early Diagnosis, Therapy, and Follow-up of Differentiated Thyroid Cancer**
Christoph Reiners and Valentina Drozd
- 08 GADD45B Transcript Is a Prognostic Marker in Papillary Thyroid Carcinoma Patients Treated With Total Thyroidectomy and Radioiodine Therapy**
Mateus C. Barros-Filho, Julia B. H. de Mello, Fabio A. Marchi, Clóvis A. L. Pinto, Igor C. da Silva, Patricia K. F. Damasceno, Milena B. P. Soares, Luiz P. Kowalski and Silvia R. Rogatto
- 19 Petal-Like Calcifications in Thyroid Nodules on Ultrasonography: A Rare Morphologic Characteristic of Calcification Associated With Aggressive Biological Behavior**
Qinghai Peng, Qi Zhang, Sijie Chen and Chengcheng Niu
- 27 Breast Cancer After Treatment of Differentiated Thyroid Cancer With Radioiodine in Young Females: What We Know and How to Investigate Open Questions. Review of the Literature and Results of a Multi-Registry Survey**
Christoph Reiners, Rita Schneider, Tamara Platonova, Mikhail Fridman, Uwe Malzahn, Uwe Mäder, Alexis Vrachimis, Tatiana Bogdanova, Jolanta Krajewska, Rossella Elisei, Fernanda Vaisman, Jasna Mihailovic, Gracinda Costa and Valentina Drozd
- 44 Contrast-Enhanced Ultrasound of Primary Squamous Cell Carcinoma of the Thyroid: A Case Report**
Sijie Chen, Qinghai Peng, Qi Zhang and Chengcheng Niu
- 50 Feasibility Study Shows Multicenter, Observational Case-Control Study Is Practicable to Determine Risk of Secondary Breast Cancer in Females With Differentiated Thyroid Carcinoma Given Radioiodine Therapy in Their Childhood or Adolescence; Findings Also Suggest Possible Fertility Impairment in Such Patients**
Valentina Drozd, Rita Schneider, Tamara Platonova, Galina Panasiuk, Tatjana Leonova, Nataliya Oculevich, Irina Shimanskaja, Irina Vershenya, Tatjana Dedovich, Tatjana Mitjukova, Inge Grelle, Johannes Biko and Christoph Reiners
- 59 Radiation Exposure to the Thyroid After the Chernobyl Accident**
Vladimir Drozdovitch
- 68 Advances on circRNAs Contribute to Carcinogenesis and Progression in Papillary Thyroid Carcinoma**
Xiaoqin Xu and Jiexian Jing

- 75** *The Contribution of Genetic Variants to the Risk of Papillary Thyroid Carcinoma in the Kazakh Population: Study of Common Single Nucleotide Polymorphisms and Their Clinicopathological Correlations*
Zhanna Mussazhanova, Tatiana I. Rogounovitch, Vladimir A. Saenko, Ainur Krykpayeva, Maira Espenbetova, Bauyrzhan Azizov, Hisayoshi Kondo, Katsuya Matsuda, Zhanna Kalmatayeva, Raushan Issayeva, Zhanar Yeleubayeva, Madina Madiyeva, Aray Mukanova, Marat Sandybayev, Saltanat Bolsynbekova, Zhanna Kozykenova, Shunichi Yamashita and Masahiro Nakashima
- 85** *Diagnostic Value of Sonographic Features in Distinguishing Malignant Partially Cystic Thyroid Nodules: A Systematic Review and Meta-Analysis*
Xinlong Shi, Ruifeng Liu, Luying Gao, Yu Xia and Yuxin Jiang
- 94** *Fine Needle Biopsy Versus Core Needle Biopsy Combined With/Without Thyroglobulin or BRAF 600E Mutation Assessment for Detecting Cervical Nodal Metastasis of Papillary Thyroid Carcinoma*
Xiaojun Zhang, Xu Zhang, Wei Du, Liyuan Dai, Ruihua Luo, Qigen Fang and Hong Ge
- 101** *Risk Stratification in Patients With Follicular Neoplasm on Cytology: Use of Quantitative Characteristics and Sonographic Patterns*
Ming-Hsun Wu, Kuen-Yuan Chen, Min-Shu Hsieh, Argon Chen and Chiung-Nien Chen
- 110** *Predictive Value of Thyroglobulin Changes for the Curative Effect of Radioiodine Therapy in Patients With Metastatic Differentiated Thyroid Carcinoma*
Congcong Wang, Ruiguo Zhang, Renfei Wang, Zhaowei Meng, Guizhi Zhang, Feng Dong, Yajing He and Jian Tan



Editorial: Radiation as Risk Factor, Early Diagnosis, Therapy, and Follow-up of Differentiated Thyroid Cancer

Christoph Reiners^{1,2*} and Valentina Drozd³

¹ University Hospital Würzburg, Würzburg, Germany, ² Department of Nuclear Medicine, Würzburg, Germany, ³ Foundation Arnica, Minsk, Belarus

Keywords: differentiated thyroid cancer, diagnosis, treatment, follow-up, treatment side effects

Editorial on the Research Topic

Radiation as Risk Factor, Early Diagnosis, Therapy, and Follow-up of Differentiated Thyroid Cancer

INTRODUCTION

There are a number of risk factors for differentiated thyroid cancer (DTC) that have been well known for many years (1, 2). Among them are the female gender (3), a family history of thyroid cancer, and some inherited diseases, e.g., familial adenomatous polyposis and Cowden disease (4).

The most relevant risk factor for DTC without any doubt is radiation exposure of the thyroid in childhood (5). There is some evidence that follicular thyroid cancers are more prevalent in iodine deficient populations and that benign thyroid diseases (like goiter) or obesity are risk factors for DTC too (6, 7). Recently, environmental pollutants like nitrate have been blamed for increasing the risk of DTC with combined radiation exposure to the thyroid gland (8).

Unfortunately—with the exception of one paper on radiation exposure and another one on genetic predisposition—no articles were submitted to better understand these risk factors and to develop strategies for prevention of DTC in a broad sense. Nevertheless, the 12 papers of this Research Topic focusing on diagnosis, treatment, and follow-up of DTC present interesting information relevant for patient care.

RADIATION EXPOSURE/GENETIC PREDISPOSITION

Drozdovitch from Bethesda, USA contribute a review on “Radiation Exposure to the Thyroid after the Chernobyl Accident” presenting individual and population-average thyroid doses after Chernobyl. Mean individual doses in screening cohorts amount to 0.27 Gy in Belarus and 0.19 Gy Ukraine. In evacuees of Belarus, 0.68 Gy are reported for adults and 3.1 Gy for children of 0-7 years old, whereas these doses for Ukrainian evacuees amount to 0.28 Gy in adults and 1.2 Gy in children. Without any doubt, these doses in children are relevant for DTC induction. Importantly,

OPEN ACCESS

Edited and reviewed by:

Terry Francis Davies,
Icahn School of Medicine at Mount
Sinai, United States

*Correspondence:

Christoph Reiners
reiners_c@ukw.de

Specialty section:

This article was submitted to
Thyroid Endocrinology,
a section of the journal
Frontiers in Endocrinology

Received: 19 October 2021

Accepted: 20 October 2021

Published: 06 December 2021

Citation:

Reiners C and Drozd V (2021)
Editorial: Radiation as Risk Factor,
Early Diagnosis, Therapy, and Follow-
up of Differentiated Thyroid Cancer.
Front. Endocrinol. 12:797969.
doi: 10.3389/fendo.2021.797969

more than 90% of these doses in children could have been prevented if milk and food contaminated with I-131 would have been withdrawn.

Mussazhanova et al. from Nagasaki, Japan investigate “The Contribution of Genetic Variants to the Risk of Papillary Thyroid Carcinoma in the Kazakh Population: Study of Common SNPs and their Clinicopathological Correlations”. Single nucleotide polymorphisms (SNIPs) were genotyped in a cohort of 485 PTC patients and a control group of this population (N=1,008), both not exposed to radiation. Five SNIPs adjusted for age and sex show a suggestive association with unidirectional independent effects of FOXE1/PTCSC2, FOXE1 5'UTR, NRG1 intron1, PTCSC3/NKX2-1, BATF upstream contributing to 30-40% of PTC risk.

DIAGNOSIS

Shi et al. from Beijing, China review the “Diagnostic Value of Sonographic Features in Distinguishing Malignant Partially Cystic Thyroid Nodules” performing a meta-Analysis of 8 high quality studies with 2,004 patients. The highest odds ratios (OR) are described for eccentric localization [OR 17.22 (6.53–45.41), marked or mild hypo-echogenicity [OR 5.97 (2.47–14.43)], and microcalcification [OR 38.76 (6.10–31.97)].

Wu et al. from Taipei, Taiwan investigate human observers versus computer software comparing US TIRADS criteria versus FNA Bethesda malignancy risk categories “Risk stratification in patients with follicular neoplasm on cytology: use of quantitative characteristics and sonographic patterns”. Interestingly, the computer system leads to no significant diagnostic improvement. However, the patient sample of 22 DTC cases compared to 43 benign nodules is too small to derive definitive conclusions.

In a small patient sample too, Peng et al. from Changsha, China report on “Petal-like calcifications in thyroid nodules on ultrasonography: a rare morphologic characteristic of calcification associated with aggressive biological behavior”. The authors describe flower-petal like calcifications defined as many hyperechogenic spots around solid nodules in 18 cases of PTC, 13 of which had central and 5 of which had lateral lymph node metastasis.

Chen et al. from Changsha, China contribute a case report on “Contrast-enhanced ultrasound of primary squamous cell carcinoma of the thyroid”. In a 59 year old male with clinically aggressive cancer, reduced blood flow is described as a typical sign of squamous cell cancer of the thyroid.

In a single center comparison of 174 PTC and 12 control cases, Zhang et al. from Zhengzhou China study “Fine needle biopsy versus core needle biopsy combined with/without thyroglobulin or BRAF 600E mutation assessment for detecting cervical nodal metastasis of papillary thyroid carcinoma”. The authors conclude that sensitivity and specificity of fine needle aspiration biopsy cytology can be increased by combining it with thyroglobulin measurement in the washout. However, 12 control cases are not sufficient for a statistically reliable judgment.

TREATMENT/FOLLOW-UP

A comprehensive review on circulating RNAs, Xu and Jing from Taiyuan, China explore how “Advances on circRNAs contribute to carcinogenesis and progression in papillary thyroid carcinoma”. The authors discuss its regulatory roles, pathological mechanisms, and their clinical and therapeutic significance. They show that dysregulated circRNAs correlate with aggressive clinical behavior of PTC. For predicting prognosis more long-term follow-up studies are needed. The role of these biomarkers for targeted therapy is still unclear.

“Predictive value of thyroglobulin changes for the curative effect of radioiodine therapy in patients with metastatic differentiated thyroid carcinoma” is the title of a contribution of Wang et al. from Tianjin, China. In this single center study 117 patients with metastatic DTC, 71% showed partial or complete remission after radioiodine therapy. Mean Delta-TG of 22% on TSH-suppressive levothyroxine treatment predicted response with a sensitivity of 86.7% and specificity of 88.2%.

In a laborious single center study with 202 patients (median follow-up 10.7 years), Barros-Filho et al. from Sao Paulo, Brazil propose that “GADD45B transcript is a prognostic marker in papillary thyroid carcinoma patients treated with total thyroidectomy and radioiodine therapy”. Alterations of BRAF, RAS, RET and TERT were the transcriptome profiled in a subgroup of 48 patients. No mutation was associated with the recurrence risk. However, 8 promising genes were identified showing down-expression in the response group after thyroidectomy and radioiodine therapy exclusively. As the best candidate, GADD45B transcript is described as an independent marker of recurrence with shorter disease-free survival and a hazard ratio of 2.9 (95% 1.2-7.0).

TREATMENT/SIDE EFFECTS

Reiners et al. from Würzburg, Germany contribute a review of the literature and results of a multi-registry survey in 7,565 female DTC patients on “Breast Cancer after Treatment of Differentiated Thyroid Cancer With Radioiodine in Young Females: What We Know, and How to Investigate Open Questions”. The general breast cancer risk in DTC survivors is low, ~2%, slightly higher in females than in males. RAI presumably does not substantially influence breast cancer risk after DTC. However, data from patients given RAI at young ages are sparse and insufficient to make definitive conclusions regarding age dependence of the risk of breast cancer as a SPM after RAI of DTC. In conclusion, a potential international multicenter study of female patients undergoing RAI of DTC as children, adolescents, or young adults, with a sufficient sample size, is recommended.

In the same context, Drozd et al. from Minsk, Belarus performed a feasibility study in 111 females from Belarus with DTC after RAI and a control group of 90 DTC patients without RAI. The title of the study is “Feasibility Study Shows Multicenter, Observational Case-Control Study is Practicable to Determine

Risk of Secondary Breast Cancer in Females with Differentiated Thyroid Carcinoma Given Radioiodine Therapy in their Childhood or Adolescence; Findings also Suggest Possible Fertility Impairment in Such Patients". The main objective of the study was to develop and test a comprehensive protocol, which later could be used for a consecutive study in much larger, multicenter international patient sample. The protocol developed is described as comprehensive and practicable.

Additional findings in this small sample are that patients given RAI significantly less frequently need 2nd surgeries than

controls (23%, 26/111 vs. 39%, 35/90, $P < 0.05$) and that RAI patients appear to have more frequent reproductive difficulties than controls: 78% (87/111) of the former vs. 93% (84/90) of the latter had a history of pregnancy ($P < 0.001$).

AUTHOR CONTRIBUTIONS

Both authors listed have made a substantial, direct, and intellectual contribution to the work and approved it for publication.

REFERENCES

1. Reiners C, Demidchik YE, Drozd VM, Biko J. Thyroid Cancer in Infants and Adolescents After Chernobyl. *Minerva Endocrinol* (2008) 33:381–95.
2. Drozd V, Saenko V, Branovan DI, Brown K, Yamashita S, Reiners CA. Search for Causes of Rising Incidence of Differentiated Thyroid Cancer in Children and Adolescents After Chernobyl and Fukushima: Comparison of the Clinical Features and Their Relevance for Treatment and Prognosis. *Int J Environ Res Public Health* (2021) 18:3444. doi: 10.3390/ijerph18073444
3. Kilfoy BA, Devesa SS, Ward MH, Zhang Y, Rosenberg PS, Holford TR, et al. Gender Is an Age-Specific Effect Modifier for Papillary Cancers of the Thyroid Gland. *Cancer Epidemiol Biomarkers Prev* (2009) 18:1092–100. doi: 10.1158/1055-9965
4. Nosé V. Familial Thyroid Cancer: A Review. *Mod Pathol* (2011) 24(Suppl 2):19–33. doi: 10.1038/modpathol.2010.147
5. Drozd V, Branovan DI, Reiners C. Increasing Incidence of Thyroid Carcinoma: Risk Factors and Seeking Approaches for Primary Prevention. *Int J Thyroidol* (2020) 13:95–110. doi: 10.11106/ijt.2020.13.2.95
6. Kitahara CM, Farkas DK, Jørgensen JOL, Cronin-Fenton D, Sørensen HT. Benign Thyroid Diseases and Risk of Thyroid Cancer: A Nationwide Cohort Study. *J Clin Endocrinol Metab* (2018) 103:2216–24. doi: 10.1210/jc.2017-02599
7. Steele CB, Thomas CC, Henley SJ, Massetti GM, Galuska DA, Augurs-Collins T, et al. Vital Signs: Trends in Incidence of Cancers Associated With Overweight and Obesity - United State-2014. *Morb Mortal Wkly Rep* (2017) 66:1052–8. doi: 10.15585/mmwr.mm6639e1
8. Drozd VM, Branovan I, Shiglik N, Biko J, Reiners C. Thyroid Cancer Induction: Nitrates as Independent Risk Factors or Risk Modulators After Radiation Exposure, With a Focus on the Chernobyl Accident. *Eur Thyroid J* (2018) 7:67–74. doi: 10.1159/000485971

Conflict of Interest: The authors declare that the research was conducted in the absence of any commercial or financial relationships that could be construed as a potential conflict of interest.

Publisher's Note: All claims expressed in this article are solely those of the authors and do not necessarily represent those of their affiliated organizations, or those of the publisher, the editors and the reviewers. Any product that may be evaluated in this article, or claim that may be made by its manufacturer, is not guaranteed or endorsed by the publisher.

Copyright © 2021 Reiners and Drozd. This is an open-access article distributed under the terms of the Creative Commons Attribution License (CC BY). The use, distribution or reproduction in other forums is permitted, provided the original author(s) and the copyright owner(s) are credited and that the original publication in this journal is cited, in accordance with accepted academic practice. No use, distribution or reproduction is permitted which does not comply with these terms.



GADD45B Transcript Is a Prognostic Marker in Papillary Thyroid Carcinoma Patients Treated With Total Thyroidectomy and Radioiodine Therapy

Mateus C. Barros-Filho^{1*}, Julia B. H. de Mello¹, Fabio A. Marchi¹, Clóvis A. L. Pinto², Igor C. da Silva³, Patricia K. F. Damasceno⁴, Milena B. P. Soares^{4,5}, Luiz P. Kowalski⁶ and Silvia R. Rogatto^{7*}

¹ International Research Center-CIPE, A. C. Camargo Cancer Center, São Paulo, Brazil, ² Department of Pathology, A. C. Camargo Cancer Center, São Paulo, Brazil, ³ Department of Pathology, São Rafael Hospital, Salvador, Brazil, ⁴ Gonçalo Moniz Institute, Fiocruz, Salvador, Brazil, ⁵ Health Technology Institute, SENAI CIMATEC, Salvador, Brazil, ⁶ Department of Head and Neck Surgery and Otorhinolaryngology, A. C. Camargo Cancer Center, São Paulo, Brazil, ⁷ Department of Clinical Genetics, Vejle University Hospital, Institute of Regional Health Research, University of Southern Denmark, Odense, Denmark

OPEN ACCESS

Edited by:

Christoph Reiners,
University Hospital
Würzburg, Germany

Reviewed by:

Vasyl Vasko,
Uniformed Services University of the
Health Sciences, United States
Trevor Edmund Angell,
University of Southern California,
United States

*Correspondence:

Mateus C. Barros-Filho
mfilho@accamargo.org.br
Silvia R. Rogatto
silvia.regina.rogatto@rsyd.dk

Specialty section:

This article was submitted to
Thyroid Endocrinology,
a section of the journal
Frontiers in Endocrinology

Received: 19 February 2020

Accepted: 14 April 2020

Published: 30 April 2020

Citation:

Barros-Filho MC, de Mello JBH, Marchi FA, Pinto CAL, da Silva IC, Damasceno PKF, Soares MBP, Kowalski LP and Rogatto SR (2020) GADD45B Transcript Is a Prognostic Marker in Papillary Thyroid Carcinoma Patients Treated With Total Thyroidectomy and Radioiodine Therapy. *Front. Endocrinol.* 11:269. doi: 10.3389/fendo.2020.00269

Currently, there is a lack of efficient recurrence prediction methods for papillary thyroid carcinoma (PTC). In this study, we enrolled 202 PTC patients submitted to total thyroidectomy and radioiodine therapy with long-term follow-up (median = 10.7 years). The patients were classified as having favorable clinical outcome (PTC-FCO, no disease in the follow-up) or recurrence (PTC-RE). Alterations in *BRAF*, *RAS*, *RET*, and *TERT* were investigated ($n = 202$) and the transcriptome of 48 PTC (> 10 years of follow-up) samples was profiled. Although no mutation was associated with the recurrence risk, 68 genes were found as differentially expressed in PTC-RE compared to PTC-FCO. Pathway analysis highlighted a potential role of cancer-related pathways, including signal transduction and FoxO signaling. Among the eight selected genes evaluated by RT-qPCR, *SLC2A4* and *GADD45B* showed down-expression exclusively in the PTC-FCO group compared to non-neoplastic tissues (NT). Increased expression of *GADD45B* was an independent marker of shorter disease-free survival [hazard ratio (HR) 2.9; 95% confidence interval (CI95) 1.2–7.0] in our cohort and with overall survival in the TCGA dataset (HR = 4.38, CI95 1.2–15.5). In conclusion, *GADD45B* transcript was identified as a novel prognostic marker candidate in PTC patients treated with total thyroidectomy and radioiodine therapy.

Keywords: papillary thyroid cancer, prognostic markers, *BRAF* mutation, *GADD45B*, *TERT* promoter mutation, transcription profiling

INTRODUCTION

The incidence of thyroid carcinoma has tripled over the last 35 years, affecting more than 560,000 people worldwide in 2018 (1). Papillary thyroid carcinoma (PTC) represents 80–85% of all thyroid cancer, presenting a high cure rate and a 5-years overall survival of 98% (2). However, recurrence is a frequent event (10–25%) related to patient morbidity and may occur over 20 years after the

initial treatment (3, 4). Clinical-pathological features, such as distant and lymph node metastasis, extrathyroidal extension, and tall cell histologic variant, are associated with more aggressive PTC (5). Nonetheless, the discovery of reliable biomarkers to determine the risk of relapse could be of great value in clinical practice. Low-risk PTC may be eligible for minimalistic surgical approaches (such as thyroid lobectomy) or active surveillance. On the other hand, a more aggressive intervention (such as total thyroidectomy, prophylactic neck dissection, or radioiodine therapy) could be reserved for high risk PTC (5).

The most common genetic driver alterations found in PTC are *BRAF* (60%) and *RAS* (13%) point mutations, *TERT* promoter mutation (9%), and *RET/PTC* fusion (6%) (6). *BRAF* and *TERT* mutations have been frequently associated with more aggressive thyroid carcinomas (7–10). Although the coexistence of both alterations has a synergic effect (11), their role in the prognosis of PTC is still controversial (12, 13).

Gene expression profiling has been widely evaluated in thyroid cancer for biomarker discovery, especially for diagnostic purposes (14–17). Transcriptomic-based studies have revealed predictors candidates of prognosis, including overexpression of *MUC1* (18), *MEDAG* (19), and *SPHK1* (20), and down-expression of *FMO1* (21), and *FOXF1* (22). Signatures of multigene classifiers were also reported (23, 24). Although many prognostic candidates have been suggested, most of them were not confirmed in distinct cohorts (25). The inclusion of a limited number of patients treated with or without radioiodine and followed by short periods could explain the lack of reproducibility.

In this study, we evaluated a cohort of 202 PTC patients (69% of them with more than 10 years of follow-up) with standardized treatment (total thyroidectomy and radioiodine therapy). We reported that the most common genomic alterations (*BRAF*, *RAS*, *RET*, and *TERT*) found in PTC were not related to the recurrence risk in the long-term follow-up. The transcriptomic profiling (microarray) revealed potential recurrence biomarkers, of which a higher expression of *GADD45B* (Growth arrest and DNA-damage-inducible, beta) was an independent marker of shorter disease-free survival (confirmed by RT-qPCR).

MATERIALS AND METHODS

Patient Selection Criteria

Patients with pathological confirmation of PTC treated from July 2001 to December 2010 at A. C. Camargo Cancer Center, São Paulo, Brazil, were retrospectively included in this study. The samples were selected according to the availability of fresh-frozen tissues at our BioBank. The Ethics Committee in Human Research for the Institution approved this study (Protocol n° 1410/10), which was conducted according to the Helsinki Declaration. The tumor specimens obtained from the thyroidectomy were reviewed by an experienced pathologist (CP) using blinded interpretation.

In order to standardize the treatment strategy used in our cohort, only patients submitted to total thyroidectomy followed by radioiodine therapy were enrolled. Patients with other cancer types prior to the thyroid cancer diagnosis were excluded

to avoid bias in the prognostic analysis. We also excluded samples with low RNA quality (RNA integrative number < 5). Patients with no evidence of active disease at the follow-up, defined as negative image test by ultrasonography and serum thyroglobulin (< 1 ng/mL with suppressed TSH), were classified as having favorable clinical outcome (FCO). Recurrence (RE) was defined as persistent or recurrent PTC after the definitive treatment with pathologic confirmation (fine-needle aspiration biopsy or surgery) or combined imaging (Computed Tomography or Positron Emission Tomography with Computed Tomography) and strong biochemical evidence (persistent serum thyroglobulin > 2 ng/mL with suppressed TSH < 0.1 mIU/L or thyroglobulin > 5 ng/mL with induced TSH > 30 mIU/L). Due to the presence of late recurrence during the natural history of PTC (3), we have included only patients followed up for more than 5 years in the FCO group. Based on the fact that the microarray assays were used as a “discovery set,” we adopted a minimum follow-up of 10 years.

Following these criteria, a total of 202 patients were included (Table S1). The sample distribution according to the molecular approaches is summarized in Figure S1. We also included 15 non-neoplastic thyroid (NT) tissues in the RT-qPCR analysis. The NT tissues were obtained from surrounding PTC samples showing no histological alterations, hyperplastic, or inflammatory changes in the remaining thyroid parenchyma.

Detection of Genomic Alterations

Nucleic acids (DNA and RNA) were isolated, as previously described (26). Adequate quantity and quality for 202 DNA and 178 RNA PTC specimens were obtained. Point mutations in *BRAF* (codon 600), *KRAS* (codon 12/13), *HRAS* (codon 61), and *KRAS* (codon 61) were evaluated by pyrosequencing and *RET* rearrangements (*RET/PTC1* and *RET/PTC3*) by RT-qPCR, as previously described (27). *TERT* promoter mutations (C228T and C250T hotspots) were investigated by direct Sanger sequencing, as described elsewhere (28).

Gene Expression Profiling

Gene expression microarray experiments were performed in 48 PTC using the SurePrint G3 8x60K platform (Agilent Technologies Inc., Santa Clara, CA, USA), co-hybridized with a pool of nine non-neoplastic thyroid tissues, as previously described (15). This data was generated in a previous study (15) and is available in the GEO database (accession number GSE50901). The probes representing protein-coding genes were selected and quantile-normalized using BRB ArrayTools software (v. 4.4.0). Groups were compared using the limma package ($P < 0.01$) (29), adopting a fold change (FC) ≥ 1.5 to define differential expression. Since male patients usually present a worse prognosis (30), representing a potential bias in our study, genes found as more or less expressed according to gender and mapped in X or Y chromosomes were excluded. Hierarchical clustering analysis was performed with Euclidean distance and complete linkage using ComplexHeatmap package (31) available for R program.

In silico Molecular Analysis

Genes differentially expressed identified in the microarray analysis were subjected to an *in silico* exploration, employing two pathway-enrichment tools, KOBAS (v.3.0; kobas.cbi.pku.edu.cn/) and pathDIP (<http://ophid.utoronto.ca/pathdip/>), using KEGG, Reactome and PANTHER databases. Experimentally detected and computational predicted protein-protein interactions (minimum confidence level for predicted associations of 99%) were used in the pathDIP tool, while literature curated known pathway memberships were used in KOBAS. Pathways highlighted by both tools were designated as putatively disrupted (hypergeometric test with Benjamini and Hochberg correction $P < 0.05$).

Reverse Transcription Quantitative PCR (RT-qPCR) Analysis

Eight genes (*ELMO1*, *F2RL2*, *FOXP2*, *GADD45B*, *HGD*, *JUND*, *S1PR1*, and *SLC2A4*) were selected for RT-qPCR investigation using TaqMan Low Density Arrays® (TLDA; Applied Biosystems, Foster City, CA, USA) in 72 PTC, including 38 samples tested prior by microarray, 34 independent cases, and 15 additional non-neoplastic thyroid samples (histological normal pattern tissue surrounding tumor). The gene selection considered the *P*-value (*FOXP2*, *GADD45B*, *HGD*, *JUND*, and *SLC2A4* were among the top 15 lowest *P*-values), fold change (*F2RL2* had the highest FC) and pathway analysis (*ELMO1*, *GADD45B*, *S1PR1*, and *SLC2A4* were members of FoxO signaling or Signal Transduction pathways). Two references (*EIF2B1* and *PUM1*) were selected among five transcripts (*18S*, *EIF2B1*, *PUM1*, *TBP*, and *YWHAZ*) using geNorm (32) to obtain the normalized target gene relative expression. *GADD45B* (target) and reference genes (*EIF2B1* and *PUM1*) were further evaluated in 106 PTCs using individual Taqman assays (Applied Biosystems, Hs04188837_g1, Hs00426752_m1 and Hs00472881_m1, respectively). The reactions were assembled in duplicates (10 ng of cDNA) according to the manufacturer instructions, using automatic pipetting (QIagility, QIAGEN, Courtaboeuf, France). The amplifications were carried out with 7900HT Real Time PCR System (Applied Biosystems). Normalization was implemented following the Pfaffl method (33).

TCGA Database

Disease-free survival, overall survival, *GADD45B* expression (RNA sequencing, log₂ transformed RSEM+1), and *BRAF* mutation (exome sequencing) data from PTC patients were retrieved from the UCSC Xena Browser (<https://xenabrowser.net/datapages/>, accessed in October 2019). In total, 490 PTC subjects had both follow-up and gene expression information available for the analysis.

Statistical Analysis

Statistical analysis and illustrations were performed with BRB ArrayTools (v. 4.4.0), SPSS (v. 21.0; SPSS, Chicago, IL, USA) and Graphpad Prism (v. 5.0; GraphPad Software Inc., La Jolla, CA, USA) software. Genomic alterations were confronted with clinical-pathological features using Fisher exact test with multiple hypothesis correction (Bonferroni test). Relative expression

obtained by RT-qPCR was compared among biological groups with Student *t*-test and ANOVA (Tukey *post-hoc* test). A two-tailed $P < 0.05$ value was adopted as significant. Gene expression values were dichotomized in bellow and above the median (RT-qPCR from our cohort and RNA sequencing from TCGA) to perform the survival analyses. The Kaplan–Meier method was used to plot the disease-free and overall survival. Cox proportional-hazards regression was used in the univariate and multivariate survival analysis to estimate the hazard ratio (HR) and 95% confidence intervals (CI95). Variables significantly associated ($P < 0.05$) in the univariate were included in the multivariate model (conditional backward elimination) (SPSS (v. 21.0; SPSS, Chicago, IL, USA)).

RESULTS

PTC Relapse Risk Was Not Associated With *BRAF*, *RAS*, *RET*, and *TERT* Alterations

We detected *BRAF*V600E mutation in 62.4% (126/202) of our cases. *RAS* mutation was found in 2.5% (5/198) (all in *NRAS*), *TERT* promoter mutations in 2.6% (5/193; 1 C228T and 4 C250T), and *RET* rearrangement in 9.2% (16/174; 11 *RET/PTC1* and 5 *RET/PTC3*) of the tumors. Only two cases presented concurrent alterations in *BRAF*, *RAS*, and *RET*, one classical variant (*BRAF* and *RET/PTC*), and one follicular variant (*BRAF* with *NRAS*). Four of five *TERT* positive cases also presented *BRAF* mutations. These four *BRAF/TERT* concurrent mutations were from patients older than 55 years, tumors larger than 1 cm with extrathyroidal extension. Three were classic variants, and the patients had a favorable clinical outcome. One patient presented a diffuse sclerosing variant of PTC that progressed with distant metastasis and died due to the disease. Tumors harboring *BRAF* mutations were correlated with the classical variant of PTC ($P = 0.007$) and the presence of extra-thyroidal extension ($P = 0.025$). However, no significant association was found after a multiple-comparison correction (Table 1). *RAS* mutations were prevalent in the follicular variant, *TERT* in older patients, and *RET/PTC* in patients with lymph node metastasis (all significant after the multiple-comparison correction). No significant difference was observed between the assessed alterations with the risk of relapse (Table 1).

Gene Expression Profile as a Predictor of PTC Recurrence

Gene expression profile of PTC from patients with recurrence (PTC-RE) was compared with PTC from patients with favorable clinical outcome (PTC-FCO). The microarray analysis unveiled 61 differentially expressed genes (17 less and 44 more expressed in PTC-RE compared to PTC-FCO) (Table S2). A supervised hierarchical clustering analysis including the differentially expressed genes revealed a “high risk” group comprising eight of 13 PTC-RE, and a “low risk” group containing 34 of 35 PTC-FCO (Figure 1).

TABLE 1 | Clinical-pathological characteristics according to the status of *BRAF*, *RAS*, and *TERT* mutations and *RET* rearrangements in papillary thyroid carcinomas.

Variables	<i>BRAF</i> (N = 202)		<i>RAS</i> (N = 198)		<i>TERT</i> (N = 193)		<i>RET</i> (N = 174)	
	Mutated/total (%)	P	Mutated/total (%)	P	Mutated/total (%)	P	Fusion/total (%)	P
Age								
<55 years	106/175 (61)	0.206	5/171 (3)	1.000	1/167 (1)	0.001	16/150 (11)	0.132
≥55 years	20/27 (74)		0/27 (0)		4/26 (15)		0/24 (0)	
Gender								
Female	95/155 (61)	0.609	3/152 (2)	0.330	4/149 (3)	1.000	11/135 (8)	0.359
Male	31/47 (66)		2/46 (4)		1/44 (2)		5/39 (13)	
Tumor Size								
≤1 cm	58/91 (64)	0.771	2/89 (2)	1.000	0/85 (0)	0.068	6/78 (8)	0.606
>1 cm	68/111 (61)		3/109 (3)		5/108 (5)		10/96 (10)	
Multifocal								
No	67/113 (59)	0.464	3/112 (3)	1.000	3/107 (3)	1.000	10/97 (10)	0.793
Yes	55/85 (65)		2/82 (2)		2/82 (2)		6/73 (8)	
Variant								
Classical	103/150 (69)	0.007	0/147 (0)	<0.001	3/142 (2)	0.571	12/132 (9)	0.090
Follicular	16/37 (43)		4/36 (11)		1/36 (3)		1/30 (3)	
Other ^a	7/15 (47)		1/15 (7)		1/15 (7)		3/12 (25)	
Invasion^b								
No	112/179 (63)	0.804	5/175 (3)	1.000	3/170 (2)	0.080	12/156 (8)	0.130
Yes	11/19 (58)		0/19 (0)		2/19 (11)		3/15 (20)	
ETE								
No	64/116 (55)	0.025	5/112 (4)	0.077	1/113 (1)	0.081	9/101 (9)	0.795
Yes	57/80 (71)		0/80 (0)		4/74 (5)		7/69 (10)	
Node Status								
cN0, pN0	83/134 (62)	0.879	5/133 (4)	0.174	4/127 (3)	0.662	5/119 (4)	0.002
pN1	43/68 (63)		0/65 (0)		1/66 (2)		11/55 (20)	
Recurrence^c								
No	105/169 (62)	1.000	5/167 (3)	1.000	4/161 (2)	1.000	14/152 (9)	1.000
Yes	21/33 (64)		0/31 (0)		1/32 (3)		2/22 (9)	

N, number of samples tested; ETE, extrathyroidal extension; P-value, Fisher exact test; in bold, statistically significant after Bonferroni correction ($P = 0.05$ divided by nine variables = $P < 0.0056$).

^atall cells, solid, oncocyctic, sclerosing and mucosecretory histological variants.

^bVascular and/or perineural invasions.

^cLocoregional recurrence (N = 29) and distant metastases (N = 4, all in the lung).

Potentially Disrupted Pathways Associated With Recurrence in PTC

To better understand the gene list obtained in the microarray analysis, we performed an *in silico* molecular analysis using pathDIP (<http://ophid.utoronto.ca/pathdip/>) and KOBAS (v.3.0; kobas.cbi.pku.edu.cn/) tools. We found an enrichment of signal transduction, peptide ligand-binding receptors, FoxO signaling, and platelet activation, signaling and aggregation pathways (P adjusted < 0.05) (Table 2).

Confirmation of Genes Differentially Expressed in PTC by RT-qPCR and Their Association With Clinical Outcome

Eight targets (*ELMO1*, *F2RL2*, *FOXP2*, *GADD45B*, *HGD*, *JUND*, *S1PR1*, and *SLC2A4*) and two reference genes (*EIF2B1* and *PUM1*) were assayed by RT-qPCR (N = 72; TLDA method).

ELMO1, *FOXP2*, *HGD*, and *JUND* were less expressed, and *F2RL2* and *S1PR1* more expressed in both PTCs groups compared to non-neoplastic thyroid tissues. *GADD45B* and *SLC2A4* were less expressed only in the PTC-FCO group compared to NT. However, only *GADD45B* showed a significant difference between the PTC-RE and PTC-FCO (more expressed in PTC-RE) (Figure 2).

GADD45B Expression as a Prognostic Marker

A total of 106 PTC samples with available RNA was used to evaluate the *GADD45B* expression level by RT-qPCR assays using *EIF2B1* and *PUM1* as references. Combining both PCR sets (TLDA and Taqman individual assay), a cohort with 178 PTC samples was established. A higher expression of *GADD45B* (median expression as the threshold) was confirmed as a factor

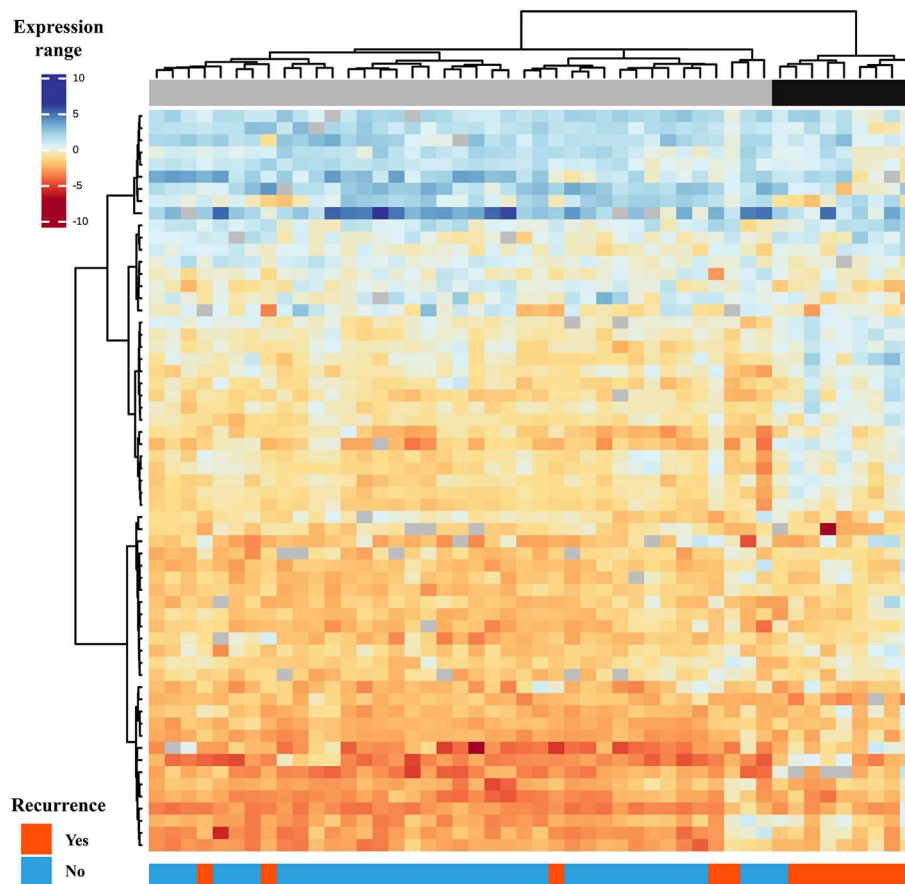


FIGURE 1 | Supervised hierarchical clustering analysis comprising 61 genes differentially expressed in primary PTC-RE compared to PTC-FCO (samples in columns and genes in rows). Two major groups are shown: the first (gray) is enriched by patients with favorable clinical outcomes and the second (black) by patients who relapsed in the follow-up.

related to shorter disease-free survival ($HR = 3.6$, $CI95$ 1.5–8.4; $P = 0.003$) (**Figure 3A**). Multivariate analysis revealed that *GADD45B* and cervical lymph node metastasis are independent predictors markers of relapse ($P = 0.015$, $HR = 2.9$, and $P = 0.009$, $HR = 3.0$, respectively) (**Table 3**).

Using the RNA sequencing data of PTC ($N = 490$) from the TCGA database (no standardized treatment), *GADD45B* also exhibited a prognostic role, being more expressed in patients with shorter overall survival (overall survival analysis: $HR = 4.38$, $CI95$ 1.2–15.5; $P = 0.022$) (**Figure 3B**). However, no association with the recurrence risk was observed (disease-free survival analysis: $HR = 0.69$, $CI95$ 0.35–1.4; $P = 0.279$) (**Figure S2**).

DISCUSSION

In general, PTC is an indolent disease and recurrence can appear long periods after surgery, making the identification of molecular prognostic markers a challenge (34). Herein, we investigated the most common gene alterations described in PTC, as well as transcriptomic data, to identify markers able to anticipate the outcome of patients treated with total thyroidectomy followed by

radioiodine therapy. Only patients with a minimum follow-up of 10 years were included in the large-scale gene expression analysis, while specific mutations/rearrangements and mRNAs levels were evaluated in patients followed for at least 5 years.

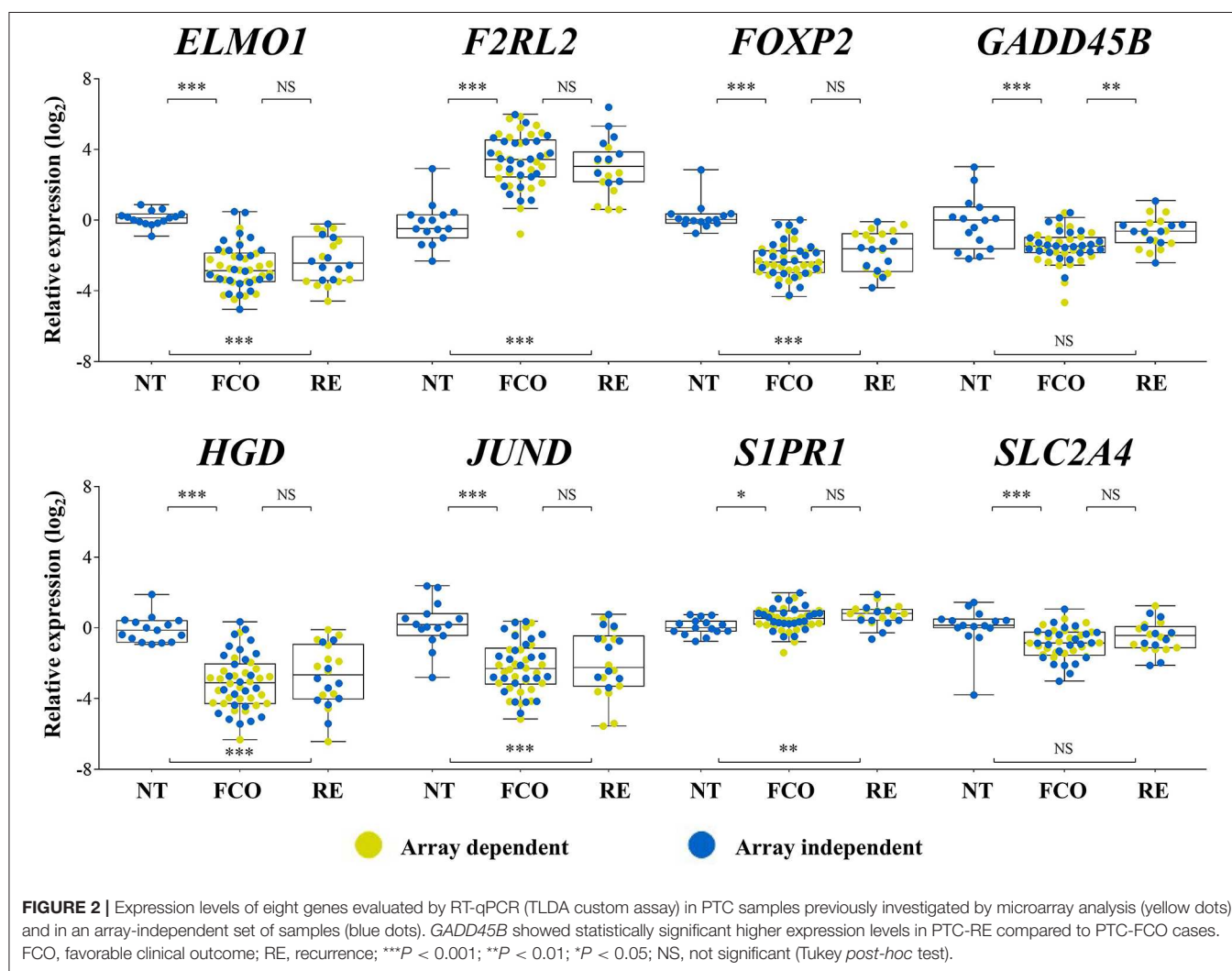
Among the 202 PTC cases evaluated in this study, *BRAF* mutation was detected with a high frequency (62.4%), while *RAS* mutation (2.5%), *RET* fusions (9.2%), and *TERT* promoter mutation (2.6%) were uncommon. These frequencies are comparable to the ones available in the TCGA database (*BRAF*: 59.7%, *RAS*: 13% *RET*: 6.3% *TERT*: 9.4%) (6). Although reports in the literature show that *BRAF* and *TERT* mutations are related to aggressive thyroid tumors (8, 9, 35, 36), no association was found with the recurrence risk in our set of cases. This result may be explained by the inclusion of patients treated exclusively by total thyroidectomy and radioiodine therapy. This criterion was adopted to avoid treatment-related bias, which resulted in the exclusion of very low-risk cases and enriched our sample set with a more aggressive phenotype.

Our results were consistent with the association amongst *BRAF* mutation with extra-thyroidal extension and the classical histological variant (6, 35, 37). Albeit rare in our cohort, *RAS*

TABLE 2 | Biological pathways potentially altered in PTC from relapsed patients using KOBAS 3.0 and PathDip tools.

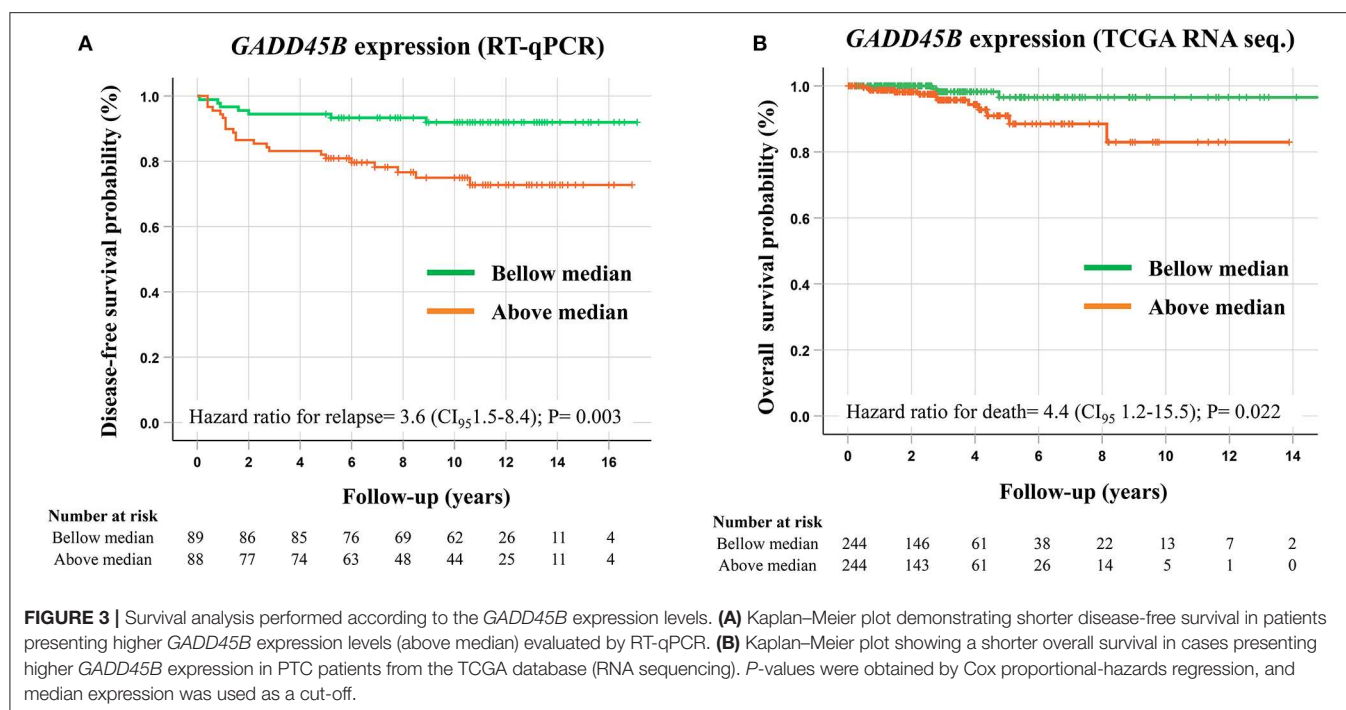
Pathway name	Deregulated genes in pathway	KOBAS 3.0		PathDIP	
		<i>P</i>	<i>FDR</i>	<i>P</i>	<i>FDR</i>
Signal transduction (Reactome)	<i>F2RL3, FLRT1, APOA1, ELMO1, PPP1R15A, CHEK1, GNA14, F2RL2, RAG2, CCL25, JUNB, GPR83, RHOB, S1PR1</i>	<0.001	0.001	<0.001	0.024
Platelet activation, signaling and aggregation (Reactome)	<i>PCDH7, APOA1, GNA14, F2RL2, RHOB, F2RL3</i>	<0.001	0.001	<0.001	0.019
FoxO signaling pathway (KEGG)	<i>S1PR1, SLC2A4, GADD45B, RAG2</i>	<0.001	0.003	<0.001	0.023
Peptide ligand-binding receptors (Reactome)	<i>CCL25, F2RL2, F2RL3</i>	0.004	0.049	<0.001	0.023

P-value from hypergeometric test; False Discovery Rate (FDR) estimated by Benjamini-Hochberg method.



mutation was associated with the follicular variant, as previously described (6, 38, 39). Five of 16 *RET/PTC* cases were *RET/PTC3* (*NCOA4-RET* translocation), an alteration frequently associated with ionizing radiation (40). Nonetheless, those patients have not declared any known prior exposure to radiation. Similar to previous reports, *RET/PTC* inversion was associated with lymph

node involvement (39, 41). However, *RET* fusions are often observed in young patients, who have a higher frequency of lymph node metastases (39, 42). We found that 44% (7/16) of our *RET/PTC* positive cases were from patients younger than 30 years, compared to only 16% (25/158) of the *RET/PTC* negative cases. Conversely, *TERT* promoter mutation was previously



described as being predominantly found in older patients (6, 43), as we observed in our dataset (range of 54–66 years). Telomerase activation is essential to cancer development by keeping the telomere length and overcoming senescence (44). Thyroid follicle cells from old individuals are *TERT*-deficient and present short-length telomeres (43). In older patients, *TERT* promoter mutation is suggested to be a consequence of the constant proliferation and activation of the telomerase, due to telomere crisis (43). Despite the small number of cases ($N = 4$) harboring both *BRAFV600E* and *TERT* promoter mutation, their clinical-pathological profile suggests a more aggressive phenotype (older patients with larger tumors and extrathyroidal extension). Even though only two patients from our whole cohort died due to the disease, one of them presented a *BRAF/TERT* concurrent mutation (diffuse sclerosing variant of PTC).

To our knowledge, no previous study has used high-throughput gene expression analysis to evaluate PTC cases with standardized treatment and long-term follow-up. Although the analysis of a homogenous cohort can eliminate the influence of some confounding factors, different histological types are frequently compared (18, 23, 45). The molecular basis of the thyroid tumor de-differentiation was studied by gene expression microarray in tumors with different degrees of aggressiveness (31 well-differentiated and 13 poorly/undifferentiated thyroid carcinomas) (23). A signature of 29 genes correctly separates 96% of tumors (42/44) according to prognosis, by grouping well-differentiated carcinomas that relapsed together with poorly/undifferentiated carcinomas (23). However, the authors included patients followed for almost 19 years in the unfavorable prognosis group and cases accompanied for <1 year categorized in the good prognosis group. A panel of 63 proteins (tissue microarray) was assessed in 12 anaplastic thyroid cancer

associated with a well-differentiated component (45). The authors reported that the expression pattern of eight proteins (β -catenin, E-cadherin, thyroglobulin, topoisomerase II α , VEGF, p53, BCL-2, and MIB-1) was able to separate anaplastic tumors from their differentiated components with 96% accuracy. Similarly, the signature of 61 differentially expressed genes found in our study was able to correctly classify PTC-RE from PTC-FCO with 87.5% accuracy (61.5% sensitivity and 97.5% specificity). No overlap between the markers found in our study with those aforementioned was found.

Among the pathways enriched by the differentially expressed genes found in our study was the FoxO signaling. This pathway is mainly activated by extracellular pro-apoptotic signals via membrane receptors, promoting downstream activation of forkhead box O3 (FOXO3), and inducing the expression of pro-apoptotic genes in the nucleus (46, 47). *BRAFV600E* directly inhibits the pro-apoptotic signals from the FoxO pathway (46). Therefore, this pathway is fundamental for the molecular pathogenesis of PTC (48). SLC2A4 (also known as GLUT4), *GADD45B*, S1PR1, and RAG1 are downstream factors induced by the FoxO pathway (49–52). These transcripts are more expressed in PTC-RE compared to PTC-FCO. However, only *GADD45B* was confirmed by RT-qPCR with the inclusion of a new group of samples (SLC2A4 and S1PR1 were also tested). Curiously, lower *GADD45B* expression was also associated with *BRAF* mutation in our dataset (by RT-qPCR) and confirmed in the TCGA dataset (RNA sequencing for *GADD45B* analysis and exome sequencing for *BRAF* genotyping) (Figure S3).

GADD45B is a member of the GADD45 family (Growth arrest and DNA-damage-inducible), which regulates cell proliferation through the participation of DNA replication and repair mechanisms (53), G2/M checkpoint control (54), and apoptosis

TABLE 3 | Univariate and multivariate analysis, contrasting the risk of relapse of PTC patients with clinical, pathological and molecular features.

Variables	Univariate analysis		Multivariate analysis	
	HR (CI _{95%})	P	HR (CI _{95%})	P
Age				
<55 years	1.0			
≥55 years	0.6 (0.2–2.1)	0.476		
Gender				
Female	1.0		1.0	
Male	2.3 (1.1–4.6)	0.020	1.6 (0.7–3.4)	0.241
Tumor Dimension				
≤1 cm	1.0			
>1 cm	2.0 (1.0–5.0)	0.062		
Multicentricity				
No	1.0			
Yes	2.0 (1.0–4.0)	0.062		
Histological Variant				
Classical	1.0			
Other	2.0 (0.8–5.2)	0.148		
Vascular/Perineural Invasion				
No	1.0		1.0	
Yes	3.2 (1.4–7.4)	0.007	1.8 (0.6–4.9)	0.271
Extrathyroidal Extension				
No	1.0			
Yes	1.8 (0.9–3.7)	0.091		
Lymph Node Metastasis				
No	1.0		1.0	
Yes	4.1 (2.0–8.4)	<0.001	3.0 (1.3–6.9)	0.009
BRAF Mutation				
No	1.0			
Yes	1.1 (0.5–2.2)	0.867		
RAS Mutation				
No	1.0			
Yes	0 (0–848.7)	0.542		
RET/PTC				
No	1.0			
Yes	1.0 (0.2–4.4)	0.972		
TERT Promoter Mutation				
No	1.0			
Yes	1.4 (0.2–10.4)	0.728		
GADD45B Expression				
Below median	1.0		1.0	
Above median	3.6 (1.5–8.4)	0.003	2.9 (1.2–7.0)	0.015

HR, Hazard ratio; CI, confidence interval. P-value, Cox proportional-hazards regression. The bold values are statistically significant.

(55). GADD45 family genes are rapidly induced in response to a variety of stress signals, such as ionizing radiation, pro-apoptotic inflammatory cytokines, mitogen stimulation, and xenobiotics (56). In contrast to the pro-apoptotic effect of *GADD45A* and *GADD45G* (57), *GADD45B* presents dual pro and anti-apoptotic roles (58). The mechanism responsible for inhibiting apoptosis has already been shown to attenuate JNK activation (c-Jun N-terminal kinase) (59) and induce p53 degradation

(58). Decreased *GADD45B* gene expression levels have been described in several human tumors, such as lymphoma, thyroid, breast, cervical, lung, and esophageal cancers, often by epigenetic regulation (60–64). Conversely, increased *GADD45B* expression levels were associated with shorter recurrence-free and overall survival in the most prevalent and aggressive human cancer types (65). Since we have included non-neoplastic thyroid samples in the RT-qPCR analysis, it was possible to note that *GADD45B* was underexpressed exclusively in the PTC-FCO. *GADD45B* showed high expression variability in NT samples, in agreement with the TCGA dataset (**Figure S3**). It has been proposed that genetic and epigenetic alterations can occur in the earliest carcinogenesis steps, which can also be detected in histological “normal” tissues surrounding tumors (66, 67). *GADD45B* deficient cells have been reported to be more sensitive to ultraviolet light-induced apoptosis (68). On the other hand, increased *GADD45B* expression has been related to chemotherapy resistance (69) and survival of tumor cells resistant to ultraviolet light and gamma radiation in medium with low nutrient availability (70). Hence, it is possible that *GADD45B* deficient PTCs are more susceptible to radioiodine therapy (all patients included in our study received radioiodine therapy after surgery).

Higher expression of *GADD45B* was an independent factor for shorter disease-free survival in our internal dataset and shorter overall survival in the TCGA cohort. Likewise, high *GADD45B* protein expression was an independent marker of poorer prognosis in stage II colorectal cancer and a potential marker to indicate post-operative chemotherapy (71). In thyroid cancer, an accurate recurrence predictive biomarker could aid in the de-intensification of the treatment in low risk patients (72). Even though it is widely used and proven to be effective, radioiodine therapy enhances the risk for second primary tumors (mainly hematological malignancies) and alterations in salivary glands (73, 74). The evaluation of *GADD45B* expression could be incorporated in combination with clinical-pathological information in the routine to aid in the risk stratification of PTC patients. This analysis could be performed using RT-qPCR assay in post-surgical tumor samples, which has the potential to improve the indication and the intensity of radioiodine therapy and TSH suppression, and the medical surveillance frequency. Although a protein analysis using immunohistochemistry could improve even more the applicability of the test in the clinical setting, the RT-qPCR is more sensitive and has wider dynamic range quantification.

In conclusion, we showed that increased expression of *GADD45B* was an independent marker of poor prognosis of PTC, whereas genomic alterations in *BRAF*, *RAS*, *RET*, and *TERT* were not associated with the risk of recurrence in our cohort of PTC patients treated with total thyroidectomy and radioiodine therapy in a long-term follow-up.

DATA AVAILABILITY STATEMENT

All large scale data analyzed in this study are publicly available: GEO database (accession number GSE50901) and TCGA consortium (UCSC Xena Browser; <https://xenabrowser.net/datapages/>).

ETHICS STATEMENT

The studies involving human participants were reviewed and approved by Ethics Committee in Human Research of A. C. Camargo Cancer Center Protocol n° 1410/10. The patients/participants provided their written informed consent to participate in this study.

AUTHOR CONTRIBUTIONS

MB-F, SR, and LK conceived and designed the study. MB-F and JM conducted the experiments. MB-F and FM performed bioinformatics analyses. MB-F, PD, and IS performed statistical analyses. CP performed the histopathological evaluation. JM, PD, IS, CP, and MS contributed to data interpretation. All authors participated in the preparation and approved the final version of the manuscript.

FUNDING

This research was funded by grants from the Fundação de Amparo à Pesquisa do Estado de São Paulo (FAPESP) (2015/17707-5 and 2015/20748-5).

REFERENCES

1. Ferlay J, Colombet M, Soerjomataram I, Mathers C, Parkin DM, Pineros M, et al. Estimating the global cancer incidence and mortality in 2018: GLOBOCAN sources and methods. *Int J Cancer*. (2019) 144:1941–53. doi: 10.1002/ijc.31937
2. Lim H, Devesa SS, Sosa JA, Check D, Kitahara CM. Trends in thyroid cancer incidence and mortality in the united states, 1974–2013. *JAMA*. (2017) 317:1338–48. doi: 10.1001/jama.2017.2719
3. Hay ID, Thompson GB, Grant CS, Bergstralh EJ, Dvorak CE, Gorman CA, et al. Papillary thyroid carcinoma managed at the mayo clinic during six decades (1940–1999): temporal trends in initial therapy and long-term outcome in 2,444 consecutively treated patients. *World J Surg*. (2002) 26:879–85. doi: 10.1007/s00268-002-6612-1
4. Mazzaferri EL, Jhiang SM. Long-term impact of initial surgical and medical therapy on papillary and follicular thyroid cancer. *Am J Med*. (1994) 97:418–28. doi: 10.1016/0002-9343(94)90321-2
5. Tuttle RM, Alzahrani AS. Risk stratification in differentiated thyroid cancer: from detection to final follow-up. *J Clin Endocrinol Metab*. (2019) 104:4087–100. doi: 10.1210/je.2019-00177
6. Cancer Genome Atlas Research Network. Integrated genomic characterization of papillary thyroid carcinoma. *Cell*. (2014). 159:676–90. doi: 10.1016/j.cell.2014.09.050
7. Liu C, Chen T, Liu Z. Associations between BRAF(V600E) and prognostic factors and poor outcomes in papillary thyroid carcinoma: a meta-analysis. *World J Surg Oncol*. (2016) 14:241. doi: 10.1186/s12957-016-0979-1
8. Pozdeyev N, Gay LM, Sokol ES, Hartmaier R, Deaver KE, Davis S, et al. Genetic analysis of 779 advanced differentiated and anaplastic thyroid cancers. *Clin Cancer Res*. (2018) 24:3059–68. doi: 10.1158/1078-0432.ccr-18-0373
9. Krasner JR, Alyouha N, Pustaszzeri M, Forest VI, Hier MP, Avior G, et al. Molecular mutations as a possible factor for determining extent of thyroid surgery. *J Otolaryngol Head Neck Surg*. (2019) 48:51. doi: 10.1186/s40463-019-0372-5
10. Rusinek D, Pfeifer A, Krajewska J, Oczko-Wojciechowska M, Handkiewicz-Junak D, Pawlaczek A, et al. Coexistence of TERT promoter mutations and the BRAF V600E alteration and its impact on histopathological features of papillary thyroid carcinoma in a selected series of polish patients. *Int J Mol Sci*. (2018) 19:2647. doi: 10.3390/ijms19092647

SUPPLEMENTARY MATERIAL

The Supplementary Material for this article can be found online at: <https://www.frontiersin.org/articles/10.3389/fendo.2020.00269/full#supplementary-material>

Supplementary Figure 1 | Flowchart summarizing the number of cases evaluated according to each methodology applied in the study. We excluded: °two samples due to poor quality of the Sanger sequencing; and #four samples without conclusive results for *KRAS*, *HRAS* and *NRAS* mutation. *Four samples were not tested for *RET/PTC* (RNA was used for expression assays); +TaqMan Low Density Arrays (TLDA); °Taqman individual assay.

Supplementary Figure 2 | Kaplan–Meier plot comparing the disease-free survival of PTC patients from TCGA according to the *GADD45B* expression (RNA sequencing). *P* values were obtained by Cox proportional-hazards regression and median expression was used as cut-off.

Supplementary Figure 3 | *GADD45B* expression levels according to the *BRAF* mutation status. (A) Boxplots illustrating the *GADD45B* transcript evaluated by RT-qPCR in our internal sample set (NT = 15; PTC BRAF− = 61; PTC BRAF+ = 118). (B) *GADD45B* transcript evaluated by RNA sequencing in the TCGA dataset (NT = 59; PTC BRAF− = 196; PTC BRAF+ = 273). NT: non-neoplastic thyroid tissue; PTC: papillary thyroid carcinoma; BRAF−: Negative for BRAF mutation; BRAF+: Positive for BRAF mutation; *****P* < 0.001; **P* < 0.05; NS: not significant (Tukey post-hoc test).

11. Xing M, Liu R, Liu X, Murugan AK, Zhu G, Zeiger MA, et al. BRAF V600E and TERT promoter mutations cooperatively identify the most aggressive papillary thyroid cancer with highest recurrence. *J Clin Oncol*. (2014) 32:2718–26. doi: 10.1200/jco.2014.55.5094
12. Gouveia C, Can NT, Bostrom A, Grenert JP, van Zante A, Orloff LA. Lack of association of BRAF mutation with negative prognostic indicators in papillary thyroid carcinoma: the University of California, San Francisco, experience. *JAMA Otolaryngol Head Neck Surg*. (2013) 139:1164–70. doi: 10.1001/jamaoto.2013.4501
13. de Biase D, Gandolfi G, Ragazzi M, Eszlinger M, Sancisi V, Gugnoni M, et al. TERT Promoter mutations in papillary thyroid microcarcinomas. *Thyroid*. (2015) 25:1013–9. doi: 10.1089/thy.2015.0101
14. Alexander EK, Kennedy GC, Baloch ZW, Cibas ES, Chudova D, Diggans J, et al. Preoperative diagnosis of benign thyroid nodules with indeterminate cytology. *N Engl J Med*. (2012) 367:705–15. doi: 10.1056/NEJMoa1203208
15. Barros-Filho MC, Marchi FA, Pinto CA, Rogatto SR, Kowalski LP. High diagnostic accuracy based on CLDN10, HMGA2, and LAMB3 transcripts in papillary thyroid carcinoma. *J Clin Endocrinol Metab*. (2015) 100:E890–9. doi: 10.1210/je.2014-4053
16. Wojtas B, Pfeifer A, Oczko-Wojciechowska M, Krajewska J, Czarniecka A, Kukulska A, et al. Gene expression (mRNA) Markers for differentiating between malignant and benign follicular thyroid tumours. *Int J Mol Sci*. (2017) 18:e1184. doi: 10.3390/ijms18061184
17. Macerola E, Poma AM, Proietti A, Romani R, Torregrossa L, Ugolini C, et al. Digital gene expression analysis on cytology smears can rule-out malignancy in follicular-patterned thyroid tumors. *J Mol Diagn*. (2019) 22:179–87. doi: 10.1016/j.jmoldx.2019.09.008
18. Wreesmann VB, Sieczka EM, Socci ND, Hezel M, Belbin TJ, Childs G, et al. Genome-wide profiling of papillary thyroid cancer identifies MUC1 as an independent prognostic marker. *Cancer Res*. (2004) 64:3780–9. doi: 10.1158/0008-5472.can-03-1460
19. Song Y, Fu LJ, Li HT, Qiu XG. Evaluation of MEDAG gene expression in papillary thyroid microcarcinoma: associations with histological features, regional lymph node metastasis and prognosis. *Sci Rep*. (2019) 9:5800. doi: 10.1038/s41598-019-41701-4
20. Li J, Zhang B, Bai Y, Liu Y, Jin J. Upregulation of sphingosine kinase 1 is associated with recurrence and poor prognosis in papillary thyroid carcinoma. *Oncol Lett*. (2019) 18:5374–82. doi: 10.3892/ol.2019.10910

21. Luo J, Zhang B, Cui L, Liu T, Gu Y. FMO1 gene expression independently predicts favorable recurrence-free survival of classical papillary thyroid cancer. *Future Oncol.* (2019) 15:1303–11. doi: 10.2217/fon-2018-0885
22. Gu Y, Hu C. Bioinformatic analysis of the prognostic value and potential regulatory network of FOXF1 in papillary thyroid cancer. *Biofactors.* (2019) 45:902–11. doi: 10.1002/biof.1561
23. Montero-Conde C, Martin-Campos JM, Lerma E, Gimenez G, Martinez-Guitarte JL, Combalia N, et al. Molecular profiling related to poor prognosis in thyroid carcinoma. Combining gene expression data and biological information. *Oncogene.* (2008) 27:1554–61. doi: 10.1038/sj.onc.1210792
24. Londero SC, Jespersen ML, Kroghdahl A, Bastholt L, Overgaard J, Schytte S, et al. Gene-expression classifier in papillary thyroid carcinoma: validation and application of a classifier for prognostication. *Anticancer Res.* (2016) 36:749–56. Available online at: <http://ar.iiajournals.org/content/36/2/749.long>
25. Kempf E, de Beyer JA, Cook J, Holmes J, Mohammed S, Nguyen TL, et al. Overinterpretation and misreporting of prognostic factor studies in oncology: a systematic review. *Br J Cancer.* (2018) 119:1288–96. doi: 10.1038/s41416-018-0305-5
26. Barros-Filho MC, Dos Reis MB, Beltrami CM, de Mello JBH, Marchi FA, Kuasne H, et al. DNA methylation-based method to differentiate malignant from benign thyroid lesions. *Thyroid.* (2019) 29:1244–54. doi: 10.1089/thy.2018.0458
27. Beltrami CM, Dos Reis MB, Barros-Filho MC, Marchi FA, Kuasne H, Pinto CAL, et al. Integrated data analysis reveals potential drivers and pathways disrupted by DNA methylation in papillary thyroid carcinomas. *Clin Epigenetics.* (2017) 9:45. doi: 10.1186/s13148-017-0346-2
28. Camargo Barros-Filho M, Barreto Menezes de Lima L, Bisarro Dos Reis M, Bette Homem de Mello J, Moraes Beltrami C, Lopes Pinto CA, et al. PFKFB2 promoter hypomethylation as recurrence predictive marker in well-differentiated thyroid carcinomas. *Int J Mol Sci.* (2019) 20:e61334. doi: 10.3390/ijms20061334
29. Ritchie ME, Phipson B, Wu D, Hu Y, Law CW, Shi W, et al. limma powers differential expression analysis for RNA-sequencing and microarray studies. *Nucleic Acids Res.* (2015) 43:e47. doi: 10.1093/nar/gkv007
30. Zahedi A, Bondaz L, Rajaraman M, Leslie WD, Jefford C, Young JE, et al. Risk for Thyroid cancer recurrence is higher in men than in women independent of disease stage at presentation. *Thyroid.* (2019). doi: 10.1089/thy.2018.0775. [Epub ahead of print].
31. Gu Z, Eils R, Schlesner M. Complex heatmaps reveal patterns and correlations in multidimensional genomic data. *Bioinformatics.* (2016) 32:2847–9. doi: 10.1093/bioinformatics/btw313
32. Vandesompele J, De Preter K, Pattyn F, Poppe B, Van Roy N, De Paepe A, et al. Accurate normalization of real-time quantitative RT-PCR data by geometric averaging of multiple internal control genes. *Genome Biol.* (2002) 3:e0034. doi: 10.1186/gb-2002-3-7-research0034
33. Pfaffl MW. A new mathematical model for relative quantification in real-time RT-PCR. *Nucleic Acids Res.* (2001) 29:e45. doi: 10.1093/nar/29.9.e45
34. Dong W, Horiuchi K, Tokumitsu H, Sakamoto A, Noguchi E, Ueda Y, et al. Time-Varying pattern of mortality and recurrence from papillary thyroid cancer: lessons from a long-term follow-Up. *Thyroid.* (2019) 29:802–8. doi: 10.1089/thy.2018.0128
35. Kim TH, Park YJ, Lim JA, Ahn HY, Lee EK, Lee YJ, et al. The association of the BRAF(V600E) mutation with prognostic factors and poor clinical outcome in papillary thyroid cancer: a meta-analysis. *Cancer.* (2012) 118:1764–73. doi: 10.1002/cncr.26500
36. Donati B, Ciarrocchi A. Telomerase and telomeres biology in thyroid cancer. *Int J Mol Sci.* (2019) 20:e2887. doi: 10.3390/ijms20122887
37. Oler G, Cerutti JM. High prevalence of BRAF mutation in a Brazilian cohort of patients with sporadic papillary thyroid carcinomas: correlation with more aggressive phenotype and decreased expression of iodide-metabolizing genes. *Cancer.* (2009) 115:972–80. doi: 10.1002/cncr.24118
38. Zhu Z, Gandhi M, Nikiforova MN, Fischer AH, Nikiforov YE. Molecular profile and clinical-pathologic features of the follicular variant of papillary thyroid carcinoma. An unusually high prevalence of ras mutations. *Am J Clin Pathol.* (2003) 120:71–7. doi: 10.1309/nd8d-9laj-trct-g6qd
39. Adeniran AJ, Zhu Z, Gandhi M, Steward DL, Fidler JP, Giordano TJ, et al. Correlation between genetic alterations and microscopic features, clinical manifestations, and prognostic characteristics of thyroid papillary carcinomas. *Am J Surg Pathol.* (2006) 30:216–22. doi: 10.1097/01.pas.0000176432.73455.1b
40. Nikiforov YE, Rowland JM, Bove KE, Monforte-Munoz H, Fagin JA. Distinct pattern of ret oncogene rearrangements in morphological variants of radiation-induced and sporadic thyroid papillary carcinomas in children. *Cancer Res.* (1997) 57:1690–4.
41. Wang YL, Zhang RM, Luo ZW, Wu Y, Du X, Wang ZY, et al. High frequency of level II-V lymph node involvement in RET/PTC positive papillary thyroid carcinoma. *Eur J Surg Oncol.* (2008) 34:77–81. doi: 10.1016/j.ejso.2007.08.012
42. Collins BJ, Chiappetta G, Schneider AB, Santoro M, Pentimalli F, Fogelfeld L, et al. RET expression in papillary thyroid cancer from patients irradiated in childhood for benign conditions. *J Clin Endocrinol Metab.* (2002) 87:3941–6. doi: 10.1210/jcem.87.8.8748
43. Liu T, Wang N, Cao J, Sofiadis A, Dinets A, Zedenius J, et al. The age- and shorter telomere-dependent TERT promoter mutation in follicular thyroid cell-derived carcinomas. *Oncogene.* (2014) 33:4978–84. doi: 10.1038/onc.2013.446
44. Yuan X, Larsson C, Xu D. Mechanisms underlying the activation of TERT transcription and telomerase activity in human cancer: old actors and new players. *Oncogene.* (2019) 38:6172–83. doi: 10.1038/s41388-019-0872-9
45. Wiseman SM, Griffith OL, Deen S, Rajput A, Masoudi H, Gilks B, et al. Identification of molecular markers altered during transformation of differentiated into anaplastic thyroid carcinoma. *Arch Surg.* (2007) 142:717–27. doi: 10.1001/archsurg.142.8.717
46. Ikenoue T, Hikiba Y, Kanai F, Tanaka Y, Imamura J, Imamura T, et al. Functional analysis of mutations within the kinase activation segment of B-Raf in human colorectal tumors. *Cancer Res.* (2003) 63:8132–7. Available online at: <https://cancerres.aacrjournals.org/content/63/23/8132>
47. Lehtinen MK, Yuan Z, Boag PR, Yang Y, Villen J, Becker EB, et al. A conserved MST-FOXO signaling pathway mediates oxidative-stress responses and extends life span. *Cell.* (2006) 125:987–1001. doi: 10.1016/j.cell.2006.03.046
48. Xing M. Molecular pathogenesis and mechanisms of thyroid cancer. *Nat Rev Cancer.* (2013) 13:184–99. doi: 10.1038/nrc3431
49. Nakae J, Biggs WH, 3rd, Kitamura T, Caveness WK, Wright CV, Arden KC, et al. Regulation of insulin action and pancreatic beta-cell function by mutated alleles of the gene encoding forkhead transcription factor Foxo1. *Nat Genet.* (2002) 32:245–53. doi: 10.1038/ng890
50. Tran H, Brunet A, Grenier JM, Datta SR, Fornace AJ, Jr., et al. DNA repair pathway stimulated by the forkhead transcription factor FOXO3a through the Gadd45 protein. *Science.* (2002) 296:530–4. doi: 10.1126/science.1068712
51. Amin RH, Schlissel MS. Foxo1 directly regulates the transcription of recombination-activating genes during B cell development. *Nat Immunol.* (2008) 9:613–22. doi: 10.1038/ni.1612
52. Fabre S, Carrette F, Chen J, Lang V, Semichon M, Denoyelle C, et al. FOXO1 regulates L-Selectin and a network of human T cell homing molecules downstream of phosphatidylinositol 3-kinase. *J Immunol.* (2008) 181:2980–9. doi: 10.4049/jimmunol.181.5.2980
53. Smith ML, Ford JM, Hollander MC, Bortnick RA, Amundson SA, Seo YR, et al. p53-mediated DNA repair responses to UV radiation: studies of mouse cells lacking p53, p21, and/or gadd45 genes. *Mol Cell Biol.* (2000) 20:3705–14. doi: 10.1128/mcb.20.10.3705-3714.2000
54. Vairapandi M, Azam N, Balliet AG, Hoffman B, Liebermann DA. Characterization of MyD118, Gadd45, and proliferating cell nuclear antigen (PCNA) interacting domains. PCNA impedes MyD118 AND Gadd45-mediated negative growth control. *J Biol Chem.* (2000) 275:16810–9. doi: 10.1074/jbc.275.22.16810
55. Takekawa M, Saito H. A family of stress-inducible GADD45-like proteins mediate activation of the stress-responsive MTK1/MEKK4 MAPKKK. *Cell.* (1998) 95:521–30. doi: 10.1016/s0092-8674(00)81619-0
56. Moskalev AA, Smit-McBride Z, Shaposhnikov MV, Plyusina EN, Zhavoronkov A, Budovsky A, et al. Gadd45 proteins: relevance to aging, longevity and age-related pathologies. *Ageing Res Rev.* (2012) 11:51–66. doi: 10.1016/j.arr.2011.09.003
57. Song L, Li J, Zhang D, Liu ZG, Ye J, Zhan Q, et al. IKKbeta programs to turn on the GADD45alpha-MKK4-JNK apoptotic cascade specifically via p50 NF-kappaB in arsenite response. *J Cell Biol.* (2006) 175:607–17. doi: 10.1083/jcb.200602149

58. Yu Y, Huang H, Li J, Zhang J, Gao J, Lu B, et al. GADD45beta mediates p53 protein degradation via Src/PP2A/MDM2 pathway upon arsenite treatment. *Cell Death Dis.* (2013) 4:e637. doi: 10.1038/cddis.2013.162
59. Papa S, Zazzeroni F, Bubici C, Jayawardena S, Alvarez K, Matsuda S, et al. Gadd45 beta mediates the NF-kappa B suppression of JNK signalling by targeting MKK7/JNKK2. *Nat Cell Biol.* (2004) 6:146–53. doi: 10.1038/ncb1093
60. Ying J, Srivastava G, Hsieh WS, Gao Z, Murray P, Liao SK, et al. The stress-responsive gene GADD45G is a functional tumor suppressor, with its response to environmental stresses frequently disrupted epigenetically in multiple tumors. *Clin Cancer Res.* (2005) 11:6442–9. doi: 10.1158/1078-0432.ccr-05-0267
61. Zerbini LF, Libermann TA. GADD45 deregulation in cancer: frequently methylated tumor suppressors and potential therapeutic targets. *Clin Cancer Res.* (2005) 11:6409–13. doi: 10.1158/1078-0432.ccr-05-1475
62. Guo W, Dong Z, Guo Y, Chen Z, Kuang G, Yang Z. Methylation-mediated repression of GADD45A and GADD45G expression in gastric cardia adenocarcinoma. *Int J Cancer.* (2013) 133:2043–53. doi: 10.1002/ijc.28223
63. Iacobas DA, Tuli NY, Iacobas S, Rasamny JK, Moscatello A, Geliebter J, et al. Gene master regulators of papillary and anaplastic thyroid cancers. *Oncotarget.* (2018) 9:2410–24. doi: 10.18632/oncotarget.23417
64. Do H, Kim D, Kang J, Son B, Seo D, Youn H, et al. TFAP2C increases cell proliferation by downregulating GADD45B and PMAIP1 in non-small cell lung cancer cells. *Biol Res.* (2019) 52:35. doi: 10.1186/s40659-019-0244-5
65. Verzella D, Bennett J, Fischietti M, Thotakura AK, Recordati C, Pasqualini F, et al. GADD45beta loss ablates innate immunosuppression in cancer. *Cancer Res.* (2018) 78:1275–92. doi: 10.1158/0008-5472.can-17-1833
66. Feinberg AP, Ohlsson R, Henikoff S. The epigenetic progenitor origin of human cancer. *Nat Rev Genet.* (2006) 7:21–33. doi: 10.1038/nrg1748
67. Yim JH, Choi AH, Li AX, Qin H, Chang S, Tong ST, et al. Identification of Tissue-Specific DNA Methylation signatures for thyroid nodule diagnostics. *Clin Cancer Res.* (2019) 25:544–51. doi: 10.1158/1078-0432.CCR-18-0841
68. Gupta M, Gupta SK, Hoffman B, Liebermann DA. Gadd45a and Gadd45b protect hematopoietic cells from UV-induced apoptosis via distinct signaling pathways, including p38 activation and JNK inhibition. *J Biol Chem.* (2006) 281:17552–8. doi: 10.1074/jbc.M600950200
69. Cheng TC, Manorek G, Samimi G, Lin X, Berry CC, Howell SB. Identification of genes whose expression is associated with cisplatin resistance in human ovarian carcinoma cells. *Cancer Chemother Pharmacol.* (2006) 58:384–95. doi: 10.1007/s00280-005-0171-8
70. Engelmann A, Speidel D, Bornkamm GW, Deppert W, Stocking C. Gadd45 beta is a pro-survival factor associated with stress-resistant tumors. *Oncogene.* (2008) 27:1429–38. doi: 10.1038/sj.onc.1210772
71. Zhao Z, Gao Y, Guan X, Liu Z, Jiang Z, Liu X, et al. GADD45B as a prognostic and predictive biomarker in stage ii colorectal cancer. (2018) 9:e70361. doi: 10.3390/genes9070361
72. Lowenstein LM, Basourakos SP, Williams MD, Troncoso P, Gregg JR, Thompson TC, et al. Active surveillance for prostate and thyroid cancers: evolution in clinical paradigms and lessons learned. *Nat Rev Clin Oncol.* (2019) 16:168–84. doi: 10.1038/s41571-018-0116-x
73. Teng CJ, Hu YW, Chen SC, Yeh CM, Chiang HL, Chen TJ, et al. Use of radioactive iodine for thyroid cancer and risk of second primary malignancy: a nationwide population-based study. *J Natl Cancer Inst.* (2016) 361:108. doi: 10.1093/jnci/djv314
74. Selvakumar T, Nies M, Klein Hesselink MS, Brouwers AH, van der Horst-Schrivers ANA, Klein Hesselink EN, et al. Long-term effects of radioiodine treatment on salivary gland function in adult survivors of pediatric differentiated thyroid carcinoma. *J Nucl Med.* (2018) 60:2 172–177. doi: 10.2967/jnumed.118.212449

Conflict of Interest: The authors declare that the research was conducted in the absence of any commercial or financial relationships that could be construed as a potential conflict of interest.

Copyright © 2020 Barros-Filho, de Mello, Marchi, Pinto, da Silva, Damasceno, Soares, Kowalski and Rogatto. This is an open-access article distributed under the terms of the Creative Commons Attribution License (CC BY). The use, distribution or reproduction in other forums is permitted, provided the original author(s) and the copyright owner(s) are credited and that the original publication in this journal is cited, in accordance with accepted academic practice. No use, distribution or reproduction is permitted which does not comply with these terms.



Petal-Like Calcifications in Thyroid Nodules on Ultrasonography: A Rare Morphologic Characteristic of Calcification Associated With Aggressive Biological Behavior

Qinghai Peng, Qi Zhang, Sijie Chen and Chengcheng Niu*

Department of Ultrasound Diagnosis, Second Xiangya Hospital, Central South University, Changsha, China

OPEN ACCESS

Edited by:

Christoph Reiners,
University Hospital
Würzburg, Germany

Reviewed by:

Roberto Vita,
University of Messina, Italy
Sriram Gubbi,
National Institutes of Health (NIH),
United States

*Correspondence:

Chengcheng Niu
niu.chengcheng@csu.edu.cn

Specialty section:

This article was submitted to
Thyroid Endocrinology,
a section of the journal
Frontiers in Endocrinology

Received: 05 February 2020

Accepted: 14 April 2020

Published: 22 May 2020

Citation:

Peng Q, Zhang Q, Chen S and Niu C
(2020) Petal-Like Calcifications in
Thyroid Nodules on Ultrasonography:
A Rare Morphologic Characteristic of
Calcification Associated With
Aggressive Biological Behavior.
Front. Endocrinol. 11:271.
doi: 10.3389/fendo.2020.00271

This study investigated a rare ultrasonographically detected thyroid petal-like calcification and its relationship with thyroid carcinoma and biological behavior. We described the clinical and ultrasonographical features of thyroid nodules with petal-like calcifications in 18 patients undergoing thyroid surgery and cervical lymph node dissection. All of the thyroid nodules with petal-like calcifications were papillary thyroid carcinomas (PTCs). Of the 18 patients, 13 (72.2%) had cervical central lymph node metastasis, and five (27.8%) had cervical lateral lymph node metastasis. Petal-like calcifications occurred in malignant thyroid nodules with a high incidence of lymph node metastasis, which may be a specific ultrasonographic feature associated with the aggressive biological behavior of PTC.

Keywords: petal-like calcifications, conventional ultrasound, contrast-enhanced ultrasound, papillary thyroid carcinoma, lymph node metastasis

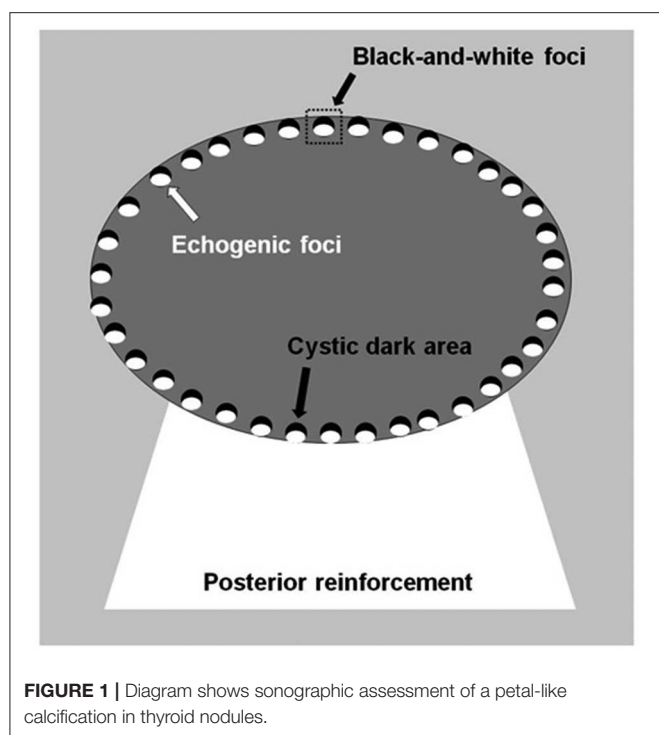
INTRODUCTION

Calcifications are commonly detected by ultrasonographic images in thyroid nodules and could be classified into various patterns (1–6). Taki et al. classified calcifications into microcalcifications, intranodular coarse calcifications, peripheral calcifications, and calcified spots (7). Kim et al. further classified peripheral calcifications into annular-like peripheral calcifications and crescent-like peripheral calcifications (2, 3). Among these subtypes, microcalcifications are known to be highly associated with papillary thyroid carcinoma (PTC) (4, 5). Kobayashi et al. reported that, out of 941 PTC patients, 32.0% patients had microcalcifications, and, out of 407 thyroid nodules with microcalcification, 301 (74.0%) were PTC (4). Yin et al. reported that, among 339 thyroid nodules with microcalcification, 210 (61.9%) of them were PTC, and, of 312 PTC patients, 210 (63.1%) had microcalcifications (5). However, to our knowledge, there are no studies on the ultrasonographic features of petal-like calcifications in thyroid nodules. In this study, we investigated the detection of petal-like calcifications by ultrasound and their relationship with thyroid carcinoma and biological behavior.

METHODS

Patients

A total of 18 patients with 18 nodules with petal-like calcifications that were detected with preoperative conventional ultrasound (US) and contrasted-enhanced ultrasound (CEUS) and underwent postoperative histopathologic analysis following resected hemithyroidectomy or total



thyroidectomy from December 2016 to November 2019 were enrolled in this prospective study. Of the 18 patients, five underwent cervical central and lateral lymph node dissection, and 13 only underwent central lymph node dissection.

Ultrasound Examination

The thyroid nodules were imaged with a Siemens Acuson S3000 US scanner equipped with a 9L4 linear array transducer (Siemens Medical Solutions, Mountain View, CA, USA; transducer frequency: 4–9 MHz) and/or an 18L6 linear array transducer (6–18 MHz). Petal-like calcifications appeared as scattered hyperechogenic spots < 2 mm in diameter around solid thyroid nodules with the appearance of flower petals and had a cystic-like dark area ahead of each hyperechogenic spot. The cystic dark area and hyperechogenic spot constituted black-and-white foci (Figure 1). The thyroid nodules with petal-like calcifications often showed acoustic posterior reinforcement. In addition to age, sex, and serum thyroid hormone, which included thyroid-stimulating hormone (TSH), free thyroxine, free triiodothyronine, thyroid peroxidases antibody (A-TPO), and thyroglobulin antibody (A-TG), the US features of the thyroid nodules were recorded, including tumor size, composition, shape, margin, echogenicity, posterior reinforcement, vascularity, and capsule contact with protrusion (8, 9). The US performance of the thyroid nodules was classified according to the Thyroid Imaging Reporting and Data System (TI-RADS) diagnostic classification by Kwak et al. (10).

CEUS was performed using contrast pulsed sequencing technology with a low mechanical index following intravenous injection of SonoVue microbubbles (Bracco, Italy). CEUS

videos were recorded for at least 60 s with dedicated software (Contrast Dynamics, Mountain View, CA, USA). With respect to the surrounding thyroid parenchyma enhancement, the time-intensity curves (TICs) of the thyroid nodules with regions of interest (ROIs) were acquired, and CEUS features were classified (8, 9), including enhancement type, peak intensity (PI), time to peak (TP), and area under the curve (AUC). The PI, TP, and AUC of the nodules are reported as indices by the ratio of the region of interest in the nodules to the region of interest in the thyroid parenchymal tissue.

Histopathological Diagnosis

The histopathological results obtained after surgery were used as the only reference standard for the final diagnoses of the thyroid nodules. Patients were staged according to the eighth edition of the American Joint Committee on Cancer (AJCC)/Tumor Lymph Node Metastasis (TNM) staging system (11–13).

RESULTS

In this study, a total of 18 patients with 18 nodules with petal-like calcifications were summarized for their clinical, ultrasonographic and pathologic characteristics. The clinical characteristics of the 18 patients with petal-like calcifications were summarized in Table 1. After surgery, all the patients with petal-like calcifications were histopathologically confirmed as the histological classic variant PTC. A total of 18 PTC patients (four men and 14 women, age mean: 30.17 ± 7.29 y, range: 18–40 y) with petal-like calcifications were included in the analysis. Of the 18 patients, nine (50.0%) had Hashimoto thyroiditis, six (33.3%) had multiple nodules, six (33.3%) had A-TPO increased, and five (27.8%) had A-TG increased.

The ultrasonographic characteristics of the thyroid nodules with petal-like calcifications are outlined in Table 2. Among the 18 thyroid nodules in the 18 PTC patients, all nodules were solid in composition; only one (5.6%) had taller than wider shapes, 11 (61.1%) had ill-defined margins (Figures 2–4), 17 (94.4%) had marked hypoechoic or hypoechoic echogenicity (Figures 2–4), seven (38.9%) had acoustic posterior reinforcement (Figures 2, 3), 12 (66.7%) had capsule contact with protrusion (Figure 4), and six (33.3%) had internal vascularity (Figures 2, 4). From CEUS examination, 11 (61.1%) nodules had a hyper- or iso-enhancement type (Figures 3, 4), which meant the majority of the nodules underwent a higher or equal enhancement compared with those of parenchymal tissue. Fifteen (83.3%) had a centripetal perfusion pattern (Figures 3, 4), representing most of the nodules received the perfusion of microbubbles from the periphery to the center. Twelve (66.7%) had a PI index ≥ 1 (Figures 3, 4), indicating that 66.7% of nodules had a higher PI than those of parenchymal tissue. Eight (44.4%) had a TP index ≥ 1 (Figure 4), implying that 44.4% of nodules had a longer or equal time to peak as the parenchymal tissue. And 10 (55.6%) had an AUC index ≥ 1 (Figures 3, 4), showing that 55.6% of nodules had a higher AUC than those of parenchymal tissue. According to the Kwak TI-RADS classification, 18 nodules (100%) were classified as category 4c (three or four suspicious US features; high possibility of malignancy).

TABLE 1 | Clinical characteristics.

Characteristics	n	%
SEX		
Male	4	22.2
Female	14	77.8
Age (years)	30.17 ± 7.29 (18–40)	
≤ 55 y	18	100
> 55 y	0	0
MULTIFOCALITY		
Yes	6	33.3
No	12	66.7
HASHIMOTO THYROIDITIS		
Yes	9	50.0
No	9	50.0
TSH		
Normal	18	100.0
Abnormal	0	0
FREE THYROXINE		
Normal	18	100.0
Abnormal	0	0
FREE TRIIODOTHYRONINE		
Normal	18	100.0
Abnormal	0	0
A-TPO		
Increased	6	33.3
Normal	12	66.7
A-TG		
Increased	5	27.8
Normal	13	72.2

TSH, thyroid-stimulating hormone; A-TPO, thyroid peroxidases antibody; A-TG, thyroglobulin antibody.

The pathologic characteristics of all the patients are summarized in **Table 3**. Of the 18 patients, five underwent cervical central and lateral lymph node dissection, and 13 underwent central lymph node dissection. According to the eighth edition of the AJCC/TNM staging system, all patients were in TNM stage I and had no obvious distant metastases (M0 classification). The mean diameter of PTCs with petal-like calcifications was 16.72 ± 9.01 mm (range: 6–34 mm), and 13 (72.2%) patients had a tumor size > 10 mm (T1 classification). After histopathological diagnosis, five (27.8%) patients were shown to have both cervical central and lateral lymph node metastasis (N1b classification), eight (44.4%) were shown to have cervical central lymph node metastasis (N1a classification), and the last five (27.8%) had no cervical lymph node metastasis (N0 classification).

DISCUSSION

High-resolution US is recommended for preoperative screening of malignant thyroid nodules from benign nodules and

TABLE 2 | Ultrasonographic characteristics.

Characteristics	n	%
Conventional US parameters		
TALLER THAN WIDE SHAPE		
Yes	1	5.6
No	17	94.4
ILL-DEFINED MARGIN		
Yes	11	61.1
No	7	38.9
HYPOECHOIC ECHOGENICITY		
Yes	17	94.4
No	1	5.6
POSTERIOR TRANSLUCENCY		
Yes	7	38.9
No	11	61.1
CAPSULE CONTACT WITH PROTRUSION		
Yes	12	66.7
No	6	33.3
INTERNAL VASCULARITY		
Yes	6	33.3
No	12	66.7
CEUS parameters		
HYPER-OR ISO ENHANCEMENT TYPE		
Yes	11	61.1
No	7	38.9
CENTRIPETAL PERFUSION PATTERN		
Yes	15	83.3
No	3	16.7
PI INDEX ≥ 1		
Yes	12	66.7
No	6	33.3
TP INDEX ≥ 1		
Yes	8	44.4
No	10	55.6
AUC Index ≥ 1		
Yes	10	55.6
No	8	44.4

US, ultrasound; CEUS, contrast-enhanced ultrasound; PI, peak intensity; TP, time to peak; AUC, area under the curve.

evaluating cervical lymph node metastasis (14–16). Previous studies have reported that PTC with cervical lymph node metastasis exhibits aggressive behavior and is associated with a poor prognosis (13, 14). As one of the more suspicious thyroid sonographic features, microcalcification has been proven to be highly predictive of central compartment lymph node metastases (17, 18). However, to our knowledge, it is rare for ultrasound to detect thyroid nodule petal-like calcifications, and their relationship with thyroid carcinoma has never been reported before.

In the present study, we collected 18 thyroid nodules with petal-like calcifications, which appeared as many scattered

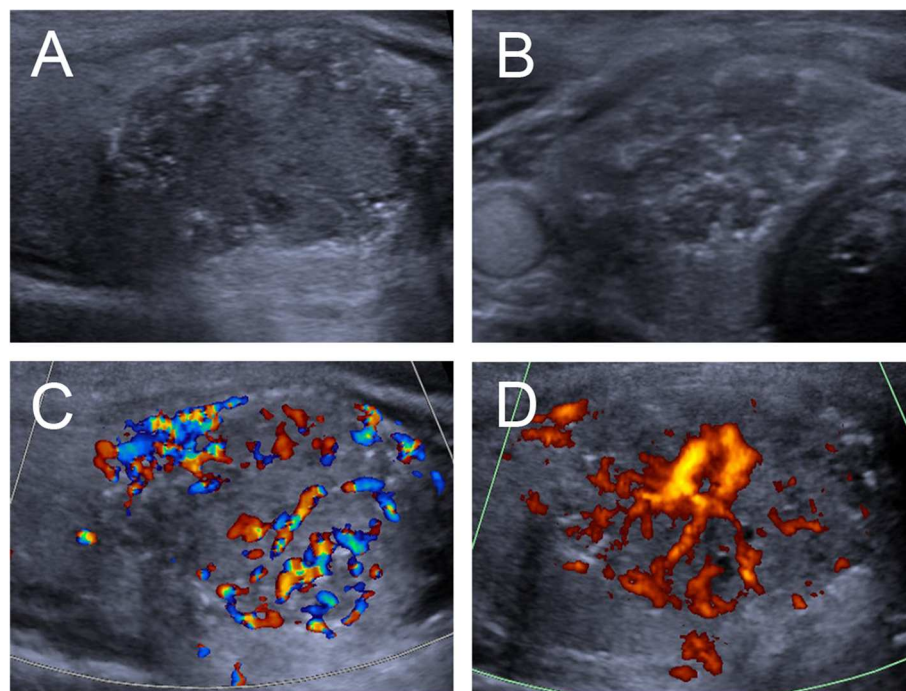


FIGURE 2 | Ultrasound images of an 18-y-old female PTC patient with petal-like calcification of the right thyroid lobe. **(A)** Longitudinal and **(B)** Horizontal gray-scale sonograms; the thyroid nodules had a solid component, hypoechoic echogenicity, and ill-defined margin. **(C)** Color Doppler and **(D)** Energy Doppler sonograms showed abundant internal and peripheral vascularities.

hyperechogenic spots around solid thyroid nodules with the appearance of flower petals, with a cystic-like dark area ahead of each hyperechogenic spot. The histopathologic result from all the patients was PTC, and 13 (72.2%) patients had cervical lymph node metastasis; however, previous studies have indicated that only 60–75% of thyroid nodules with microcalcification were PTC (4, 5), which indicates that petal-like calcifications in thyroid nodules are a fairly special sonographic characteristic of PTC and are highly associated with cervical lymph node metastasis. Fortunately, owing to the young mean age of our sample population, all patients in this study were in TNM stage I according to the eighth edition of the AJCC/TNM staging system.

According to the Kwak TI-RADS classification, five US suspicious features (solid composition, marked hypo-echogenicity or hyper-echogenicity, irregular or microlobulated margins, taller-than-wide shape, and presence of microcalcifications) were used to categorize the thyroid nodules, with TI-RADS scores of 3 (no suspicious US features), 4a (one suspicious US feature), 4b (two suspicious US features), 4c (three or four suspicious US features), and 5 (five suspicious US features) (10). In the current study, all thyroid nodules with petal-like calcifications presented with a solid composition and microcalcifications, two suspicious US features according to the Kwak TI-RADS classification guidelines from 2011 (10). In addition, the majority of these nodules had ill-defined margins and marked hypoechoic or hypoechoic echogenicity. The nodules consequently had a high TI-RADS classification due to the presence of three or four suspicious US features.

Furthermore, CEUS characteristics showed that the majority of nodules had a hyper- or isoenhancement type, a centripetal perfusion pattern, a PI index ≥ 1 and an AUC index ≥ 1 . Huang et al. reported that hyper- or iso-enhancement was one of the most useful US features for predicting the presence of cervical central lymph node metastasis (18), which is consistent with our results, demonstrating that the plentiful blood supply of the thyroid tumor may be associated with the aggressive biological behavior of PTC.

This study had many limitations. Firstly, all of the nodules with petal-like calcifications identified in our study ended up being PTC. So, data on whether benign thyroid nodules display such petal-like calcifications is lacking in our study. The sample size of our study population was small. Second, an unavoidable selection bias existed due to only patients who underwent surgery included in this study. A large-scale study is needed in the future to evaluate the association of petal-like calcifications with their corresponding pathogenetic characteristic.

CONCLUSIONS

In conclusion, we first reported a special pattern of calcification in thyroid nodules, petal-like calcifications, which only occurred in malignant nodules with a high incidence of lymph node metastasis. This kind of calcification appears as numerous scattered hyperechogenic spots around solid thyroid nodules with the appearance of flower petals, with a cystic-like dark area ahead of each hyperechogenic spot in ultrasonographic

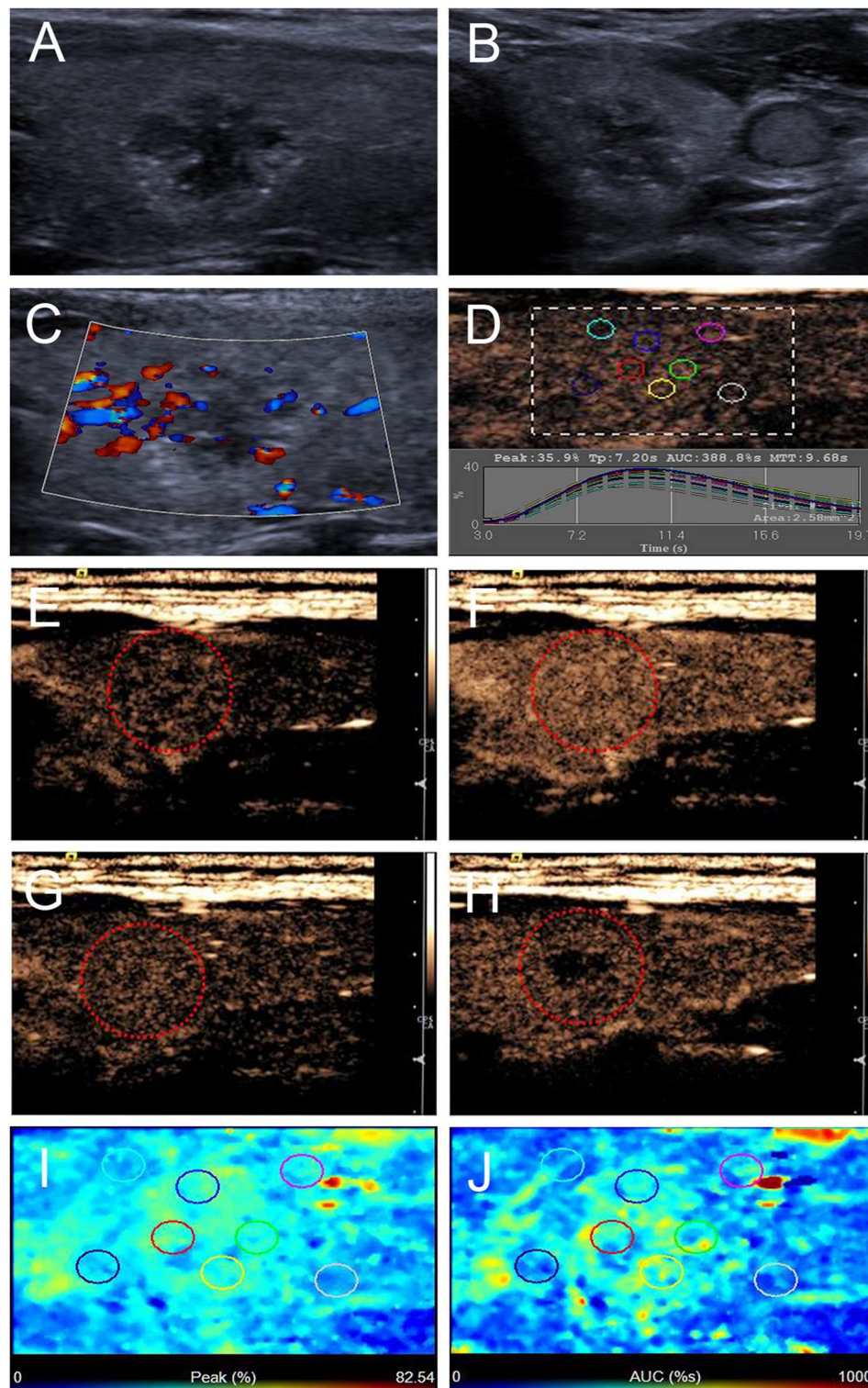


FIGURE 3 | Ultrasound images of a 26-y-old female PTC patient with petal-like calcification of the left thyroid lobe. **(A)** Longitudinal and **(B)** horizontal gray-scale sonograms; the thyroid nodule had a solid component, hypoechoic echogenicity and ill-defined margin. **(C)** Color Doppler sonogram showed moderate peripheral vascularity. **(D)** TICs of the thyroid nodule and peripheral thyroid parenchyma with different regions of interest (different color circles). **(E–H)** CEUS sonograms of the thyroid nodule **(E)** at 6 s (wash-in), **(F)** 9 s (time to peak), **(G)** 15 s (wash-out), and **(H)** 33 s (wash-out), revealing diffuse and homogeneous enhancement (circle) across the whole lesion, and the center of the lesion washed out clearly at 33 s. **(I)** Parametric color map showing that peak intensity values for the nodule were partially green, and the adjacent thyroid parenchyma was blue, indicating that the peak intensity of the nodule was higher than that of the peripheral thyroid parenchyma. **(J)** Parametric color map showing that AUC values for the nodule were mixed with green and yellow, and adjacent thyroid parenchyma was blue, indicating that the AUC of the nodule was higher than that of the peripheral thyroid parenchyma.

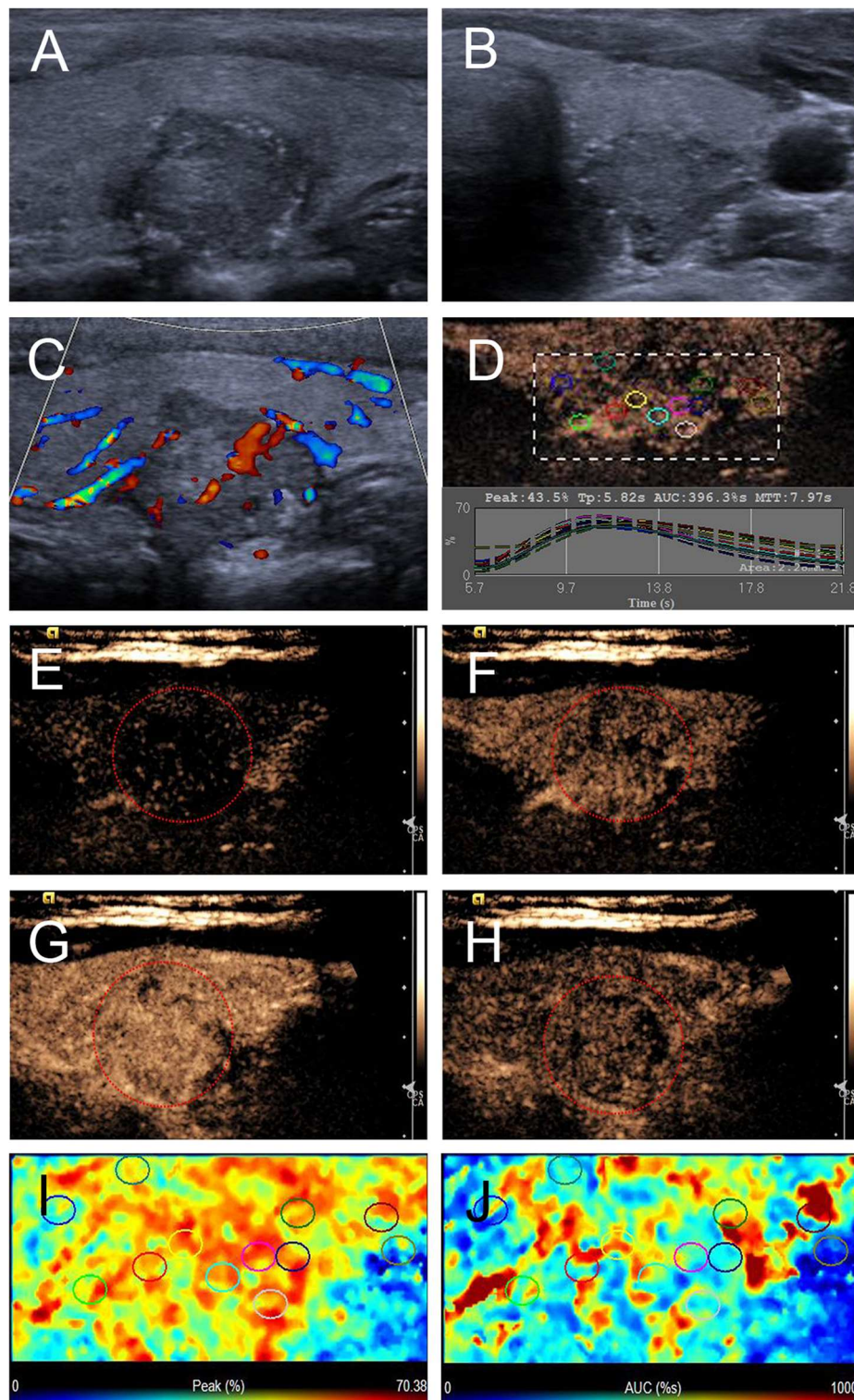


FIGURE 4 | Ultrasound images of a 26-y-old female PTC patient with petal-like calcification of the left thyroid lobe. **(A)** Longitudinal and **(B)** horizontal gray-scale sonograms; the thyroid nodule had a solid component, hypoechoic echogenicity, ill-defined margin, and capsule contact with protrusion. **(C)** Color Doppler sonogram showed moderate internal and peripheral vascularity. **(D)** TICs of the thyroid nodule and peripheral thyroid parenchyma with different regions of interest (different color circles). **(E–H)** CEUS sonograms of the thyroid nodule **(E)** at 6 s (wash-in), **(F)** 9 s (wash-in), **(G)** 11 s (time to peak), and **(H)** 15 s (wash-out), revealing diffuse, and heterogeneous enhancement (circle) across the whole lesion. **(I)** Parametric color map showing that peak intensity values for the nodule were mixed with red and yellow, and adjacent thyroid parenchyma were blue and yellow, indicating that the peak intensity of the nodule was higher than that of the peripheral thyroid parenchyma. **(J)** Parametric color map showing that AUC values for the nodule were mixed with blue, yellow and red, and adjacent thyroid parenchyma were almost the same, indicating that the AUC of the nodule was equal to that of the peripheral thyroid parenchyma.

TABLE 3 | Pathological characteristics according to eighth edition of AJCC/TNM classification system.

Characteristics	n	%
Tumor size (mm)	16.72 ± 9.01 (6–34)	
≤ 10 mm	5	27.8
> 10 mm	13	72.2
T CLASSIFICATION		
T1	13	72.2
T2	5	27.8
N CLASSIFICATION		
N0	5	27.8
N1a	8	44.4
N1b	5	27.8
M CLASSIFICATION		
M0	18	100
TNM stage		
I	18	100

images, which is called black-and-white foci. In addition, the majority of these nodules had ill-defined margins, marked hypoechoic or hypoechoic echogenicity, capsule contact with protrusion, a hyper- or isoenhancement type, a centripetal perfusion pattern, a PI index ≥ 1 and an AUC index ≥ 1 . Therefore, petal-like calcifications in thyroid nodules may be a specific ultrasonographic feature associated with the aggressive biological behavior of PTC.

REFERENCES

- Park M, Shin JH, Han BK, Ko EY, Hwang HS, Kang SS, et al. Sonography of thyroid nodules with peripheral calcifications. *J Clin Ultrasound*. (2009) 37:324–8. doi: 10.1002/jcu.20584
- Kim BK, Choi YS, Kwon HJ, Lee JS, Heo JJ, Han YJ, et al. Relationship between patterns of calcification in thyroid nodules and histopathologic findings. *Endocr J*. (2013) 60:155–60. doi: 10.1507/endocrj.ej12-0294
- Kim BK, Lee EM, Kim JH, Oak SY, Kwon SK, Choi YS, et al. Relationship between ultrasonographic and pathologic calcification patterns in papillary thyroid cancer. *Medicine*. (2018) 97:e12675. doi: 10.1097/MD.00000000000012675
- Kobayashi K, Fujimoto T, Ota H, Hirokawa M, Yabuta T, Masuoka H, et al. Calcifications in thyroid tumors on ultrasonography: calcification types and relationship with histopathological type. *Ultrasound Int Open*. (2018) 4:E45–51. doi: 10.1055/a-0591-6070uio0137
- Yin L, Zhang W, Bai W, He W. Relationship between morphologic characteristics of ultrasonic calcification in thyroid nodules and thyroid carcinoma. *Ultrasound Med Biol*. (2020) 46:20–5. doi: 10.1016/j.ultrasmedbio.2019.09.005
- Malhi HS, Velez E, Kazmierski B, Gulati M, Deurduian C, Cen SY, et al. Peripheral thyroid nodule calcifications on sonography: evaluation of malignant potential. *AJR Am J Roentgenol*. (2019) 213:672–5. doi: 10.2214/AJR.18.20799
- Taki S, Terahata S, Yamashita R, Kinuya K, Nobata K, Kakuda K, et al. Thyroid calcifications: sonographic patterns and incidence of cancer. *Clin Imaging*. (2004) 28:368–71. doi: 10.1016/S0899-7071(03)00190-6
- Peng Q, Niu C, Zhang M, Peng Q, Chen S. Sonographic characteristics of papillary thyroid carcinoma with coexistent hashimoto's thyroiditis:

DATA AVAILABILITY STATEMENT

The raw data supporting the conclusions of this article will be made available by the authors, without undue reservation, to any qualified researcher.

ETHICS STATEMENT

The studies involving human participants were reviewed and approved by the ethics committee of the Second Xiangya Hospital of Central South University. The patients/participants provided their written informed consent to participate in this study. Written informed consent was obtained from the individual(s) for the publication of any potentially identifiable images or data included in this article.

AUTHOR CONTRIBUTIONS

CN contributed to the conception and design of the work. QP and CN participated to data analysis and manuscript writing. QZ and SC participated to data collection and patient follow-up.

ACKNOWLEDGMENTS

This project was funded by the National Natural Science Foundation of China (Grant No. 81974267 and 81601883), Hunan Provincial Natural Science Foundation of China (Grant 2018JJ3861 and 2018JJ2575), and Hunan Provincial Health Commission Research Foundation Project (B2019166).

- conventional ultrasound, acoustic radiation force impulse imaging and contrast-enhanced ultrasound. *Ultrasound Med Biol*. (2019) 45:471–80. doi: 10.1016/j.ultrasmedbio.2018.10.020
- Peng Q, Niu C, Zhang Q, Zhang M, Chen S, Peng Q. Mummified thyroid nodules: conventional and contrast-enhanced ultrasound features. *J Ultrasound Med*. (2019) 38:441–52. doi: 10.1002/jum.14712
- Kwak JY, Han KH, Yoon JH, Moon HJ, Son EJ, Park SH, et al. Thyroid imaging reporting and data system for US features of nodules: a step in establishing better stratification of cancer risk. *Radiology*. (2011) 260:892–9. doi: 10.1148/radiol.11110206
- Casella C, Ministrini S, Galani A, Mastriale F, Cappelli C, Portolani N. The new TNM staging system for thyroid cancer and the risk of disease downstaging. *Front Endocrinol*. (2018) 9:541. doi: 10.3389/fendo.2018.00541
- Suh S, Kim YH, Goh TS, Lee J, Jeong DC, Oh SO, et al. Outcome prediction with the revised American joint committee on cancer staging system and American thyroid association guidelines for thyroid cancer. *Endocrine*. (2017) 58:495–502. doi: 10.1007/s12020-017-1449-4
- Lamartina L, Grani G, Arvat E, Nervo A, Zatelli MC, Rossi R, et al. 8th edition of the AJCC/TNM staging system of thyroid cancer: what to expect (ITCO#2). *Endocr Relat Cancer*. (2018) 25:L7–11. doi: 10.1530/ERC-17-0453
- Haugen BR, Alexander EK, Bible KC, Doherty GM, Mandel SJ, Nikiforov YE, et al. American thyroid association management guidelines for adult patients with thyroid nodules and differentiated thyroid cancer: the American thyroid association guidelines task force on thyroid nodules and differentiated thyroid cancer. *Thyroid*. (2016) 26:1–133. doi: 10.1089/thy.2015.0020
- Tessler FN, Middleton WD, Grant EG, Hoang JK, Berland LL, Teefey SA, et al. ACR Thyroid imaging, reporting and data system (TI-RADS): white

- paper of the ACR TI-RADS committee. *J Am Coll Radiol.* (2017) 14:587–95. doi: 10.1016/j.jacr.2017.01.046
16. American Thyroid Association Guidelines Taskforce on Thyroid, Differentiated Thyroid C, Cooper DS, Doherty GM, Haugen BR, Kloos RT, et al. Revised American thyroid association management guidelines for patients with thyroid nodules and differentiated thyroid cancer. *Thyroid.* (2009) 19:1167–214. doi: 10.1089/thy.2009.0110
 17. Chen J, Li XL, Zhao CK, Wang D, Wang Q, Li MX, et al. Conventional ultrasound, immunohistochemical factors and BRAF(V600E) mutation in predicting central cervical lymph node metastasis of papillary thyroid carcinoma. *Ultrasound Med Biol.* (2018) 44:2296–306. doi: 10.1016/j.ultrasmedbio.2018.06.020
 18. Hong YR, Yan CX, Mo GQ, Luo ZY, Zhang Y, Wang Y, et al. Conventional US, elastography, and contrast enhanced US features of papillary thyroid microcarcinoma predict central compartment lymph node metastases. *Sci Rep.* (2015) 5:7748. doi: 10.1038/srep07748

Conflict of Interest: The authors declare that the research was conducted in the absence of any commercial or financial relationships that could be construed as a potential conflict of interest.

Copyright © 2020 Peng, Zhang, Chen and Niu. This is an open-access article distributed under the terms of the Creative Commons Attribution License (CC BY). The use, distribution or reproduction in other forums is permitted, provided the original author(s) and the copyright owner(s) are credited and that the original publication in this journal is cited, in accordance with accepted academic practice. No use, distribution or reproduction is permitted which does not comply with these terms.



Breast Cancer After Treatment of Differentiated Thyroid Cancer With Radioiodine in Young Females: What We Know and How to Investigate Open Questions. Review of the Literature and Results of a Multi-Registry Survey

OPEN ACCESS

Edited by:

Jacqueline Jonklaas,
Georgetown University, United States

Reviewed by:

Joanna Klubo-Gwiezdzinska,
National Institutes of Health (NIH),
United States
Yevgeniya Kushchayeva,
University of South Florida,
United States

*Correspondence:

Christoph Reiners
reiners_c@ukw.de

†Present address:

Alexis Vrachimis,
German Oncology Center, Limassol,
Cyprus

Specialty section:

This article was submitted to
Thyroid Endocrinology,
a section of the journal
Frontiers in Endocrinology

Received: 23 January 2020

Accepted: 14 May 2020

Published: 10 July 2020

Citation:

Reiners C, Schneider R, Platonova T, Fridman M, Malzahn U, Mäder U, Vrachimis A, Bogdanova T, Krajewska J, Elisei R, Vaisman F, Mihailovic J, Costa G and Drozd V (2020) Breast Cancer After Treatment of Differentiated Thyroid Cancer With Radioiodine in Young Females: What We Know and How to Investigate Open Questions. Review of the Literature and Results of a Multi-Registry Survey. *Front. Endocrinol.* 11:381. doi: 10.3389/fendo.2020.00381

Christoph Reiners^{1*}, Rita Schneider¹, Tamara Platonova², Mikhail Fridman², Uwe Malzahn¹, Uwe Mäder¹, Alexis Vrachimis^{3†}, Tatiana Bogdanova⁴, Jolanta Krajewska⁵, Rossella Elisei⁶, Fernanda Vaisman⁷, Jasna Mihailovic⁸, Gracinda Costa⁹ and Valentina Drozd²

¹ University Hospital, Würzburg, Germany, ² The International Fund "Help for Patients With Radiation-Induced Thyroid Cancer 'ARNICA'", Minsk, Belarus, ³ University Hospital, Münster, Germany, ⁴ Institute of Endocrinology and Metabolism, Kiev, Ukraine, ⁵ M. Skłodowska-Curie National Research Institute of Oncology, Gliwice, Poland, ⁶ University Hospital, Pisa, Italy, ⁷ National Cancer Institute, Rio de Janeiro, Brazil, ⁸ Institute of Oncology Vojvodina, Sremska Kamenica, Serbia, ⁹ University Hospital, Coimbra, Portugal

Published studies on the risk of radiation-induced second primary malignancy (SPM) after radioiodine treatment (RAI) of differentiated thyroid cancer (DTC) refer mainly to patients treated as middle-aged or older adults and are not easily generalizable to those treated at a younger age. Here we review available literature on the risk of breast cancer as an SPM after RAI of DTC with a focus on females undergoing such treatment in childhood, adolescence, or young adulthood. Additionally, we report the results of a preliminary international survey of patient registries from academic tertiary referral centers specializing in pediatric DTC. The survey sought to evaluate the availability of sufficient patient data for a potential international multicenter observational case-control study of females with DTC given RAI at an early age. Our literature review identified a bi-directional association of DTC and breast cancer. The general breast cancer risk in adult DTC survivors is low, ~2%, slightly higher in females than in males, but presumably lower, not higher, in those diagnosed as children or adolescents than in those diagnosed at older ages. RAI presumably does not substantially influence breast cancer risk after DTC. However, data from patients given RAI at young ages are sparse and insufficient to make definitive conclusions regarding age dependence of the risk of breast cancer as a SPM after RAI of DTC. The preliminary analysis of data from 10 thyroid cancer registries worldwide, including altogether 6,449 patients given RAI for DTC and 1,116 controls, i.e., patients not given RAI, did not show a significant increase of breast cancer incidence after RAI.

However, the numbers of cases and controls were insufficient to draw statistically reliable conclusions, and the proportion of those receiving RAI at the earliest ages was too low. In conclusion, a potential international multicenter study of female patients undergoing RAI of DTC as children, adolescents, or young adults, with a sufficient sample size, is feasible. However, breast cancer screening of a larger cohort of DTC patients is not unproblematic for ethical reasons, due to the likely, at most slightly, increased risk of breast cancer post-RAI and the expected ~10% false-positivity rate which potentially produced substantial “misdiagnosis.”

Keywords: differentiated thyroid carcinoma, radioiodine therapy, iodine-131, long-term complications, young females, childhood and adolescence, second primary malignancy, breast cancer

INTRODUCTION

Treatment of differentiated thyroid cancer (DTC) in childhood, adolescence, or early adulthood with surgery, radioiodine (iodine-131, I-131) therapy (RAI), and thyroid hormone replacement achieves 10-year survival rates of 95%, with relatively low recurrence rates of 10–30% (1). However, an excellent long-term survival may be partly offset by an increased risk for second primary malignancy (SPM) related to RAI or other causes.

According to a systematic review by Clement et al. (2), the risk for SPM is increased after RAI of DTC. For many years, the gastrointestinal tract (salivary glands, stomach, and colorectum), the genitourinary tract (kidneys and bladder), and the hematopoietic system (blood cells) have been considered to be at risk to develop SPM after RAI (2–4). However, a recent meta-analysis did not find an increased risk of solid cancers after RAI (5).

Since I-131 is concentrated by the sodium iodide symporter and that molecule is expressed in the mammary gland (6), the female breast may receive relevant radiation doses between 0.2 and 2 Gy from repeated courses, with cumulative activities of 1–15 GBq (7). Based on the recently introduced radiation risk assessment tool of the United States National Cancer Institute, a dose of 2 Gy to the breast of a 10-year-old girl hypothetically doubles her lifetime risk for breast cancer, whereas in a 50-year-old woman, the risk increases only by 20% (8).

OBJECTIVE AND SCOPE

Published studies on the risk of radiation-induced SPM, including breast cancer in DTC, refer mainly to middle-aged and older adult survivors. These studies are not easily generalizable to those treated as children, adolescents, or young adults since the patients who are still growing are more sensitive to radiation, and the patients treated earlier in life may have a longer potential latency period. Therefore, we here (1) review available literature on the risk of breast cancer as an SPM (A) independent of the type of treatment of RAI and (B) after RAI of DTC, with a focus on young females, and (2) report the results of our preliminary international multi-registry survey to evaluate the availability of patient data for a sufficiently powered multicenter international study of DTC patients given RAI as children, adolescents, or

young adults. This research project was sponsored by the German Federal Office for Radiation Protection.

REVIEW OF THE LITERATURE

Methods

The literature included in the analysis was identified by two independent reviewers (VD and RS), principally using an automated literature search for English language papers published from 1984 to 2018 regarding breast cancer after RAI of DTC. The search was carried out using the online Medline (PubMed), Cochrane, and Embase databases. The main search terms were “thyroid” OR “breast” OR “mamma” AND “cancer” OR “malignancy” OR “carcinoma” OR “tumor” AND “second primary malignancy” AND “radioiodine therapy.” Besides the automated search, a manual search for additional relevant publications was made of the bibliographies of the papers identified automatically.

Systematic reviews, meta-analyses, cohort studies, and case-control studies were included. Case reports, single-center studies with small databases or study samples ($N < 500$), narrative reviews of the literature, editorials, and letters to the editor were excluded. Also excluded were publications regarding studies not differentiating between synchronous and metachronous SPMs.

From the publications fulfilling the inclusion criteria, the following information (if available) were extracted:

- First author, date, country
- Setting (e.g., hospital registry and population-based registry), single-center or multicenter design
- Duration of the study and of the follow-up time
- Study sample characteristics (number, gender, and age of patients/controls), exclusion criteria in the study
- DTC characteristics (histology and TNM stage)
- Surgery, RAI yes/no, cumulative I-131 activity as a surrogate for radiation dose
- SPM (of all kinds/breast cancer) before/after RAI
- Latency period, age dependency, dose dependency of SPM, and breast cancer incidence (correlation with I-131 activity)
- Risk estimates for secondary breast cancer after DTC (independent of treatment) and for secondary breast cancer after RAI of DTC, expressed as one or more of the following:

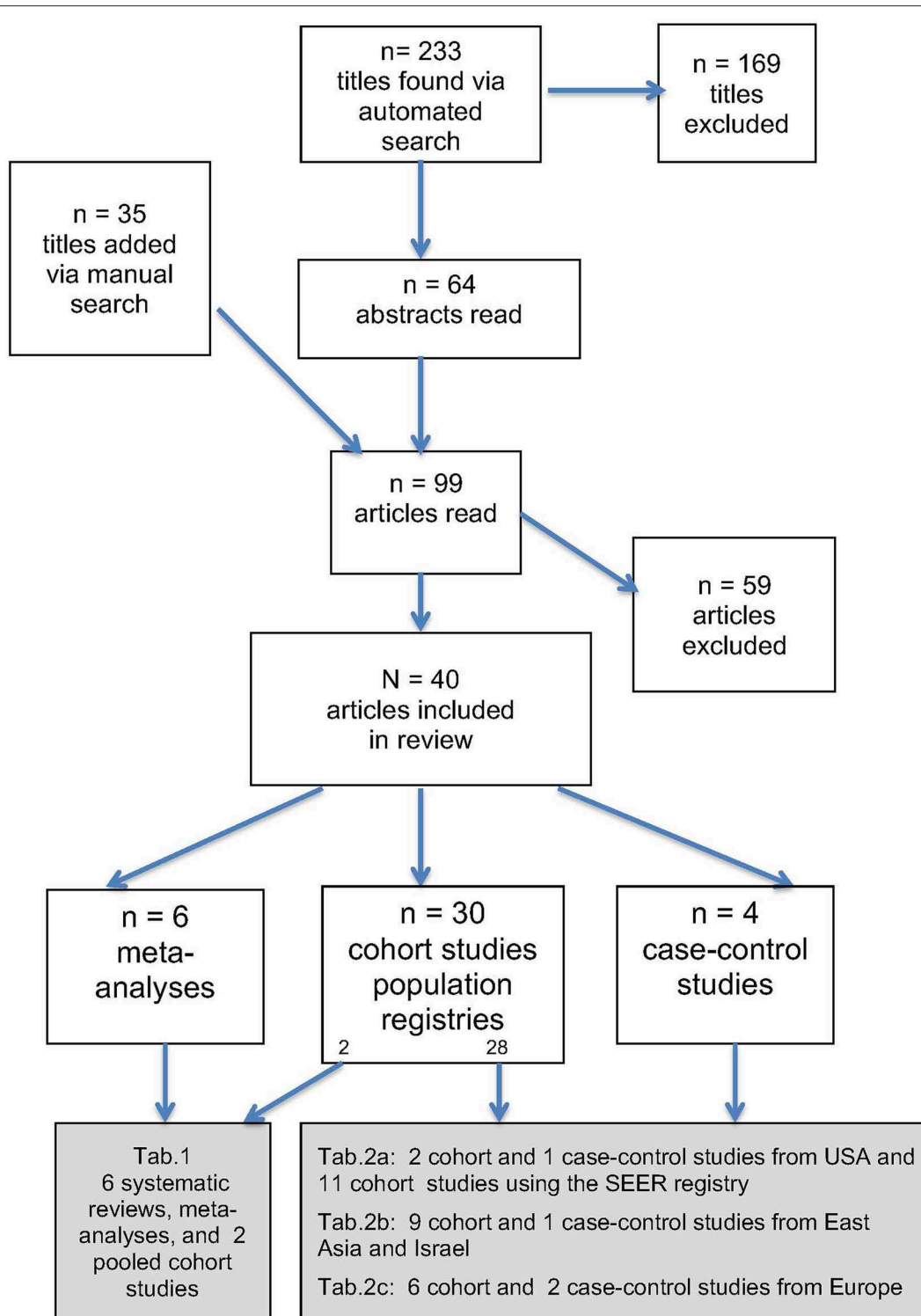


FIGURE 1 | Flow diagram describing the literature search process.

- absolute number
- excess absolute risk
- excess relative risk

- observed/expected incidence (O/E)
- odds ratio
- relative risk

- standardized incidence ratio (SIR)
- incidence rate ratio
- hazard ratio (HR)

with corresponding 95% confidence interval (CI).

Because of the heterogeneity and the variable design of the studies in the literature, only a qualitative and not a pooled analysis was performed.

Results

Publications Included

Using the search strategy described above, a total of 233 citations were found (**Figure 1**), 169 of which were excluded because the publications were unrelated to DTC, represented duplicate publication of the same studies, or were otherwise deemed not to be relevant. In addition to the 64 publications located through the automated search that were deemed to be of potential interest based on their abstracts, a manual search considering the bibliographies of the review articles retrieved 35 citations deemed to be of potential interest based on their abstracts. Thus, 99 full-text articles were read, of which 59 were excluded for the following reasons: small number of clinical observations by single centers ($n = 12$), case reports ($n = 11$), letters to the editor ($n = 4$), and unclear specification if the breast cancer was diagnosed before or after DTC ($n = 32$) (the papers could be excluded on more than one grounds).

Thus, altogether 40 publications were included in our analysis (**Figure 1**); they are cited and summarized in four tables. The main criterion for the assignment of a publication to a particular table was the type of study: **Table 1**—systematic reviews and meta-analyses and **Table 2**—cohort or case-control studies. Since the majority of the studies analyzed were large single-center cohort or case-control studies, resulting in a large number of publications, such articles were assigned to “sub-tables” according to the region of origin (**Table 2A**—USA, **Table 2B**—East Asia and Israel, and **Table 2C**—Europe). Within the tables, the studies are arranged according (1) to country of origin and (2) year of publication (chronological order from earliest to most recent).

Specifically, **Table 1** is a list of the results of six systematic reviews and meta-analyses. In addition, two large multinational pooled cohort studies are shown.

The majority of the included published studies ($n = 28$) were cohort studies of large population-based tumor registries (**Tables 2A–2C**). The US Surveillance, Epidemiology, and End Results (SEER) Registry (**Table 2A**) served as the database for 11 publications. Besides the studies using the SEER registry, **Table 2A** presents three other American analyses: one single-center cohort study, one cohort study analyzing the SEER database plus a local registry, and one case-control study.

Seven cohort studies (**Table 2B**) from East Asia also used large registries, e.g., the databases of the Korean Central Cancer Registry, the Taiwanese National Health Insurance, and the Taiwanese National Cancer Registry. Three cohort studies (**Table 2B**) analyzed the Israel National Cancer Registry. From Europe (**Table 2C**), six large cohort studies were found.

Finally, four case-control studies (**Tables 2B, 2C**) were included in our review, the largest of which included more than 4,000 cases (46).

A considerable proportion of the articles tried to take the patients' age at the diagnosis of DTC into consideration. However, only two studies focused on the risk of breast cancer after RAI for DTC in children and adolescents (3, 25).

It should be mentioned that, of 40 studies, 22 dealt with the general risk of breast cancer after DTC, not taking into account the form of treatment. Fourteen of the 40 studies dealt both with the general risk and the RAI-dependent risk. Conversely, four studies considered only the risk of breast cancer after treatment of DTC with RAI.

Risk of Breast Cancer After DTC (Independent of Therapy)

Three large meta-analyses and two large pooled cohort studies (**Table 1**) revealed a generally increased risk for breast cancer as an SPM in DTC patients, too, with significant SIRs of about 1.2 (9, 11, 13–15). Interestingly, only one of the meta-analyses gave an indication to exclude such an effect (5).

Eight of the 12 cohort studies examining the SEER registry and other registries from the USA (**Table 2A**) also described significant, if weak, increases of breast cancer risk in DTC survivors, with SIRs of ca. 1.2 or O/E values of ca. 1.2 (3, 17, 18, 21–24, 26).

On the other hand, three studies on the SEER registry (16, 20, 25) and two other cohort studies from the USA (25, 28) did not reveal such increases of breast cancer risk in DTC survivors (**Table 2A**).

Slightly higher, and again significant, increases of breast cancer risk in patients after a diagnosis of DTC have been described by nine of 17 cohort and case-control studies from East Asia, Israel, and Europe (**Tables 2B, 2C**) (29, 31–34, 36, 37, 43, 46). The SIRs in these studies ranged between 1.3 and 1.5, with the exception of 2.5 in patients from a Korean registry (**Table 2B**) (46).

On the contrary, seven of the same 17 studies (**Tables 2B, 2C**), including one from Israel (35), four from Scandinavia (38–40, 42) as well as two from France and Slovenia (44, 45), did not show an increased general risk for breast cancer in DTC patients. Hall et al. (40) did find such an association, but only in their subgroup at follow-up of >10 years (**Table 2C**).

Studies looking at age as a risk modifier and comparing subgroups of adult patients suggested no clear age dependency of SIRs (**Table 2A**) (3, 16, 25). Brown et al. (3) compared the risk of breast cancer in two groups of relatively young DTC survivors, those younger than 25 years of age and those 25–49 years of age, respectively (**Table 2A**). The authors only found a significantly increased risk for breast cancer in the older group. A similar observation was made by Vassilopoulou-Sellin et al. (16), who found an increased risk for breast cancer in women ages 40–49 years, but not in younger patients (**Table 2A**). Most interestingly for our survey regarding age-related risks, the only study specifically addressing young patients, an analysis of the SEER database performed by Adly et al. (25), did not find an increased risk for breast cancer in patients younger than age 20

TABLE 1 | Breast cancer risk in DTC survivors and/or DTC survivors given RAI: systematic reviews, meta-analyses, and internationally pooled cohort studies.

References, country	Study design, setting	Study period, length of FU (y), exclusion if FU < x(y), lost to FU (%)	Age range or mean age at DTC diagnosis (y)	DTC cases (TR), DTC with RAI (TR)	BC cases (BT), BC with RAI (BR)	BC risk after DTC, BC risk after RAI. Risks (95%CI)	BC risk status after DTC:	BC risk status after RAI:
Subramanian et al. (9), USA, Canada	Systematic review of the literature and meta-analysis, 8 pooled studies	1966–2006, 6–15 y		TC 60,490		SIR(BT) = 1.25 (1.17–1.32)	↑	
Sawka et al. (10), Canada	Systematic review of the literature and meta-analysis, 2 pooled studies	1966–2008, 9–13 y, 1 y excluded		TC 16,502, TR 8,473		RR(BR) = 0.86 (0.64–1.16)		⇔
Joseph et al. (11), Australien	Systematic review of the literature and meta-analysis, 18 pooled studies	1946–2015, <2 y excluded		TC 223,782		SIR(BT) = 1.24(1.16–1.33)	↑	
Zhang et al. (12), China	Systematic review of the literature and meta-analysis, 6 pooled studies	1934–2009, 7.8–12 y	42–50 y	TC 17,914, TR 9,000	BR 96	RR(BR) = 0.61 (0.47–0.79)		⇔
Nielsen et al. (13), USA	Systematic review of the literature and meta-analysis, 18 pooled studies	1934–2009, 7.8–12 y		TC 44,879	BT 5,791	OR(BT) = 1.18 (1.09–1.26)	↑	
Yu et al. (5), Canada	Systematic review of the literature and meta-analysis, 7 pooled studies	2008–2017, 7–13 y		TC 68,481	BT 1,276	RR(BR) = 0.8 (0.53–1.21)	⇔	
Rubino et al. (14), France	Pooled 3-cohort study, French, Swedish, Italian cohorts	1934–1995, 13 y, <2 y excluded	44 y	TC 6,841	BT 128, BR 54	SIR(BT) = 1.3 (1.0–1.5), SIR(BR) = 1.2 (0.9–1.6), RR = 0.8 (0.5–1.1)	↑	⇔
Sandeep et al. (15), Europe, Canada, Australia, Singapore	Pooled cohort study 13 cancer registries of Europe, Canada, Australia, Singapore	1953–2000, 25 y, <1 y excluded		TC 39,002	BT 552	SIR(BT) = 1.31 (1.21–1.43)	↑	

Some data may be absent in particular rows if the data were not reported in the publication. Up arrows (↑) denote increased risk, horizontal arrows (⇔) denote no increased risk. Unless otherwise noted, the "DTC patients" group includes both patients receiving RAI and those not receiving RAI.

BC, breast cancer; CI, confidence interval; DTC, differentiated thyroid cancer; FU, follow-up; OR, odds ratio; RAI, radioiodine therapy; RR, relative risk; SIR, standardized incidence ratio.

TABLE 2A | Breast cancer risk in DTC survivors and/or DTC survivors given RAI: cohort and case-control studies from USA.

References, country	Study design, setting	Study period, length of FU (y), exclusion if FU < x (y), lost to FU (%)	Age range or mean age at DTC diagnosis (y)	DTC cases (TC), DTC with RAI (TR)	BC cases (BT), BC with RAI (BR)	BC risk after DTC (BT), BC risk after RAI (BR), Risks (95% CI)	BC risk status After DTC	BC risk status after RAI
Vassilopoulou-Sellin et al. (16), USA	Cohort study, University of Texas and SEER registry	1944–1997, <2 y	42 y	TC 1,013	BT 24, BR 14	All ages RR(BT) = 3.9 (0.5–28.6), 40–49 y RR(BT) = 3.0 (1.17–8.62)	⇔	↑
Chen et al. (17), USA	Cohort study SEER Registry	1973–1994 <2 y	48.6 y	TC 23,080	BT 252	RR(BT) = 3.9 (1.04–1.33)	↑	
Ronckers et al. (18), USA	Cohort study SEER Registry	1973–2000, 8 y, <2 mo	43 y	TC 29,456	BT 530, BR 53	O/E(BT) = 1.21 (1.11–1.32), O/E(BR) = 1.18 vs. O/E (no BR) = 1.28	↑	⇔
Bhattacharyya et al. (19), USA	Cohort study SEER Registry	1988–2001, RAI 5.2 y, no RAI 4.7 y,	RAI 43.5 y, no RAI 54 y	TC 29,231, TR 10,349	BT 424, BR 112	Prevalence of BR 1.08% of BT without RAI 1.6%,		⇔
Chuang et al. (20), USA	Cohort study SEER Registry	1973–2000, RAI 15 y no RAI 11.1 y, <6 mo	> 18 y	TC 26,639	BT 462, BR 344	RR(BT) = 1.02 (0.81–1.29), RR(BR) = 0.86 (0.6–1.24)	⇔	⇔
Brown et al. (3), USA	Cohort study SEER Registry	1973–2002, 8.6 y	42 y	TC 30,278	BT 597, BR 76	All ages O/E(BT) = 1.22 (1.12–1.32), < 25y O/E(BT) = 1.16 (0.58–2.08) All ages O/E(BR) = 1.21 (0.95–1.52)	↑	⇔
Kim et al. (21), USA	Cohort study SEER Registry	1973–2008		TC 52,103	BT 1,041	SIR(BT) = 1.13 (1.06–1.20), SIR(BR) = 1.14 (0.98–1.31)	↑	⇔
Kuo et al. (22), USA	Cohort study, SEER Registry	1990–2011	46 y	TC 38,158, TR 16,670	BT 954, BR 384	OR(BT) = 1.02 (1.01–1.02), OR(BR) = 0.94 (0.82–1.08)	↑	⇔
Upreti et al. (23), USA	Cohort study SEER Registry	2004–2010, <6 mo, 12.8 y	> 18 y	TC 12,603	BT 291	O/E(BT) = 1.19 (1.06–1.34)	↑	
Endo et al. (24), USA	Cohort study, SEER Registry	1992–2013, <6 mo	61 y	TC 75,992	BT 727, BR 245	O/E(BT) = 1.17 (1.09–1.26), O/E (BR) = 1.08 (0.95–4.7), O/E(no BR) = 1.12 (1.01–1.24)	↑	⇔
Adly et al. (25), USA	Cohort study, SEER Registry	1973–2013	16 y	TC 1,769	BT 9	SIR (BT) = 0.96 (0.44–1.83)	⇔	
Ron et al. (26), USA	Cohort study, Connecticut Tumor Registry	1935–1978, < 2, mo 1 6%	47.3 y	TC 1,618, TR 281	BT 34, BR 8	SIR(BT) = 1.89 (1.31–2.64), SIR(BR) = 2.57 (1.1–5.07)	↑	↑
Simon et al. (27), USA	Case-control study National Institute of Child Health and Human	1961–1995	35–64 y	TC 23	BT 4,575	OR(BT) = 2.7 (1.2–5.9)	↑	
Canchola et al. (28), USA	Cohort study, California Cancer Registry	1988–1999, <1 y		TC 10,932	BT invasive 78, BT <i>in situ</i> 23	SIR (invasive) = 0.9 (0.7–1.1), SIR (<i>in situ</i>) = 1.6 (1.0–2.4)	⇔ ↑	

Some data may be absent in particular rows if the data were not reported in the publication. Up arrows (↑) denote increased risk, horizontal arrows ⇔ denote no increased risk. Unless otherwise noted, the “DTC patients” group includes both patients receiving RAI and those not receiving RAI.

BC, breast cancer; CI, confidence interval; DTC, differentiated thyroid cancer; FU, follow-up; O/E, observed/expected ratio; OR, odds ratio; RAI, radioiodine therapy; RR, relative risk; SIR, standardized incidence ratio.

TABLE 2B | Breast cancer risk in DTC survivors and/or DTC survivors given RAI: cohort and case-control studies from Asia.

References, country	Study design, setting	Study period, length of FU (y), excluded if FU <x(y), lost to FU (%)	Age range or mean age at DTC diagnosis (y)	DTC cases (TC), DTC with RAI (TR)	BC cases (BT), BC with RAI (BR)	BC risk after TC, BC risk after RAI, Risks (95% CI)	BC risk status after DTC	BC risk status after RAI
Cho et al. (29), Korea	Cohort study, Korean Central Cancer Registry	1993–2010, <2 mo excluded	45.2 y	TC 178,844	BT 599	SIR(BT) = 1.20 (1.11–1.30)	↑	
Ahn et al. (30), Korea	Cohort study, Registry of Seoul National University Hospital	1973–2012, 5 y, <2 y excluded	45.2 y	TC 6,150, TR 3,631	BT 99	HR(BR) = 0.49 (0.22–1.06)		⇔
Ahn et al. (30), Korea	Case-control study, Registry of Seoul National University Hospital	1970–2009, 5 y, <2	43.4 y	TC 4,243	BT 55	SIR(BT) = 2.45 (1.83–2.96)	↑	
Khang et al. (31), Korea	Cohort study, Registry of Seoul National University Hospital	1976–2010, 7 y, <1 y excluded	46.4 y	TC 2,468, TR 1,396	BT 17	BT was more frequent, in the no RAI group.	↑	
Lu et al. (32), Taiwan	Cohort study, Taiwan Cancer	1979–2006, 7.1 y, <1 mo excluded	45.2 y	TC 19,068	BT 102	SIR(BT) = 1.42 (1.16–1.72)	↑	
Teng et al. (33), Taiwan	Cohort study, Taiwan National Health Insurance Database	1997–2010, 6.5 y, <1 y	46 y	TC 20,235, TR 11,799	BT 158	SIR(BT) = 1.48 (1.26–1.73), HR(BR) = 0.99 (0.96–1.02)	↑	⇔
Lin et al. (34), Taiwan	Cohort study, Taiwan National Health Insurance Database	2000–2011, 5.9 y	46 y	TC 10,361, TR 7,069	BT 129, BR 91	HR(BT) = 1.31(1.07–1.61), HR(BR) = 1.34(1.06–1.69)	↑	↑ No correlation with activity
Sadetzki et al. (35), Israel	Cohort study, Israel National Cancer Registry	1960–1998, 9.4 y, <1 y excluded		TC 4,911	BT 70	SIR(BT) = 1.07 (0.84–1.34)	⇔	
Hirsch et al. (36), Israel	Cohort study, Israel National Cancer Registry, Rabin Medical Center Thyroid Cancer Registry	9.3 y, <2 y excluded	48.1 y	TC 1,943, TR 1,574	BT 49, BR 39	The most common SPM was breast cancer(49 from 173)	↑	
Izkhakov et al. (37) Israel	Cohort study, Israel National Cancer Registry	1980–2011, 9.7 y, <1 y excluded	51.2 y (Jews), 41.4 y (Arabs)	TC 11,538	BT 258	SIR(BT) = 1.44(1.26–1.61)	↑	

Some data may be absent in particular rows if the data were not reported in the publication. Numbers in parentheses represent 95% CI's. Up arrows (↑) denote increased risk, horizontal arrows (⇔) denote no increased risk. Unless otherwise noted, the "DTC patients" group includes both patients receiving RAI and those not receiving RAI.

BC, breast cancer; CI, confidence interval; DTC, differentiated thyroid cancer; FU, follow-up; HR, hazard ratio; RAI, radioiodine therapy; SIR, standardized incidence ratio.

TABLE 2C | Breast cancer risk in DTC survivors and/or DTC survivors given RAI: cohort and case-control studies from Europe.

References, country	Study design, setting	Study period, length of FU (y), excluded if FU < x(y), Lost to FU (%)	Age range or mean age at DTC diagnosis (y)	DTC cases (TC), TC with RAI (TR)	BC cases (BT), BC with RAI (BR)	BC risk after TC, BC risk after RAI, risks (95% CI)	BC risk status after DTC	BC risk status after RAI
Osterlind et al. (38), Denmark	Cohort study, Denmark Cancer	1943–1980, 5.9 y		TC 1,351	BT 11	SIR(BT) = 0.96 (0.76–1.20)	⇔	
Hall et al. (39), Sweden	Cohort study, Swedish Cancer	1958–1975, <1 y excluded	49 y	TC 2,968	BT 45	SIR(BT) = 0.99 (0.72–1.33)	⇔	
Hall et al. (40), Sweden	Cohort study, Registry of 6 university hospitals	1950–1975, 14–16 y, <2 y excluded	5–75 y	TC 1,955, TR 834	BT 36, BR 9	SIR(BT) = 1.37 (0.91–2.00) FU > 10 y SIR(BT) = 1.75 (1.06–2.74), SIR(BR) = 0.74 (0.34–1.40), O/R(BR) = 0.47 (0.21–1.08)	⇔ ↑	⇔
Hall et al. (41), Sweden	Case-control study, oncologic centers of 6 hospitals	1950–1975, 50 y	5–75 y	TC 1,955, TR 834	BR 36, no BR 107			⇔
Akslen and Glatre (42), Norway	Cohort study, Cancer Registry of Norway	1955–1985, 8.8 y, <2 mo excluded		TC 2,720	BT 33	SIR(BT) = 1.03 (0.71–1.44)	⇔	
Adjadj et al. (43), France	Case-control study, 3 French cancer centers	1934–1995, 12 y, <2 y excluded, 21% lost to FU, 15% died	42 y	TC 2,365	BT 48	SIR(BT) = 1.3 (1.0–1.7), SIR(BR) = 1.2 (0.2–6.2)	↑	⇔
Berthe et al. (44), France	Cohort study, Basse-Normandie Cohort	1960–1998, <1 y excluded	47 y	TC 875	BT 12	SIR(BT) = 1.19 (0.62–2.08)	⇔	
Edhemovic et al. (45), Slovenia	Cohort study, Cancer Registry of Slovenia	1971–1993, 5.2 y, <1 Mo excluded	54.9 y	TC 894	BT 4	SIR(BT) = 1.12 (0.31–2.87)	⇔	

Some data may be absent in particular rows if the data were not reported in the publication. Numbers in parentheses represent 95% CIs. Up arrows (↑) denote increased risk, horizontal arrows (⇔) denote no increased risk. Unless otherwise noted, the “DTC patients” group includes both patients receiving RAI and those not receiving RAI.

BC, breast cancer; CI, confidence interval; DTC, differentiated thyroid cancer; FU, follow-up; HR, hazard ratio; OR, odds ratio; RAI, radioiodine therapy; SIR, standardized incidence ratio.

years at the time of DTC diagnosis and who were followed up for up to 40 years (**Table 2A**).

Few studies have investigated the latency times between diagnosis of DTC and detection of breast cancer. The above-mentioned study of the Korean National University Hospital, Seoul, database with the highest SIR, 2.5 (**Table 2B**) (46), reported in patients older than 30 years a mean latency time between diagnoses of DTC and breast cancer of 6.6 (minimum–maximum, 3.3–7.8) years. In patients diagnosed with DTC when younger than age 30 years, the mean latency time was considerably longer, 17.9 (minimum–maximum, 13.9–20.4) years.

Studies Comparing Breast Cancer Risk in Patients With DTC Receiving vs. Not Receiving RAI

The first cohort study describing an increased risk for breast cancer after DTC, that of Ron et al. (26), already focused on radiation as a risk factor for the former malignancy and reported a significantly increased SIR of 2.6 after radiation therapy (**Table 2A**). However, in the study of Ron et al. (26), the group of patients with radiation treatment was small ($n = 8$) and the type of treatment (percutaneous radiation therapy, RAI) was not specified.

On the contrary, two meta-analyses and one large pooled cohort study (**Table 1**) comparing the risk of breast cancer as an SPM in DTC patients given or not given RAI did not find an increased risk after RAI (10, 12, 14).

The absence of an association between RAI of DTC and breast cancer was confirmed by all seven studies on the risk of breast cancer after such treatment upon examining the US SEER Registry (**Table 2A**) (3, 18–22, 24). The same conclusions were drawn in five of six studies in other countries, e.g., Korea and Taiwan (**Table 2B**) (30, 33), the Scandinavian nations (40, 41), and France (**Table 2C**) (43).

In detail, Ahn et al. (30) noted that the risk of breast cancer was not associated with RAI (**Table 2B**); even for relatively high cumulative activities of ≥ 4.4 GBq, no effect was demonstrated. Lin et al. (34) showed that there was a small increase of breast cancer risk in DTC patients post-RAI (**Table 2B**), but not as high as that associated with DTC *per se*. Most importantly, in patients receiving cumulative activities of > 4.4 GBq in comparison to patients receiving < 4.4 GBq, the risk for breast cancer was not increased.

Brown et al. (3) did not find a correlation with RAI in any age group or when comparing breast cancer risk in two subgroups of relatively young patients after DTC—those < 25 years old vs. those 25–49 years of age, respectively (**Table 2A**). Of interest is that Vassilopoulou-Sellin et al. (16) found, independent of RAI, an increased risk for breast cancer in women aged 40–49, but not in younger patients (**Table 2A**).

Adly et al. (25) also analyzed the SEER Registry data but focused on young patients (**Table 2A**). These investigators concluded that the overall risk of all kinds of SPM was significantly increased (SIR 1.5; 95%CI, 1.08–1.98) in patients undergoing RAI for DTC, being higher in females and White patients. Additionally, the cumulative incidence of all kinds of SPM after RAI of DTC in children appeared to increase steadily

with survival after the primary treatment. The overall risk of SPM in patients with RAI was found to be significantly higher than expected compared to the risk in the general population. Based on this study, the pediatric thyroid cancer survivors are at an increased risk of developing SPM of the organs highly exposed to radiation by RAI: salivary glands, gums, and other parts of the mouth, the stomach, as well as the kidneys. By contrast, a significant increase of breast cancer as SPM in patients given RAI as children was not observed (SIR 0.96; 95%CI, 0.44–1.83).

INTERNATIONAL MULTI-REGISTRY SURVEY

Participating Registries and Study Design

The second part of this report addresses a survey of patient registries from institutions known by the authors to specialize in treating children and adolescents with DTC. This preliminary study evaluated the availability of sufficient patient data to conduct an adequately powered international multicenter observational case–control study regarding breast cancer risk in female DTC survivors who were treated with RAI at a young age. Altogether eight academic tertiary referral centers from Germany, Ukraine, Poland, Italy, Brazil, Serbia, and Portugal agreed to participate. In addition, the German-Belarusian Foundation “ARNICA” contributed two separate datasets, one from their registry and the other from a dedicated smaller database which was set up for a “pilot study” that sought to test the feasibility of a multicenter international study on breast cancer risk in DTC survivors (Drozd et al., submitted). The nine institutions participating in the registry survey were:

- Foundation “ARNICA,” Minsk, Belarus (feasibility study sample and routine registry)
- Institute of Endocrinology and Metabolism, Kiev, Ukraine
- Instituto Nacional do Cancer—INCA, Rio de Janeiro, Brazil
- Institute of Oncology Vojvodina, Department of Nuclear Medicine, Sremska Kamenica, Serbia
- Department of Nuclear Medicine, University Hospital, Coimbra, Portugal
- Department of Nuclear Medicine, University Hospital, Münster, Germany
- Department of Endocrinology, University Hospital, Pisa, Italy
- Clinic of Nuclear Medicine and Endocrine Tumors, M. Skłodowska-Curie Memorial Cancer Center and Institute of Oncology, Gliwice, Poland
- Department of Nuclear Medicine, University Hospital, Würzburg, Germany

In the registry survey, in 2014–2015, the participating centers answered questionnaires requesting the most relevant information regarding breast cancer in female survivors of DTC, particularly those receiving RAI at an early age. These queries included the database's total number of female DTC survivors diagnosed during childhood or adolescence with or without a history of RAI, the percentage of DTC survivors who were ages < 18 or < 40 years of age at the time of the primary treatment, the cumulative activity of I-131 administered for

RAI, and the follow-up regimen after RAI. Queries were also made regarding the incidence of SPM, specifically breast cancer, both before and after the DTC diagnosis. The registry study was performed with anonymous, aggregated patient data.

The pilot observational cohort study alluded to above was performed in collaboration with the Foundation “ARNICA” and other organizations in Belarus and Germany in 2016–2017 (Drozd et al., submitted). In this feasibility study, selected female patients given RAI for their DTC in childhood or adolescence and control patients not given RAI underwent clinical, imaging, and laboratory examinations as part of a screening program for breast cancer. As noted previously, the dedicated database that was created for the pilot study also was analyzed in the present study. To avoid duplicate publication, any patients in the dedicated database who also were in the Foundation “ARNICA” Registry were excluded from all analyses of the latter.

Number and Origin of Patients and Controls

Tables 3A, 3B show the key aggregated data for each of the nine centers and 10 databases included in our survey. The cohorts comprised altogether 7,565 female DTC survivors given RAI (“RAI patients,” $n = 6,449$) or not given RAI (“controls,” $n = 1,116$). The number of RAI patients per institution varied considerably from 15 to 1,644 and the number of controls from 0 to 419.

The three largest groups of RAI patients, with more than 1,000 cases each, were contributed by the participating centers in Münster, Kiev, and Pisa. By contrast, by far the largest “no RAI” control group was provided by the Foundation “ARNICA,” Minsk, with a total of more than 500 controls (pilot study database plus registry). **Table 3A** is firstly a list of the three cohorts from Minsk and Kiev, which included a considerable proportion of young patients who developed DTC after the Chernobyl reactor accident in 1986 (1, 47).

Cohort Characteristics

It is apparent from **Tables 3A, 3B** that not all information was provided by all centers. However, the data supplied seemed to suffice to answer the survey’s most important questions about the number and the main characteristics of the patients/survivors under observation.

Age Distribution

The data in **Tables 3A, 3B** are listed according to the patients’ and the controls’ ages at the time of the first treatment (surgery and/or RAI). **Table 3A** shows the young patient groups from five centers, who were between 12 and 16 years of age at the time of their initial treatment. Only the patients and the controls from Kiev were older, with mean ages of 26–30 years. However, because the Kiev cohorts included 16% of patients and 32% of controls not older than 18 years, we present their data in **Table 3A**, too, directly adjacent to the data from Minsk.

The cohorts from the four other centers (**Table 3B**), which together contributed approximately two-thirds of the RAI patients (4,110/6,449), mirrored the typical age distribution for

patients with DTC, with mean ages at surgery/first RAI between 43 and 48 years.

Cumulative I-131 Activity

Except for the cohort from Kiev, all centers reported their cumulative activity of I-131 (in GBq) administered for RAI (**Tables 3A, 3B**). The mean cumulative activities of the centers in Minsk (registry), Würzburg, Münster, and Coimbra ranged between 6.0 and 10.0 GBq, whereas the highest mean cumulative activities, >10–12 GBq, were applied in patients from Minsk (pilot study sample) as well as in Rio de Janeiro and Sremska Kamenica. The relatively high cumulative activities can be explained by the young age of the patient cohorts from Belarus, Brazil, and Serbia. That demographic characteristic presumably corresponded to a relatively aggressive disease and hence to high rates of nodal or distant metastases or both, requiring a greater I-131 activity to be effectively treated.

Duration of Follow-Up

Eight of the nine centers (**Tables 3A, 3B**) provided information about the mean duration of follow-up after RAI in RAI patients and after surgery in controls (when available). On average, the centers in Minsk and Pisa had the longest mean follow-up times, slightly over 15 years. The mean follow-up times of the centers in Gliwice, Rio de Janeiro, and Sremska Kamenica ranged between 11 and 13 years. The shortest follow-up times were reported from Münster, with about 9 years, and Würzburg and Coimbra, with about 5 years.

Second Primary Malignancies

Again, eight of the nine centers provided data about SPM and breast cancer before and after the diagnosis of DTC (**Tables 3A, 3B**). There was considerable inhomogeneity of the data reported, which can be explained by the age distribution of the different cohorts. In the very young cohorts from Minsk (pilot study sample), Rio de Janeiro, Sremska Kamenica, and Coimbra, no breast cancer cases were reported in patients or controls. The relatively large cohorts of patients ($n = 909$) and controls ($n = 419$) of the Minsk registry included a low number of breast cancer cases, eight and five, respectively, before the diagnosis of DTC. After the DTC diagnosis, there was one additional case of breast cancer and three additional cases of other SPM in the RAI patient group as compared to no case of breast cancer and one case of another SPM in the control group.

The rates of SPM and breast cancer were higher in the much older cohorts from Würzburg, Münster, Gliwice, and Pisa. The rates before and after the diagnosis of DTC reported by the latter three centers were very similar, ranging between 0.5 and 2.5% (median, 0.9%) for breast cancer and 0.6–4.5% (median, 1.9%) for SPM other than breast cancer. The exceptionally high rate of other malignancies before DTC in the Würzburg cohort may be explained, at least partially, by detection bias due to the existence of a comprehensive local clinical cancer registry and a follow-up program. In that cohort, systematic differences in the cumulative incidences of breast cancer and other SPM between RAI patients and controls were not recognizable.

TABLE 3A | Registry survey: RAI patient and control cohort characteristics by center - young age groups.

Study Center	Feasibility study sample, ARNICA		Registry, ARNICA		Institute of Endocrinology & Metabolism		National Tumor-Institute (INCA)		Dept. Nuclear Medicine, Institute of Oncology Vojvodina		Dept. Nuclear Medicine, University Hospital	
City, country	Minsk, Belarus		Minsk, Belarus		Kiev, Ukraine		Rio de Janeiro, Brazil		Sremska Kamenica, Serbia		Coimbra, Portugal	
N (% of combined study sample)	202 (2.7%)		1,328 (17.6%)		1,297 (17.1%)		89 (1.2%)		32 (0.4%)		15 (0.2%)	
Cohorts	RAI patients	Controls*	RAI patients	Controls	RAI patients	Controls	RAI patients	Controls	RAI patients	Controls	RAI patients	Controls
n (% of RAI patient or control cohort)	102 (1.6%)	100 (9.0%)	909 (14.1%)	419 (37.5%)	1,199 (18.6%)	98 (8.8%)	81 (1.3%)	8 (0.7%)	32 (10.5%)	0	15 (0.2)	0
Current age (years, M \pm SD)	30.1 \pm 1.9	34.3 \pm 5.3	28.5 \pm 5.2	36.7 \pm 5.9		36.7 \pm 5.9	25.6 \pm 9.6	31.2 \pm 8.9	29.3 \pm 6.1		21.5 \pm 5.1	
Age at first surgery (years, M \pm SD)	11.9 \pm 3.2	17.6 \pm 6.6	13.3 \pm 3.3	23.6 \pm 9.1	29.6 \pm 8.1	26.2 \pm 7.6	14.50 \pm 3.0	14.5 \pm 3.3	15.8 \pm 3.9		14.2 \pm 2.6	
<18 years, <i>n</i> (%)				134 (32%)	190 (15.8%)	134 (32%)					15 (100%)	
<40 years, <i>n</i> (%)				416 (99.3%)	1,125 (93.8%)	416 (99.3%)						
Age at first RAI (years, M \pm SD)	12.8 \pm 3.0		14.3 \pm 3.4				14.5 \pm 3.0		16.9 \pm 0.81		15.5 \pm 2.0	
<18 years, <i>n</i> (%)									17 (53%)		15 (100%)	
<40 years, <i>n</i> (%)									15 (47%)			
Cumul. I-131 activity (GBq, M \pm SD)	11.8 \pm 9.5		6.6 \pm 3.8				10.4 \pm 5.5		10.9 \pm 0.2		7.2 \pm 8.0	
Follow-up duration (years, M \pm SD)	17.3 \pm 3.2	15.9 \pm 3.4	17.4 \pm 2.8	13.6 \pm 6.2			11.1 \pm 8.4	16.2 \pm 8.2	13.1 \pm 7.4		5.4 \pm 4.5	
SPM before DTC												
Breast cancer, <i>n</i> (%)	0	0	0	0			0	0	0		0	
Other cancers, <i>n</i> (%)	0	0	8 (0.9%)	5 (1.2%)					0		0	
SPM after DTC/RAI												
Breast cancer, <i>n</i> (%)			1 (0.9%)	0			0	0	0		0	
Other cancers, <i>n</i> (%)			3 (0.3%)	1 (0.2%)					0		0	

Cumul., cumulative; Dept., department; DTC, differentiated thyroid carcinoma; follic., I = 131, iodine-131; M \pm SD, mean + standard deviation; RAI, radioiodine therapy; SPM, second primary malignancy.

*Controls were patients with DTC who had not received RAI.

TABLE 3B | Registry survey: RAI patient and control cohort characteristics by center - all age groups.

Study center	Dept. Nuclear Medicine, University Hospital		Dept. Endocrinology, University Hospital		Dept.Nuclear Medicine & Endocrinology, MSC Memorial Cancer Center		Dept.Nuclear Medicine University Hoispital	
City/country	Münster, Germany		Pisa, Italy		Gliwice, Poland		Würzburg, Germany	
N (% of combined study sample)	1,808 (23.9%)		1,091 (14.4%)		867 (11.5%)		836 (11.1%)	
Cohorts	RAI patients	Controls*	RAI patients	Controls	RAI patients	Controls	RAI patients	Controls
n (% of RAI patient or control cohort)	1,644 (25.5%)	164 (14.7%)	1,091 (16.9%)	0	650 (10.1%)	217 (19.4%)	726 (11.3%)	110 (9.9%)
Current age (years, M \pm SD)	56.3 \pm 16.2	55.5 \pm 13.3						
Age at first surgery (years, M \pm SD)	47.6 \pm 15.9	48.8 \pm 13.1	44.13 \pm 3.0		43.3 \pm 4.9	43.9 \pm 2.1	45.6 \pm 16.1	46.7 \pm 15.5
<18 years, <i>n</i> (%)					44 (6.8%)	7 (3.2%)		
<40 years, <i>n</i> (%)					241 (37.1%)	76 (35.0%)		
Age at first RAI (years, M \pm SD)	47.8 \pm 15.9						45.7 \pm 16.1	
<18 years, <i>n</i> (%)	34 (2.1%)						30 (4.1%)	
<40 years, <i>n</i> (%)	544 (33.1%)						244 (33.6%)	
Cumul. I-131 activity (GBq, M \pm SD)	7.8 \pm 10.1		6.0 \pm 6.5		4.0 \pm 5.8		7.5 \pm 6.6	
Follow-up duration (years, M \pm SD)	8.6 \pm 6.8	6.8 \pm 6.1	16.1 \pm 10.4		11.4 \pm 3.9	10.9 \pm 4.3	4.7 \pm 3.72	5.74 \pm 4.08
SPM before DTC								
Breast cancer, <i>n</i> (%)	10 (0.6%)	3 (1.8%)	5 (0.5%)		4 (0.6%)	0	5 (0.7%)	1 (0.9%)
Other cancers, <i>n</i> (%)	20 (1.2%)	1 (0.6%)	9 (0.8%)		10 (1.5%)	0	107(14.7%)	5 (4.5%)
SPM after DTC/RAI								
Breast cancer, <i>n</i> (%)	16 (1.0%)	2 (1.2%)	27 (2.5%)		11 (1.6%)	0	9 (1.2%)	2 (1.8%)
Other cancers, <i>n</i> (%)	13 (0.8%)	4 (2.4%)	42 (3.8%)		14 (2.2%)	2 (0.9%)	19 (2.6%)	4 (3.6%)

Cumul., cumulative; Dept., department; DTC, differentiated thyroid carcinoma; I = 131, iodine-131; M \pm SD, mean + standard deviation; RAI, radioiodine therapy; SPM, second primary malignancy.

*Controls were patients with DTC who had not received RAI.

DISCUSSION

Literature Review

Breast Cancer Risk in Differentiated Thyroid Cancer Patients Generally Increased, Influence of RAI Questionable

In a comprehensive systematic review and meta-analysis, Nielsen et al. (13) investigated the relationship between breast cancer and DTC. Interestingly, these authors, in line with earlier investigators (17, 48), described a bi-directional association, meaning that the risk of breast cancer was increased in patients with DTC and *vice versa*.

The majority of studies addressing this issue that are referenced here (22/34) indicate that there is a generally increased risk for breast cancer after diagnosis of DTC, independent of therapy. This observation was reflected in five of six systematic reviews, meta-analyses, and pooled studies (Table 1). The observation also was echoed in eight of 12 cohort studies using the SEER registry or other registries from the USA (Table 2A) and nine of 16 studies analyzing other registries (Tables 2B, 2C).

In the general population of the USA, breast cancer risk in women below age 45 years corresponds to approximately one case in 87, or 1.2% (49). To give a rough estimate of the risk in DTC survivors, a SIR of 1.5, the maximum value for 90% of the studies listed in Table 1, would mean that, with the diagnosis of DTC, the general risk of 1.2% could be increased by 50%, to ~1.8%, in women younger than 45 years of age.

However, the only study specifically focusing on children and adolescents younger than 20 years old does not suggest an increased breast cancer risk in patients with DTC (25). There is some indication that the latency times for breast cancer after DTC in young patients are much longer than in adults, often lasting 20 years or more, so that the studies examining this risk have to focus on long observation times (30).

Beyond the generally increased risk for breast cancer in DTC survivors independent of treatment, a history of RAI seems not to have any additional influence on this risk (Tables 1, 2A, 2C), based on published findings of all SEER studies, all meta-analyses, and nearly all cohort studies from a variety of countries. There are two exceptions describing an increased risk in cohorts after RAI, but correlations of the degree of risk with the therapeutic activity of I-131 were not found (26, 34). Two additional studies examined the possibility of a higher risk of breast cancer in young patients given RAI, which was not confirmed (3, 16).

Assessing the hypothesis of a generally increased risk for SPMs other than breast cancer in DTC patients/survivors was not an objective of the present study. However, in young (as well as adult) DTC patients after RAI, a generally increased risk for SPM seems to exist, specifically in organs and tissues relatively highly irradiated by RAI, e.g., salivary glands, gums, and other parts of the mouth, the stomach, and the kidneys (25).

Limitations and Weaknesses of Published Studies

Concerning the risk of breast cancer in DTC survivors given RAI at a young age—the original focus of this review—data are inconclusive for many reasons. A general problem of critically

reviewing publications from, e.g., tumor registries is that non-independent data sets from identical registries are analyzed and published repeatedly. This plays an important role in the context of our review because 11 of 40 studies utilized the SEER registry and, similarly, three studies from Korea, two studies from Taiwan, three studies from Israel, and two studies from Sweden all refer to the same respective databases from those countries (Tables 2A, 2C). As expected, the systematic reviews and the meta-analyses used these same databases, too. To give an example, the six such studies cited here (Table 1) in five cases include patients from Hall et al. (39–41), in four cases include those of Rubino et al. (14), and in three cases each were the samples of Adjadj et al. (43), Berthe et al. (44), and Brown et al. (3).

Generally, the risk for breast cancer in DTC patients independent of therapy may be overestimated since the samples in 36 studies on the general risk of breast cancer in DTC patients included a large proportion of patients who were treated with RAI. Therefore, the studies' estimates of breast cancer risk in "all DTC survivors" might be conservatively high—because any increased risk due to RAI would materially elevate risk in the overall group.

Detection bias is possibly the most relevant limitation for most of the studies published since patients with a cancer diagnosis tend to participate more strictly in cancer screening programs, e.g., for breast cancer. Detection bias, by the way, may be the cause for the surprisingly high rate, 14.7%, of SPM other than breast cancer before the diagnosis of DTC in the Würzburg registry. Another limitation of the literature is that the published studies often did not differentiate between synchronous and metachronous SPMs; indeed that is one reason why more than 30 papers were excluded from this literature review.

In addition, when comparing DTC patients after RAI with DTC controls without a history of that treatment, selection may have introduced a relevant bias. That is because the indication for RAI depends on tumor stage, and RAI usually is not performed in patients with the frequently favorable stage pT1N0M0 (50). Conversely, patients treated with RAI tend to suffer from more advanced DTC, and this propensity for more aggressive malignancy may also be reflected in a predisposition for SPM such as breast cancer.

Only one case-control study (28) investigated the risk of breast carcinoma *in situ* vs. invasive breast cancer in DTC patients, separately describing such an increased risk for carcinoma *in situ* only (Table 2A).

Latency times between radiation exposure and manifestation of solid cancers tend to require a minimum of 4–5 years, with the consequence that SPM presenting earlier probably is not radiation-induced. In some studies that we evaluated, the patients were excluded if the SPM appeared within a month, several months, or even longer periods of up to 2 years after the diagnosis of DTC—which may be still too short an exclusion threshold.

On the other hand, maximum latency times for radiation-induced SPM may reach up to 30–40 years after treatment. The studies analyzed here had mostly relatively short mean observation times of <10 years ($n = 12$ studies; median, 7 years) and less often long follow-up times of 10–20 years (n

= 7 studies, median 12 years). According to the American Thyroid Association's "Management Guidelines for Children with Thyroid Nodules and Differentiated Thyroid Cancer," the minimum follow-up time for studies on outcomes and long-term side effects of DTC therapy in children and adolescents should be at least 10 years (50).

A severe drawback in the context of potentially RAI-induced breast cancer in DTC patients is that data about the therapeutic activity of I-131 (in mCi or GBq) are mostly not reported. Moreover, this activity is merely a surrogate for the radiation dose to breast tissue (in Gy), which only can be determined by individual measurements of uptake and effective half-time of I-131 in the body and the breast specifically. Regarding radiation exposure in general, a history of frequent diagnostic radiological examinations or accidental irradiation (e.g., in the case of Chernobyl) may play an important role, confounding the interpretation of the impact of RAI.

Nielsen et al. (13) discussed possible confounders influencing breast cancer risk after DTC, including genetic susceptibility, obesity, and hormones (estrogen and thyroid-stimulating hormone). Different histological subtypes of DTC should be studied separately, given findings thus far regarding genetic tumor profiles. Up to now, some studies have been published about obesity as common risk factor for DTC and breast cancer [e.g., (51)]. As to the role of estrogens and thyroid-stimulating hormone as common risk factors for DTC and breast cancer, a number of *in vitro* and animal studies have been published, but only a few studies in humans (52–54). In any case, levothyroxine therapy, aiming at thyroid-stimulating hormone suppression in patients with advanced DTC, is suspected to increase breast cancer risk independent of DTC (55). In addition, endocrine disruptors like nitrate may play a role in the pathogenesis of DTC and breast cancer (56, 57).

While six of nine cohort and case–control studies published from 1984 to 2000 did not show an increased risk for breast cancer after DTC, 15 of 17 studies published in 2000 and later demonstrated such an increased risk. It may be speculated that, in the later period, which is characterized by a sharp increase in DTC incidence worldwide, some common risk factors such as endocrine disruptors may have affected the incidence of breast cancer as well as DTC.

Finally, with respect to the scope of this review, to obtain an estimate of the risk of breast cancer as an SPM after RAI of DTC with a focus on young females, it is difficult to draw proper conclusions. That is because only two studies referenced here concentrated on those given such therapy as children or adolescents (3, 25). These studies described an increasing risk with age after adolescence for different types of SPM after RAI for DTC; however, these tumor entities did not include breast cancer.

Since the data are not sufficient to draw any conclusions about age dependence of breast cancer risk after RAI of DTC, it seems to be reasonable and necessary to evaluate whether relevant data in large-enough samples of young DTC patients can be collected in a systematic international multicenter survey which should be carried out as a case–control study applying multivariate statistical methods.

International Multi-Registry Survey

Our registry study was performed with the goal of assessing the potential sample size for a larger and more detailed study, allowing firmly evidence-based conclusions to be drawn on the real risk of breast cancer before and after treatment of DTC with RAI in young females. One important finding of our survey was that usually registries covering the whole age spectrum of patients with DTC contain only very low percentages of those <18 years old, ranging between 2 and 7% (the situation in Münster, Würzburg, and Gliwice registries in our survey). Since dedicated registries of children and adolescents with DTC are rare and tend to contain only low numbers of cases, it might not be possible to restrict the limit of "young age" at the time of RAI to 18 years. To ensure the recruitment of a sample size enabling sufficient statistical power, the age limit at the time of RAI probably should be increased to 40 years, which would cover about 35% of patients with DTC.

Based on the maximum breast cancer rates in our registry survey (see Section Cumulative I-131 Activity) and on published data (5), it is assumed that—independent of treatment—about 2% of female DTC survivors develop breast cancer. As noted earlier, RAI for DTC with cumulative activities of 10–15 GBq I-131 corresponds to radiation doses to the female breast of between 2 and 3 Gy, which may double/triple the lifetime risk for breast cancer (8). We estimated that sample sizes of at least 4,340 cases below age 40 years at the time of RAI and 660 controls will be necessary under the assumption of an HR of 2.76 to reject the zero hypothesis of no effect of RAI, with a power of 80% (58).

Taking into account that about 3,200 of the patients in this registry study already met the age <40 years criterion, it seems to be feasible to recruit 30% more cases by including additional patients from other DTC specialist centers in Germany and abroad. Regarding the controls not receiving RAI, this survey already identified 650 of the 660 necessary patients for a subsequent study.

CONCLUSIONS

To summarize today's state of knowledge, independent of DTC treatment, there appears to be a bi-directional association of DTC itself and breast cancer. Nonetheless, the risk of breast cancer in adult DTC survivors is low, about 2%, slightly higher in females than in males, but based on the literature, presumably lower in children and adolescents than in older age groups. RAI is assumed not to substantially influence the lifetime risk of breast cancer after DTC, but data from those given such treatment as children or adolescents are sparse.

The literature review and multicenter registry survey reported here lead to the following recommendation: an international multicenter study with a sufficiently high number of female DTC survivors is feasible; that study should have a case–control design and include female patients <40 years of age with DTC diagnosed 20–30 years earlier. For reasons of compliance and practicability, such a design should be preferred over a longitudinal study lasting several decades.

However, especially given the likely at most slightly increased risk for breast cancer after RAI, breast cancer screening of a large cohort of female DTC survivors who received breast doses between 0.2 and 2 Gy from cumulative RAI activities of 1–15 GBq I-131 (7) is not unproblematic for ethical reasons. These reasons are related to an expected high rate of false-positive findings of ultrasonographic screening for breast cancer—in the range of 10%—and a resultant uncertain frequency of “misdiagnosis.” On similar grounds, the International Late Effects of Childhood Cancer Guideline Harmonization Group does not recommend routine breast cancer surveillance in female childhood, adolescent, or young adult cancer survivors treated with chest radiation doses <10 Gy (59). Such concerns apply in an even more pronounced way to the control cohort not affected by RAI-related radiation exposure as a potential risk-increasing factor. Hence, RAI patients and controls should be especially actively involved in choices regarding breast cancer screening, in a “shared decision-making” approach, and particular attention should be paid to the education of potential study participants regarding this possible issue (60).

AUTHOR CONTRIBUTIONS

CR contributed to concept development, study management, critical review of the literature, and editing of the final manuscript. RS contributed to study management, literature search, critical review of the literature, and language editing. TP contributed to the management and the analysis of thyroid cancer database in Minsk. MF contributed to the histology review

of thyroid cancer database in Minsk. UMä contributed to the supply of registry data from Würzburg. UMa contributed to the statistical analysis and writing the statistics section of the manuscript. AV contributed to the supply of registry data from Münster. TB contributed to the supply of registry data from Kiev. JK contributed to the supply of registry data from Gliwice. RE contributed to the supply of registry data from Pisa. FV contributed to the supply of registry data from Rio de Janeiro. JM contributed to the supply of registry data from Sremska Kamenica. GC contributed to the supply of registry data from Coimbra. VD contributed to the study management, literature search, critical review of the literature, supply of feasibility study data from Minsk, and drafting of the manuscript. All authors contributed to the critical review. All authors contributed to the article and approved the submitted version.

FUNDING

This project was funded by the German Federal Office for Radiation Protection (File Number 35615S424). The funder played no role in determining the content of the manuscript or in the decision regarding whether to submit the manuscript for publication.

ACKNOWLEDGMENTS

An English language medical editor, Robert J. Marlowe, Spencer-Fontayne Corporation, Jersey City, NJ, USA, assisted in the revision of the original version of this paper.

REFERENCES

- Reiners C, Biko J, Haenscheid H, Hebestreit H, Kirinjuk S, Baranowski O, et al. Twenty-five years after Chernobyl: outcome of radioiodine treatment in children and adolescents with very-high risk radiation induced differentiated thyroid carcinoma. *J Clin Endocrinol Metab.* (2013) 98:3039–48. doi: 10.1210/jc.2013-1059
- Clement SC, Peeters RP, Ronckers CM, Links TP, van den Heuvel-Eibrink MM, Nieveen van Dijkum EJ, et al. Intermediate and long-term adverse effects of radioiodine therapy for differentiated thyroid carcinoma – A systematic review. *Cancer Treat Rev.* (2015) 41:925–34. doi: 10.1016/j.ctrv.2015.09.001
- Brown AP, Chen J, Hitchcock YJ, Szabo A, Shrieve DC, Tward JD. The risk of second primary malignancies up to three decades after the treatment of differentiated thyroid cancer. *J Clin Endocrinol Metab.* (2008) 93:504–15. doi: 10.1210/jc.2007-1154
- Kumagai A, Reiners C, Drozd V, Yamashita S. Childhood thyroid cancers and radioactive iodine therapy: necessity of precautionary radiation health risk management. *Endocr J.* (2007) 54:839–47. doi: 10.1507/endocrj.K07E-012
- Yu CY, Saeed O, Goldberg AS, Farooq S, Fazelzad R, Goldstein DP, et al. A systematic review and meta-analysis of subsequent malignant neoplasm risk after radioactive iodine treatment of thyroid cancer. *Thyroid.* (2018) 28:1662–73. doi: 10.1089/thy.2018.0244
- Poole VL, McCabe CJ. Iodide transport and breast cancer. *J Endocrinol.* (2015) 227:R1–12. doi: 10.1530/JOE-15-0234
- Travis CC, Stabin MG. 131I ablation treatment in young females after the Chernobyl accident. *J Nucl.* (2006) 47:1723–7.
- United States National Cancer Institute. RadRat Tool (2020). Available online at: <https://radiationcalculators.cancer.gov/radrat/> (accessed April 19, 2020).
- Subramanian S, Goldstein DP, Parlea L, Thabane L, Ezzat S, Ibrahim-Zada I, et al. Second primary malignancy risk in thyroid cancer survivors: a systematic review and meta-analysis. *Thyroid.* (2007) 17:1277–88. doi: 10.1089/thy.2007.0171
- Sawka AM, Thabane L, Parlea L, Ibrahim-Zada I, Tsang RW, Brierley JD, et al. Second primary malignancy risk after radioactive iodine treatment for thyroid cancer: a systematic review and meta-analysis. *Thyroid.* (2009) 19:451–7. doi: 10.1089/thy.2008.0392
- Joseph K, Ediramanne S, Eslick G. The association between breast cancer and thyroid cancer: a meta-analysis. *Breast Canc Res Treat.* (2015) 152:173–81. doi: 10.1007/s10549-015-3456-6
- Zhang Y, Liang J, Li H, Cong H, Lin Y. Risk of second primary breast cancer after radioactive iodine treatment in thyroid cancer: a systematic review and meta-analysis. *Nucl Med Commun.* (2016) 37:110–5. doi: 10.1097/MNM.0000000000000419
- Nielsen SM, White MG, Hung S, Aschebrook-Kilfoy B, Kaplan EL, Angelos P, et al. The breast-thyroid cancer link: a systematic review and meta-analysis. *Cancer Epidemiol Biomark.* (2016) 25:231–8. doi: 10.1158/1055-9965.EPI-15-0833
- Rubino C, de Vathaire F, Dottorini ME, Hall P, Schwartz C, Couette JE, et al. Second primary malignancies in thyroid cancer patients. *Br J Cancer.* (2003) 89:1638–44. doi: 10.1038/sj.bjc.6601319
- Sandeep TC, Strachan MW, Reynolds RM, Brewster DH, Scél G, Pukkala E, et al. Second primary cancers in thyroid cancer patients: a multinational record linkage study. *J Clin Endocrinol Metab.* (2006) 91:1819–25. doi: 10.1210/jc.2005-2009
- Vassilopoulou-Sellin R, Palmer L, Taylor S, Cooksley CS. Incidence of breast carcinoma in women with thyroid carcinoma. *Cancer.* (1999) 85:696–705.

- doi: 10.1002/(SICI)1097-0142(19990201)85:3<696::AID-CNCR20>3.0.CO;2-4
17. Chen AY, Levy L, Goepfert H, Brown BW, Spitz MR, Vassilopoulou-Sellin R. The development of breast cancer in women with thyroid cancer. *Cancer*. (2001) 92:225–31. doi: 10.1002/1097-0142(20010715)92:2<225::AID-CNCR1313>3.0.CO;2-B
 18. Ronckers CM, McCarron P, Ron E. Thyroid cancer and multiple primary tumors in the SEER cancer registries. *Int J Cancer*. (2005) 117:281–8. doi: 10.1002/ijc.21064
 19. Bhattacharyya N, Chien W. Risk of second primary malignancy after radioactive iodine treatment for differentiated thyroid carcinoma. *Ann Otol Rhinol Laryngol*. (2006) 15:607–10. doi: 10.1177/000348940611500806
 20. Chuang S-C, Hashibe M, Yu G-P, Le AD, Cao W, Hurwitz EL, et al. Radiotherapy for primary thyroid cancer as a risk factor for second primary cancers. *Cancer Lett*. (2006) 238:42–52. doi: 10.1016/j.canlet.2005.06.015
 21. Kim C, Bi X, Pan D, Chen Y, Carling T, Ma S, et al. The risk of second cancers after diagnosis of primary cancer is elevated in thyroid microcarcinomas. *Thyroid*. (2013) 23:575–82. doi: 10.1089/thy.2011.0406
 22. Kuo JH, Chabot JA, Lee JA. Breast cancer in thyroid cancer survivors: an analysis of the surveillance, epidemiology, and end results-9 database. *Surgery*. (2016) 159:23–30. doi: 10.1016/j.surg.2015.10.009
 23. Uprety D, Khanal A, Arjyal L, Bista A, Basnet B, Kandel P, et al. The risk of secondary primary malignancy in early stage differentiated thyroid cancer: a US population-based study. *Acta Oncol*. (2016) 55:1375–7. doi: 10.1080/0284186X.2016.1196829
 24. Endo M, Liu JR, Dougan M, Lee JS. Incidence of second malignancies in patients with papillary thyroid cancer from surveillance, epidemiology, and end results 13 datasets. *J Thyroid Res*. (2018) 2018:8765369. doi: 10.1155/2018/8765369
 25. Adly MH, Soby M, Rezak MR, Ishak M, Afifi MA, Shafie AE, et al. Risk of second malignancies among survivors of pediatric thyroid cancer. *Int J Clin Oncol*. (2018) 23:625–33. doi: 10.1007/s10147-018-1256-9
 26. Ron E, Curtis R, Hoffman DA, Flannery JT. Multiple primary breast and thyroid cancer. *Br J Cancer*. (1984) 49:87–92. doi: 10.1038/bjc.1984.13
 27. Simon MS, Tang M-T, Bernstein L, Norman SA, Weiss L, Burkman TM, et al. Do thyroid disorders increase the risk of breast cancer? *Cancer Epidemiol Biomark*. (2002) 11:1574–8.
 28. Canchola AJ, Horn-Ross PL, Purdie DM. Risk of second primary malignancies in women with papillary thyroid cancer. *Am J Epidemiol*. (2006) 163:521–7. doi: 10.1093/aje/kwj072
 29. Cho YY, Lim J, Oh C-M, Ryu J, Jung K-W, Chung J-H, et al. Elevated risks of subsequent primary malignancies in patients with thyroid cancer: a nationwide, population-based study in Korea. *Cancer*. (2015) 121:259–68. doi: 10.1002/cncr.29025
 30. Ahn HY, Min HS, Yeo Y, Ma SH, Hwang Y, An JH, et al. Radioactive iodine therapy did not significantly increase the incidence and recurrence of subsequent breast cancer. *J Clin Endocrinol Metab*. (2015) 100:3486–93. doi: 10.1210/JC.2014-2896
 31. Khang AR, Cho SW, Choi HS, Ahn HY, Yoo WS, Kim KW, et al. The risk of second primary malignancy is increased in differentiated thyroid cancer patients with a cumulative (131)I dose over 37 GBq. *Clin Endocrinol*. (2015) 83:117–23. doi: 10.1111/cen.12581
 32. Lu C-H, Lee K-D, Chen P-T, Chen C-C, Kuan F-C, Huang C-E, et al. Second primary malignancies following thyroid cancer: a population-based study in Taiwan. *Eur J Endocrinol*. (2013) 169:577–85. doi: 10.1530/EJE-13-0309
 33. Teng CJ, Hu YW, Chen SC, Yeh CM, Chiang HL, Chen TJ, et al. Use of radioactive iodine for thyroid cancer and risk of second primary malignancy: a nationwide population-based study. *J Nat Cancer Inst*. (2016) 08:1–8. doi: 10.1093/jnci/djv314
 34. Lin CY, Lin CL, Huang WS, Kao CH. Risk of breast cancer in patients with thyroid cancer receiving or not receiving I-131 treatment: a nationwide population-based cohort study. *J Nucl Med*. (2016) 57:685–90. doi: 10.2967/jnumed.115.164830
 35. Sadetzki S, Calderon-Margalit R, Peretz C, Novikov I, Barchan M, Papa MZ. Second primary breast and thyroid cancers (Israel). *Cancer Causes Control*. (2003) 14:367–75. doi: 10.1023/A:1023908509928
 36. Hirsch D, Shohat T, Gorsheim A, Robenshtok E, Shimon I, Benbassat C. Incidence of non- thyroidal primary malignancy and the association with I-131 treatment in patients with differentiated thyroid cancer. *Thyroid*. (2016) 26:1110–6. doi: 10.1089/thy.2016.0037
 37. Izhakov E, Barchana M, Lipshitz I, Silverman BG, Stern N, Keinan-Boker L. Trends of second primary malignancy in patients with thyroid cancer: a population based cohort study in Israel. *Thyroid*. (2017) 27:793. doi: 10.1089/thy.2016.0481
 38. Osterlind A, Olsen JH, Lynge E, Ewertz M. Second cancer following cutaneous melanoma and cancers of the brain, thyroid, connective tissue, bone and eye in Denmark, 1943–1989. *Nat Cancer Inst Monogr*. (1985) 68:361–88.
 39. Hall P, Holm LE, Lundell G. Second primary tumors following thyroid cancer. A Swedish record linkage study. *Acta Oncol*. (1990) 29:869–73. doi: 10.3109/02841869009096381
 40. Hall P, Holm LE, Lundell G, Bjelkengren G, Larsson LG, Lindberg S, et al. Cancer risks in thyroid cancer patients. *Brit J Cancer*. (1991) 64:159–63. doi: 10.1038/bjc.1991.261
 41. Hall P, Holm L-E, Undell G, Ruden B-I. Tumors after radiotherapy for thyroid cancer. A case-control study within a cohort of thyroid cancer patients. *Acta Oncologica*. (1992) 31:403–7. doi: 10.3109/02841869209088279
 42. Akslen LA, Glatte E. Second malignancies in thyroid cancer patients: a population-based survey of 3658 cases from Norway. *Eur J Cancer*. (1992) 28:91–195. doi: 10.1016/S0959-8049(05)80085-1
 43. Adjadj E, Rubino C, Shamsaldin A, Le MG, Schlumberger M, de Vathaire F. The risk of multiple primary breast and thyroid carcinomas - role of the radiation dose. *Cancer*. (2003) 98:1309–17. doi: 10.1002/cncr.11626
 44. Berthe E, Henry-Amar M, Michels JJ, Rame JB, Berthet P, Babin E, et al. Risk of second primary cancer following differentiated thyroid cancer. *Eur J Nucl Med Mol Imaging*. (2004) 31:685–91. doi: 10.1007/s00259-003-1448-y
 45. Edhemovic I, Volk N, Auersperg M. Second primary cancers following thyroid cancer in Slovenia. A population-based cohort study. *Eur J Cancer*. (1998) 3:1813–4.
 46. An JH, Hwangbo Y, Ahn HY, Keam B, Lee KE, Han W, et al. A possible association between thyroid cancer and breast cancer. *Thyroid*. (2015) 35:1330–8. doi: 10.1089/thy.2014.0561
 47. Fridman M, Drozd V, Demidchik YL, Levin L, Branovan D. Second primary malignancy in Belarus patients with post-Chernobyl papillary thyroid carcinoma. *Thyroid*. (2015) 25(Suppl. 1):A22–3.
 48. Van Fossen VL, Wilhelm SM, Eaton JL, McHenry CR. Association of thyroid, breast and renal cell cancer: a population-based study of the prevalence of second malignancies. *Ann Surg Oncol*. (2013) 20:1341–7. doi: 10.1245/s10434-012-2718-3
 49. Anders CK, Johnson R, Litton J, Phillips M, Bleyer A. Breast cancer before age 40 years. *Semin Oncol*. (2009) 36:237–49. doi: 10.1053/j.seminoncol.2009.03.001
 50. Francis GL, Waguespack SG, Bauer AJ, Angelos P, Benvenega S, Cerutti JM, et al. Management guidelines for children with thyroid nodules and differentiated thyroid cancer. *Pediatrics*. (2018) 142:716–59. doi: 10.1089/thy.2014.0460
 51. Xu L, Port M, Landi S, Gemignani F, Cipollini M, Elisei R, et al. Obesity and the risk of papillary thyroid cancer: a pooled analysis of three case-control studies. *Thyroid*. (2014) 24:966–74. doi: 10.1089/thy.2013.0566
 52. Henderson BE, Ross R, Bernstein L. Estrogens as a cause of human cancer: the Richard and Hinda Rosenthal Foundation award lecture. *Cancer Res*. (1988) 48:246–53.
 53. Fang Y, Yao L, Sun J, Yang R, Chen Y, Tian J, et al. Does thyroid dysfunction increase the risk of breast cancer? A systematic review and meta-analysis. *J Endocrinol Invest*. (2017) 40:1035–47. doi: 10.1007/s40618-017-0679-x
 54. Weng C-H, Okawa ER, Roberts MB, Park SK, Umbricht CB, Manson JAE, et al. Breast cancer risk in postmenopausal women with medical history of thyroid disorder in the women's health initiative. *Thyroid*. (2020) 30:519–30. doi: 10.1089/thy.2019.0426
 55. Hercbergs A, Mousa SA, Leinung M, Lin HY, Davis P. Thyroid hormone in the clinic and breast cancer. *Horm Cancer*. (2018) 9:139–43. doi: 10.1007/s12672-018-0326-9
 56. Veselik DJ, Divekar S, Dakshanamurthy S, Storch GB, Turner JM, Graham KL, et al. Activation of estrogen receptor-alpha by the anion

- nitrite. *Cancer Res.* (2008) 68:3950–8. doi: 10.1158/0008-5472.CAN-07-2783
57. Drozd VM, Branovan I, Shiglik N, Biko J, Reiners C. Thyroid cancer induction: nitrates as independent risk factors or risk modulators after radiation exposure, with a focus on the Chernobyl accident. *Eur Thyroid J.* (2018) 7:67–74. doi: 10.1159/000485971
 58. Reiners C, Schneider R, Drozd V, Dedovich T, Leonova T, Mitjukova T, et al. *Brustkrebsrisiko nach Radiojodtherapie des Schilddrüsenkarzinoms. Bundesamt für Strahlenschutz Forschungsvorhaben.* (2018). Available online at: <http://doris.bfs.de/jspui/handle/urn:nbn:de:0221-2019013117429> (accessed April 19, 2020).
 59. Mulder RL, Kremer LCM, Hudson MM, Bhatia S, Landier W. Recommendations for breast cancer surveillance for female childhood, adolescent and young adult cancer survivors treated with chest radiation: a report from the International Late Effects of Childhood Cancer Guideline Harmonization Group. *Lancet Oncol.* (2013) 14:e621–9. doi: 10.1016/S1470-2045(13)70303-6
 60. Elwyn G, Cochran N, Pignogne M. Shared decision making—the importance of diagnosing preferences. *JAMA Intern Med.* (2017) 177:1239–40. doi: 10.1001/jamainternmed.2017.1923

Conflict of Interest: The authors declare that the research was conducted in the absence of any commercial or financial relationships that could be construed as a potential conflict of interest.

Copyright © 2020 Reiners, Schneider, Platonova, Fridman, Malzahn, Mäder, Vrachimis, Bogdanova, Krajewska, Elisei, Vaisman, Mihailovic, Costa and Drozd. This is an open-access article distributed under the terms of the Creative Commons Attribution License (CC BY). The use, distribution or reproduction in other forums is permitted, provided the original author(s) and the copyright owner(s) are credited and that the original publication in this journal is cited, in accordance with accepted academic practice. No use, distribution or reproduction is permitted which does not comply with these terms.



Contrast-Enhanced Ultrasound of Primary Squamous Cell Carcinoma of the Thyroid: A Case Report

Sijie Chen^{1,2}, Qinghai Peng^{1,2}, Qi Zhang^{1,2} and Chengcheng Niu^{1,2*}

¹ Department of Ultrasound Diagnosis, The Second Xiangya Hospital, Central South University, Changsha, China, ² Research Center of Ultrasonography, The Second Xiangya Hospital, Central South University, Changsha, China

OPEN ACCESS

Edited by:

Christoph Reinert,
University Hospital
Würzburg, Germany

Reviewed by:

Pasqualino Malandrino,
University of Catania, Italy
Daniela Pasquali,
University of Campania Luigi
Vanvitelli, Italy

*Correspondence:

Chengcheng Niu
niuchengcheng@csu.edu.cn

Specialty section:

This article was submitted to
Cancer Endocrinology,
a section of the journal
Frontiers in Endocrinology

Received: 21 February 2020

Accepted: 25 June 2020

Published: 11 August 2020

Citation:

Chen S, Peng Q, Zhang Q and Niu C
(2020) Contrast-Enhanced Ultrasound
of Primary Squamous Cell Carcinoma
of the Thyroid: A Case Report.
Front. Endocrinol. 11:512.
doi: 10.3389/fendo.2020.00512

Introduction: Primary squamous cell carcinoma of the thyroid (ThyPSCC) is an extremely rare aggressive malignancy with a poor prognosis. However, almost no report thus far has investigated the microvasculature of ThyPSCC imaged using contrast-enhanced ultrasound.

Case Report: A 59-year-old male patient presented to our hospital with progressively worsening hoarse voice symptoms for 20 days and was diagnosed with left unilateral vocal fold palsy. Ultrasonography revealed a solitary marked hypoechoic thyroid nodule with an unclear boundary in the inferior part of the left lobe. Color Doppler flow imaging showed a poor blood flow signal inside this nodule. Contrast-enhanced ultrasound images showed a persistent low peak enhancement of the nodule from its periphery to its center. The time-intensity curve displayed a wash-in time of 10 s, a time to peak of 37 s, a peak signal intensity of 24.5%, and a wash-out time of 70 s for the thyroid tumor. Finally, left hemithyroidectomy of the thyroid tumor was performed, and histopathologic and immunohistochemical evaluations confirmed the diagnosis of ThyPSCC. Postoperatively, the patient received a combination therapy of chemotherapy, radiotherapy, and targeted therapy, but the patient died 4 months after surgery.

Conclusion: Primary squamous cell carcinoma of the thyroid is a rare but aggressive malignancy of the thyroid. Herein, we reported a case of ThyPSCC and its ultrasonography and pathologic findings.

Keywords: thyroid cancer, thyroid nodules (TNs), thyroid ultrasound (US), primary squamous cell carcinoma, contrast enhanced ultrasound (CEUS)

INTRODUCTION

Primary squamous cell carcinoma of the thyroid (ThyPSCC) is a rare thyroid malignancy with high aggressiveness and poor prognosis, comprising ~0.1–1% of all primary thyroid carcinomas (1–6). Owing to the rapidly progressing and highly invasive nature of the malignancy, patients with ThyPSCC often present at an advanced stage and are difficult to diagnose in the early stage because of its rare incidence and lack of typical imaging findings (7, 8).

Thyroid ultrasonography and fine-needle aspiration biopsy (FNAB) are the diagnostic tools of choice for evaluating patients with suspected thyroid nodules (9). Contrast-enhanced ultrasound (CEUS), as a relatively novel US technique, is used to investigate the microvasculature of thyroid nodules and improve the diagnostic accuracy of thyroid nodules accompanied by the use of Thyroid

Imaging Reporting and Data Systems for ultrasonographic features (10–13). However, very few published studies have reported the use of ultrasonography for ThyPSCC. To our knowledge, this is the first case describing the CEUS findings of ThyPSCC.

CASE REPORT

A 59-year-old male patient presented to our hospital with progressively worsening hoarse voice symptoms for 20 days and was diagnosed with left unilateral vocal fold palsy. A high-resolution ultrasound instrument (Siemens Acuson S3000, Mountain View, CA, USA) equipped with a 4- to 9-MHz linear probe was used. Thyroid ultrasonography revealed a solitary $3.1 \times 2.8 \times 2.6\text{-cm}^3$ marked hypoechoic thyroid nodule with an unclear boundary in the inferior part of the left lobe (**Figure 1A**). This nodule exhibited many malignant ultrasound features, such as solid components, hypoechogenicity, and microlobulated margins. Color Doppler flow imaging (CDFI) showed poor blood flow signals in the nodule (**Figure 1B**). Contrast-enhanced ultrasound was performed with a bolus intravenous injection of 3.0 mL of SonoVue (Bracco, Milan, Italy) followed by 5 mL of saline. Contrast pulse sequencing technology was used, and the time-intensity curves (TICs) of the nodule were calculated. The nodule began to be slowly enhanced from the periphery to the center at 10 s (wash-in time), and the enhancement

reached its peak [time to peak (TTP)] at 37 s with a peak intensity of 24.5%. Then, the nodule slowly declined until all the microbubbles washed out at 70 s (**Figures 1C,D**). Based on its malignant conventional ultrasound features and the poor microvasculature revealed by CEUS, we inferred that the nodule was a malignant tumor.

After neck ultrasonography, the positron emission tomography-computed tomography was carried for evaluating the situation of distant metastases. Positron emission tomography-computed tomography showed a mass with increased glucose metabolism in the inferior part of the left thyroid lobe (**Figure 2A**), which indicated it as a malignant mass, whereas there was no evidence of lymph nodes metastasis and distant metastases. Then, ultrasonography-guided FNAB was performed for the left thyroid mass immediately. Cytologic examination by fine-needle aspiration (FNA) revealed sheets of tumor cells with giant deep-stained nuclei (Bethesda category V) (**Figure 2B**). Finally, a left hemithyroidectomy of the thyroid tumor was undertaken. The lower edge of the tumor reached the upper mediastinum, and the depth of the tumor invaded the esophagus and trachea, which could not be completely removed. According to the eighth edition of the American Joint Committee on Cancer/Tumor Lymph Node Metastasis (TNM) staging system (14), the patient was in TNM stage III (T4a N0 M0). Histopathological examination of hematoxylin and eosin staining showed that a carcinoma in the inferior

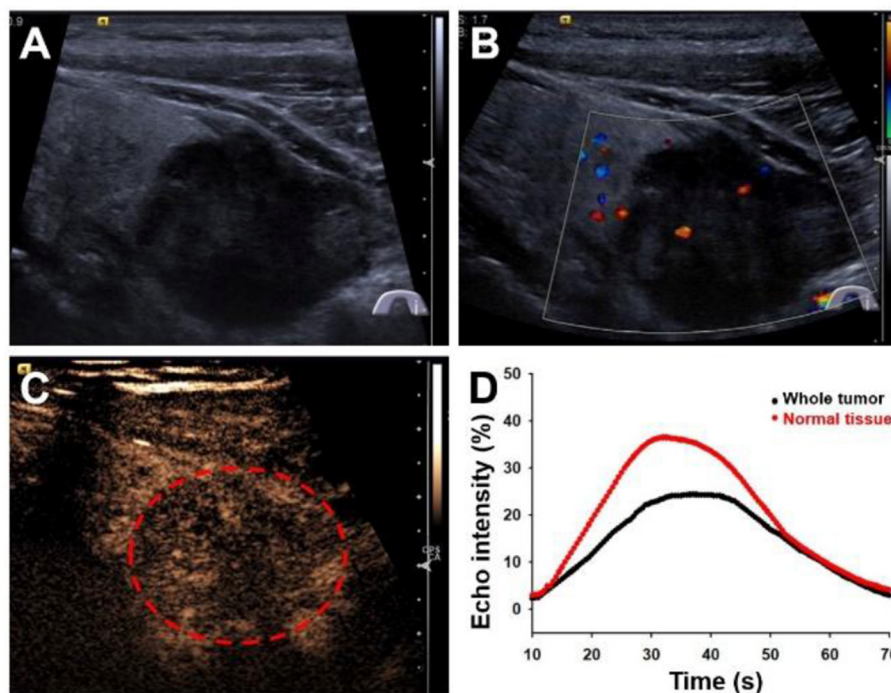


FIGURE 1 | Ultrasonography images of primary squamous cell carcinoma of the thyroid. **(A)** Longitudinal gray-scale sonography revealed a solid marked hypoechoic thyroid nodule in the inferior part of the left lobe. **(B)** Color Doppler flow imaging showed a poor blood flow signal inside this nodule. **(C)** Contrast-enhanced ultrasound image showed a persistent low peak enhancement of the nodule at 37 s. **(D)** Time-intensity curves displayed the wash-in time of 10 s, TTP of 37 s, peak signal intensity of 24.5%, and wash-out time of 70 s for the thyroid tumor.

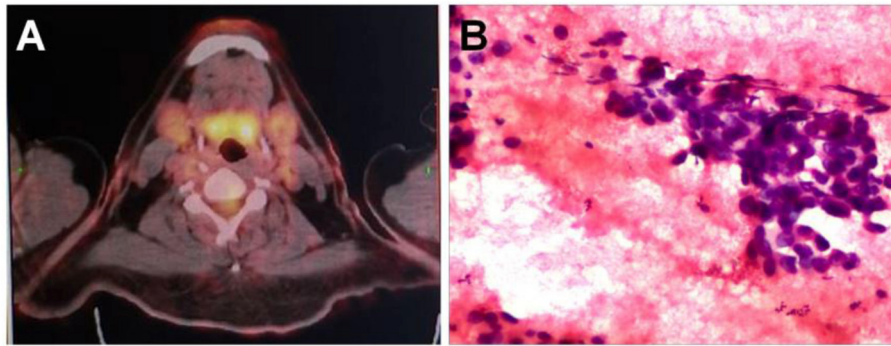


FIGURE 2 | (A) A positron emission tomography–computed tomography scan showed increased ^{18}F -fluorodeoxyglucose metabolism in the left neck mass. **(B)** Preoperative fine-needle aspiration cytology of the mass demonstrated a few sheets of malignant-looking tumor cells with giant deep stained nuclei (hematoxylin and eosin, magnification $\times 400$).

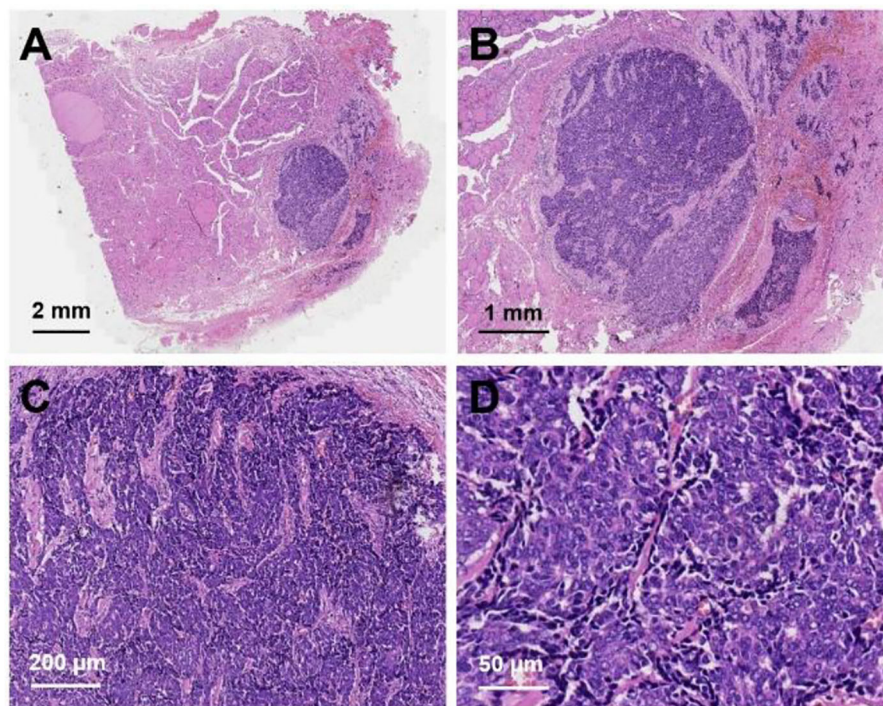


FIGURE 3 | Hematoxylin and eosin staining of primary squamous cell carcinoma of the thyroid: **(A)** magnification $\times 8$, **(B)** magnification $\times 20$, **(C)** magnification $\times 100$, **(D)** magnification $\times 400$.

part of the thyroid lobe (**Figure 3A**) had no obvious palisade arrangement, intercellular bridges, or keratinization with a cancer pearl (**Figures 3B–D**). Immunohistochemically, tumor cells were positive for cytokeratin 19 (CK19, **Figure 4A**), cytokeratin 5 and 6 (CK5/6, **Figure 4B**), epithelial membrane antigen (EMA, **Figure 4C**), p40 (**Figure 4D**), p63 (**Figure 5A**), and Ki-67 (30%+, **Figure 5B**) and negative for thyroglobulin (TG, **Figure 5C**) and thyroid transcription factor 1 (TTF-1, **Figure 5D**). In view of these findings, the tumor was diagnosed as poorly differentiated ThyPSCC. Postoperatively, the patient

received two cycles of chemotherapy with docetaxel/cisplatin, intensity-modulated radiotherapy, and nimotuzumab-targeted therapy. However, the patient died 4 months after surgery.

DISCUSSION

Primary squamous cell carcinoma of the thyroid is a thyroid malignancy with extremely rare incidence, and the clinical diagnosis and treatment guidelines for this disease have no consensus (4). The biological behavior of ThyPSCC is aggressive,

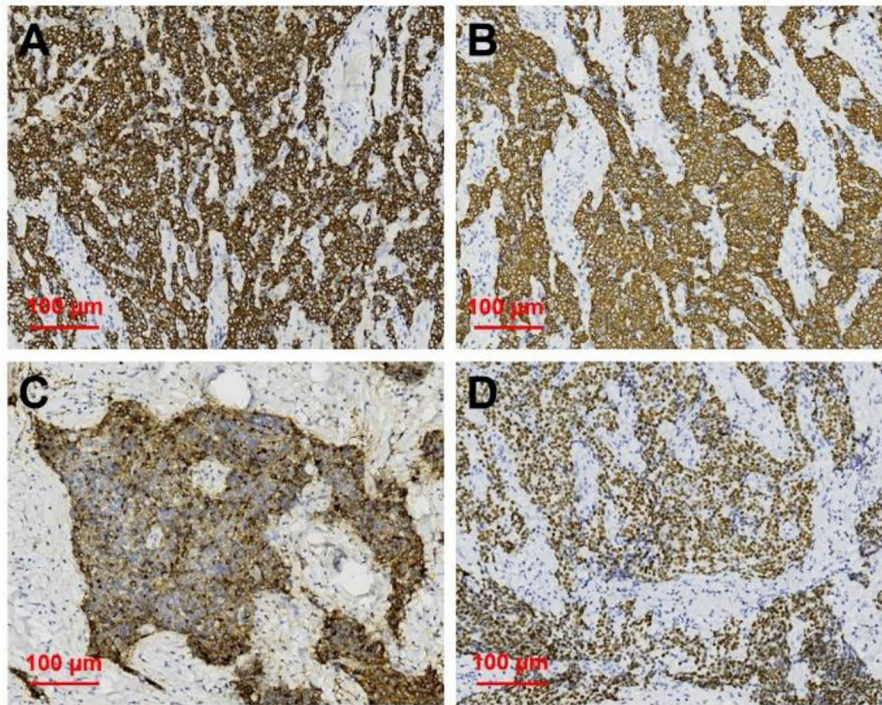


FIGURE 4 | Immunohistochemical staining of primary squamous cell carcinoma of the thyroid (magnification $\times 200$). Immunohistochemical staining for **(A)** CK19, **(B)** CK5/6, **(C)** EMA, **(D)** p40, all of which were deeply stained (positive).

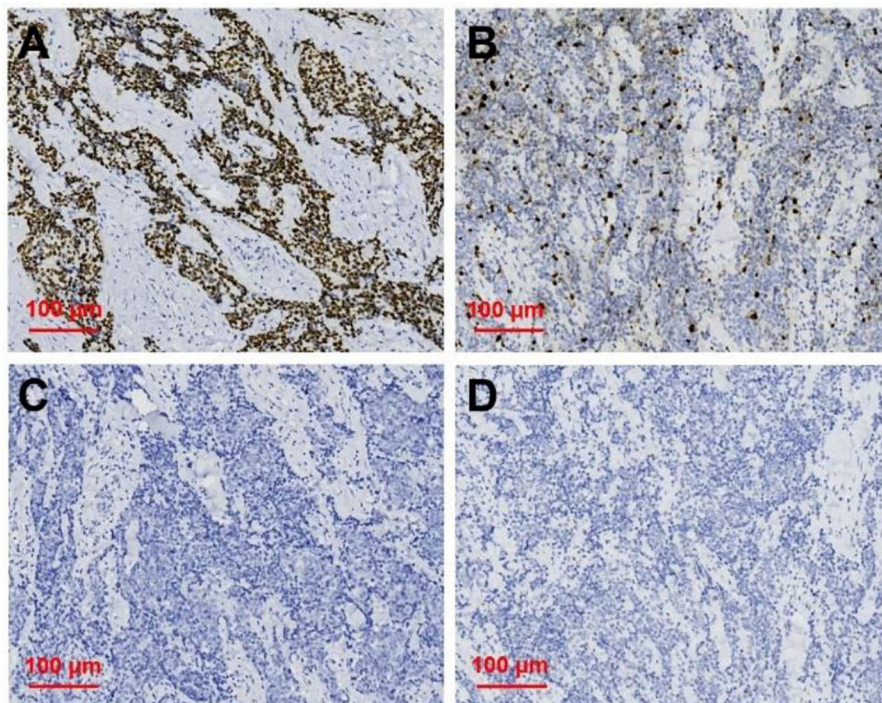


FIGURE 5 | Immunohistochemical staining of primary squamous cell carcinoma of the thyroid (magnification $\times 200$). Immunohistochemical staining for **(A)** p63, **(B)** Ki67, **(C)** TG, **(D)** TTF-1, and p63 was deeply stain (positive); Ki67 proliferation index was 30%; TG and TTF-1 did not stain (negative).

and the prognosis is poor, with a median overall survival of 4–24 months, which depends on the different tumor grades (1). Yang et al. using the Surveillance, Epidemiology, and End Results Program database, reported that poorly differentiated tumor grade occupied the highest percentages of all graded tumors, and the median survival was 4 months, which is similar to the survival time in our case (1).

High-frequency ultrasound, as the basic imaging modality in the diagnosis of thyroid nodules, has found gradually increasing differentiated thyroid cancers over recent years (15, 16). The ultrasonography imaging findings of ThyPSCC have seldom been published. Regarding the ultrasonography findings, Chen et al. (17) reported that ThyPSCC presented as a thyroid mass with eggshell calcification, peripheral soft tissue with a blurred margin, and minimal vascular signals on CDFI sonography. In the case of Jang et al. (7), ThyPSCC presented as a large, well-defined, lobulated, heterogeneously hypoechoic mass with diffuse microcalcifications on ultrasonography. Kondo et al. (18) reported that a well-differentiated ThyPSCC showed a cystic hypoechoic mass with a smooth margin and rapidly grew with margin change blurring in 1 year. In our case, this poorly differentiated ThyPSCC presented as a solitary marked hypoechoic thyroid mass with an irregular margin and unclear boundary with a normal thyroid. The irregular margin and unclear boundary with normal thyroid corresponded to tumor invasion with adjacent tissue infiltration, which is consistent with the findings during the operation that tumor invasion with the esophagus cannot be completely removed. Poor blood flow signals on CDFI sonography and persistent hypoenhancement on CEUS of the mass are consistent with squamous cell carcinoma, which has no obvious vascularity on pathologic examination.

Many studies have investigated the application of CEUS to improve the diagnostic accuracy of thyroid nodules, despite its usage in ThyPSCC being scarce. Zhang et al. (15) found that high/circular/equal enhancement indicated benign thyroid nodules, and low enhancement indicated malignant thyroid nodules. Ma et al. (19) investigated whether incomplete, no ring or heterogeneous enhancement, later wash-in time, and low peak intensity on CEUS were independent risk factors in predicting malignant thyroid nodules. Deng et al. (20) detected that papillary thyroid carcinomas (PTCs) exhibited low enhancement, a lower peak signal intensity, and a lower area under the curve (AUC) than peripheral thyroid parenchyma on CEUS (13, 20). In our study, the TICs of CEUS for ThyPSCC showed a wash-in time of 10 s, a TTP of 37 s, a peak signal intensity as low as 24.5%, and a wash-out time of 70 s. This is similar to the results of PTCs with a slow wash-in time, a lower peak signal intensity, and a lower AUC, as in previous reports (13). To our knowledge, no reports on CEUS imaging findings of ThyPSCC have appeared in the English-language literature. According to Jang et al. (7), ThyPSCC showed a large heterogeneously enhancing thyroid mass with a large central non-enhancing portion on enhanced CT, which corresponded well with the squamous cell carcinoma portion with a necrotic

portion in pathologic staining. Because of the rapid growth of squamous tumor cells, relatively few interstitial blood vessels in tumors were related to the low peak signal intensity and low AUC on CEUS.

With increasing malignancy in squamous cell carcinoma, the typical squamous cell carcinoma findings of intercellular bridges and keratinized cancer pearl can decrease or disappear. Immunohistochemical staining is useful in diagnosing primary thyroid cancer. In this case, positivity for CK5/6 and EMA and negativity for TTF-1 and TG expression predicted squamous cell carcinoma derivation and excluded the possibility of these common tumors (3, 21). Further positivity for p63 and Ki67 expression as poor prognostic markers was associated with its poorly differentiated tumor grade (7, 22).

CONCLUSION

Primary squamous cell carcinoma of the thyroid is an extremely rare tumor, and very few studies describe its ultrasonographic imaging findings. It is difficult to establish a clinical guideline for diagnosis. Our case presents the CEUS features of ThyPSCC, indicating that the TICs of ThyPSCC are similar to the enhancing parameters of PTCs with a slow wash-in time, a lower peak signal intensity, and a lower AUC.

DATA AVAILABILITY STATEMENT

The datasets generated for this study are available on request to the corresponding author.

ETHICS STATEMENT

The studies involving human participants were reviewed and approved by the Ethics Committee of Second Xiangya Hospital, Central South University, China. The patients/participants provided their written informed consent to participate in this study. Written informed consent was obtained from the individual(s) for the publication of any potentially identifiable images or data included in this article.

AUTHOR CONTRIBUTIONS

All authors listed have made a substantial, direct and intellectual contribution to the work, and approved it for publication.

FUNDING

This project was funded by the National Natural Science Foundation of China (81974267), Hunan Provincial Natural Science Foundation of China (2018JJ2575), and Hunan Provincial Health Commission Research Foundation Project (B2019166).

REFERENCES

- Yang S, Li C, Shi X, Ma B, Xu W, Jiang H, et al. Primary squamous cell carcinoma in the thyroid gland: a population-based analysis using the SEER database. *World J Surg.* (2019) 43:1249–55. doi: 10.1007/s00268-019-04906-2
- Limberg J, Ullmann TM, Stefanova D, Finnerty BM, Beninato T, Fahey TJ, et al. Prognostic characteristics of primary squamous cell carcinoma of the thyroid: a national cancer database analysis. *World J Surg.* (2020) 44:348–55. doi: 10.1007/s00268-019-05098-5
- Koyama S, Fujiwara K, Nosaka K, Fukuhara T, Morisaki T, Miyake N, et al. Immunohistochemical features of primary pure squamous cell carcinoma in the thyroid: an autopsy case. *Case Rep Oncol.* (2018) 11:418–24. doi: 10.1159/000490410
- Wang SS, Ye DX, Wang B, Xie C. The expressions of keratins and P63 in primary squamous cell carcinoma of the thyroid gland: an application of raman spectroscopy. *Onco Targets Ther.* (2020) 13:585–91. doi: 10.2147/OTT.S229436
- Yasumatsu R, Sato M, Uchi R, Nakano T, Hashimoto K, Kogo R, et al. The treatment and outcome analysis of primary squamous cell carcinoma of the thyroid. *Auris Nasus Larynx.* (2018) 45:553–7. doi: 10.1016/j.anl.2017.07.009
- Kao NH, Tan CS, H, Koh AJ. The utility of immunohistochemistry in differentiating metastatic primary squamous cell carcinoma of the thyroid from a primary lung squamous cell carcinoma. *Case Rep Endocrinol.* (2019) 2019:1–4. doi: 10.1155/2019/8641267
- Jang JY, Kwon KW, Kim SW, Youn I. Primary squamous cell carcinoma of thyroid gland with local recurrence: ultrasonographic and computed tomographic findings. *Ultrasonography.* (2014) 33:143–8. doi: 10.14366/usg.13022
- Raggio B, Barr J, Ghandour Z, Friedlander P. Primary squamous cell carcinoma of the thyroid. *Ochsner J.* (2019) 19:290–2. doi: 10.31486/toj.18.0002
- Haugen BR, Alexander EK, Bible KC, Doherty GM, Mandel SJ, Nikiforov YE, et al. 2015 American thyroid association management guidelines for adult patients with thyroid nodules and differentiated thyroid cancer: the American thyroid association guidelines task force on thyroid nodules and differentiated thyroid cancer. *Thyroid.* (2016) 26:1–133. doi: 10.1089/thy.2015.0020
- Tessler FN, Middleton WD, Grant EG, Hoang JK, Berland LL, Teeffey SA, et al. ACR thyroid imaging, reporting and data system (TI-RADS): white paper of the ACR TI-RADS committee. *J Am Coll Radiol.* (2017) 14:587–95. doi: 10.1016/j.jacr.2017.01.046
- Kwak JY, Han KH, Yoon JH, Moon HJ, Son EJ, Park SH, et al. Thyroid imaging reporting and data system for US features of nodules: a step in establishing better stratification of cancer risk. *Radiology.* (2011) 260:892–9. doi: 10.1148/radiol.11110206radiol.11110206
- Peng Q, Niu C, Zhang Q, Zhang M, Chen S. Mummified thyroid nodules: conventional and contrast-enhanced ultrasound features. *J Ultrasound Med.* (2018) 38:441–52. doi: 10.1002/jum.14712
- Peng Q, Niu C, Zhang M, Chen S. Sonographic characteristics of papillary thyroid carcinoma with coexistent hashimoto's thyroiditis: conventional ultrasound, acoustic radiation force impulse imaging and contrast-enhanced ultrasound. *Ultrasound Med Biol.* (2019) 45:471–80. doi: 10.16/j.ultrasmedbio.2018.10.020
- Casella C, Ministrini S, Galani A, Mastroianni F, Cappelli C, Portolani N. The new TNM staging system for thyroid cancer and the risk of disease downstaging. *Front Endocrinol.* (2018) 9:541. doi: 10.3389/fendo.2018.00541
- Zhang Y, Zhou P, Tian SM, Zhao YF, Li JL, Li L. Usefulness of combined use of contrast-enhanced ultrasound and TI-RADS classification for the differentiation of benign from malignant lesions of thyroid nodules. *Eur Radiol.* (2017) 27:1527–36. doi: 10.1007/s00330-016-4508-y
- Zhang YZ, Xu T, Gong HY, Li CY, Ye XH, Lin HJ, et al. Application of high-resolution ultrasound, real-time elastography, and contrast-enhanced ultrasound in differentiating solid thyroid nodules. *Medicine.* (2016) 95:e5329. doi: 10.1097/MD.0000000000000532900005792-201611080-00016
- Chen CY, Tseng HS, Lee CH, Chan PW. Primary squamous cell carcinoma of the thyroid gland with eggshell calcification: sonographic and computed tomographic findings. *J Ultrasound Med.* (2010) 29:1667–70. doi: 10.7863/jum.2010.29.11.1667
- Kondo T, Matsuyoshi A, Matsuyoshi H, Goto R, Ono K, Honda Y, et al. A case of primary thyroid squamous cell cancer: transformation from benign tumour associated with chronic thyroiditis? *BMJ Case Rep.* (2009) 2009:bcr10.2008.1137. doi: 10.1136/bcr.2008.1137
- Ma JJ, Ding H, Xu BH, Xu C, Song LJ, Huang BJ, et al. Diagnostic performances of various gray-scale, color doppler, and contrast-enhanced ultrasonography findings in predicting malignant thyroid nodules. *Thyroid.* (2014) 24:355–63. doi: 10.1089/thy.2013.0150
- Deng J, Zhou P, Tian SM, Zhang L, Li JL, Qian Y. Comparison of diagnostic efficacy of contrast-enhanced ultrasound, acoustic radiation force impulse imaging, and their combined use in differentiating focal solid thyroid nodules. *PLoS ONE.* (2014) 9:e90674. doi: 10.1371/journal.pone.0090674PONE-D-13-30329
- Struller F, Senne M, Falch C, Kirschniak A, Konigsrainer A, Muller S. Primary squamous cell carcinoma of the thyroid: case report and systematic review of the literature. *Int J Surg Case Rep.* (2017) 37:36–40. doi: 10.1016/j.ijscr.2017.06.011
- Wang W, Ouyang Q, Meng C, Jing L, Li X. Treatment optimization and prognostic considerations for primary squamous cell carcinoma of the thyroid. *Gland Surg.* (2019) 8:683–90. doi: 10.21037/gs.2019.11.07

Conflict of Interest: The authors declare that the research was conducted in the absence of any commercial or financial relationships that could be construed as a potential conflict of interest.

Copyright © 2020 Chen, Peng, Zhang and Niu. This is an open-access article distributed under the terms of the Creative Commons Attribution License (CC BY). The use, distribution or reproduction in other forums is permitted, provided the original author(s) and the copyright owner(s) are credited and that the original publication in this journal is cited, in accordance with accepted academic practice. No use, distribution or reproduction is permitted which does not comply with these terms.



Feasibility Study Shows Multicenter, Observational Case-Control Study Is Practicable to Determine Risk of Secondary Breast Cancer in Females With Differentiated Thyroid Carcinoma Given Radioiodine Therapy in Their Childhood or Adolescence; Findings Also Suggest Possible Fertility Impairment in Such Patients

OPEN ACCESS

Edited by:

Gabriella Pellegriti,
University of Catania, Italy

Reviewed by:

Massimo Salvatori,
Catholic University of the Sacred
Heart, Italy
Agnese Barnabei,
Azienda Sanitaria Locale Roma 1, Italy

*Correspondence:

Valentina Drozd
vm.drozd@gmail.com
Christoph Reiners
Reiners_C@ukw.de

Specialty section:

This article was submitted to
Cancer Endocrinology,
a section of the journal
Frontiers in Endocrinology

Received: 29 May 2020

Accepted: 27 August 2020

Published: 28 October 2020

Citation:

Drozd V, Schneider R, Platonova T, Panasiuk G, Leonova T, Oculevich N, Shimanskaja I, Vershenya I, Dedovich T, Mitjukova T, Grelle I, Biko J and Reiners C (2020) Feasibility Study Shows Multicenter, Observational Case-Control Study Is Practicable to Determine Risk of Secondary Breast Cancer in Females With Differentiated Thyroid Carcinoma Given Radioiodine Therapy in Their Childhood or Adolescence; Findings Also Suggest Possible Fertility Impairment in Such Patients. *Front. Endocrinol.* 11:567385. doi: 10.3389/fendo.2020.567385

Valentina Drozd^{1*}, Rita Schneider², Tamara Platonova¹, Galina Panasiuk¹, Tatjana Leonova³, Nataliya Oculevich⁴, Irina Shimanskaja¹, Irina Vershenya⁵, Tatjana Dedovich¹, Tatjana Mitjukova¹, Inge Grelle², Johannes Biko² and Christoph Reiners^{2*}

¹ International Foundation "Arnica," Minsk, Belarus, ² Department of Nuclear Medicine, University Hospital, Würzburg, Germany, ³ The Center of Thyroid Tumors, Minsk City Oncological Dispensary, Minsk, Belarus, ⁴ Center of Medical Rehabilitation and Balneotherapy, Minsk, Belarus, ⁵ Clinical Laboratory "MedEx-Lab," Minsk, Belarus

Objective: This single-center, observational case-control feasibility study sought to test key elements of a protocol for an eventual long-term international observational case-control study of a larger patient cohort, to evaluate the risk of breast cancer as a second primary malignancy in females with differentiated thyroid cancer (DTC) given radioiodine therapy (RAI) during childhood or adolescence.

Patients: Females developing DTC after the Chernobyl accident in Belarus and ≤ 19 years old at the time of thyroid surgery were enrolled: patients given RAI ($n = 111$) and controls of similar age not given RAI ($n = 90$).

Results: One case of breast cancer was newly diagnosed among the RAI patients, but none in controls. Patients given RAI significantly less frequently needed 2nd surgeries than did controls (23%, 26/111 vs. 39%, 35/90, $P < 0.05$); the main indication for such procedures usually is suspicion of local recurrence. RAI patients appeared to have had more frequent reproductive difficulties than did controls: 78% (87/111) of the former vs. 93% (84/90) of the latter had a history of pregnancy ($P < 0.01$), and the mean number of pregnancies was 1.5 ± 1.2 in RAI patients vs. 1.9 ± 1.1 in controls ($P < 0.05$). Most notably, infertility was observed in 23% (26/111) of RAI patients vs. 4% (4/90) of controls ($P < 0.01$).

In conclusion, a international observational case-control study on breast cancer after DTC in patients given RAI vs. not given RAI appears to be feasible. Additional research and everyday clinical attention should be devoted to reproductive function after RAI in young females.

Keywords: thyroid cancer, radiation-induced thyroid cancer, radioiodine therapy, breast cancer risk, infertility

INTRODUCTION

Most cases of differentiated thyroid cancer (DTC) in childhood, adolescence, and early adulthood can be successfully treated with surgery, radioiodine [iodine-131 (I-131)] therapy (RAI), and thyroid hormone replacement, resulting in 10-year survival rates of 95% and low recurrence rates of 10–30% (1). However, excellent long-term survival may be restricted by an increased risk for second primary malignancy related to RAI and/or other factors (2, 3). It is well-known that the gastrointestinal tract (salivary glands, stomach, colorectum), the genitourinary tract (kidneys, bladder), and the hematopoietic system (leukocytes) are at risk to develop a second primary malignancy after RAI (2–4). I-131 is concentrated by the sodium-iodide symporter, which is expressed not only in thyrocytes, but in epithelial cells of salivary glands, of the stomach, and of the mammary gland too (5). Thus, the female breast may receive relevant radiation doses of 0.4–0.6 Gy from one course of RAI with 6 GBq (6). We recently reviewed the literature on breast cancer as a second primary malignancy after RAI of DTC with a focus on young patients, and concluded that there is a general association between DTC and breast cancer. The risk for breast cancer after DTC in adults is low—about 2%—and RAI is assumed not to influence that risk substantially, but data in patients given RAI as children and adolescents are sparse. Systematic studies about breast cancer risk in young TC patients after RAI therefore are needed (7, 8).

MATERIALS AND METHODS

Objective and Scope

In addition to the literature review mentioned above, we performed a preliminary multicenter registry survey to evaluate the availability of sufficient patient data for a subsequent international multicenter observational case-control study in children and adolescents with DTC (7, 8). In parallel, to develop a protocol for such a multicenter study, we performed an observational case-control feasibility study in small samples of young female patients with DTC after RAI and of controls with DTC not treated with RAI. Both the survey and the feasibility study were sponsored by the German Federal Office for Radiation Protection (8). The sponsor had no involvement in the content or the decision to publish this paper.

Patients and Study Design

As part of a variety of collaborative international humanitarian and scientific projects on radiation-induced DTC in Belarusian patients after the Chernobyl nuclear reactor accident (3, 8–15)

after thyroid surgery in Minsk (Belarus), children and adolescents with advanced DTC were treated with high-activity RAI in two German academic tertiary referral centers, the University Hospitals of Essen (1992–1993) and Würzburg (1994–2007). Altogether, more than 1,000 cycles of RAI were performed in roughly 250 patients (14) with one or more of pT4 pN1, or pM1 TNM tumor stages. Selection was made without direct influence from the German side.

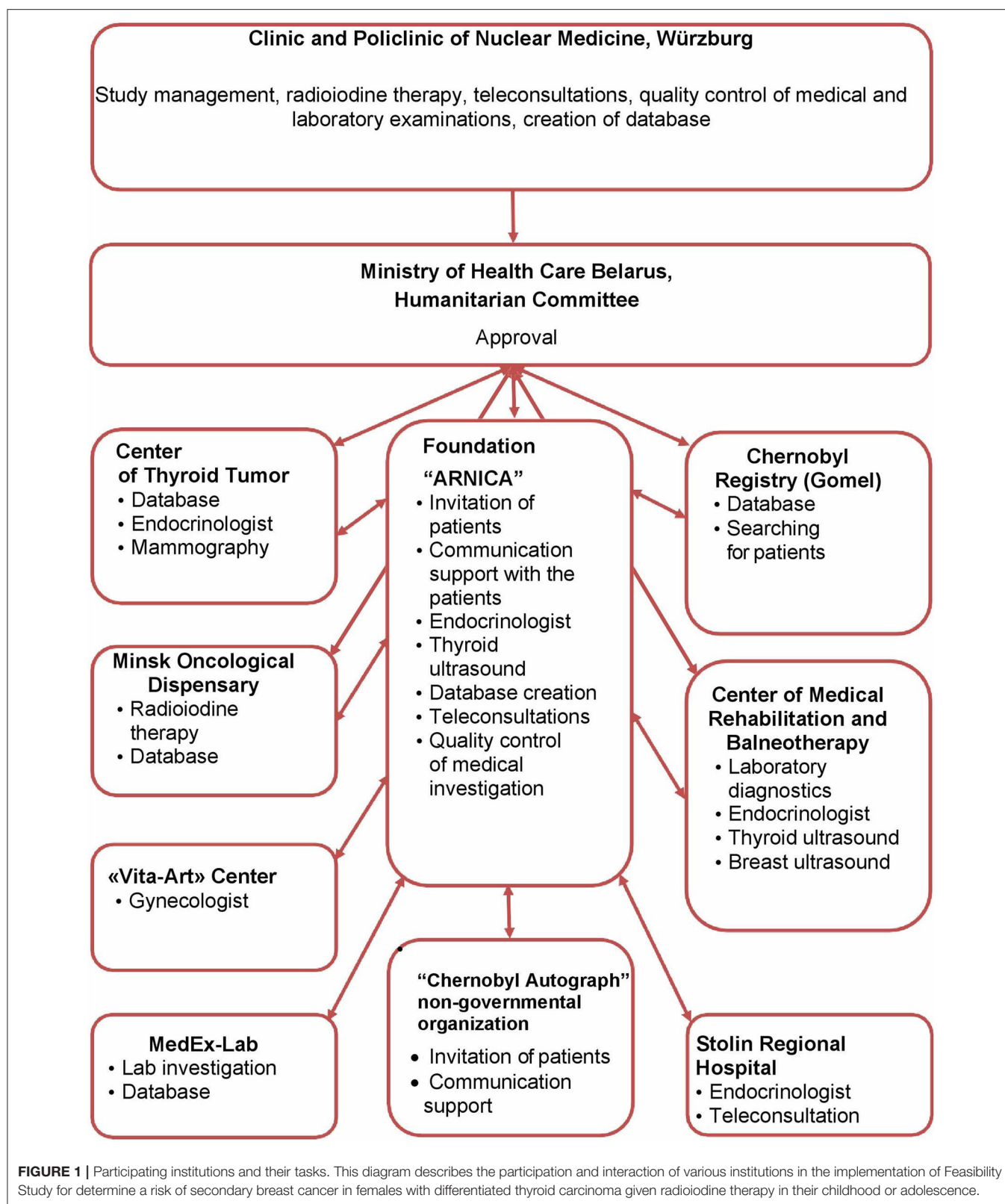
With approval of the Ministry of Health and the Humanitarian Committee of Belarus, following treatment in Germany, the patients were followed-up in Minsk by experienced endocrinologists and gynecologists of the Center of Thyroid Tumors, Minsk City Oncological Dispensary, the International Foundation “Arnica,” the “Vita-Art” Health Center, and the “MedEx-Lab” clinical laboratory in cooperation with institutions in Belarus including the Chernobyl Registry, the Center of Medical Rehabilitation and Balneotherapy, the Stolin Regional Hospital, and the “Chernobyl Autograph” non-governmental organization (Figure 1).

We decided to carry out our observational case-control feasibility study in roughly 100 female patients who were age ≤ 19 years at the time of thyroid surgery during the 1992–2007 treatment period (“RAI patients”). An equal number of patients with DTC of similar age who did not receive RAI would serve as controls. More than 200 potential “RAI patients” group members and ca. 120 potential controls, all females, received invitations for a comprehensive cost-free health check in the outpatient clinic of the “Arnica” Foundation and the “Vita-Art” Health Center. Reimbursement of study participants’ travel costs was guaranteed.

Study Protocol and Quality Assurance

In all participants, the medical and radiological history related to the Chernobyl accident was documented using questionnaires developed for this study. In addition, in the RAI patient group, relevant RAI-related data, e.g., therapeutic activity per course, number of courses, and cumulative activities (in GBq), were registered.

Patients and controls underwent clinical examination including palpation and sonographic examination of the neck and breast. If abnormalities were detected in the breast screening sonogram, then mammography, magnetic resonance imaging, or both followed. The breast cancer screening program used in this study was recommended by the International Late Effects of Childhood Cancer Guideline Harmonization Group (16) for young patients with non-breast cancers who had radiation exposure of the breast. Ultrasonography equipment consisted of a Logiq E” Scanner with 12 MHz-probe (GE Healthcare, Chicago,



IL, USA). For quality assurance of breast imaging, findings were documented according to the BI-RADS classification, 5th edition (17).

Study participants also underwent comprehensive biochemical screening based on testing which was carried out at "MedEx-Lab" clinical laboratory in Minsk, with quality

control at the laboratory of the Clinic and Polyclinic for Nuclear Medicine in Würzburg, Germany. For classification of remission/progression after therapy of DTC, thyroglobulin and anti-thyroglobulin antibody status were determined. Levothyroxine replacement was checked with determination of thyroid-stimulating hormone (TSH) and free thyroxine (fT4) concentrations. Variables of calcium-phosphate metabolism (parathormone, calcium, and phosphorus levels) were also quantitated. As part of the general health check, blood cell counts, lipid, liver, and pancreas status, and sex hormone status were determined. An automatic immunochemical analyser (COBAS e 411, Roche Diagnostics, Risch-Rotkreuz, Switzerland) was used to measure hormone variables and the COBAS INTEGRA 400 plus automatic analyser (Roche Diagnostics) served for determination of other biochemical variables. The clinical laboratory in Minsk used commercial control sera (Lyphochek® 1, 2, 3; Biorad Company, Hercules, CA, USA) for daily quality assurance checks as well as for external comparisons with the lab of the Clinic and Polyclinic for Nuclear Medicine in Würzburg. Both labs followed the rules of the authorities in Belarus and Germany that govern participation in blinded studies.

Database, Data Protection, and Patients' Rights

A customized Access database (Microsoft, Redmond, WA, USA) was created for this study. A trained medical documentation assistant entered into this database de-identified data from the records of the study medical and biochemical examinations, which data had been generated by physicians and laboratory staff. The medical documentation assistant regularly made plausibility checks and flagged missing data. Before enrolment, study participants gave their informed consent for participation in the study and were over 18 at the time of data collection and analysis of de-identified data.

Statistics

Aggregate tabulated results are presented here with arithmetic means \pm standard deviations (SDs) and/or medians and minimum–maximum ranges, as appropriate. For intergroup statistical comparisons, Student *t*-test was used for constant variables and chi-square test for frequencies. Results with probability of error $<5\%$ were considered to be significant.

RESULTS

Study Group

Altogether 111 RAI patients and 90 controls, respectively, were enrolled in the study, which was performed from 2016–2017. Selected characteristics of these groups of study participants are presented in **Table 1**.

The RAI patient and control groups differed in certain demographic, disease, and treatment characteristics; most differences were attributable to history of RAI being the key criterion for inclusion into one or the other of the groups. On average, RAI patients were ca. 1.5 years younger at the time of surgery than were the controls ($P < 0.002$). Unsurprisingly, all

TABLE 1 | Characteristics of RAI patients and controls.

Variable	RAI patients <i>n</i> = 111	Control <i>n</i> = 90	<i>P</i>
Age at thyroid surgery (years)			
Mean \pm SD	12.7 \pm 3.4	14.3 \pm 3.4	<0.002
Median (minimum–maximum)	12.3 (4.2–18.9)	14.7 (6.8–18.9)	
Extent of thyroid surgery % (<i>n</i>)			
Total thyroidectomy	100% (111)	53% (48)	<0.001
Hemithyroidectomy	0 (0.0%)	47% (42)	
Number of surgeries for DTC % (<i>n</i>) of subjects in category			
1	72% (80)	59% (53)	<0.05
2	23% (26)	39% (35)	<0.05
>2	5% (5)	2% (2)	n.s.
pTNM stage % (<i>n</i>)			
T1	43% (48)	90% (81)	<0.001
T2	37% (41)	9% (8)	<0.001
T3	20% (22)	1% (1)	<0.001
N0	9% (10)	60% (54)	<0.001
N1	91% (101)	40% (36)	<0.001
M0	75% (83)	100% (90)	<0.05
M1*	25% (28)	0 (0%)	<0.001
Radioiodine therapy RAI courses (<i>n</i>)			
Mean \pm SD	2.9 \pm 2.1	–	ND
Median (minimum–maximum)	2 (0–10)	–	ND
Cumulative RAI activity (GBq)			
Mean \pm SD	10.6 \pm 9.5	–	ND
Median (minimum–maximum)	7.4 (2.0–43.0)	–	ND
Age at enrolment (years)			
Mean \pm SD	33.4 \pm 2.6	35.3 \pm 3.8	<0.001
Median (minimum–maximum)	32.6 (28.3–42.3)	34.6 (27.2–43.1)	
Duration of follow-up after thyroid surgery (years)			
Mean \pm SD	20.9 \pm 3.9	20.7 \pm 4.0	n.s.
Median (minimum–maximum)	21.3 (13.6–27.3)	21.6 (10.5–29.4)	

Due to rounding, percentages may not add up to 100%.

ND, not done; n.s., not statistically significant; RAI, radioiodine ($I-131$) therapy; SD, standard deviation.

*Based on post-operative $I-131$ whole body scan.

patients given RAI had undergone total thyroidectomy, because as complete as possible resection of thyroid tissue (whether malignant or healthy) is a precondition for RAI. In contrast, only a bit more than half of controls had undergone such surgery ($P < 0.001$). RAI patients less frequently needed a second surgical intervention (23 vs. 39%, $P < 0.05$). Significantly larger proportions of RAI patients had $>pT1$ primary tumor, presence of lymph node metastasis, or distant involvement, reflecting disease characteristics likely to have contributed to the decision for or against RAI. In both groups, however $>95\%$ of cases were histologically classified as papillary cancers.

Regarding Chernobyl-related radiation exposure, there were no inter-group differences in residence on contaminated ground, consumption of contaminated food and milk, or use of iodine thyroid blocking around the time of the accident, the last of which was reported in $<5\%$ of members of either group (data

not shown). The respective percentages of family members of RAI patients or controls with thyroid cancer (7 vs. 4%), breast cancer (6 vs. 8%) or any type of cancer (30 vs. 29%) showed no statistically significant differences. Additionally, there were no differences in BMI, age at menarche, regularity of the menstrual cycle, prevalence of diabetes, alcohol abuse, or use of oral contraceptives.

Concerning reproductive history, 78% of RAI patients (87/111) and 93% of controls (84/90) reported history of pregnancy, a statistically significant difference ($P < 0.01$). The mean numbers of pregnancies also differed between these groups (1.5 ± 1.2 vs. 1.9 ± 1.1 ; $P < 0.05$). In the RAI group, 50% of mothers (44/87) had practiced breast-feeding, in the control group, 53% (45/84). Remarkably, infertility according to the World Health Organization definition, i.e., inability to become pregnant despite regular sexual intercourse without contraception, was observed in 23% of RAI patients (26/111). Two of these 26 women were treated for infertility for a long time and then were able to give birth to healthy children using *in vitro* fertilization. Only 4% of controls (4/90) ($P < 0.01$) were treated for infertility and in this group, 2 women were not married.

Current Physical and Biochemical Findings

Enlarged neck lymph nodes, reflecting possible DTC recurrence, were detected by ultrasound in 14% of the RAI group (16/111) and 27% in the control group (24/90) ($P < 0.05$). DTC recurrences were found sonographically and subsequently histologically verified by fine needle aspiration biopsy in 2 control patients (2%), but no RAI patient.

Presumably due to their having completely-excised thyroid glands, RAI patients needed higher mean thyroid hormone replacement doses of levothyroxine than did controls, 2.3 ± 0.5 $\mu\text{g/kg}$ body weight vs. 2.0 ± 0.9 $\mu\text{g/kg}$ body weight ($P < 0.001$). However, mean fT4 values did not differ between the groups, nor did mean TSH concentrations (Table 2).

Additionally, thyroglobulin levels were below the level of detectability (1 pg/mL) in a significantly greater proportion of RAI patients ($P < 0.001$). Presumably due to RAI patients' more frequent radical operations, decreased parathormone levels (<15 pg/mL) signaling postoperative hypoparathyroidism, a well-known complication of thyroid surgery, were much more frequent in that group than in the control group ($P < 0.001$). Corresponding to a greater frequency of decreased parathormone levels after thyroidectomy and RAI, blood calcium was decreased in 36% of RAI patients (40/111) and 21% of controls (19/90) ($P < 0.05$), while phosphate was increased in 28% (32/111) and 9% (8/90), respectively ($P < 0.002$).

Neither RAI patients nor controls differed, or showed significant abnormalities in blood cell counts (data not shown). Concerning blood lipid values, however, while the groups did not differ, they both had a high prevalence of abnormalities. Total cholesterol was above the reference range in 47% of RAI patients (52/111) and 43% of controls (39/90), while low-density lipoprotein was above the reference range in 73% of RAI patients (81/111) and 72% of controls (65/90). High-density lipoprotein levels were below the reference range in 43% and 44% of these groups, respectively. No abnormalities were seen

TABLE 2 | Current biochemical findings by category, % (n).

Variable (relationship to reference range)	Reference range	RAI patients n = 111	Controls n = 90	P-value
TSH (mIU/L)				
≤ 0.10 (below)	0.27–4.2	45% (50)	40% (36)	n.s.
> 0.10 –0.27 (within)		12% (13)	11% (10)	n.s.
> 0.27 –4.2 (within)		36% (40)	44% (40)	n.s.
> 4.2 (above)		7% (8)	4% (4)	n.s.
fT4 (pmol/L)				
< 12 (below)	12–22	1% (1)	3% (3)	n.s.
12–22 (within)		55% (61)	62% (56)	n.s.
> 22 (above)		44% (49)	34% (31)	n.s.
Tg (ng/mL)				
< 1.0 (within)	$< 1^*$	93% (103)	54% (49)	< 0.001
≥ 1.0 (above)		7% (8)	46% (41)	< 0.001
PTH (ng/mL)				
< 15 (below)	15–65	35% (39)	9% (8)	< 0.001
15–65 (within)		64% (71)	87% (78)	< 0.001
> 65 (above)		1% (1)	4% (4)	n.s.

Due to rounding, percentages may not add up to 100%.

fT4, free thyroxine; n.s., not significant; PTH, parathormone; Tg, thyroglobulin; TSH, thyroid-stimulating hormone.

*After thyroidectomy.

in the liver enzymes alanine aminotransferase and or aspartate aminotransferase. Elevated blood glucose levels were found in 5% of RAI patients (6/111) and 8% of controls (7/90). Neither the differences in liver enzymes, nor those in blood glucose were significant.

Regarding the sex hormones, there were no significant inter-group differences in luteinizing hormone, follicle-stimulating hormone, anti-Müllerian hormone, prolactin, estrogen, or testosterone concentrations (data not shown). Progesterone levels were less frequently abnormally decreased in RAI patients compared to controls (16%, 18/111 vs. 41%, 41/90; $P < 0.01$).

Breast-Related Findings

Previous events of clinical relevance to breast cancer such as breast trauma, lumps, local pain, or mastitis were only rarely reported, in one to three patients, with no differences between groups. Similarly, findings like skin abnormalities, conspicuous or secreting mammillae, and palpable indurations or lumps on inspection and palpation were rare and evenly distributed among RAI patients vs. controls.

Table 3 summarizes the results of breast sonography. Sixty-one percent of RAI patients (68/111) and 68% of controls (61/90) had completely normal findings. This difference was not statistically significant; nor were the differences regarding frequencies of diffuse changes, focal lesions, cysts, fibromas, or detectable lymph nodes. Ninety-six percent of sonograms in patients given RAI and of 100% in controls were classified into non-suspicious BI-RADS categories.

TABLE 3 | Breast ultrasonography findings.

Variable	RAI patients <i>n</i> = 111	Controls <i>n</i> = 90	<i>P</i>
Normal findings, % (<i>n</i>)			
Yes	61% (68)	68% (61)	n.s.
No	39% (43)	32% (29)	
Diffuse changes, % (<i>n</i>)			
Yes	26% (29)	22% (20)	n.s.
No	74% (82)	78% (70)	
Focal lesions, % (<i>n</i>)			
Yes	11% (13)	9% (8)	n.s.
No	88% (98)	91% (82)	
Largest focal lesion (mm), mean ± SD	8.1 ± 4.5	7.5 ± 3.1	n.s.
Cysts, %(<i>n</i>)	5% (5)	3% (3)	n.s.
Fibroma, % (<i>n</i>)	4% (4)	0% (0)	n.s.
Lymph nodes, % (<i>n</i>)			
None	97% (108)	99% (89)	n.s.
Single	3% (3)	1% (1)	n.s.
Multiple	0% (0)	0% (0)	
Localization of lymph nodes, % (<i>n</i>)			
Axillary	3% (3)	1% (1)	n.s.
Other	0% (0)	0% (0)	
BI-RADS category, <i>n</i> (%)			
Category 0	0% (0)	0% (0)	n.s.
Category 1	61% (68)	68% (61)	n.s.
Category 2	35% (39)	32% (29)	n.s.
Category 3	4% (4)	0% (0)	n.s.
Category 4	0% (0)	0% (0)	n.s.
Category 5	0% (0)	0% (0)	n.s.

Due to rounding, percentages may not add up to 100%.

BI-RADS, breast imaging-reporting and data system; n.s., not statistically significant; RAI, radioiodine ($I-131$) treatment.

In the 4 RAI patients with BI-RADS category 3 findings, the suspicious lesions were removed surgically, with a histological diagnosis of fibroma in 3 cases and carcinoma in 1.

DISCUSSION

The aim of this observational case-control feasibility study in two small samples ($n = \text{ca. } 100$ each) of young female patients of similar age, whose treatment for DTC either included or did not include RAI, was to develop a protocol for a larger multicenter study with a sufficiently large sample to reliably test the hypothesis “RAI does not increase the risk for breast cancer compared to DTC patients without RAI.” Based on our previously-mentioned literature review and international registry survey, we assumed this risk to be $\sim 2.5\%$ and concluded that at least 4,340 patients and 660 controls would be needed to test the hypothesis with adequate statistical power, 80% (7).

This feasibility study delivered a number of expected results. First, concerning numbers of subjects in both groups, it was not surprising that it was more difficult in our patient population to recruit controls ($n = 90$) than patients given RAI ($n = 111$). Most children and adolescents with DTC after the Chernobyl accident

presented with relatively advanced tumor stages, in which RAI is indicated. This can be deduced from the observation that 100% of the RAI had (near-) total thyroidectomy, 57% were classified postoperatively as tumor stage $>pT1$, and 91% as $pN1$ and 40% as $pM1$ stages.

Second, an imaging protocol following the recommendations (16) to use the BI-RADS classification (17) in young patients with primary malignancy of non-breast tissues, but radiation exposure of the breast, proved to be feasible. Four cases of BI-RADS category 3 findings were detected among the RAI patients and histologically verified, among them 1 case of breast cancer. This single case, and the lack of cases among the controls, do not allow any statistical conclusions to be drawn regarding breast cancer risk associated with RAI. However, the breast cancer case provides additional evidence for the still-unproven assumption that this tumor is in general rare in young females with DTC (7). On the other hand, at least 3 cases of SPM other than breast cancer, all cancer of the cervix uteri, which were not in the focus of this study, were found by history in 111 RAI patients. These observations align to some extent with data published by Fridman et al. (18) demonstrating that the prevalence of SPM in 4,237 patients treated in Belarus for post-Chernobyl papillary DTC between 1990–2015 was 1% after a 15-year follow-up. Among the 41 patients who developed SPM, hematological malignancies (9 cases), cervical cancer (7 cases), breast cancer (4 cases), and colon carcinoma (4 cases) were most frequently observed (18).

Third, quality checks suggest that our study had reliable biochemistry results. Thyroglobulin levels in blood should be undetectable if no healthy or cancerous thyroid tissue, i.e., no local residues, involved lymph nodes, or distant metastases remain after therapy. The finding that thyroglobulin levels were statistically more frequently measurable in controls than in RAI patients corresponds conversely to the more complete surgical removal of thyroid tissue, and to additional destruction of such tissue by RAI.

According to the current American Thyroid Association guidelines (19), it seems that too high a percentage—40%—of our controls had complete TSH suppression. On the other hand, the corresponding frequency of complete suppression, 45%, in our higher-risk RAI patient group seems to have been too low. There is a debate about TSH target values in the literature, addressing potential cardiovascular complications of complete TSH suppression in low-risk patients (19, 20) such as, e.g., our control group. Additionally, chronic levothyroxine overdosage is suspected of increasing breast cancer risk independent of DTC (21). Reasons for the possibly suboptimal degree of TSH suppression in many of our patients may include the supply situation of levothyroxine necessitating that patients frequently switch among different thyroid hormone preparations. The explanation also may include laboratory monitoring at irregular intervals, since levothyroxine regimens in athyroid individuals must be titrated and re-titrated over time, according to circulating TSH levels.

Not completely unexpected was the appreciable prevalence of laboratory constellations of hypoparathyroidism, i.e., increased circulating phosphate, decreased parathormone, and calcium.

However, mostly due to complications of the generally more radical surgery in the RAI patients, the percentage of below-normal parathormone blood levels, 35%, in that group was relatively high, compared to the 9% in controls. Obviously, medication for substitution therapy of hypoparathyroidism needs specific attention in patients treated for DTC at a young age, especially those undergoing total thyroidectomy. Increased levels of serum cholesterol in roughly 45% of patients and controls seem surprising. However, in a recent narrative review of studies focusing on this issue, Bianco and Taylor (22) stressed that a high percentage of patients on levothyroxine replacement after thyroidectomy who have normal TSH levels have elevated cholesterol, and that indeed, >50% of such patients need statins.

This study also had two interesting and particularly noteworthy findings. First, RAI patients significantly less frequently needed 2 or more surgical interventions than did controls (23% vs. 39%, $P < 0.05$). The main indication for 2nd intervention is usually suspicion of local recurrence; notably, ca. 20 of the approximately 120 subjects who were approached to participate as controls had to be excluded because they already had been diagnosed with a DTC recurrence.

Second, only 78% of the post-RAI patients, compared to 93% of controls, reported a history of pregnancy, and the mean numbers of pregnancies differed significantly between groups (1.5 ± 1.2 vs. 1.9 ± 1.1 , $P > 0.05$). Remarkably, infertility defined according to recent international standards (23) as inability to become pregnant despite regular sexual intercourse without contraception, was observed in 23% of post-RAI patients, vs. only 4% of controls ($P < 0.01$). It should be noted that Chart of European Health Information Gateway (WHO) for the Belarus demonstrated that fertility rate in 2016 (time of practical implementation of study) was 1.7 births per woman (24). About each fifth couple in Belarus faces infertility, and male infertility accounts for 50% of infertile couples (25).

The literature contains high-level evidence of transient testicular dysfunction in males after RAI, but only very low-level evidence, and conflicting findings, regarding female reproductive outcomes (2, 6). For example, a study by Nies et al. (26) demonstrated that female survivors of DTC who received 131-I treatment during childhood did not appear to have major abnormalities in reproductive characteristics nor in predictors of ovarian failure (26). Giusti et al. (27) found no difference in anti-Müllerian hormone levels in two relatively small samples of patients with DTC undergoing or not undergoing RAI, and that infertility must be considered a low risk, but concluded that 1 out of 2 women with DTC suffer from menstrual dysregulation independent of RAI (27). Yaish et al. (28), however, observed a significant decrease of anti-Müllerian hormone levels 3 months after RAI, with only partial recovery after 12 months. The Yaish et al. study had some limitations, however, because the cohort was inhomogeneous, including patients with DTC or Graves' disease. Further, no control group with similar fluctuations of TSH levels, but not given RAI, was studied (28). Taken together with the limitations of the literature, our observations regarding reproductive history suggest the need for additional, systematic study of the associations of DTC, RAI, thyroid

hormone replacement therapy, and gynecological comorbidities, e.g., cervical cancer as an SPM, with female fertility.

Our study has some strengths, and some limitations too. In the former category, the investigation was carried out by experienced clinicians following a strict predefined and quality-assured protocol. Additionally, patients and controls matched well-regarding history of Chernobyl-related radiation exposure, family history of DTC, breast cancer, or other types of cancer, and frequency of potentially confounding breast cancer risk factors, e.g., high BMI, diabetes, alcohol abuse, older age at menarche, irregular menstrual cycle, and use of oral contraceptives. Study groups were relatively small in absolute terms, but large for a single center following patients with childhood DTC. Moreover, follow-up times, ranging between 10–30 years (mean 20 ± 4.0 years) after thyroid surgery, were long. The study results provided assurance that the follow-up protocol properly had among its main focuses the identification of recurrences, optimization of levothyroxine dosing, and replacement therapy for hypoparathyroidism. A weakness of this study is that all participants had been exposed to radiation from the Chernobyl reactor accident, which influences the risk and possibly the clinical behavior of DTC notably (29) and questionably the risk of BC too (30).

In conclusion, a sufficiently-powered subsequent international, multicenter, observational case-control study on breast cancer risk in female patients with DTC given or not given RAI in childhood or adolescence appears to be feasible; key elements of the required protocol for that study, including necessary quality controls, were successfully tested in such patients. Based on the findings of the present study and the results of a corresponding comprehensive literature review (7), the risk for breast cancer in DTC survivors seems not to be high. However, the risk in DTC subtypes, the influence of age (taking into account exposure to RAI around puberty), genetic predisposition for BC by familial history and genotyping as well as genome wide association studies of DTC should be addressed more in detail and additional attention should be paid to reproductive function after RAI. It may be argued that more aggressive DTC, deserving high activities of RAI, could occur in patients with genetic predisposition to second primary cancer. According to a recent review on genome wide association studies a gradual increase in the general risk for differentiated thyroid cancer can be demonstrated with the strongest SNPs but the overall prediction ability appears to be very limited. Up to now, the clinical aggressiveness of DTC and its risk for SPM's by "genomic profiling" is not possible (31).

DATA AVAILABILITY STATEMENT

All datasets generated for this study are included in the article/supplementary material.

ETHICS STATEMENT

The studies involving human participants were reviewed and approved by Ministry of Health of Belarus. The

patients/participants provided their written informed consent to participate in this study.

AUTHOR CONTRIBUTIONS

VD: concept development, study management, patients' examination in Minsk, analysis of thyroid cancer database, writing and editing manuscript. RS: study management, management and analysis of thyroid cancer database in Minsk, language editing. TP: database management and analysis of thyroid cancer database in Minsk, statistical data processing. GP: patients' examination in Gomel, analysis of thyroid cancer database in Gomel. TL, NO, and IS: patients' examination in Minsk, analysis of thyroid cancer database in Minsk. IV: laboratory tests, quality control, analysis of thyroid cancer database in Minsk. TD: study management and analysis of thyroid cancer database in Minsk, statistical data processing. TM: laboratory tests, analysis of thyroid cancer database in Minsk. IG: quality control of laboratory tests, analysis of

thyroid cancer database in Minsk. JB: concept development, study management, patients' examination in Minsk and in Würzburg. CR: concept development, study management, patient's examination in Minsk and in Würzburg, analysis of thyroid cancer database, writing and editing manuscript. All authors critical review and approval of final version of manuscript.

FUNDING

The project has been funded by the German Federal Office for Radiation Protection (File No. 35615S424) and supported by the charitable association Medical Help for Chernobyl Children, Würzburg.

ACKNOWLEDGMENTS

This manuscript was edited by Robert J. Marlowe, Spencer-Fontayne Corporation, Jersey City, NJ, USA.

REFERENCES

1. Jarzab B, Handkiewicz-Junak D, Włoch J. Juvenile differentiated thyroid carcinoma and the role of radioiodine in its treatment: a qualitative review. *Endocr Relat Cancer*. (2005) 12:773–803. doi: 10.1677/erc.1.00880
2. Brown AP, Chen J, Hitchcock YJ, Szabo A, Shrieve DC, Tward JD. The risk of second primary malignancies up to three decades after the treatment of differentiated thyroid cancer. *J Clin Endocrinol Metab*. (2008) 93:504–15. doi: 10.1210/jc.2007-1154
3. Kumagai A, Reiners C, Drozd V, Yamashita S. Childhood thyroid cancers and radioactive iodine therapy: necessity of precautionary radiation health risk management. *Endocr J*. (2007) 2007:839–847. doi: 10.1507/endocrj.K07E-012
4. Clement SC, Peeters RP, Ronckers CM, Links TP, van den Heuvel-Eibrink MM, Nieveen van Dijkum EJ, et al. Intermediate and long-term adverse effects of radioiodine therapy for differentiated thyroid carcinoma – a systematic review. *Cancer Treat Rev*. (2015) 41:925–34. doi: 10.1016/j.ctrv.2015.09.001
5. Poole VL, McCabe CJ. Iodide transport and breast cancer. *J Endocrinol*. (2015) 227:R1–12. doi: 10.1530/JOE-15-0234
6. Travis CC, Stabin MG. ¹³¹I ablation treatment in young females after the Chernobyl accident. *J Nucl Med*. (2007) 47:1723–7.
7. Reiners C, Schneider R, Platonova T, Fridman M, Malzahn U, Mäder U, et al. (2020). Breast cancer after treatment of thyroid cancer with radioiodine in young females: what we know about this and how to investigate open questions - review of the literature and results of a preliminary multicentric survey. *Front. Endocrinol*. 11:381. doi: 10.3389/fendo.2020.00381
8. Reiners C, Schneider R, Arnold K, Hertlein M, Sauer E, Drozd V, et al. *Brustkrebsrisiko nach Radiojodtherapie des Schilddrüsenkarzinoms. Bundesamt für Strahlenschutz – Forschungsvorhaben 3615S42421*. (2018). Available online at: <http://nbn-resolving.de/urn:nbn:de:0221-2019013117429>. (accessed July 10, 2020).
9. Demidchik YE, Demidchik EP, Reiners C, Biko J, Mine M, Saenko VA, et al. Comprehensive clinical assessment of 740 cases of surgically treated thyroid cancer in children of Belarus. *Ann Surg*. (2006) 243:525–32. doi: 10.1097/01.sla.0000205977.74806.0b
10. Drozd V, Poljanskaya O, Ostapenko V, Demidchik Y, Biko I, Reiners C. Systematic ultrasound screening as a significant tool for early detection of thyroid carcinoma in Belarus. *J Pediatr Endocrinol Metab*. (2002) 15:979–84. doi: 10.1515/JPEM.2002.15.7.979
11. Farahati J, Reiners C, Demidchik EP. Is the UICC/AJCC classification of primary tumor in childhood thyroid carcinoma valid? *J Nucl Med*. 40:2125.
12. Fridman M, Savva N, Krasko O, Mankovskaya S, Branovan DI, Schmid KW, et al. Initial presentation and late results of treatment of post-chernobyl papillary thyroid carcinoma in children and adolescents of Belarus. *J Clin Endocrinol Metab*. (2014) 99:2932–41. doi: 10.1210/jc.2013-3131
13. Reiners C, Demidchik YE, Drozd VM, Biko J. Thyroid cancer in infants and adolescents after chernobyl. *Minerva Endocrinol*. (2008) 33:381–95.
14. Reiners C, Biko J, Haenscheid H, Hebestreit H, Kirinjuk S, Baranowski O, et al. Twenty-five years after chernobyl: outcome of radioiodine treatment in children and adolescents with very high-risk radiation-induced differentiated thyroid carcinoma. *J Clin Endocrinol Metab*. (2013) 98:3039–48. doi: 10.1210/jc.2013-1059
15. Verburg FA, Biko J, Diessl S, Demidchik Y, Drozd V, Rivkees SA, et al. I-131 activities as high as safely administrable (AHASA) for the treatment of children and adolescents with advanced differentiated thyroid cancer. *J Clin Endocrinol Metab*. (2011) 96:E1268–71. doi: 10.1210/jc.2011-0520
16. Mulder RL, Kremer LC, Hudson MM, Bhatia S, Landier W, Levitt G, et al. Recommendations for breast cancer surveillance for female survivors of childhood, adolescent, and young adult cancer given chest radiation: a report from the international late effects of childhood cancer guideline harmonization group. *Lancet Oncol*. (2013) 14:e621–9. doi: 10.1016/S1470-2045(13)70303-6
17. *American College of Radiologists BI-RADS Atlas 5th Edition*. (2013). Available online at: <https://shop.acr.org/Default.aspx?TabID=55&ProductId=66931383> (accessed November 25, 2019).
18. Fridman M, Drozd V, Demidchik Y, Levin L, Branovan I, Shiglik N, et al. Second primary malignancy in Belarus patients with post-chernobyl papillary thyroid carcinoma. *Thyroid*. (2015) 25 (Suppl. 1):A22A23. doi: 10.1089/thy.2015.29004
19. Haugen BR, Alexander EK, Bible KC, Doherty GM, Mandel SJ, Nikiforov YE, et al. 2015 American thyroid association management guidelines for adult patients with thyroid nodules and differentiated thyroid cancer. *Thyroid*. (2016) 26:1–133. doi: 10.1089/thy.2015.0020
20. American Academy of Pediatrics. Management guidelines for children with thyroid nodules and differentiated thyroid cancer. *Pediatrics*. (2018) 142:e20183063. doi: 10.1542/peds.2018-3063
21. Hercbergs A, Mousa SA, Leinung M, Lin HY, Davis PJ. Thyroid hormone in the clinic and breast cancer. *Hormones Cancer*. (2018) 9:139–43. doi: 10.1007/s12672-018-0326-9
22. Bianco AC, Taylor P. Levothyroxine treatment and cholesterol in hypothyroidism. *Nat Rev Endocrinol*. (2020) 16:193–4. doi: 10.1038/s41574-020-0323-2

23. Zegers-Hochschild F, Adamson GD, Dyer S, Racowsky C, de Mouzon J, Sokol R, et al. The international glossary on infertility and fertility care, 2017. *Hum Reprod.* (2017) 32:1786–801. doi: 10.1093/humrep/dex234
24. World Health Organization. *Chart of European Health Information Gateway.* (2020). Available online at: [https://gateway.euro.who.int/en/indicators/hfa_25-0080-total-fertility-rate/visualizations/?country=WHO_EURO;EU_MEMBERS;EU_BEFORE_MAY2004;EU_AFTER_MAY2004;CIS;CARINFONET;SEEHN;NORDIC#id=\\$18832](https://gateway.euro.who.int/en/indicators/hfa_25-0080-total-fertility-rate/visualizations/?country=WHO_EURO;EU_MEMBERS;EU_BEFORE_MAY2004;EU_AFTER_MAY2004;CIS;CARINFONET;SEEHN;NORDIC#id=$18832) (accessed July 25, 2020).
25. *The United Nations Population Fund (UNFPA).* (2020). Available online at: <https://belarus.unfpa.org/en/topics/reproductive-health-0> (accessed July 25, 2020).
26. Nies M, Cantineau A, Arts E, van den Berg MH, van Leeuwen FE, Muller Kobold AC, et al. Long-term effects of radioiodine treatment on female fertility in survivors of childhood differentiated thyroid carcinoma. *Thyroid.* (2020) 30:1169–76. doi: 10.1089/thy.2019.0560
27. Giusti M, Mittica M, Comite P, Campana C, Gay S, Mussap M. Anti-müllerian hormone in pre-menopausal females after ablative radioiodine treatment for differentiated thyroid cancer. *Endocrine.* (2018) 60:516–23. doi: 10.1007/s12020-017-1510-3
28. Yaish I, Azem F, Gutfeld O, Silman Z, Serebro M, Sharon O, et al. A single radioactive iodine treatment has a deleterious effect on ovarian reserve in women with thyroid cancer: results of a prospective pilot study. *Thyroid.* (2018) 28:522–7. doi: 10.1089/thy.2017.0442
29. Cardis E, Howe G, Ron E, Bebesko V, Bogdanova T, Bouville A, et al. Cancer consequences of the chernobyl accident: 20 years on. *J Radiol Protect.* (2006) 26:127–40. doi: 10.1088/0952-4746/26/2/001
30. Leung KM, Shabat G, Lu P, Fields AC, Lukashenko A, Davids JS, et al. Trends in solid tumor incidence in ukraine 30 years after chernobyl. *J Glob Oncol.* (2019) 5:1–10. doi: 10.1200/JGO.19.00099
31. Saenko VA, Rogounovitch TI. Genetic polymorphism predisposing to differentiated thyroid cancer: a review of major findings of the genome-wide association studies. *Endocrinol. Metab.* (2018) 33:164–74. doi: 10.3803/EnM.2018.33.2.164

Conflict of Interest: The authors declare that the research was conducted in the absence of any commercial or financial relationships that could be construed as a potential conflict of interest.

Copyright © 2020 Drozd, Schneider, Platonova, Panasiuk, Leonova, Oculevich, Shimanskaja, Vershenya, Dedovich, Mitjukova, Grelle, Biko and Reiners. This is an open-access article distributed under the terms of the Creative Commons Attribution License (CC BY). The use, distribution or reproduction in other forums is permitted, provided the original author(s) and the copyright owner(s) are credited and that the original publication in this journal is cited, in accordance with accepted academic practice. No use, distribution or reproduction is permitted which does not comply with these terms.



Radiation Exposure to the Thyroid After the Chernobyl Accident

Vladimir Drozdovitch*

Division of Cancer Epidemiology and Genetics, National Cancer Institute, NIH, DHHS, Bethesda, MD, United States

Introduction: The Chernobyl accident resulted in a considerable release of radioactivity to the atmosphere, particularly of Iodine-131 (^{131}I), with the greatest contamination occurring in Belarus, Ukraine, and western part of Russia.

Material and Methods: Increase in thyroid cancer and other thyroid diseases incidence in population exposed to Chernobyl fallout in these counties was the major health effect of the accident. Therefore, a lot of attention was paid to the thyroid doses, mainly, the ^{131}I intake during two months after the accident. This paper reviews thyroid doses, both the individual for the subjects of radiation epidemiological studies and population-average doses. Exposure to ^{131}I intake and other exposure pathways to population of affected regions and the Chernobyl cleanup workers (liquidators) are considered.

Results: Individual thyroid doses due to ^{131}I intake varied up to 42 Gy and depended on the age of the person, the region where a person was exposed, and their cow's milk consumption habits. Population-average thyroid doses among children of youngest age reached up to 0.75 Gy in the most contaminated area, the Gomel Oblast, in Belarus. Intake of ^{131}I was the main pathway of exposure to the thyroid gland; its mean contribution to the thyroid dose in affected regions was more than 90%. The mean thyroid dose from inhalation of ^{131}I for early Chernobyl cleanup workers was estimated to be 0.18 Gy. Individual thyroid doses due to different exposure pathways varied among 1,137 cleanup workers included in the epidemiological studies up to 9 Gy. Uncertainties associated with dose estimates, in terms of mean geometric standard deviation of individual stochastic doses, varied in range from 1.6 for doses based on individual-radiation measurements to 2.6 for "modelled" doses.

Conclusion: The ^{131}I was the most radiologically important radionuclide that resulted in radiation exposure to the thyroid gland and cause an increase in the rate of thyroid cancer and other thyroid diseases in population exposed after the Chernobyl accident.

Keywords: Chernobyl, thyroid, radiation, exposure, Iodine-131

INTRODUCTION

The Chernobyl accident that occurred on 26 April 1986 led to widescale radioactive contamination of territories in Belarus, Ukraine and the western part of Russia. The accident resulted in the release from the damaged reactor of a large amount of radionuclides into the atmosphere, including the radiologically significant short-lived Iodine-131 (^{131}I), Tellurium-132 (^{132}Te), Iodine-133 (^{133}I), and

OPEN ACCESS

Edited by:

Christoph Reiners,
University Hospital Würzburg,
Germany

Reviewed by:

Michele Minuto,
University of Genoa, Italy
Francesco Frasca,
University of Catania, Italy

*Correspondence:

Vladimir Drozdovitch
drozdovv@mail.nih.gov

Specialty section:

This article was submitted to
Thyroid Endocrinology,
a section of the journal
Frontiers in Endocrinology

Received: 02 June 2020

Accepted: 17 November 2020

Published: 05 January 2021

Citation:

Drozdovitch V (2021) Radiation
Exposure to the Thyroid After
the Chernobyl Accident.
Front. Endocrinol. 11:569041.
doi: 10.3389/fendo.2020.569041

long-lived Caesium-134 and Caesium-137 (^{134}Cs and ^{137}Cs) (1). Two main groups of people were exposed to radioactive fallout: (1) representatives of the population in the contaminated territories in Belarus, Ukraine, and Russia; and (2) cleanup workers (emergency and recovery workers or liquidators) who were the first responders or participated in cleanup activities at the site of the Chernobyl nuclear power plant (NPP) and in the 30-km zone around the NPP. Young children were among the population groups most affected by accident as they consumed cow's milk contaminated with ^{131}I .

The increase of thyroid cancer among persons who were exposed to Chernobyl fallout during childhood and adolescence were reported a few years after the accident, first in Belarus (2) and in Ukraine (3), and later in Russia (4). A number of radiation epidemiology studies have demonstrated an increased risk of thyroid cancer and other thyroid diseases associated with exposure of the thyroid gland to ^{131}I (5–12). Results from these and other studies conducted in the affected population (13–15) suggested that an increase in the incidence of thyroid cancer in individuals exposed in childhood and adolescence was the main health effect of the Chernobyl accident. The excess odds ratios (EOR) of radiation-related thyroid cancer derived in these cohort and case-control studies were similar within the range of uncertainties and varied from 1.36 Gy^{-1} (95% confidence interval (CI): 0.39–4.15) (10) to 8.4 Gy^{-1} (95% CI: 4.1–17.3) (14). An increased risk of thyroid cancer, not statistically significant, (EOR/Gy = 3.91, 95% CI: –1.49, 65.7) has been reported in individuals exposed *in utero* (16, 17). Studies among Chernobyl cleanup workers, who were exposed as adults, also reported an increased risk of thyroid cancer after exposure to external irradiation and internal irradiation from ^{131}I intake (18–20).

Since the main health effect of the Chernobyl accident is an increase in the incidence of thyroid cancer and other thyroid diseases, a lot of efforts have been devoted to the assessment of radiation thyroid doses. The main purpose of this paper is to summarize the methods and results of reconstruction of radiation doses to the thyroid of the population exposed to the Chernobyl accident.

THYROID DOSES TO THE MEMBERS OF THE GENERAL PUBLIC

In the aftermath of the Chernobyl accident, the radiation absorbed dose to the thyroid gland for the members of the general public resulted mainly from intake of ^{131}I . In brief, the radionuclides, which were released into atmosphere during the accident, deposited on the ground surface, and contaminated the pasture grass and leafy vegetables covering the ground. The grazing cows ate contaminated grass and some fraction of the radioactivity was transferred to their milk. The consumption of fresh cow's milk contaminated with ^{131}I was the main pathway of thyroid exposure while the ^{131}I intake with leafy vegetables and inhaled contaminated air playing a minor role. The radiation dose due to ^{131}I intake is the highest for the thyroid gland as iodine accumulates in this organ. Thyroid doses in children are higher

than that of adults is because of the smaller size of the thyroid gland in children. Since the half-life of ^{131}I is 8.02 days, radiation exposure to the thyroid gland occurred during the first two months after the accident when the activity of ^{131}I in the environment became negligible.

In addition, there were other contributors to the thyroid exposure, which were typically rather small for most individuals, but relatively important for those with no or little milk consumption: (1) internal irradiation due to intake of short-lived radioiodine and radiotellurium isotopes (^{132}I , ^{133}I , ^{135}I , $^{131\text{m}}\text{Te}$, and ^{132}Te); (2) external irradiation from gamma-emitted radionuclides deposited on the ground; and (3) internal irradiation resulting from intake of long-lived ^{134}Cs and ^{137}Cs .

There are two types of doses to the members of general public: (1) an individual dose for a specified person that takes into account (i) information on individual whereabouts and consumption history collected, typically, by means of personal interview and (ii) individual-based radiation measurements, if available; and (2) a population-average dose for an unspecified individual that is estimated using generic values of dosimetry models. Estimates of individual dose are required for radiation epidemiological studies while the population-average doses are used for the radiation protection of population by comparing of exposure levels in population groups of different ages living in different territories.

Radiation thyroid doses are also classified as “instrumental” doses, which are estimated using individual-based radiation measurements, and ‘modelled’ doses, which are estimated using dosimetry models.

Radiation and Thyroid Volume Measurements Available for Exposure Assessment

The following information was available to reconstruct radiation doses to the population in Belarus, Ukraine and Russia:

- About 400,000 measurements of ^{131}I thyroidal activity that were derived from gamma-spectrometric and radiometric measurements (called “direct thyroid measurements”) made between 26 April and 30 June 1986 among the population resided in contaminated areas (21–23). These measurements were used to estimate the thyroid doses due to ^{131}I intake for measured individuals.
- ^{137}Cs ground deposition density measured in almost every contaminated settlement in Belarus, Ukraine and Russia (24).
- Ground deposition densities of ^{131}I and other gamma-emitting radionuclides (^{95}Zr , ^{95}Nb , ^{103}Ru , ^{106}Ru , ^{134}Cs , ^{141}Ce , ^{144}Ce), measured in some locations (25–28).
- Activity concentration of ^{131}I and total beta-activity in cow's milk (29–31).
- More than 600,000 measurements of radiocesium activity in individuals living in contaminated territories made using whole-body counter (32–35);
- Thyroid volume-values measured by the Sasakawa Memorial Health Foundation in Belarus, Ukraine, and Russia in the 1990s (36–38).

Thyroid Doses from Intake of ^{131}I Individual Thyroid Doses for the Subjects of Epidemiological Studies

The most reliable individual thyroid doses were estimated based on the results of measurements of ^{131}I thyroidal activity carried out in the most contaminated oblasts (regions) in Belarus, Ukraine, and Russia (**Figure 1**). There are two cohort studies that used estimates of individual ^{131}I thyroidal activity available for each cohort member and provided the uncertainties associated with estimates of thyroid doses due to ^{131}I intake. These two thyroid screening cohorts consist of people who were 0–18 years old at the time of the accident (ATA), 11,732 individuals in the Belarusian-American (BelAm) cohort and 13,204 individuals in the Ukrainian-American (UkrAm) cohort (39). The BelAm cohort includes persons who resided ATA in Gomel and Mogilev Oblasts as well as in the city of Minsk; UkrAm cohort consists of residents of Chernihiv, Kyiv, and Zhytomyr Oblasts (see **Figure 1**).

Information on residential history, consumption of cows' milk, dairy products, and leafy vegetables as well as the administration of stable iodine necessary for the assessment of the individual thyroid doses was collected for each cohort member by means of personal interviews (40, 41). Another two screening thyroid cohorts consist of persons exposed *in utero*, 2,965 and 2,582 individuals in Belarus and Ukraine, respectively (16, 42). A fraction of the cohorts' members, around 10% in Belarus and 28% in Ukraine, was subject to direct thyroid measurements (43, 44). Practically the same methodology was used to assess the individual thyroid doses in the BelAm and UkrAm cohorts as well as in the Belarusian and Ukrainian *in utero* cohorts.

In the BelAm and UkrAm studies, thyroid doses due to ^{131}I intake were calculated in a stochastic mode using a Monte-Carlo simulation procedure that provides an estimate of the uncertainties (41, 45). In accordance with this procedure, 1,000 *individual stochastic* thyroid doses were calculated, considering the classification of errors as shared or unshared. The distribution of *individual stochastic* thyroid doses for cohort members was approximately lognormal; the geometric standard deviation (GSD) of this distribution characterized the uncertainty of dose estimates.

Table 1 shows the distribution of individual thyroid doses in these four cohorts. More than 2/3 of the subjects of the BelAm and UkrAm cohorts received thyroid doses less than 0.5 Gray (Gy) and of the Belarusian and Ukrainian *in utero* cohorts received thyroid doses less than 0.05 Gy. Individual thyroid doses varied widely from 0 to 39, 42, 15, and 3.2 Gy in the BelAm, UkrAm, Belarusian and Ukrainian *in utero* cohorts, respectively.

The *individual stochastic* doses were characterized by the GSDs from 1.3 to 5.1 with (an arithmetic mean (AM) of 1.8, a geometric mean (GM) of 1.7) for the BelAm cohort, and from 1.3 to 10.6 (AM of 1.6, GM of 1.5) for the UkrAm cohort. The uncertainties in thyroid doses were mainly defined by sources of unshared (classical) errors: the derivation of ^{131}I activity in the cohort member's thyroid from direct thyroid measurements and the values of thyroid mass (41, 45, 46).

If the result of measurement of ^{131}I thyroidal activity was not available for the individual, thyroid doses were estimated using two types of models:

- Purely empirical models that were based on the correlation between environmental contamination (deposition density of ^{131}I or ^{137}Cs , ^{131}I activity concentration in cow's milk) and



FIGURE 1 | Areas in Belarus, Ukraine, and Russia. Territories with ^{137}Cs ground deposition density greater than 37 kBq m^{-2} are shown in gray.

TABLE 1 | Distribution (%) of thyroid doses from intake of ^{131}I and mean, median, and maximal dose among subjects of the screening cohorts in Belarus and Ukraine (41, 43–45).

Thyroid dose (Gy)	Belarusian cohort ^a	Ukrainian cohort ^a	Belarusian in utero cohort ^b	Ukrainian in utero cohort ^b
<0.05	16.9	18.1	67.3	73.9
0.05–0.199	25.6	32.9	18.4	17.0
0.2–0.499	24.0	21.4	9.2	6.2
0.5–0.99	15.9	12.3	3.3	1.9
1.0–4.99	15.9	13.4	1.6	1.0
5–9.99	1.3	1.3	0.2	–
≥10	0.4	0.6	0.03	–
Arithmetic mean	0.68	0.65	0.12	0.072
Median dose	0.27	0.19	0.014	0.012
Maximal dose	39	42	15	3.2
N of persons	11,732	13,204	2,965	2,582

^aDistribution is shown for arithmetic mean of individual stochastic doses.

^bPrenatal thyroid dose.

thyroid doses derived from direct thyroid measurements done among individuals of different ages (21, 22, 29, 47–49); and

- An environmental transfer model that considers a process of ^{131}I activity transfer to the human thyroid with contaminated milk and/or leafy vegetables for ingestion or with contaminated ground-level air for inhalation (50, 51).

To estimate the individual modelled thyroid doses, a personal interview was conducted to collect information on the whereabouts and consumption history for a given person. Individual thyroid doses estimated using the models, called “modelled” doses, were associated with uncertainties arose mainly from the estimates of ^{131}I ground deposition density in the place of residence, the transfer of ^{131}I to cow’s milk, and estimates of the thyroid mass (46, 47, 52).

Table 2 presents the thyroid doses due to ^{131}I by age and by country of residence among the subjects of the case-control study of thyroid cancer in Belarus and Russia (**Figure 1**), which was coordinated by the International Agency for Research on Cancer

TABLE 2 | Thyroid doses due to ^{131}I intake at different ages and by country of residence among subjects of the case-control study of thyroid cancer in Belarus and Russia (53).

Age (year)	Thyroid dose ^a (Gy)	
	Belarus	Russia
<2	0.70	0.43
2–4.9	0.51	0.14
5–9.9	0.38	0.033
10–14.9	0.19	0.021
15–18	0.20	0.020
Arithmetic mean (Gy)	0.54	0.10
Median dose (Gy)	0.29	0.022
Maximal dose (Gy)	8.7	4.9
N of persons	1,695	534

^aArithmetic mean of individual stochastic doses.

(IARC). Data from the table show that the thyroid dose decreased with increasing age. The thyroid dose in Russia was estimated to be more than five times lower than that in Belarus, 0.10 vs. 0.54 Gy for mean. The *individual stochastic* doses were characterized by the GSDs from 1.59 to 3.61 (AM of 1.94, GM of 1.89). The uncertainties in thyroid doses were defined by the shared (Berkson) errors in parameters of the model and by unshared (classical) errors related to the estimates of thyroid-mass values (52, 53).

Population Average Dose Estimates

Thyroid doses from intake of ^{131}I for population groups were estimated using a combination of the methods indicated above. The following groups of population were considered (54, 55): evacuees from the 30-km zone around Chernobyl NPP and residents of the contaminated areas in the most affected countries, Belarus, Ukraine and Russia.

Evacuees. More than 100,000 persons were evacuated in the weeks after the accident from the most contaminated 30-km zone around the Chernobyl NPP in Ukraine and Belarus. The thyroid doses varied with place of residence, date of evacuation, and the age of the evacuees. Evacuees from Belarusian villages received the highest doses, the average thyroid dose was estimated to be 0.68 Gy for adults and 3.1 Gy for young children (0–7 years old) vs. 0.28 Gy and 1.2, respectively, for evacuees from Ukrainian villages (54). The thyroid doses for the residents evacuated from the town of Pripyat were 0.28 Gy for adults and 0.99 Gy for young children received mainly due to the ^{131}I intake with cow’s milk during their stay in the villages where they were evacuated (56). The population-weighted average thyroid dose for the entire evacuated population was 0.47 Gy. It should be noted that dose estimates were based on direct thyroid measurements carried out among evacuated persons.

Residents of the Contaminated Areas. **Table 3** shows estimates of thyroid doses due to ^{131}I for the populations of Belarus, Ukraine, and Russia (1, 57). Population-average thyroid doses depended on the varied from region to region dates of fallout and ^{131}I ground deposition densities, and on the dates when pasture grazing season started. The latter is vital, since cow’s milk was the main source of ^{131}I intake to the exposed population. The highest Oblast-average thyroid dose due to ^{131}I intake among the three countries was realized in the most contaminated Gomel Oblast in Belarus, it varied from 0.15 Gy for adults to 0.75 Gy for young children. The highest dose in Ukraine was found in Zhytomyr Oblast, 0.06 Gy for adults and 0.23 Gy for children 0–7 years old; and in Russia in Bryansk Oblast, 0.026 Gy for adults and 0.16 Gy for children 0–7 years old.

Thyroid Doses from Pathways Other than Intake of ^{131}I

Thyroid doses for most individuals were mainly due to ^{131}I intake. However, there were other exposure pathways with typically small contribution to the thyroid dose: (1) intake of short-lived radioiodine and radiotellurium isotopes (^{132}I , ^{133}I , ^{135}I , $^{131\text{m}}\text{Te}$, and ^{132}Te); (2) external irradiation from gamma-emitting radionuclides deposited on the ground (mainly $^{140}\text{Ba} + ^{140}\text{La}$, $^{95}\text{Zr} + ^{90}\text{Nb}$, and $^{132}\text{Te} + ^{132}\text{I}$ shortly after the

TABLE 3 | Estimates of thyroid doses due to ^{131}I intake for the populations of Belarus, Ukraine, and Russia (1, 5).

Region	Size of population	Thyroid dose (Gy)	
		1 year	Adults
Belarus			
Brest Oblast	1,408,000	0.12	0.026
Vitebsk Oblast	1,410,000	0.007	0.002
Gomel Oblast	1,651,000	0.75	0.15
Grodno Oblast	1,154,000	0.028	0.006
Minsk Oblast	1,587,000	0.016	0.005
Minsk City	1,518,000	0.10	0.018
Mogilev Oblast	1,280,000	0.13	0.031
Ukraine			
Chernihiv Oblast	1,416,000	0.15	0.037
Kyiv Oblast	1,685,000	0.20	0.053
Kyiv City	2,565,000	0.094	0.024
Rivne Oblast	1,164,000	0.15	0.029
Zhytomyr Oblast	1,548,000	0.23	0.060
Russia			
Bryansk Oblast	1,473,000	0.16	0.026
Kaluga Oblasts	1,041,000	0.013	0.002
Orel Oblasts	863,000	0.058	0.009
Tula Oblasts	1,863,000	0.044	0.006

accident and ^{134}Cs and ^{137}Cs in the long term); and (3) intake of long-lived ^{134}Cs and ^{137}Cs . The methods used to estimate thyroid doses from these pathways are described elsewhere (28, 33, 34, 47, 58, 59).

Table 4 shows the contribution of minor exposure pathways to the individual thyroid doses reconstructed for the subjects of epidemiological studies. The contribution varied from 5 to 8% for subjects of the studies conducted in Belarus and was about 10% for subjects in Russia.

However, the contribution of minor pathways may be substantial for some individuals. For evacuees from Prip'yat-town, which is located near the Chernobyl NPP, the inhalation intake of short-lived radioiodine and radiotellurium isotopes (^{132}I , ^{133}I , and ^{132}Te) contributed about 30% to the total thyroid dose due to inhalation (61). For the IARC coordinated case-control study of thyroid cancer in Belarus and Russia, it was estimated that for 19 out of 1,615 (1.3% of the total) study subjects, the contribution of external irradiation and ingestion of radiocesium isotopes to the thyroid dose was higher than 50% (60). These individuals were relocated from contaminated residents shortly after the accident or did not consume locally

produced foodstuffs and, therefore, were exposed to relatively small doses from ^{131}I intake in April–June 1986 but received high doses from long-lived sources of exposure in subsequent years.

THYROID DOSES TO THE CHERNOBYL CLEANUP WORKERS

Following the Chernobyl accident, more than 500,000 cleanup workers participated from 26 April 1986 to 31 December 1990 in cleanup activities on the reactor site and in the restricted 30-km zone around the Chernobyl NPP (1). Cleanup workers consisted of different occupational groups, including Chernobyl NPP personnel, nuclear workers, military, construction workers, and support staff, who performed work on decontamination and maintenance at the Chernobyl site, construction and safeguard at various locations (62, 63).

Basically, the cleanup workers received doses due to external irradiation (64–66). However, during the 10-day period of atmospheric releases of radioactivity from destroyed Unit 4, the cleanup workers also were exposed to internal irradiation due to inhalation of ^{131}I and short-lived ^{132}I , ^{133}I , ^{135}I , ^{131m}Te , and ^{132}Te . In addition, cleanup workers, who resided in contaminated areas in Belarus, Ukraine and Russia received thyroid doses due to ^{131}I intake with cow's milk, dairy products and leafy vegetables produced at their places of residence.

Cleanup Workers With Direct Thyroid Measurements

A group of 594 Chernobyl cleanup workers was measured for ^{131}I thyroidal activity between 30 April and 5 May 1986 (67). At the time of the direct thyroid measurement, each person provided information on his or her cleanup activities since 26 April 1986 as well as on stable iodine administration. As measured individuals were the operation personnel of the Chernobyl NPP, only inhalation intake of ^{131}I with contaminated air was considered in calculation of the thyroid doses.

Table 5 shows the distribution of thyroid doses for cleanup workers with direct thyroid measurements. The average thyroid dose among the cleanup workers was 0.18 Gy and the median was 0.11 Gy. About 73% of the cleanup workers received thyroid

TABLE 4 | Contribution of minor exposure pathways to the individual thyroid dose reconstructed for the subjects of epidemiological studies (34, 40, 43, 60).

Pathway	Mean contribution (%) of minor exposure pathways to the individual thyroid dose among the subjects of the study				
	Belarusian–American cohort Belarus	Belarusian <i>in utero</i> cohort Belarus	Case-control study Belarus	Case-control study Belarus	Case-control study Russia
Intake of short-lived radionuclides ^a	2.0	— ^b	2.0	1.6	0.7
External irradiation	4.5	3.6	1.8	3.4	6.3
^{137}Cs ingestion	1.5	1.8	1.0	1.3	2.3
All minor exposure pathways	8.0	5.4	4.8	6.3	9.3

^aShort-lived radioiodine (^{132}I , ^{133}I , ^{135}I) and radiotellurium (^{131m}Te and ^{132}Te) isotopes.

^bNot considered.

TABLE 5 | Distribution of the thyroid doses from inhalation of ^{131}I for the 594 Chernobyl cleanup workers with direct thyroid measurements (67).

Dose interval (Gy)	N	%	Mean dose in interval (Gy)
<0.02	34	5.7	0.014
0.02–0.049	89	15.0	0.036
0.050–0.099	150	25.2	0.076
0.10–0.199	156	26.3	0.14
0.20–0.499	129	21.7	0.31
0.50–0.999	30	5.1	0.68
≥1.0	6	1.0	1.8
Entire study population	594	100.0	0.18

doses between 0.05 and 0.50 Gy. The highest individual thyroid dose due to ^{131}I intake estimated among Chernobyl cleanup workers based on direct thyroid measurement was 4.5 Gy.

Thyroid Doses for the Subjects of Epidemiological Studies

Two case-control thyroid-cancer studies were conducted among Chernobyl cleanup workers: (1) a study nested within cohorts of Belarusian, Russian, and Baltic (Latvia, Lithuania and Estonia) cleanup workers that was coordinated by the IARC and included 530 subjects (19); and (2) a collaborative study of the National Research Center for Radiation Medicine (Kyiv, Ukraine) and the U.S. National Cancer Institute that was nested in a cohort of Ukrainian cleanup workers and included 607 subjects (68). Individual thyroid doses were estimated for the study subjects

due to (a) external irradiation during a cleanup mission using the RADRUE method (65), (b) internal irradiation during a cleanup mission due to inhalation of (b) ^{131}I and (c) short-lived radioiodine and radiotellurium isotopes as well as from (d) intake of ^{131}I during residence (69). A dosimetry questionnaire was administered to each cleanup worker or his proxy to collect detailed information about (a) the cleanup worker's routes to and from his or her work place(s) at the Chernobyl site and in the 30-km zone, (b) the details about the cleanup activities, (c) residential history between 26 April and 30 June 1986, and (d) consumption of locally produced foodstuffs (only for Ukrainian cleanup workers). To estimate the uncertainties in doses, *individual stochastic* doses for each considered exposure pathway were calculated using Monte Carlo simulations.

Table 6 provides the thyroid doses from different exposure pathways reconstructed for the subjects of epidemiological studies among the Chernobyl cleanup workers. The mean thyroid dose from all exposure pathways was 0.19, 0.10, 0.058, and 0.20 Gy for cleanup workers from Belarus, Russia, Baltic States and Ukraine, respectively. The thyroid dose was formed mainly due to external irradiation, except for Belarusian cleanup workers who were, mainly, residents of the 30-km zone and their dose was defined by ^{131}I intake during cleanup mission and residence. The thyroid doses during residence were not calculated for Russian and Baltic States cleanup workers as ^{131}I deposition densities in their locations of residence were negligible compared to those of Belarusian and Ukrainian cleanup workers.

TABLE 6 | Thyroid doses from different exposure pathways reconstructed for subjects of case-control studies of thyroid cancer among Chernobyl cleanup workers (19, 69).

Exposure pathways ^a	Thyroid dose (Gy) for Chernobyl cleanup workers from			
	Belarus	Russia	Baltic States	Ukraine
<i>External irradiation</i>				
Arithmetic mean	0.0095	0.10	0.057	0.14
Median	0.0018	0.044	0.039	0.020
Range	~0–0.30	4.8×10^{-5} –0.82	7.3×10^{-4} –0.26	1.5×10^{-5} –3.6
<i>Inhalation of ^{131}I^b</i>				
Arithmetic mean	0.13	–	6.8×10^{-4}	0.044
Median	0.024	–	6.8×10^{-4}	0.012
Range	3.3×10^{-5} –3.2	–	5.2×10^{-5} –0.0014	~0–1.7
<i>Inhalation of short-lived radionuclides</i>				
Arithmetic mean	–	–	–	0.011
Median	–	–	–	0.0016
Range	–	–	–	~0–0.38
<i>Intake of ^{131}I during residence</i>				
Arithmetic mean	0.11	–	–	0.042
Median	0.060	–	–	0.0073
Range	2.9×10^{-5} –0.73	–	–	~0–3.4
<i>External irradiation during residence</i>				
Arithmetic mean	0.0050	–	–	–
Median	0.0011	–	–	–
Range	1.5×10^{-5} –0.051	–	–	–
<i>Total</i>				
Arithmetic mean ^c	0.19	0.10	0.058	0.20
Median	0.067	0.044	0.040	0.047
Range	1.9×10^{-4} –3.3	4.8×10^{-5} –0.82	7.3×10^{-4} –0.26	1.5×10^{-4} –9.0

^aDuring the cleanup mission, otherwise indicated.

^bBoth, inhalation and ingestion of ^{131}I for cleanup workers from Belarus.

^cArithmetic mean, median, and range of thyroid doses are given for the study subjects who were exposed to the specific exposure pathway. Therefore, the arithmetic mean of total dose is not equal to the sum of arithmetic means of components of the dose.

For the IARC-coordinated study, the GSDs of the *individual stochastic* doses due to external irradiation varied from 1.1 to 5.8 with a mean of 1.9, while for the thyroid doses due to ^{131}I intake during residence, the GSDs varied from 1.9 to 2.5 with a mean of 2.2 (70). The uncertainties of the *individual stochastic* doses in the Ukrainian-American study were characterized by a mean GSD of 2.0, 1.8, 2.0 and 2.6 for external irradiation, inhalation of ^{131}I , inhalation of short-lived radionuclides, and exposure to ^{131}I intake during residence, respectively (69).

CONCLUSIONS

This paper considers the radiation exposure to the thyroid after the Chernobyl accident. The most important radiological consequence of the accident was exposure to ^{131}I , which led to an increase in the rate of thyroid cancer and other thyroid diseases in the exposed population. The thyroid doses were mainly defined by the consumption of cow's milk contaminated with ^{131}I . Individual thyroid doses due to ^{131}I intake varied up to 42 Gy and depended on the age of person, the region where people were exposed, and their cow's milk consumption habits. In addition to exposure due to ^{131}I , the intake of short-lived radioiodine and radiotellurium isotopes, external irradiation, and the intake of long-lived ^{134}Cs and ^{137}Cs contributed to the thyroid dose of the members of public, typically, not more than 10%.

The mean thyroid dose due to ^{131}I inhalation in a group of 594 early Chernobyl cleanup workers was 0.18 Gy. Individual thyroid doses were also reconstructed for 1,137 cleanup workers included in two case-control studies of thyroid cancer. Their thyroid dose from different exposure pathways, i.e., external

irradiation, inhalation of ^{131}I and short-lived radionuclides during the cleanup mission, and ^{131}I intake during residence, varied within a wide range from essential zero to 9 Gy.

AUTHOR CONTRIBUTIONS

The author confirms being the sole contributor of this work and has approved it for publication.

FUNDING

This work was funded by the Intramural Research Program of the National Cancer Institute (USA), Division of Cancer Epidemiology and Genetics.

ACKNOWLEDGMENTS

The author gratefully acknowledges the contribution of the late Drs. Yuri Gavrilin, Valeri Khrouch, Ilya Likhtarov, and Nickolas Luckyanov to the design, development, and implementation of the dosimetry for the studies considered in the paper. The author also gratefully acknowledges the contribution of Lynn Anspaugh, Elena Bakhanova, André Bouville, Mikhail Balonov, Vadim Chumak, Mykola Chepurny, Ivan Golovanov, Victor Kryuchkov, Lionella Kovgan, Semion Kutsen, Sergii Masiuk, Victor Minenko, Sergey Shinkarev, Valeri Stepanenko, Paul Voillequé, Irina Zvonova, and many others to the dosimetry methods applied in the reviewed studies.

REFERENCES

- United Nations Scientific Committee on the Effects of Atomic Radiation (UNSCEAR). *Sources and Effects of Ionizing Radiation, UNSCEAR 2008 Report. Annex D: Health effects due to radiation from the Chernobyl accident. Sales No. E.11.IX.3*. New York: United Nations (2011).
- Kazakov VS, Demidchik EP, Astakhova LN. Thyroid cancer after Chernobyl. *Nature* (1992) 359:21. doi: 10.1038/359021a0
- Prisyazhiuk A, Pjatak OA, Buzanov VA, Reeves GK, Beral V. Cancer in the Ukraine, post Chernobyl. *Lancet* (1991) 338:1334–5. doi: 10.1016/0140-6736(91)92632-c
- Ivanov VK, Tsyb AF, Matveenko YG, Parshkov YM, Maksyutov MA, Gorskiy AI, et al. Radiation epidemiology of cancer- and non-cancer thyroid diseases in Russia after the ChNPP accident: Prognostication and risk estimation. *Radiat Risk* (1995) 1:3–29.
- Brenner AV, Tronko MD, Hatch M, Bogdanova TI, Oliynyk VA, Lubin JH, et al. I-131 dose response for incident thyroid cancers in Ukraine related to the Chernobyl accident. *Environ Health Perspect* (2011) 119:933–9. doi: 10.1289/ehp.1002674
- Cahoon EK, Nadirov EA, Polanskaya ON, Yauseyenko VV, Velalkin IV, Minenko VF, et al. Risk of prevalent thyroid nodules in residents of Belarus exposed to Chernobyl fallout as children and adolescents. *J Clin Endocrinol Metab* (2017) 102:2207–21. doi: 10.1210/jc.2016-3842
- Ostroumova E, Brenner A, Oliynyk V, McConnell R, Robbins J, Terekhova G, et al. Subclinical hypothyroidism after radioiodine exposure: Ukrainian-American cohort study of thyroid cancer and other thyroid diseases after the Chernobyl accident (1998–2000). *Environ Health Perspect* (2009) 117:745–50. doi: 10.1289/ehp.0800184
- Ostroumova E, Rozhko A, Hatch M, Furukawa K, Polyanskaya O, McConnell RJ, et al. Measures of thyroid function among Belarusian children and adolescents exposed to Iodine-131 from the accident at the Chernobyl nuclear plant. *Environ Health Perspect* (2013) 121:865–71. doi: 10.1289/ehp.1205783
- Tronko MD, Howe GR, Bogdanova TI, Bouville AC, Epstein OV, Brill AB, et al. A cohort study of thyroid cancer and other thyroid diseases after the Chernobyl accident: thyroid cancer in Ukraine detected during first screening. *J Natl Cancer Inst* (2006) 98:896–903. doi: 10.1093/jnci/djj244
- Tronko M, Brenner A, Bogdanova T, Shpak V, Hatch M, Oliynyk V, et al. Thyroid neoplasia risk is increased nearly 30 years after the Chernobyl accident. *Int J Cancer* (2017) 141:1585–8. doi: 10.1002/ijc.30857
- Zablotska LB, Ron E, Rozhko AV, Hatch M, Polyanskaya ON, Brenner AV, et al. Thyroid cancer risk in Belarus among children and adolescents exposed to radioiodine after the Chernobyl Accident. *Br J Cancer* (2011) 104:181–7. doi: 10.1038/sj.bjc.6605967
- Zablotska LB, Nadyrov EA, Polyanskaya ON, McConnell RJ, O'Kane P, Lubin J, et al. Risk of thyroid follicular adenoma among children and adolescents in Belarus exposed to Iodine-131 after the Chernobyl accident. *Am J Epidemiol* (2015) 182:781–90. doi: 10.1093/aje/kwv127
- Astakhova LN, Anspaugh LR, Beebe GW, Bouville A, Drozdovitch VV, Garber V, et al. Chernobyl-related thyroid cancer in children of Belarus: a case-control study. *Radiat Res* (1998) 150:349–56. doi: 10.2307/3579983
- Cardis E, Kesminiene A, Ivanov V, Malakhova I, Shibata Y, Khrouch V, et al. Risk of thyroid cancer after exposure to ^{131}I in childhood. *J Natl Cancer Inst* (2005) 97:724–32. doi: 10.1093/jnci/dji129
- Davis S, Stepanenko V, Rivkind N, Kopecky KJ, Voillequé P, Shakhhtar V, et al. Risk of thyroid cancer in the Bryansk Oblast of the Russian Federation

- after the Chernobyl power station accident. *Radiat Res* (2004) 162:241–8. doi: 10.1667/rr3233
16. Hatch M, Brenner A, Bogdanova T, Derevyanko A, Kuptsova N, Likhtarev I, et al. A screening study of thyroid cancer and other thyroid diseases among individuals exposed in utero to Iodine-131 from Chornobyl fallout. *J Clin Endocrinol Metab* (2009) 94:899–906. doi: 10.1210/jc.2008-2049
 17. Hatch M, Brenner AV, Cahoon EK, Drozdovitch V, Little MP, Bogdanova T, et al. Thyroid cancer and benign nodules after exposure in utero to fallout from Chernobyl benign thyroid nodules. *J Clin Endocrinol Metab* (2019) 104:41–8. doi: 10.1210/jc.2018-00847
 18. Ivanov VK, Tsyb AF, Gorsky AI, Maksyutov MA, Rastopchin EM, Konogorov AP, et al. Thyroid cancer among “liquidators” of the Chernobyl accident. *Br J Radiol* (1997) 70:937–41. doi: 10.1259/bjr.70.837.9486071
 19. Kesminiene A, Evrard AS, Ivanov VK, Malakhova IV, Kurtinaitis J, Stengrevics A, et al. Risk of thyroid cancer among Chernobyl liquidators. *Radiat Res* (2012) 178:425–36. doi: 10.1667/RR2975.1
 20. Ostroumova E, Gudzenko N, Brenner A, Gorokh Y, Hatch M, Prisyazhnyuk A, et al. Thyroid cancer incidence in Chernobyl liquidators in Ukraine: SIR analysis, 1986–2010. *Eur J Epidemiol* (2014) 29:337–42. doi: 10.1007/s10654-014-9896-1
 21. Gavrilin YI, Khrouch VT, Shinkarev SM, Krysenko NA, Skryabin AM, Bouville A, et al. Chernobyl accident: Reconstruction of thyroid dose for inhabitants of the Republic of Belarus. *Health Phys* (1999) 76:105–19. doi: 10.1097/00004032-199902000-00002
 22. Likhtarov I, Kovgan L, Vavilov S, Chepurny M, Bouville A, Luckyanov N, et al. Post-Chernobyl thyroid cancers in Ukraine. Report 1. Estimation of thyroid doses. *Radiat Res* (2005) 163:125–36. doi: 10.1667/rr3291
 23. Bratilova AA, Zvonova IA, Balonov MI, Shishkanov NG, Trushin VI, Hoshi M. ¹³¹I content in the human thyroid estimated from direct measurements of the inhabitants of Russian areas contaminated due to the Chernobyl accident. *Radiat Prot Dosimetry* (2003) 105:623–6. doi: 10.1093/oxfordjournals.rpd.a006315
 24. European Commission. Atlas on ¹³⁷Cs deposition on Europe after the Chernobyl accident. Brussels, Luxembourg: European Commission (1998).
 25. Drozdovitch V, Zhukova O, Germenchuk M, Khrutchinsky A, Kukhta T, Luckyanov N, et al. Database of meteorological and radiation measurements made in Belarus during the first three months following the Chernobyl accident. *J Environ Radioact* (2013) 116:84–92. doi: 10.1016/j.jenvrad.2012.09.010
 26. Khrushchinskii AA, Kuten SA, Minenko VF, Zhukova OM, Podgaikaya AA, Germenchuk MG, et al. Radionuclide ratios in precipitation on the territory of Belarus after the Chernobyl accident: Calculation from gamma-spectrometric measurements on soil in May–July 1986. *At Energy* (2014) 117:143–8. doi: 10.1007/s10512-014-9902-4
 27. Mück K, Pröhl G, Likhtarev I, Kovgan L, Meckbach R, Golikov V. A consistent radionuclide vector after the Chernobyl accident. *Health Phys* (2002) 82:141–56. doi: 10.1097/00004032-200202000-00002
 28. Pitkevich VA, Guba VV, Ivanov VK, Chekin SY, Tsyb AF, Vakulovsky SM, et al. Reconstruction of the composition of the Chernobyl radionuclide fallout and external radiation absorbed doses to the population in areas of Russia. *Radiat Prot Dosimetry* (1996) 64:69–92. doi: 10.1093/oxfordjournals.rpd.a031568
 29. Drozdovitch V, Germenchuk M, Bouville A. Using total beta-activity measurements in milk to derive thyroid doses from Chernobyl fallout. *Radiat Prot Dosimetry* (2006) 118:402–11. doi: 10.1093/rpd/nci360
 30. Minenko V, Viarenich K, Zhukova O, Kukhta T, Podgaikaya M, Khrutchinsky A, et al. Activity concentrations of ¹³¹I and other radionuclides in cow’s milk in Belarus during the first month following the Chernobyl accident. *J Environ Radioact* (2020) 220–221:106264. doi: 10.1016/j.jenvrad.2020.106264
 31. Zvonova IA, Bratilova AA, Balonov MI, Shutov VN, Kotik DS, Shaposhnikova EN, et al. ¹³¹I concentration in milk in Russian areas after the Chernobyl accident. In: *Full papers of IRPA-11 International Congress*. Madrid, Spain, 23–28 May 2004, Madrid: IRPA (2004).
 32. Likhtarev IA, Kovgan LN, Vavilov ES, Gluvchinsky RR, Perevznikov ON, Litvinets LN, et al. Internal exposure from ingestion of foods contaminated by ¹³⁷Cs after the Chernobyl accident. Report I. General model: Ingestion doses and countermeasure effectiveness for the adults of Rovno oblast of Ukraine. *Health Phys* (1996) 70:297–317. doi: 10.1097/00004032-199603000-00001
 33. Likhtarev IA, Kovgan LN, Vavilov ES, Perevznikov ON, Litvinets LN, Anspaugh LR, et al. Internal exposure from ingestion of foods contaminated by ¹³⁷Cs after the Chernobyl accident. Report II. Ingestion doses of the rural population of Ukraine up to 12 y after the accident (1986–1997). *Health Phys* (2000) 79:341–57. doi: 10.1097/00004032-200010000-00002
 34. Minenko VF, Ulanovsky A, Drozdovitch V, Shemiakina E, Gavrilin Y, Khrouch V, et al. Individual thyroid dose estimates for a case-control study of Chernobyl-related thyroid cancer among children of Belarus. Part II. Contributions from long-lived radionuclides and external radiation. *Health Phys* (2006) 90:312–27. doi: 10.1097/01.HP.0000183761.30158.c1
 35. Sekitani Y, Hayashida N, Karevskaya IV, Vasilitsova OA, Kozlovsky A, Omiya M, et al. Evaluation of ¹³⁷Cs body burden in inhabitants of Bryansk Oblast, Russian Federation, where a high incidence of thyroid cancer was observed after the accident at the Chernobyl nuclear power plant. *Radiat Prot Dosimetry* (2010) 141:36–42. doi: 10.1093/rpd/ncq137
 36. Ashizawa K, Shibata Y, Yamashita S, Namba H, Hoshi M, Yokoyama N, et al. Prevalence of goiter and urinary iodine excretion levels in children around Chernobyl. *J Clin Endocrinol Metab* (1997) 82:3430–3. doi: 10.1210/jcem.82.10.4285
 37. Likhtarov I, Kovgan L, Masiuk S, Chepurny M, Ivanova O, Gerasymenko V, et al. Estimating thyroid masses for children, infants, and fetuses in Ukraine exposed to (¹³¹I) from the Chernobyl accident. *Health Phys* (2013) 104:78–86. doi: 10.1097/HP.0b013e31826e188e
 38. Skryabin AM, Drozdovitch V, Belsky Y, Leshcheva SV, Mirkhaidarov AK, Voillequé P, et al. Thyroid mass in children and adolescents living in the most exposed areas to Chernobyl fallout in Belarus. *Radiat Prot Dosimetry* (2010) 142:292–9. doi: 10.1093/rpd/ncq209
 39. Stezhko VA, Buglova EE, Danilova LI, Drozd VM, Krysenko NA, Lesnikova NR, et al. A cohort study of thyroid cancer and other thyroid diseases following the Chernobyl accident: objectives, design, and methods. *Radiat Res* (2004) 161:481–92. doi: 10.1667/3148
 40. Drozdovitch V, Minenko V, Khrouch V, Leshcheva S, Gavrilin Y, Khrutchinsky A, et al. Thyroid dose estimates for a cohort of Belarusian children exposed to radiation from the Chernobyl accident. *Radiat Res* (2013) 179:597–609. doi: 10.1667/RR3153.1
 41. Likhtarov I, Kovgan L, Masiuk S, Talerko M, Chepurny M, Ivanova O, et al. Thyroid cancer study among Ukrainian children exposed to radiation after the Chernobyl accident: improved estimates of the thyroid doses to the cohort members. *Health Phys* (2014) 106:370–96. doi: 10.1097/HP.0b013e31829f3096
 42. Yauseyenko V, Drozdovitch V, Ostroumova E, Polyanskaya O, Minenko V, Brenner A, et al. Belarusian *in utero* cohort: new opportunity to evaluate health effects of prenatal and early-life exposure to ionizing radiation. *J Radiol Prot* (2020) 40:280–95. doi: 10.1088/1361-6498/ab5c08
 43. Drozdovitch V, Minenko V, Kukhta T, Trofimik S, Grakovitch R, Hatch M, et al. Thyroid dose estimates for a cohort of Belarusian persons exposed in utero and during early life to Chernobyl fallout. *Health Phys* (2020) 118:170–84. doi: 10.1097/HP.0000000000001135
 44. Likhtarov I, Kovgan L, Chepurny M, Ivanova O, Boyko Z, Ratia G, et al. Estimation of the thyroid doses for Ukrainian children exposed in utero after the Chernobyl accident. *Health Phys* (2011) 100:583–93. doi: 10.1097/HP.0b013e3181ff391a
 45. Drozdovitch V, Minenko V, Golovanov I, Khrutchinsky A, Kukhta T, Kutsen S, et al. Thyroid dose estimates for a cohort of Belarusian children exposed to ¹³¹I from the Chernobyl accident: Assessment of uncertainties. *Radiat Res* (2015) 184:203–18. doi: 10.1667/rr13791.1
 46. Likhtarev I, Minenko V, Khrouch V, Bouville A. Uncertainties in thyroid dose reconstruction after Chernobyl. *Radiat Prot Dosimetry* (2003) 105:601–8. doi: 10.1093/oxfordjournals.rpd.a006310
 47. Gavrilin Y, Khrouch V, Shinkarev S, Drozdovitch V, Minenko V, Shemiakina E, et al. Individual thyroid dose estimation for a case-control study of Chernobyl-related thyroid cancer among children of Belarus. Part 1: ¹³¹I, short-lived radioiodines (¹³²I, ¹³³I, ¹³⁵I), and short-lived radiotelluriums (^{131m}Te and ¹³²Te). *Health Phys* (2004) 86:565–85. doi: 10.1097/00004032-200406000-00002

48. Stepanenko VF, Voilleque PG, Gavrilin Y, Khrouch VT, Shinkarev SM, Orlov MY, et al. Estimating individual thyroid doses for a case-control study of childhood thyroid cancer in Bryansk Oblast, Russia. *Radiat Prot Dosimetry* (2004) 108:143–60. doi: 10.1093/rpd/nch017
49. Zvonova IA, Balonov MI, Bratilova AA. Thyroid dose reconstruction for the population of Russia after the Chernobyl accident. *Radiat Prot Dosimetry* (1998) 79:175–8. doi: 10.1093/oxfordjournals.rpd.a032386
50. Drozdovitch VV, Goulko GM, Minenko VF, Paretzke HG, Voigt G, Kenigsberg Y. Thyroid dose reconstruction for the population of Belarus after the Chernobyl accident. *Radiat Environ Biophys* (1997) 36:17–23. doi: 10.1007/s004110050050
51. Vlasov OK, Pitkevich VA. Agro-climate model for estimation of radionuclides transport on food chain and for formation of internal exposure to population. *Radiat Risk* (1999) 11:65–85.
52. Drozdovitch V, Maceika E, Khrouch V, Zvonova I, Vlasov O, Bouville A, et al. Uncertainties in individual doses in a case-control study of thyroid cancer after the Chernobyl accident. *Radiat Prot Dosimetry* (2007) 127:540–3. doi: 10.1093/rpd/ncm360
53. Drozdovitch V, Kesminiene A, Moissonnier M, Veyalkin I, Ostroumova E. Uncertainties in radiation doses for a case-control study of thyroid cancer among persons exposed in childhood to Iodine-131 from Chernobyl fallout. *Health Phys* (2020) 119:222–35. doi: 10.1097/HP.0000000000001206
54. Bouville A, Likharev I, Kovgan L, Minenko V, Shinkarev S, Drozdovitch V. Radiation dosimetry for highly contaminated Ukrainian, Belarusian and Russian populations, and for less contaminated populations in Europe. *Health Phys* (2007) 93:487–501. doi: 10.1097/01.HP.0000279019.23900.62
55. Cardis E, Howe G, Ron E, Bebesko V, Bogdanova T, Bouville A, et al. Cancer consequences of the Chernobyl accident: 20 years after. *J Radiol Prot* (2006) 26:127–40. doi: 10.1088/0952-4746/26/2/001
56. Goulko GM, Chumak VV, Chepurny NI, Henrichs K, Jacob P, Kairo IA, et al. Estimation of ¹³¹I thyroid doses for the evacuees from Pripjat. *Radiat Environ Biophys* (1996) 35:81–7. doi: 10.1007/BF02434029
57. Drozdovitch V, Bouville A, Chobanova N, Filistovic V, Ilus T, Kovačić M, et al. Radiation exposure to the population of Europe following the Chernobyl accident. *Radiat Prot Dosimetry* (2007) 123:515–28. doi: 10.1093/rpd/ncf528
58. Golikov VY, Balonov MI, Jacob P. External exposure of the population living in areas of Russia contaminated due to the Chernobyl accident. *Radiat Environ Biophys* (2002) 41:185–93. doi: 10.1007/s00411-002-0167-2
59. Likharev IA, Kovgan LN, Jacob P, Anspaugh LR. Chernobyl accident: retrospective and prospective estimates of external dose of the population of Ukraine. *Health Phys* (2002) 82:290–303. doi: 10.1097/00004032-200203000-00002
60. Drozdovitch V, Khrouch V, Maceika E, Zvonova I, Vlasov O, Bratilova A, et al. Reconstruction of radiation doses in a case-control study of thyroid cancer following the Chernobyl accident. *Health Phys* (2010) 99:1–16. doi: 10.1097/HP.0b013e3181c910dd
61. Balonov M, Kaidanovsky G, Zvonova I, Kovtun A, Bouville A, Luckyanov N, et al. Contributions of short-lived radioiodines to thyroid doses received by evacuees from the Chernobyl area estimated using early in-vivo measurements. *Radiat Prot Dosimetry* (2003) 105:593–9. doi: 10.1093/oxfordjournals.rpd.a006309
62. Bouville A, Kryuchkov V. Increased occupational radiation doses: nuclear fuel cycle. *Health Phys* (2014) 106:259–71. doi: 10.1097/HP.000000000000066
63. Chumak VV. Physical dosimetry of Chernobyl cleanup workers. *Health Phys* (2007) 93:452–61. doi: 10.1097/01.HP.0000278842.39156.93
64. Chumak VV, Sholom SV, Bakhanova EV, Pasalskaya LF, Musijachenko AV. High precision EPR dosimetry as a reference tool for validation of other techniques. *Appl Radiat Isot* (2005) 62:141–6. doi: 10.1016/j.apradiso.2004.08.029
65. Kryuchkov V, Chumak V, Maceika E, Anspaugh LR, Cardis E, Bakhanova E, et al. RADRUE method for reconstruction of gamma external doses to Chernobyl liquidators in epidemiological studies. *Health Phys* (2009) 97:275–98. doi: 10.1097/HP.0b013e3181ac9306
66. Kryuchkov VP, Kochetkov OA, Tovijanov AG. Mitigation of accident consequences at Chernobyl NPP: radiation and dosimetry issues. Moscow: Izdat (2012).
67. Drozdovitch V, Kryuchkov V, Chumak V, Kutsen S, Golovanov I, Bouville A. Thyroid doses due to Iodine-131 inhalation among Chernobyl cleanup workers. *Radiat Environ Biophys* (2019) 58:183–94. doi: 10.1007/s00411-019-00781-6
68. Cahoon E, Mabuchi K, Drozdovitch V, Little M, Hatch M, Gudzenko N, et al. Risk of thyroid cancer among Chernobyl clean-up workers in Ukraine. *Environ Epidemiol* (2019) 3:49. doi: 10.1097/01.EE9.0000606172.11860.ac
69. Drozdovitch V, Kryuchkov V, Bakhanova E, Golovanov I, Bazyka D, Gudzenko N, et al. Reconstruction of individual thyroid doses for case-control study of thyroid cancer among Ukrainian Chernobyl cleanup workers. *Health Phys* (2020) 118:18–35. doi: 10.1097/HP.0000000000001120
70. Drozdovitch V, Chumak V, Kesminiene A, Ostroumova E, Bouville A. Doses for post-Chernobyl epidemiological studies: Are they reliable? *J Radiol Prot* (2016) 36:R36–73. doi: 10.1088/0952-4746/36/3/R36

Conflict of Interest: The author declares that the research was conducted in the absence of any commercial or financial relationships that could be construed as a potential conflict of interest.

This is an open-access article distributed under the terms of the Creative Commons Attribution License (CC BY). The use, distribution or reproduction in other forums is permitted, provided the original author(s) and the copyright owner(s) are credited and that the original publication in this journal is cited, in accordance with accepted academic practice. No use, distribution or reproduction is permitted which does not comply with these terms.



Advances on circRNAs Contribute to Carcinogenesis and Progression in Papillary Thyroid Carcinoma

Xiaoqin Xu and Jiexian Jing*

Department of Etiology, Shanxi Cancer Hospital, Taiyuan, China

OPEN ACCESS

Edited by:

Christoph Reiners,
University Hospital Würzburg,
Germany

Reviewed by:

Jason David Prescott,
Johns Hopkins Medicine,
United States
Marialuisa Appetecchia,
Istituti Fisioterapici Ospitalieri (IRCCS),
Italy

*Correspondence:

Jiexian Jing
2912972872@qq.com

Specialty section:

This article was submitted to
Cancer Endocrinology,
a section of the journal
Frontiers in Endocrinology

Received: 24 April 2020

Accepted: 13 November 2020

Published: 21 January 2021

Citation:

Xu X and Jing J (2021) Advances on
circRNAs Contribute to
Carcinogenesis and Progression in
Papillary Thyroid Carcinoma.
Front. Endocrinol. 11:555243.
doi: 10.3389/fendo.2020.555243

In view of the highly increased prevalence of papillary thyroid carcinoma (PTC) year by year, it is of great importance to explore new molecular targets for anticancer strategies. Emerging evidence indicates that circular RNAs (circRNAs), characterized by a closed-loop structure and high stability, play important roles in tumorigenesis and development of human cancer by regulating multiple complex biological processes, such as cellular proliferation, metastasis, and metabolism. A comprehensive understanding of the roles of circRNAs will facilitate the development of promising future therapeutic strategies for treating cancers, including PTC. In this paper, we review the profile of circRNA in PTC, its regulatory roles, and the pathological mechanism as well as their related clinical significance. In addition, challenges of this specific field are discussed.

Keywords: papillary thyroid carcinoma, circRNA, characteristics, ceRNA, signaling pathway, diagnosis, prognosis

INTRODUCTION

Thyroid cancer (TC) is the most prevalent endocrine malignancy, accounting for nearly one third of the total head and neck malignancies globally (1, 2). Among all cases, 80%–85% of them are papillary thyroid carcinoma (PTC) (3). Although the overall 5-year survival rate of PTC can reach 97%, the 5-year survival rate of patients with advanced PTC is only 59% (4). PTC can still be life threatening and causes poor prognosis due to its invasiveness and metastasis. Extensive efforts have been conducted on research of the carcinogenesis, progression, and effective therapeutic methods of TC. Despite advances in clinical management, including surgery, radiotherapy, levothyroxine treatment, and target therapy, promising and optimal molecular therapies remain to be further explored. In addition to the DNA mutations, such as the BRAFV600E mutation, which was discovered previously, accumulating evidence indicates that non-coding RNAs (ncRNAs) also participate in the progression and pathogenesis of PTC (5–7). Among them, circular RNAs (circRNAs) have attracted increasing attention. Optimistic exploration of PTC-related circRNA likely will be beneficial to pave the way to improve clinical management.

CircRNAs are a newly identified subclass of ncRNA family, and they are produced cotranscriptionally by the spliceosome at the expense of canonical mRNA isoforms, forming a head-to-tail backsplice characterized by a covalently nonlinear, closed-loop structure that lacks either 5' to 3' polarity or a polyadenylated tail (8). Based on the biogenesis of circRNAs in human cells, they are usually classified into three types: exonic circRNAs (ecircRNAs), which are generated from the exons of pre-mRNAs; intronic circRNAs (ciRNAs), which are produced from the intronic region in the pre-mRNAs; and exon-intron circRNAs (EIciRNAs), which consist of both exons and

introns from the pre-mRNAs. Due to their closed structures, circRNAs are resistant to RNA degradation and more stable than linear RNA. Emerging evidence shows that dysregulation of circRNAs play important roles in promoting tumorigenesis and tumor progression (9). It is demonstrated that circRNAs serve as competitive endogenous RNAs (ceRNAs) or microRNA sponges, compete with microRNAs (miRNAs), and consequently regulate the target gene expression (10). Furthermore, circRNAs are also involved in various physiological and pathophysiological processes, such as modulating alternative splicing (11) and regulating protein–RNA interactions (12). Previous research have profiled the circRNAs expression of PTC and have found significantly differentiated circRNAs in PTC compared with normal thyroid tissue, which may be involved in the pathogenesis of PTC. In the following sections, we highlight

the results of recent research efforts, including the profile of markedly dysregulated circRNAs and their related regulatory networks and clinical significance in PTC as well as the current challenges in the field.

PROFILED circRNAs AND ITS ROLE IN PTC

Expression and Biological Function of circRNAs in PTC

To date, many different circRNAs have been found either upregulated or downregulated in PTC tissues compared with matched adjacent normal tissues (Table 1). In line with tissue

TABLE 1 | Dysregulated circRNAs and their biological function in PTC.

circRNA	circRNAID	chromosomelocation	Length	Host gene	Function	Tissues (T/N)	reference
Upregulation							
circRASSF2	hsa_circ_0059354	chr20:4760668-4766974	4418nt	RASSF2	cell proliferation and cell apoptosis	112pairs	(13)
circFNDC3B	hsa_circ_0006156	chr3:171965322-171969331	526nt	FNDC3B	cell proliferation and cell apoptosis	42pairs	(14)
circFOXO1	hsa_circ_0025033	chr12: 2966846-2983691	3410 nt	FOXO1	cell proliferation, clone-forming, apoptosis, migration and invasion	78pairs /20 pairs	(15, 16)
hsa_circ_0058124	hsa_circ_0058124	chr2:216270960-216274462	864nt	FN1	cell proliferation, tumorigenicity, tumor invasion, and metastasis	92pairs	(17)
hsa_circ_0039411	hsa_circ_0039411	chr16:55523562-55540586	4418nt	MMP2	cell growth, migration, invasion and cell apoptosis	46pairs	(18)
circBACH2	hsa_circ_0001627	chr6: 90959407–90981660	2995nt	BACH2	cell proliferation, migration and invasion	40pairs	(19)
circRAPGEF5	hsa_circ_0001681	chr7: 22330793–22357656	516nt	RAPGEF5	cell proliferation, migration, and invasion	30pairs	(20)
Has_circ_0008274	hsa_circ_0008274	chr11: 96485180-96489456	244nt	UGGT2	cell proliferation and invasion	142pairs	(21)
circEIF6	hsa_circ_0060060	chr20:33867368-33872594	799nt	EIF6	autophagy, cell apoptosis	6pairs	(22)
circZFR	hsa_circ_0072088	chr5:32379220-32388780	693nt	ZFR	cell proliferation, migration and invasion	41pairs	(23)
circRNA_102171	–	–	309nt	SMURF2	cell proliferation, migration and invasion, apoptosis	47pairs	(24)
circNUP214	hsa_circ_0089153	chr9:134011326-134022971	1102nt	NUP214	cell proliferation, invasion, migration and tumorigenesis	30pairs	(25)
hsa_circ_0004458	hsa_circ_0004458	chr8: 18656804-18662408	448nt	PSD3	cell proliferation, cycle, and apoptosis	48pairs	(26)
circ-0103552	hsa_circ_0103552	chr15:43294752-43314999	920nt	UBR1	cell invasion and migration	56pairs	(27)
circ_0067934	hsa_circ_0067934	chr3:170013698-170015181	170nt	PRKCI	cell proliferation, migration, and invasion and apoptosis	57pairs	(28)
circMAN1A2	–	–	–	–	–	57T/121N	(29)
circNEK6	hsa_circ_0088483	chr9:127055127-127101944	911nt	NEK6	cell growth and invasion	GSE3678 GSE93522	(30)
hsa_circRNA_007148	–	–	–	–	–	–	(31)
Down-regulation							
circ-ITCH	–	–	–	–	cell proliferation, invasion and apoptosis	14pairs	(32)
hsa_circ_0137287	hsa_circ_0137287	chr8:92301363-92307931	284nt	SLC26A7	–	120T/60N	(33)
hsa_circRNA_100395	–	–	–	–	–	–	(34)
hsa_circRNA_047771	–	–	–	–	–	–	(35)

T, Tumor tissue; N, Normal tissue.

expression level, most PTC-related circRNAs are dysregulated in corresponding PTC cell lines versus in normal thyroid cell lines. Based on gain- and loss-function experiments *in vivo* and *in vitro*, each identified circRNA displays significantly altered tumor cell biological behavior or cell phenotype in PTC cell lines, such as cell proliferation, cell cycle, apoptosis, migration, and invasion (**Table 1**), suggesting that the particular circRNA may act as an oncogenic driver or a tumor suppressor. Take cell-cycle regulation as an example; knockdown of circRASSF2, circFNDC3B, and circFOXMI caused, respectively, significant G1 phase cell-cycle arrest of TPC-1 cells ($p < 0.01$, $p < 0.01$, and $p < 0.01$, respectively). Silenced circRNA_102171 caused G2 phase arrest, and si-circ_0004458 displayed S phase reduction. In contrast, enhanced circRASSF2 expression increased the G2 phase percentage and decreased the G1 phase percentage of K1 cells ($p < 0.01$). Overexpression of circFNDC3B increased the S-phase percentage and decreased the G0/G1 phase percentage of K1 cells ($p < 0.01$). circFOXMI expression increased the S phase percentage and decreased the G0/G1 phase percentage of K1 cells ($p < 0.01$). On the basis of this series of functional experiments, circRNAs were confirmed to play oncogenic or inhibitory roles in PTC.

Biogenesis, Stability, and Subcellular Location of Profiled circRNAs in PTC

Many reports demonstrate that circRNAs are spliced and derived from the host genes (**Table 1**), and even some circRNAs may impact the mRNA expression level of their host genes. As shown in **Table 1**, characteristics of circRNAs are represented, including circRNA ID (<http://www.circbase.org>), chromosome position, spliced length, and host gene. Among them, most circRNAs are classified as ecircRNAs, such as hsa_circ_0006156 (14), Hsa_circ_0058124 (16), CircBACH2 (19), hsa_circ_0001681 (20), CircRNA_102171 (24), and hsa_circ_0004458 (26). Exceptionally, CircNEK6 is a kind of exonic circRNA encoding the mRNA NEK6. In addition, some circRNAs are not found in circBase because of limited information in current reports, including hsa_circRNA_100395, hsa_circRNA_047771, hsa_circRNA_007148, and circ-ITCH, circMAN1A2.

Generally, stability of the circRNA is critical for exerting its function. Analysis of stability for circRNA and its host gene in PTC cells, treated with transcription inhibitor actinomycin D, reveals that the half-life of circRASSF2 exceeds 24 h, whereas that of RASSF2 mRNA is only about 3 h in TPC-1 cells (13). Similarly, the half-life of circFNDC3B and circFOXMI transcript exceeds 24 h, much more stable than the corresponding host genes FNDC3B and FOXMI (14, 15), respectively. Furthermore, circRNA is resistant to RNase R digestion. This proves that circRNAs are extremely more stable than their mRNA level. Given their stability, circRNAs are appropriate for future clinical applications for PTC.

In addition, subcellular location may be related to the distinct molecular roles of various kinds of circRNAs in cells. EcircRNAs are predominantly localized in the cytoplasm (35), and ciRNAs

and ElciRNAs are preferred in the nucleus (36). Subcellular location by cell fraction assay and FISH analysis indicates that circFNDC3B (14), circBACH2 (19), circRAPGEF5 (20), and circNUP214 (25) are predominantly localized in the cytoplasm of PTC cells, and hsa_circ_0058124 primarily appears in the nucleus and also exists in cytoplasm (17). In brief, it is essential to get the properties of circRNAs to facilitate the following pathological mechanism.

PATHOLOGICAL MECHANISM OF circRNAs IN PTC

CircRNAs are widely involved in human physiological and pathological processes and can be used in various manners (37), including (1) serving as microRNA (miRNA) or protein sponges; (2) interacting with proteins, such as recruiting specific proteins, enhancing protein function, and functioning as protein scaffolding; and (3) translating into peptides. Highly abundant circRNAs have been found to contain many competing miRNA binding sites. Therefore, they can be used as RNA “sponges” to cooperatively adsorb miRNAs, thereby regulating the expression of downstream target genes that are inhibited by miRNAs through competing with endogenous RNAs (38). In cancer research, the use of circRNAs as miRNA sponges to regulate downstream target genes is widely reported.

CircRNA Serves as ceRNA Involved in PTC Progression

CircRNAs are important transcriptional regulators of gene expression, relieving the association between miRNA and target genes involved in the pathogenesis of various diseases. It is reported that circRNAs could act as miRNA sponges and regulate the expression of downstream target genes. Previous studies show that an increasing number of circRNA/miRNA/mRNA axes are identified to promote PTC progression (**Figure 1**). This well depicts the interactional network between circRNA and RNA for a better understanding of the transcriptional regulation mechanism by circRNA. Of note, some RNA regulatory network mediated by circRNA remains to be further improved. For example, circ_0025033/miR-1231 and miR-1304 (16), circ-0103552/miR-127 (27), hsa_circ100395/miR-141-3p/miR-200a-3p (34).

Signaling Pathway Modulated by PTC-Related circRNAs

CircRNAs also exert their regulatory roles to modulate signaling pathways in cancer, for instance, the wnt/ β -catenin signaling pathway (39–40), AMPK/mTOR signaling pathway (41), PI3K/AKT signaling pathways (42–44), and NOTCH pathway (45, 46). As a classical pathway, the wnt signaling pathway is involved in many phases of vertebrate embryonic development and contributes to tumorigenesis. Its aberrant

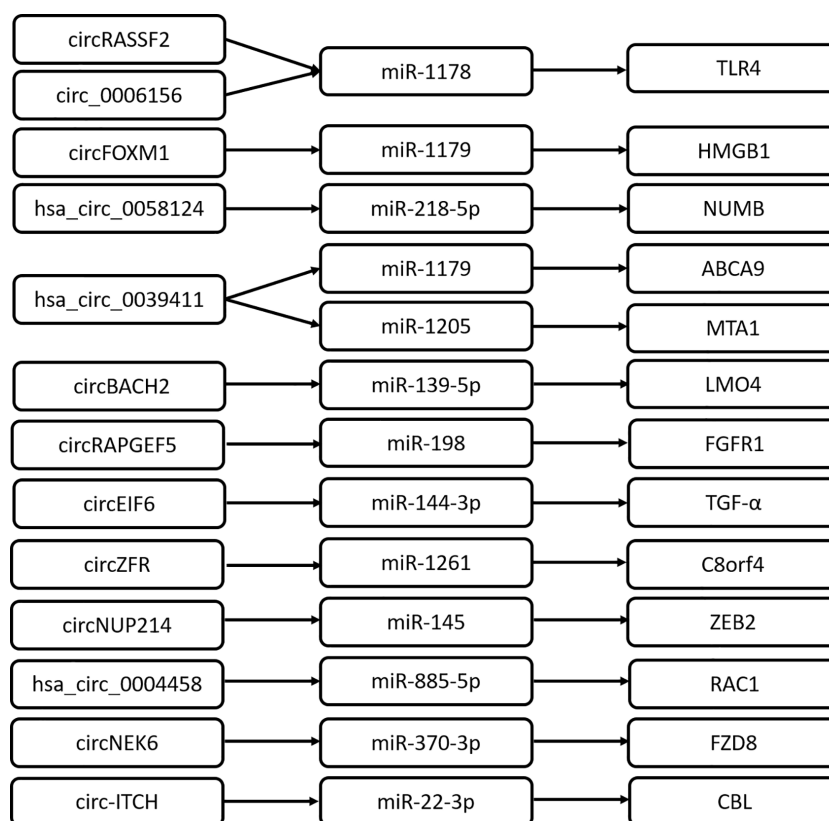


FIGURE 1 | CircRNAs play roles by acting as ceRNA in PTC.

activation could facilitate the progression of various human cancers. CircRNA_102171 directly interacts with CTNNBIP1 and impairs the formation of CTNNBIP1/ β -catenin complex (24). Consequently, circRNA_102171 promotes the interaction of β -catenin with TCF proteins; significantly enhances the expression of corresponding target genes, such as CCND1, CCND2, MYC, and SOX4; and activates the Wnt/ β -catenin pathway in a CTNNBIP1-dependent manner (24). Frizzled class receptor 8 (FZD8) is reported to be one of the cell surface receptors of the Wnt signaling pathway, which belongs to the Frizzled family of serpentine proteins. Chen F et al. find that circNEK6 binds target miR-370-3p to inhibit FZD8 degradation and the upregulated FZD8 activates the wnt signaling pathway (30). Wang M et al. reveals a novel mechanism regulating the wnt pathway by circRNA (32). Circ-ITCH sponges miR-22-3p to elevate CBL (an E3 ligase of nuclear β -catenin) expression, which leads to the inactivation of the Wnt/ β -catenin pathway and consequently attenuates PTC progression. Moreover, Yao Y et al. reports that hsa_circ_0058124 plays an oncogenic driver in PTC by downregulating the NOTCH3 signaling pathway. hsa_circ_0058124 may exert its biological effects in PTC through hsa_circ_0058124/miR-218-5p/NUMB, subsequently with repression of the NOTCH3/GATAD2A axis because NUMB is a strong suppressor of the

NOTCH pathway (17). Collectively, circRNAs modulate various pathways to activate the PTC progression program.

circRNAs ACT AS TUMOR BIOMARKERS IN PTC

The Relationship Between circRNAs and Clinicopathological Parameters in PTC

Clinical analysis reveals that dysregulated circRNAs correlate with aggressive clinicopathological characteristics of PTC, including tumor size, TNM stage, lymph node metastasis, T stage, distal metastasis, and extrathyroidal extension (Table 2). Among them, highly expressed circRASSF2 (13), circFND3B (14), circFOXM1 (15), hsa_circ_0058124 (17), circBACH2 (19), circ_0008274 (21), circZFR (23), hsa_circ_0004458 (26), circ_0067934 (28), and hsa_circRNA_007148 (31) positively correlate with a few aggressive features, whereas lower levels of hsa_circ_0137287 (22), hsa_circRNA_047771 (31), and circ-ITCH (32) negatively correlate with some clinical features. Of note, tumor size is classified by different groups in different research. For example, downregulation of hsa_circ_0137287 correlates with tumor size >2 cm. Upregulated circ_0067934 and circ_0006156 correlate with tumor size >1 cm, hsa_circ_0004458 with tumor size \geq 3 cm,

TABLE 2 | The relationship between circRNAs and clinical features of PTC.

Clinical features	Upregulated circRNAs	Downregulated circRNAs
Tumor size	circFNDC3B (14), circFOX1 (15), hsa_circ_0058124 (17), hsa_circ_0004458 (26), circ_0067934 (28)	hsa_circ_0137287 (22)
Lymph node metastasis	circRASSF2 (13), circFNDC3B (14), circFOX1 (15), hsa_circ_0058124 (17), circBACH2 (19), circ_0008274 (21), circZFR (23), hsa_circ_0004458 (26), circ_0067934 (28), hsa_circRNA_007148 (31)	hsa_circ_0137287 (22), hsa_circRNA_047771 (31), circ-ITCH (32)
TNM stage	circFNDC3B (14), circFOX1 (15), hsa_circ_0058124 (17), circBACH2 (19), circ_0008274 (21), circZFR (23), hsa_circ_0004458 (26), circ_0067934 (28)	hsa_circRNA_047771 (31), circ-ITCH (32)
T stage	circRASSF2 (13), hsa_circ_0004458 (26)	hsa_circ_0137287 (22)
Distal metastasis	circRASSF2 (13), hsa_circ_0004458 (26)	
Extrathyroidal extension	hsa_circ_0058124 (17)	hsa_circ_0137287 (22)

hsa_circ_0058124 with tumor size >2 cm, and circFOX1 with tumor size >3 cm. Generally, PTC is often combined with other types of thyroid disease, such as Hashimoto's thyroiditis (HT), nodular goiter (NG), and so on. It is reported that the level of circFOX1 is significantly associated with NG ($P = 0.009$) (15). In addition, a great deal of previous research indicates that the BRAFV600E mutation is identified as an essential genetic factor in PTC progression. The BRAFV600E mutation, which can cause activation of MAPK pathway signaling, is significantly associated with more aggressive characteristics of PTCs and facilitates risk stratification and the management of patients with thyroid nodules. A decreased hsa_circRNA_047771 expression level is associated with the BRAF^{V600E} mutation ($P < 0.05$) (31). Collectively, the association between circRNAs and aggressive clinicopathological characteristics supports that circRNAs can serve as prognostic factors for PTC patients.

Diagnostic Value of PTC-Related circRNAs

Pathological diagnosis is a gold standard method for the preoperative evaluation of thyroid nodules; however, cytology remains indeterminate for up to 30% of nodules that cannot be definitively diagnosed (47). Except for the BRAFV600E mutation, a novel molecular biomarker is required in favor of clinical diagnosis and risk stratification, especially for efficient management of cN0 papillary thyroid microcarcinoma (PTMC). Extensive exploration in recent years reveals that ncRNAs, such as miRNAs, lncRNAs, and circRNAs, could function as a promising diagnostic biomarker for PTC patients (48, 49). A receiver operating characteristic (ROC) curve was used to evaluate the diagnostic value of circRNAs in PTC tissues compared with paratumor tissues, and it was found that the area under the ROC curve (AUC) of circFNDC3B was 0.891 (95% CI = 0.820–0.961, $P < 0.0001$) (14) and of circBACH2 was 0.8631 (95% CI = 0.7774–0.9489, $P < 0.0001$) (19). More

importantly, circRNAs also serve as postsurgical diagnostic biomarkers. Lan X et al. find that hsa_circ_0137287 has a potential diagnostic value in predicting malignancy (AUC = 0.8973, 95% CI = 0.8452–0.9494, $P < 0.0001$), extrathyroidal extension (AUC = 0.6885, 95% CI = 0.5908–0.7862, $P = 0.0009$), and lymph node metastasis (AUC = 0.6691, 95% CI = 0.5641–0.7742, $P = 0.0034$), respectively (33). Additionally, hsa_circRNA_047771 (AUC = 0.876, 95% CI = 0.78–0.94, sensitivity = 87.5%, specificity = 80.0%) and hsa_circRNA_007148 (AUC = 0.846, 95% CI = 0.75–0.96, sensitivity = 82.5%, specificity = 77.5%) may be candidate diagnostic biomarkers for PTC (31). In view of, so far, limited exploration, further studies are required to discover more optimal biomarkers for diagnosis of PTC.

Predicting Roles of circRNAs for Prognosis in PTC

Previous follow-up studies indicate that most PTC patients have a good prognosis: 85% of PTC cases are highly curable for innocent biological behavior. However, it is necessary to carefully observe the recurrence and metastasis, especially for advanced PTC patients. As with other coding genes (BRAFV600E, RAS, etc.) and noncoding genes (miRNA, lncRNA, etc.), circRNAs may be potential predictors for prognosis of PTC. Kaplan–Meier survival curve analysis reveals that PTC patients with low expression of circFNDC3B display obviously longer overall survival (OS) times than those with high expression of circFNDC3B ($P < 0.05$) (14). Similar to circFNDC3B, downregulated circBACH2 had relatively longer OS ($P < 0.05$) (19), a higher expression of circZFR in PTC patients is correlated with worse prognosis (23), and patients with high expression of circ_0067934 show lower survival rates (28). Moreover, Cox proportional hazards regression model analysis also indicates that circ_0067934 is an independent risk factor for prognosis (RR = 4.385, 95% CI = 1.087–17.544, $P = 0.038$) (28), like the circ-ITCH as well (32). More importantly, it is necessary to monitor relapse and progression by reliable biomarkers in long-term follow-up studies. In addition, the relationship between circRNAs, such as circFNDC3B, circBACH2, and circZFR, and prognosis-predicting roles reveals that it is insufficient to confirm its predicting role for prognosis due to limited survival analysis. Maybe it will be more convincing if performing further analysis by Cox proportional hazards regression models. Even the researcher could observe the relationship between circRNA and recurrence and metastasis in PTC for fine management of PTC, to fully elucidate the prognostic value of circRNAs for PTC.

CHALLENGES AND PROSPECTS

To date, a handful of ncRNAs have been identified, and many have shown oncogenic or tumor-suppressive roles in human cancer, especially lncRNAs and circRNAs. However, it is just like the tip of an iceberg. Despite advances in the relationship between circRNAs and PTC, current research still has a few limitations. For example, the sample size and histological types of

TC are limited. Except for circEIF6 (22), most TC-related circRNA research does not include other TCs such as anaplastic thyroid carcinoma (ATC) and medullary thyroid carcinoma (MTC) due to their low incidence. However, it is necessary to explore further by prolonging the observation period and performing multicenter clinical studies.

Furthermore, the molecular mechanism of circRNAs in the PTC pathological process needs to be further clarified to establish RNA regulatory networks. Currently, most studies focus on the “molecular sponge” function or ceRNA role of certain circRNAs. According to ceRNA theory, artificial circRNAs engineered with diverse methods can act as potential and promising therapeutic molecular tools. Nevertheless, circRNAs represent diversity in functions. Therefore, other functions of circRNAs in TC should be explored for a more comprehensive landscape and better understanding of the mechanism in the future, such as alternative splicing, regulation of gene transcription, and crosstalk with RBPs. More importantly, it needs a series of sufficient and logically scientific proofs outside of the molecular mechanism research for a reliable but not farfetched explanation.

Additionally, in view of the clinical applications of circRNAs, further studies should pay more attention to evaluating the

diagnostic and prognostic value of circRNAs and the associations with clinical drug resistance. Notably, few reports examine PTC-related circRNAs involved in this field. Liu F et al. demonstrates that circEIF6 associates with chemo-resistance (cisplatin-resistance) by influencing cell autophagy (22). More importantly, circRNAs could be secreted into blood, saliva (50), and even exosomes (51), which play important roles in the tumor microenvironment, suggesting that the circRNA level in body liquid and FNAB samples could facilitate clinical management, such as serum circMAN1A2 (29), serum exosomal circRASSF2 (13), and circ_0006156 (14).

Taken together, it is expected to identify more promising RNA signatures and unveil the underlying mechanism of circRNAs for better understanding of the etiology and pathological progress in TC, which sheds light on the potential applications of circRNAs for translational medicines.

AUTHOR CONTRIBUTIONS

XX drafted the manuscript. JJ supervised and revised the manuscript. All authors contributed to the article and approved the submitted version.

REFERENCES

- Kitahara CM, Sosa JA. The changing incidence of thyroid cancer. *Nat Rev Endocrinol* (2016) 12(11):646–53. doi: 10.1038/nrendo.2016.110
- Cabanillas ME, McFadden DG, Durante C. Thyroid cancer. *Lancet* (2016) 388 (10061):2783–95. doi: 10.1016/S0140-6736(16)30172-6
- Fagin JA, Wells SA Jr. Biologic and clinical perspectives on thyroid Cancer. *N Engl J Med* (2016) 375(11):1054–67. doi: 10.1056/NEJMra1501993
- Kunavisarut T. Diagnostic biomarkers of differentiated thyroid cancer. *Endocrine* (2013) 44(3):616–22. doi: 10.1007/s12020-013-9974-2
- Tallini G, de Biase D, Durante C, Acquaviva G, Bisceglia M, Bruno R, et al. BRAF V600E and risk stratification of thyroid microcarcinoma: a multicenter pathological and clinical study. *Mod Pathol* (2015) 28(10):1343–59. doi: 10.1038/modpathol.2015.92
- Fuziwara CS, Kimura ET. MicroRNAs in thyroid development, function and tumorigenesis. *Mol Cell Endocrinol* (2016) 456:44–50. doi: 10.1016/j.mce.2016.12.017
- Liyanarachchi S, Li W, Yan P, Bundschuh R, Brock P, Senter L, et al. Genome-Wide Expression Screening Discloses Long Noncoding RNAs Involved in Thyroid Carcinogenesis. *J Clin Endocrinol Metab* (2016) 101(11):4005–13. doi: 10.1210/jc.2016-1991
- Jeck WR, Sharpless NE. Detecting and characterizing circular RNAs. *Nat Biotechnol* (2014) 32(5):453–61. doi: 10.1038/nbt.2890
- He J, Xie Q, Xu H, Li J, Li Y. Circular RNAs and cancer. *Cancer Lett* (2017) 396:138–44. doi: 10.1016/j.canlet.2017.03.027
- Thomson DW, Dinger ME. Endogenous microRNA sponges: evidence and controversy. *Nat Rev Genet* (2016) 17(5):272–83. doi: 10.1038/nrg.2016.20
- Ashwal-Fluss R, Meyer M, Pamudurti NR, Ivanov A, Bartok O, Hanan M, et al. circRNA biogenesis competes with pre-mRNA splicing. *Mol Cell* (2014) 56(1):55–66. doi: 10.1016/j.molcel.2014.08.019
- Ebbesen KK, Kjems J, Hansen TB. Circular RNAs: identification, biogenesis and function. *Biochim Biophys Acta* (2016) 1859(1):163–8. doi: 10.1016/j.bbagr.2015.07.007
- Wu G, Zhou W, Lin X, Sun Y, Li J, Xu H, et al. circRASSF2 Acts as ceRNA and Promotes Papillary Thyroid Carcinoma Progression through miR-1178/TLR4 Signaling Pathway. *Mol Ther Nucleic Acids* (2020) 19:1153–63. doi: 10.1016/j.omtn.2019.11.037
- Wu G, Zhou W, Pan X, Sun Z, Sun Y, Xu H, et al. Circular RNA Profiling Reveals Exosomal circ_0006156 as a Novel Biomarker in Papillary Thyroid Cancer. *Mol Ther Nucleic Acids* (2020) 19:1134–44. doi: 10.1016/j.omtn.2019.12.025
- Ye M, Hou H, Shen M, Dong S, Zhang T. Circular RNA circFOXMI Plays a Role in Papillary Thyroid Carcinoma by Sponging miR-1179 and Regulating HMGB1 Expression. *Mol Ther Nucleic Acids* (2020) 19:741–50. doi: 10.1016/j.omtn.2019.12.014
- Pan Y, Xu T, Liu Y, Li W, Zhang W. Upregulated circular RNA circ_0025033 promotes papillary thyroid cancer cell proliferation and invasion via sponging miR-1231 and miR-1304. *Biochem Biophys Res Commun* (2019) 510(2):334–8. doi: 10.1016/j.bbrc.2019.01.108
- Yao Y, Chen X, Yang H, Chen W, Qian Y, Yan Z, et al. Hsa_circ_0058124 promotes papillary thyroid cancer tumorigenesis and invasiveness through the NOTCH3/GATAD2A axis. *J Exp Clin Cancer Res* (2019) 38(1):318. doi: 10.1186/s13046-019-1321-x
- Yang Y, Ding L, Li Y, Xuan C. Hsa_circ_0039411 promotes tumorigenesis and progression of papillary thyroid cancer by miR-1179/ABCA9 and miR-1205/MTA1 signaling pathways. *J Cell Physiol* (2020) 235(2):1321–9. doi: 10.1002/jcp.29048
- Cai X, Zhao Z, Dong J, Lv Q, Yun B, Liu J, et al. Circular RNA circBACH2 plays a role in papillary thyroid carcinoma by sponging miR-139-5p and regulating LMO4 expression. *Cell Death Dis* (2019) 10(3):184. doi: 10.1038/s41419-019-1439-y
- Liu W, Zhao J, Jin M, Zhou M. circRAPGEF5 Contributes to Papillary Thyroid Proliferation and Metastasis by Regulation miR-198/FGFR1. *Mol Ther Nucleic Acids* (2019) 14:609–16. doi: 10.1016/j.omtn.2019.01.003
- Zhou GK, Zhang GY, Yuan ZN, Pei R, Liu DM. Has_circ_0008274 promotes cell proliferation and invasion involving AMPK/mTOR signaling pathway in papillary thyroid carcinoma. *Eur Rev Med Pharmacol Sci* (2018) 22(24):8772–80. doi: 10.26355/eurrev_201812_16644
- Liu F, Zhang J, Qin L, Yang Z, Xiong J, Zhang Y, et al. Circular RNA EIF6 (Hsa_circ_0060060) sponges miR-144-3p to promote the cisplatin-resistance of human thyroid carcinoma cells by autophagy regulation. *Aging (Albany NY)* (2018) 10(12):3806–20. doi: 10.18632/aging.101674
- Wei H, Pan L, Tao D, Li R. Circular RNA circZFR contributes to papillary thyroid cancer cell proliferation and invasion by sponging miR-1261 and

- facilitating C8orf4 expression. *Biochem Biophys Res Commun* (2018) 503 (1):56–61. doi: 10.1016/j.bbrc.2018.05.174
24. Bi W, Huang J, Nie C, Liu B, He G, Han J, et al. CircRNA circRNA_102171 promotes papillary thyroid cancer progression through modulating CTNNBIP1-dependent activation of β -catenin pathway. *J Exp Clin Cancer Res* (2018) 37(1):275. doi: 10.1186/s13046-018-0936-7
 25. Li X, Tian Y, Hu Y, Yang Z, Zhang L, Luo J. CircNUP214 sponges miR-145 to promote the expression of ZEB2 in thyroid cancer cells. *Biochem Biophys Res Commun* (2018) 507(1-4):168–72. doi: 10.1016/j.bbrc.2018.10.200
 26. Jin X, Wang Z, Pang W, Zhou J, Liang Y, Yang J, et al. Upregulated hsa_circ_0004458 Contributes to Progression of Papillary Thyroid Carcinoma by Inhibition of miR-885-5p and Activation of RAC1. *Med Sci Monit* (2018) 24:5488–500. doi: 10.12659/MSM.911095
 27. Zheng FB, Chen D, Ding YY, Wang SR, Shi DD, Zhu ZP. Circular RNA circ_0103552 promotes the invasion and migration of thyroid carcinoma cells by sponging miR-127. *Eur Rev Med Pharmacol Sci* (2020) 24(5):2572–8. doi: 10.26355/eurrev_202003_20526
 28. Wang H, Yan X, Zhang H, Zhan X. CircRNA circ_0067934 Overexpression Correlates with Poor Prognosis and Promotes Thyroid Carcinoma Progression. *Med Sci Monit* (2019) 25:1342–9. doi: 10.12659/MSM.913463
 29. Fan CM, Wang JP, Tang YY, Zhao J, He SY, Xiong F, et al. circMAN1A2 could serve as a novel serum biomarker for malignant tumors. *Cancer Sci* (2019) 110 (7):2180–8. doi: 10.1111/cas.14034
 30. Chen F, Feng Z, Zhu J, Liu P, Yang C, Huang R, et al. Emerging roles of circRNA_NEK6 targeting miR-370-3p in the proliferation and invasion of thyroid cancer via Wnt signaling pathway. *Cancer Biol Ther* (2018) 19 (12):1139–52. doi: 10.1080/15384047.2018.1480888
 31. Ren H, Liu Z, Liu S, Zhou X, Wang H, Xu J, et al. Profile and clinical implication of circular RNAs in human papillary thyroid carcinoma. *PeerJ* (2018) 6:e5363. doi: 10.7717/peerj.5363
 32. Wang M, Chen B, Ru Z, Cong L. CircRNA circ-ITCH suppresses papillary thyroid cancer progression through miR-22-3p/CBL/ β -catenin pathway. *Biochem Biophys Res Commun* (2018) 504(1):283–8. doi: 10.1016/j.bbrc.2018.08.175
 33. Lan X, Cao J, Xu J, Chen C, Zheng C, Wang J, et al. Decreased expression of hsa_circ_0137287 predicts aggressive clinicopathologic characteristics in papillary thyroid carcinoma. *J Clin Lab Anal* (2018) 32(8):e22573. doi: 10.1002/jcla.22573
 34. Peng N, Shi L, Zhang Q, Hu Y, Wang N, Ye H. Microarray profiling of circular RNAs in human papillary thyroid carcinoma. *PLoS One* (2017) 12(3):e0170287. doi: 10.1371/journal.pone.0170287
 35. Jeck WR, Sorrentino JA, Wang K, Slevin MK, Burd CE, Liu J, et al. Circular RNAs are abundant, conserved, and associated with ALU repeats. *RNA* (2013) 19(2):141–57. doi: 10.1261/rna.035667.112
 36. Zhang Y, Zhang XO, Chen T, Xiang JF, Yin QF, Xing YH, et al. Circular intronic long noncoding RNAs. *Mol Cell* (2013) 51(6):792–806. doi: 10.1016/j.molcel.2013.08.017
 37. Kristensen LS, Andersen MS, Stagsted LVW, Ebbesen KK, Hansen TB, Kjems J. The biogenesis, biology and characterization of circular RNAs. *Nat Rev Genet* (2019) 20(11):675–91. doi: 10.1038/s41576-019-0158-7
 38. Hansen TB, Jensen TI, Clausen BH, Bramsen JB, Finsen B, Damgaard CK, et al. Natural RNA circles function as efficient microRNA sponges. *Nature* (2013) 495:384–8. doi: 10.1038/nature11993
 39. Liang WC, Wong CW, Liang PP, Shi M, Cao Y, Rao ST, et al. Translation of the circular RNA circ β -catenin promotes liver cancer cell growth through activation of the Wnt pathway. *Genome Biol* (2019) 20(1):84. doi: 10.1186/s13059-019-1685-4
 40. Yao Y, Hua Q, Zhou Y, Shen H. CircRNA has_circ_0001946 promotes cell growth in lung adenocarcinoma by regulating miR-135a-5p/SIRT1 axis and activating Wnt/ β -catenin signaling pathway. *BioMed Pharmacother* (2019) 111:1367–75. doi: 10.1016/j.biopha.2018.12.120
 41. Shang J, Chen WM, Liu S, Wang ZH, Wei TN, Chen ZZ, et al. CircPAN3 contributes to drug resistance in acute myeloid leukemia through regulation of autophagy. *Leuk Res* (2019) 85:106198. doi: 10.1016/j.leukres.2019.106198
 42. He Y, Mingyan E, Wang C, Liu G, Shi M, Liu S. CircVRK1 regulates tumor progression and radioresistance in esophageal squamous cell carcinoma by regulating miR-624-3p/PTEN/PI3K/AKT signaling pathway. *Int J Biol Macromol* (2019) 125:116–23. doi: 10.1016/j.ijbiomac.2018.11.273
 43. Lin Q, Ling YB, Chen JW, Zhou CR, Chen J, Li X, et al. Circular RNA circCDK13 suppresses cell proliferation, migration and invasion by modulating the JAK/STAT and PI3K/AKT pathways in liver cancer. *Int J Oncol* (2018) 53(1):246–56. doi: 10.3892/ijo.2018.4371
 44. Pan H, Li T, Jiang Y, Pan C, Ding Y, Huang Z, et al. Overexpression of Circular RNA ciRS-7 Abrogates the Tumor Suppressive Effect of miR-7 on Gastric Cancer via PTEN/PI3K/AKT Signaling Pathway. *J Cell Biochem* (2018) 119(1):440–6. doi: 10.1002/jcb.26201
 45. Xu H, Zhang Y, Qi L, Ding L, Jiang H, Yu H. NFIX Circular RNA Promotes Glioma Progression by Regulating miR-34a-5p via Notch Signaling Pathway. *Front Mol Neurosci* (2018) 11:225. doi: 10.3389/fnmol.2018.00225
 46. Wu HB, Huang SS, Lu CG, Tian SD, Chen M. CircAPLP2 regulates the proliferation and metastasis of colorectal cancer by targeting miR-101-3p to activate the Notch signalling pathway. *Am J Transl Res* (2020) 12(6):2554–69.
 47. Haugen BR. American Thyroid Association Management guidelines for adult patients with thyroid nodules and differentiated thyroid cancer: what is new and what has changed? *Cancer* (2015) 123:372–81. doi: 10.1002/cncr.30360
 48. He T, Wang H, Sun J, Wu J, Gong F, Li B, et al. Altered expression of DLG1-AS1 distinguished papillary thyroid carcinoma from benign thyroid nodules[J]. *BMC Endocr Disord* (2019) 19(1):122. doi: 10.1186/s12902-019-0440-x
 49. Fu XM, Guo W, Li N, Liu HZ, Liu J, Qiu SQ, et al. The expression and function of long noncoding RNA lncRNA-ATB in papillary thyroid cancer[J]. *Eur Rev Med Pharmacol Sci* (2017) 21(14):3239–46.
 50. Bahn JH, Zhang Q, Li F, Chan TM, Lin X, Kimi Y, et al. The landscape of microRNA, Piwi-interacting RNA, and circular RNA in human saliva. *Clin Chem* (2015) 61(1):221–30. doi: 10.1373/clinchem.2014.230433
 51. Li Y, Zheng Q, Bao C, Li S, Guo W, Zhao J, et al. Circular RNA is enriched and stable in exosomes: a promising biomarker for cancer diagnosis. *Cell Res* (2015) 25(8):981–4. doi: 10.1038/cr.2015.82

Conflict of Interest: The authors declare that the research was conducted in the absence of any commercial or financial relationships that could be construed as a potential conflict of interest.

Copyright © 2021 Xu and Jing. This is an open-access article distributed under the terms of the Creative Commons Attribution License (CC BY). The use, distribution or reproduction in other forums is permitted, provided the original author(s) and the copyright owner(s) are credited and that the original publication in this journal is cited, in accordance with accepted academic practice. No use, distribution or reproduction is permitted which does not comply with these terms.



The Contribution of Genetic Variants to the Risk of Papillary Thyroid Carcinoma in the Kazakh Population: Study of Common Single Nucleotide Polymorphisms and Their Clinicopathological Correlations

OPEN ACCESS

Edited by:

Christoph Reiners,
University Hospital Würzburg,
Germany

Reviewed by:

Filippo Biscarini,
National Research Council (CNR), Italy
Akira Sugawara,
Tohoku University, Japan

*Correspondence:

Vladimir A. Saenko
saenko@nagasaki-u.ac.jp

Specialty section:

This article was submitted to
Thyroid Endocrinology,
a section of the journal
Frontiers in Endocrinology

Received: 17 March 2020

Accepted: 01 December 2020

Published: 22 January 2021

Citation:

Mussazhanova Z, Rogounovitch TI,
Saenko VA, Krykpayeva A,
Eспенbetova M, Azizov B, Kondo H,
Matsuda K, Kalmatayeva Z,
Issayeva R, Yeleubayeva Z,
Madiyeva M, Mukanova A,
Sandybayev M, Bolsynbekova S,
Kozykenova Z, Yamashita S and
Nakashima M (2021) The Contribution
of Genetic Variants to the Risk of
Papillary Thyroid Carcinoma in the
Kazakh Population: Study of Common
Single Nucleotide Polymorphisms and
Their Clinicopathological Correlations.
Front. Endocrinol. 11:543500.
doi: 10.3389/fendo.2020.543500

Zhanna Mussazhanova^{1,2}, Tatiana I. Rogounovitch³, Vladimir A. Saenko^{4*},
Ainur Krykpayeva⁵, Maira Espenbetova⁵, Bauyrzhan Azizov⁶, Hisayoshi Kondo⁷,
Katsuya Matsuda¹, Zhanna Kalmatayeva², Raushan Issayeva², Zhanar Yeleubayeva^{2,8},
Madina Madiyeva⁹, Aray Mukanova⁹, Marat Sandybayev¹⁰, Saltanat Bolsynbekova¹⁰,
Zhanna Kozykenova¹¹, Shunichi Yamashita³ and Masahiro Nakashima¹

¹ Department of Tumor and Diagnostic Pathology, Atomic Bomb Disease Institute, Nagasaki University, Nagasaki, Japan,

² Faculty of Medicine and Health Care, Al-Farabi Kazakh National University, Almaty, Kazakhstan, ³ Department of Radiation Medical Sciences, Atomic Bomb Disease Institute, Nagasaki University, Nagasaki, Japan, ⁴ Department of Radiation Molecular Epidemiology, Atomic Bomb Disease Institute, Nagasaki University, Nagasaki, Japan, ⁵ Department of Endocrinology, Semey Medical University, Semey, Kazakhstan, ⁶ Endovascular Laboratory of Training Hospital, Semey Medical University, Semey, Kazakhstan, ⁷ Biostatistics Section, Division of Scientific Data Registry, Atomic Bomb Disease Institute, Nagasaki University, Nagasaki, Japan, ⁸ Center of Morphological Examination, Kazakh Institute of Oncology and Radiology, Almaty, Kazakhstan, ⁹ Radiology and Nuclear Medicine, Semey Medical University, Semey, Kazakhstan, ¹⁰ Center of Nuclear Medicine and Oncology of Semey, Semey, Kazakhstan, ¹¹ Department of Pathological Physiology, Semey Medical University, Semey, Kazakhstan

Objective: Risk for developing papillary thyroid carcinoma (PTC), the most common endocrine malignancy, is thought to be mediated by lifestyle, environmental exposures and genetic factors. Recent progress in the genome-wide association studies of thyroid cancer leads to the identification of several genetic variants conferring risk to this malignancy across different ethnicities. We set out to elucidate the impact of selected single nucleotide polymorphisms (SNPs) on PTC risk and to evaluate clinicopathological correlations of these genetic variants in the Kazakh population for the first time.

Methods: Eight SNPs were genotyped in 485 patients with PTC and 1,008 healthy control Kazakh subjects. The association analysis and multivariable modeling of PTC risk by the genetic factors, supplemented with rigorous statistical validation, were performed.

Result: Five of the eight SNPs: rs965513 (*FOXE1/PTCSC2*, $P = 1.3E-16$), rs1867277 (*FOXE1* 5'UTR, $P = 7.5E-06$), rs2439302 (*NRG1* intron 1, $P = 4.0E-05$), rs944289 (*PTCSC3/NKX2-1*, $P = 4.5E-06$) and rs10136427 (*BATF* upstream, $P = 9.8E-03$) were significantly associated with PTC. rs966423 (*DIRC3*, $P = 0.07$) showed a suggestive association. rs7267944 (*DHX35*) was associated with PTC risk in males ($P = 0.02$), rs1867277 (*FOXE1*) conferred the higher risk in subjects older than 55 years ($P = 7.0E-05$),

and rs6983267 (*POU5F1B/CCAT2*) was associated with pT3–T4 tumors ($P = 0.01$). The contribution of genetic component (unidirectional independent effects of rs965513, rs944289, rs2439302 and rs10136427 adjusted for age and sex) to PTC risk in the analyzed series was estimated to be 30–40%.

Conclusion: Genetic factors analyzed in the present work display significant association signals with PTC either on the whole group analysis or in particular clinicopathological groups and account for about one-third of the risk for PTC in the Kazakh population.

Keywords: papillary thyroid carcinoma, single nucleotide polymorphism, case–control genetic association study, risk factors for thyroid cancer, clinicopathological correlations

INTRODUCTION

Papillary thyroid carcinoma (PTC), a well-differentiated thyroid cancer of follicular cell origin, accounts for about 80% of all thyroid cancers worldwide being the most common endocrine malignancy. According to the IARC, in 2018 thyroid cancer affected 567,233 patients worldwide, making it the 9th most prevalent human cancer (3.1%) with the average age-standardized incidence of 6.7 and mortality rate of 0.42 per 100,000 of population (1). Region-specific incidence rates vary broadly from 1.0 in Micronesia to 15.0 in North America per 100,000 of population. In Kazakhstan, the age-standardized incidence of thyroid cancer was 2.4 per 100,000 of population accounting for 1.4% of all newly diagnosed cancers in the country in 2018.

With the improvements in cancer detection and diagnosis, the incidence of thyroid cancer is growing in most countries displaying one of the fastest increases in rate among common cancers. While the advances in thyroid nodule visualization such as ultrasound imaging and their facile assessment using ultrasound-guided fine-needle aspiration cytology have likely contributed to this uptrend, the additional reasons for the increasing incidence are investigated. Besides of well-established risk factor for thyroid cancer such as ionizing radiation, other environmental agents, including iodine deficiency, natural and technogenic pollutants with hormone disrupter effects, exposures to excessive nitrate (2, 3) and various chemicals are discussed or considered.

As a complex disease, PTC is thought to be dependent not only on environmental, but also on genetic factors. Studies of familial thyroid cancer estimated the contribution of genetic component to the risk of disease to be ranging from 28 to 53% (4, 5). At the population level, hereditary factors possibly contributing to the phenotype (e.g. the development of a condition or a disease) are usually identified in genetic association studies. To date, a number of well-powered genome-wide association studies (GWAS) or target gene investigations in thyroid cancer have been performed in the groups of different ethnicities in non-exposed or exposed to radiation individuals (6–14). GWAS findings and consequent independent replication studies have convincingly demonstrated robust associations of rs965513 (*FOXE1*, forkhead box E1 and/or *PTCSC2*, papillary thyroid carcinoma

susceptibility candidate 2; chromosome 9q22.33), rs944289 (*PTCSC3*, papillary thyroid carcinoma susceptibility candidate 3 and/or *NKX2-1*, NK2 homeobox 1; 14q13.3), rs1867277 (*FOXE1*; 9q22.33), rs2439302 (*NRG1*, neuregulin 1; 8q12) and rs966423 (*DIRC3*, disrupted in renal carcinoma 3; 2q35) SNPs with differentiated thyroid cancer, principally PTC (15–27), reviewed in (28). The strength of association signal for these SNPs in terms of odds ratios (OR) ranged from 1.28 to 1.70 in most studies. More recent studies have identified associations between the rs6983267 (*POU5F1B*, POU class 5 homeobox 1B and/or *CCAT2*, colon cancer associated transcript 2; 8q24) and thyroid cancer in different populations. A systematic review with meta-analysis of four studies that included a total of 2,825 cases and 9,684 controls confirmed the G allele of the rs6983267 to be a risk factor for thyroid cancer with an OR = 1.08, $P = 0.01$ (29).

The novel GWAS candidate loci continue to emerge. A recent combined analysis of GWAS results and the Italian replication study provided evidence of association of risk for differentiated thyroid cancer with rs10136427 (*BATF*, basic leucine zipper ATF-like transcription factor, 14q24.3) with an OR = 1.40, $P = 4.35E-07$ and rs7267944 (*DHX35*, DEAH-box helicase 35, 20q12) with an OR 1.39, $P = 2.13E-08$. These associations were replicated in the Polish and Spanish populations with little evidence of population heterogeneity (the combined, OR = 1.30, $P = 9.30E-07$ and OR 1.32, $P = 1.34E-08$, respectively) (10).

To the best of the authors' knowledge, studies of rs10136427 (*BATF*, 14q24.3) and rs7267944 (*DHX35*, 20q12) in PTC have not been replicated in independent studies. We therefore aimed to examine the six well-described SNPs discussed above, namely rs965513 (*FOXE1/PTCSC2*, 9q22.33), rs944289 (*PTCSC3/NKX2-1*, 14q13.3), rs1867277 (*FOXE1*; 9q22.33), rs2439302 (*NRG1*, 8q12), rs966423 (*DIRC3*, 2q35) and rs6983267 (*POU5F1B/CCAT2*, 8q24.2), and two SNPs newly discovered to be associated with thyroid cancer (10), rs10136427 (*BATF*, 14q24.3) and rs7267944 (*DHX35*, 20q12) in a relatively large case–control series. This work is the first to characterize the eight SNPs in the Kazakh population. In addition to the classical association analysis, we estimated the contribution of the genetic variants to PTC risk, and assessed the relationships with clinicopathological characteristics of tumors in the study since available information is very limited in the literature.

MATERIAL AND METHODS

Study Population

A total of 485 patients with histologically confirmed PTC (90.3% females, mean age 54.78 ± 13.3 y.o., 18–87 y.o., range) operated from 1980 to 2015, and 1,008 healthy control subjects (78.7% females, mean age 39.0 ± 15.8 y.o., 15–83 y.o., range) of Kazakh origin were recruited. Clinicopathological information was retrieved from medical records (Table 1). The pathological classification was based on the World Health Organization definitions (30), pathological staging (pTNM, where the T category defined the anatomic extent of cancer for the tumor, N for the lymph nodes and M for distant metastases) was according to the 7th edition of TNM classification system (31). Patients and control subjects had no

history of radiation exposure. All participants or their parents/guardian gave written informed consent in accordance with the Declaration of Helsinki. A peripheral venous blood sample was collected from each participant. The protocol of this study was approved by corresponding ethics committees.

DNA Isolation and Genotyping

Blood DNA was extracted using QIAamp DNA Mini Kit (QIAGEN, Tokyo, Japan) according to the manufacturer's protocol. DNAs of sufficient quality for genotyping were obtained from all 485 PTC patients and 1,008 control participants.

Genotyping was performed with predesigned Custom Applied Biosystems TaqMan SNP Genotyping Assays (Table 2) using TaqMan Genotyping Master mix (all reagents from ThermoFisher Scientific) and 10 ng genomic DNA per 10 μ l reaction in a Light Cycler 480 (Roche, Indianapolis, IN). Cycling conditions were as follows: denaturation at 95°C for 10 min followed by 60 cycles of 92°C for 15 s and 62°C for 1 min for all SNPs. As a quality control, 15–20% of all samples were randomly selected and re-run in duplicates for each SNP. Full concordance between the experiments was observed.

Statistical Analyses

Association Analysis

We used PLINK 1.9 (32) software to run the multiplicative genetic models in the case-control sample for each SNP with age and sex as covariates. This type of model evaluates the impact of individual alleles of a polymorphic locus on the disease. The multiplicative models have been used in the vast majority of the genome-wide and replication association studies of thyroid cancer (6–27); using those in our work provided an opportunity to compare the strength of association signals (ORs) between the previous studies and our findings. The risk alleles were assigned according to the cited literature sources for consistency; summary information on the risk alleles is provided in Table 3. Multiple testing correction (the Benjamini–Hochberg method) and the adaptive label-swapping permutation test (10^6 , maximum) were performed using options available in PLINK.

Associations between each SNP and clinicopathological parameters of PTCs were assessed using logistic regression models with binary outcomes sex (F vs M), age (≥ 55 vs < 55 years old), pathological tumor (pT) category (pT3 or pT4 vs pT1 or pT2) or nodal disease (N1 vs N0, i.e. present vs absent) as dependent variables, and individual SNPs, age and sex (where

TABLE 1 | Demographic characteristics of control subjects and PTC patients, and clinicopathological data.

Characteristics	Value (%) ¹
<i>Healthy control subjects, n = 1,008</i>	
Age at sampling, M \pm SD (range)	39.0 \pm 15.8 (15–83)
Sex	
Female	793 (78.7)
Male	215 (21.3)
<i>PTC patients, n = 485</i>	
Age at diagnosis, M \pm SD (range)	54.8 \pm 13.3 (18–87)
Sex	
Female	438 (90.3)
Male	47 (9.7)
pT ²	
T1	98 (20.2)
T2	264 (54.4)
T3	85 (17.5)
T4	38 (7.8)
N category ²	
N0	259 (53.4)
N1	74 (15.3)
NX	152 (31.3)
M category ²	
M0	376 (77.5)
M1	2 (0.4)
MX	107 (22.1)

¹Mean \pm standard deviation and (range) for age in years, count data and (%) for other variables.

²The pathological cancer staging (pTNM, where the T category defines the anatomic extent of cancer for the tumor, N for the lymph nodes and M for distant metastases; 0, 1 and X in the N and M categories correspond to absent, present, and unknown, respectively) according to the 7th edition of TNM classification system (31).

TABLE 2 | TaqMan primer/probe set used for genotyping.

SNP	Chromosomal locus	Base position ¹	Nearest gene(s)	TaqMan primer/probe set
rs965513 (A/G)	9q22.33	97,793,827	FOXE1, PTCSC2	C_1593670_20
rs944289 (T/C)	14q13.3	36,180,040	NKX2-1, PTCSC3	C_1444137_10
rs1867277 (A/G)	9q22.33	97,853,632	FOXE1	C_11736668_10
rs2439302 (G/C)	8q12	32,574,851	NRG1	C_16238367_10
rs10136427 (C/T)	14q24.3	75513546	BATF	C_2676717_10
rs966423 (T,G/C)	2q35	217,445,617	DIRC3	C_1880230_10
rs7267944 (C/T)	20q12	39,318,791	DHX35	C_29372376_10
rs6983267 (G/T)	8q24.2	127,401,060	POU5F1B, CCAT2	C_29086771_20

¹Genomic location of an SNP position on GRCh38.

TABLE 3 | Summary information on the risk alleles of analyzed SNPs.

SNP	Chromosomal locus	Nearest gene(s)	Location/annotation	Risk allele function ¹	Risk allele frequency ¹	Allelic OR ¹	Replication studies	References
rs965513 (A*/G)	9q22.33	<i>FOXE1</i> , <i>PTCSC2</i>	Intergenic, long-range enhancer	Decreases the expression of <i>FOXE1</i> , unspliced <i>PTCSC2</i> and <i>TSHR</i> in normal thyroid tissue	0.09–0.61	1.40–2.81	Yes	(6–9, 16–18, 20–27, 33, 34)
rs944289 (T*/C)	14q13.3	<i>PTCSC3</i> , <i>NKX2-1</i>	Non-coding, promoter	Decreases <i>PTCSC3</i> expression by destroying a C/EBP α / β transcription factor binding site in <i>PTCSC3</i> promoter	0.46–0.70	1.12–1.60	Yes	(6, 8, 18, 20, 21, 23–27, 35)
rs1867277 (A*/G)	9q22.33	<i>FOXE1</i>	5'UTR	Upregulates <i>FOXE1</i> expression in follicular thyroid carcinoma cells through the recruitment of USF1/USF2 transcription factors	0.16–0.53	1.20–1.75	Yes	(15, 18, 20, 23, 25, 26)
rs2439302 (G*/C)	8p12	<i>NRG1</i>	Intron 1	Increases <i>NRG1</i> expression	0.23–0.54	1.29–1.53	Yes	(8, 24, 27, 33, 36)
rs10136427 (C*/T)	14q24.3	<i>BATF</i>	Intergenic	Not established	0.79–0.88	1.05–1.62	No	(10)
rs966423 (T,G*/C)	2q35	<i>DIRC3</i>	Intron	Not established	0.41–0.82	1.14–1.28	Yes	(8, 24, 27, 33)
rs7267944 (C*/T)	20q12	<i>DHX35</i>	Intergenic	Not established	0.17–0.26	1.10–1.54	No	(10)
rs6983267 (G*/T)	8q24.2	<i>POU5F1B</i> , <i>CCAT2</i>	Non-coding	Suggested to predispose chromosome 8 to chromosomal instability	0.37–0.51	0.89–1.16	Yes	(23, 24, 26, 29)

¹Information from the literature sources.

*The risk allele is indicated by an asterisk.

applicable) as explanatory variables. The LOGISTIC procedure in the 3.71 release of SAS Studio for the 9.4M5 version of SAS (SAS Institute, Cary, NC, USA) was used for these calculations.

Exact two-sided tests, permutation tests and exact test for equality of allele frequencies for stratified groups were performed using the 'HardyWeinberg' package in R (37).

All tests were two-sided, $P < 0.05$ was considered statistically significant.

Predictive Modeling of Papillary Thyroid Carcinoma

To evaluate the impact of the genetic component on PTC risk in the given case-control sample, we used multivariable logistic regression modeling. The initial full model included all eight SNPs in the study, and age and sex as explanatory variables. The reduced model was determined by stepwise or non-automatic selection of variables to achieve minimum Akaike information criterion. Statistical validation of the reduced model was performed using permutation analysis as described before (38), and bootstrapping with 0.9 sampling rate (*i.e.*, selecting 90% of data for each sample using the unrestricted random sampling method) in 10,000 replicates using the SURVEYSELECT procedure. The receiver operating characteristic (ROC) analysis was performed to assess the predictive performance of the reduced model, supplemented with the leave-one-out cross-validation.

RESULTS

Single Nucleotide Polymorphisms Association With and Impact on Papillary Thyroid Carcinoma Risk

Five of the eight SNPs displayed significant association signals in the Kazakh population with ORs similar to those in the original

studies and follow-up publications (Table 4). The strongest associations between a risk allele and sporadic PTC were observed for rs965513 (*FOXE1/PTCSC2*, 9q22.33; OR = 2.25, $P = 1.3E-16$), rs1867277 (*FOXE1* 5'UTR, 9q22.33; OR = 1.52, $P = 7.5E-06$), rs2439302 (*NRG1* intron 1, 8q12; OR = 1.46, $P = 4.0E-05$), rs944289 (*PTCSC3/NKX2-1*, 14q13.3; OR = 1.44, $P = 4.5E-06$), and rs10136427 (intergenic region upstream *BATF*, 14q24.3; OR = 1.30, $P = 9.8E-03$). rs966423 (*DIRC3*, 2q35) showed a significant association (OR = 1.25, $P = 5.8E-03$) on unadjusted analysis, but significance became marginal after adjusting for age and sex (OR = 1.18, $P = 0.07$). Adjustment for multiple testing and statistical validation (permutation) confirmed significant association of the five SNPs (rs965513, rs944289, rs1867277, rs2439302, rs10136427) and suggestive association for rs966423.

Two remaining SNPs, rs7267944 (*DHX35*, 20q12; OR = 1.04, $P = 0.71$) and rs6983267 (*POU5F1B/CCAT2*, 8q24.2; OR = 1.09, $P = 0.36$) did not display significant associations at this stage of analysis.

After obtaining evidence that certain examined SNPs display statistically significant association signals, we set out to determine the performance of a statistical model of the risk for PTC based on genetic factors. The reduced model included four SNPs: rs965513 (*FOXE1/PTCSC2*), rs944289 (*NKX2-1*, *PTCSC3*), rs2439302 (*NRG1*) and rs10136427 (*BATF*) (Table 5). Their association signals remained significant after correction for multiple testing (Bonferroni and FDR). Statistical validation confirmed significant association of these SNPs with cancer risk (permutation), and confidence intervals almost did not change on bootstrapping. Of note, the OR estimates for the four SNPs in the model were very similar to those obtained in the single-SNP models (see Table 4) indicative of independent contribution of each SNP to thyroid cancer risk. The area under the ROC curve (AUC) was 0.82 (95% CI 0.80–0.84; $P = 3.2E-183$ as compared with a random classifier); cross-validation did not demonstrate model overfit returning a

TABLE 4 | Association analysis of papillary thyroid carcinoma in the Kazakh population.¹

SNP ²	Locus	Nearest gene(s)	Risk allele frequency		OR [95%CI]	P-value	FDR ³	P-permutation
			Cases n = 485	Controls n = 1008				
rs965513[A]	9q22.33	FOXE1, PTCSC2	0.39	0.22	2.25 [1.86–2.73]	1.3E-16	1.1E-15	1.0E-06
rs944289[T]	14q13.3	NKX2-1, PTCSC3	0.55	0.46	1.44 [1.21–1.72]	4.6E-05	9.1E-05	3.4E-05
rs1867277[A]	9q22.33	FOXE1	0.43	0.32	1.52 [1.27–1.83]	7.5E-06	3.0E-05	7.0E-06
rs2439302[G]	8q12	NRG1	0.43	0.33	1.46 [1.22–1.76]	4.0E-05	9.1E-05	4.6E-05
rs10136427[C]	14q24.3	BATF	0.77	0.72	1.30 [1.07–1.59]	9.8E-03	0.02	0.01
rs966423[T,G]	2q35	DIRC3	0.40	0.35	1.18 [0.98–1.42]	0.07	0.10	0.09
rs7267944[C]	20q12	DHX35	0.23	0.24	1.04 [0.85–1.28]	0.71	0.71	0.70
rs6983267[G]	8q24.2	POU5F1B, CCAT2	0.48	0.48	1.09 [0.91–1.30]	0.36	0.41	0.44

¹The multiplicative model adjusted for age and sex.²The risk allele is specified in brackets.³False discovery rate, the Benjamini–Hochberg procedure.**TABLE 5 |** The SNP-based logistic regression model of risk for PTC in the Kazakh population.¹

SNP	Logistic regression		Multiple testing		Permutation	Bootstrap ²
	OR [95%CI]	P-value	Bonferroni	FDR	P-value	OR [95%CI]
rs965513	2.32 [1.91–2.83]	4.8E-17	2.4E-16	1.1E-16	<1.0E-04	2.36 [1.98–2.81]
rs944289	1.43 [1.19–1.72]	1.4E-04	2.8E-04	1.6E-04	1.0E-04	1.44 [1.22–1.68]
rs2439302	1.50 [1.24–1.82]	2.9E-05	8.8E-05	4.1E-05	<1.0E-04	1.51 [1.28–1.79]
rs10136427	1.32 [1.06–1.63]	1.1E-02	1.1E-02	1.1E-02	6.8E-03	1.33 [1.09–1.61]

¹The multiplicative model adjusted for age and sex.²Bootstrap sampling rate 0.9, 10,000 replicates.

similar AUC of 0.82 (0.80–0.84). The Cox and Snell pseudo-R² of the optimal model was 0.27, and the Nagelkerke pseudo-R² was 0.38 suggesting that some 30–40% of variability in the risk for PTC in the analyzed series could be explained by the model that included age, sex and the four SNPs.

Single-Nucleotide Polymorphism Association With Clinicopathological Parameters of Papillary Thyroid Carcinoma

We assessed the genetic variants association with patients' sex, age (older than 55 years old), the pT category (pT3–T4 vs pT1–T2), and regional metastasis (N1). As shown in **Table 6**, very few statistically significant associations were found. rs7267944 (*DHX35*) was negatively associated with female sex (OR = 0.40, $P = 6.1E-05$), rs1867277 (*FOXE1*) was weakly but nominally significantly associated with the older patients' age (OR = 1.32, $P = 0.03$) and rs6983267 (*POU5F1B/CCAT2*) with more advanced tumors (OR = 1.49, $P = 0.01$).

The strong association of rs7267944 (*DHX35*) with patients' sex prompted us to test its association with PTC risk using stratified sampling. While no association was found in females OR = 0.95 (95%CI 0.76–1.18, $P = 0.62$ adjusted for age), the association signal in males was significant with an OR = 1.83 (95%CI 1.09–3.09, $P = 0.02$ adjusted for age). The difference in effect size was statistically significant ($P = 0.023$, the Breslow–Day test). No deviations from Hardy–Weinberg equilibrium in the groups of PTC patients or healthy control subjects, either non-stratified or stratified by sex, was found for this genetic

variant ($P > 0.4$ for any exact two-sided test, $P > 0.4$ for any permutation test). Exact test for equality of allele frequencies for males and females in the control subjects was negative ($P = 0.06$), but in PTC patients a strong inequality was observed ($P = 8.26E-05$), in line with other statistical findings.

The modifying effect of age on rs1867277 (*FOXE1*) was tested in respective groups of patients and control subjects younger or older 55 years old. In the younger group, rs1867277 displayed an association signal with OR = 1.44 (95%CI 1.16–1.80, $P = 9.5E-04$ adjusted for sex), and in the older group with OR = 1.84 (95%CI 1.36–2.49, $P = 7.0E-05$ adjusted for sex). There was no surprise that the association was significant in both age groups as rs1867277 was significant on the whole group association analysis, which was adjusted for age (see **Table 4**). Clearly, the effect of rs1867277 on the risk for PTC was more pronounced in subject older than 55 years old, although the difference did not reach statistical significance ($P = 0.20$). No deviations from Hardy–Weinberg equilibrium in the groups of PTC patients or healthy control subjects were found for rs1867277 ($P > 0.1$ for any exact two-sided test, $P > 0.1$ for any permutation test). Exact test for equality of allele frequencies for subjects younger than 55 years old was negative ($P = 0.85$), while in older subjects the inequality existed ($P = 0.03$).

We also tested the association of rs6983267 (*POU5F1B/CCAT2*) with PTC of different pT stage. In pT1–T2 tumors, the association was insignificant with OR = 1.0 (95%CI 0.82–1.21, $P = 0.96$ adjusted for age and sex), while in pT3–T4 tumors the signal was significant, OR = 1.47 (95%CI 1.09–1.98, $P = 0.01$ adjusted for age and sex). The difference in ORs was statistically significant ($P = 0.03$). No deviations from Hardy–Weinberg

TABLE 6 | Association of the genetic variants with clinicopathological characteristics.¹

SNP	Sex (F)			Age ≥ 55 y.o.			pT3–T4 vs pT1–T2 ²			N1 vs N0 ³		
	P-trend ⁴	OR ⁵ [95% CI]	P-value	P-trend	OR ⁵ [95% CI]	P-value	P-trend	OR[95% CI]	P-value	P-trend	OR[95% CI]	P-value
rs965513[A] ⁷	0.76	1.07 [0.70–1.63]	0.76	0.09	1.25 [0.97–1.61]	0.08	0.87	1.02 [0.77–1.36]	0.88	0.50	1.14 [0.80–1.63]	0.47
rs944289[T]	0.27	1.00 [0.97–1.02]	0.71	0.25	1.18 [0.91–1.52]	0.22	0.10	0.78 [0.58–1.04]	0.09	0.78	0.96 [0.66–1.41]	0.83
rs1867277[A]	0.55	1.15 [0.75–1.75]	0.53	0.04	1.32 [1.02–1.69]	0.03	0.33	0.85 [0.64–1.13]	0.27	1.00	1.02 [0.71–1.47]	0.90
rs2439302[G]	0.06	1.52 [1.00–1.02]	0.06	0.70	0.97 [0.76–1.24]	0.79	0.37	0.88 [0.66–1.16]	0.35	0.13	0.78 [0.54–1.11]	0.17
rs10136427[C]	0.45	0.82 [0.48–1.40]	0.47	0.28	1.17 [0.87–1.59]	0.17	0.82	1.02 [0.72–1.45]	0.90	0.98	1.00 [0.64–1.57]	0.99
rs966423[T,G]	0.58	1.15 [0.72–1.82]	0.56	0.46	1.11 [0.85–1.45]	0.43	0.89	0.96 [0.70–1.30]	0.80	0.90	1.04 [0.70–1.54]	0.84
rs7267944[C]	3.4E-05	0.40 [0.26–0.63]	6.1E-05	0.41	0.84 [0.32–1.13]	0.11	0.79	0.95 [0.67–1.35]	0.79	0.96	0.96 [0.60–1.51]	0.84
rs6983267[G]	0.08	1.00 [0.98–1.02]	0.80	0.68	0.96 [0.74–1.25]	0.76	0.02	1.49 [1.09–2.02]	0.01	0.66	1.10 [0.74–1.64]	0.63

¹Multivariate logistic regression adjusted for age and sex unless otherwise specified.

²The T category (defines the anatomic extent of cancer for the tumor) from the pathological cancer staging according to the 7th edition of TNM classification system (31); here, the advanced tumors (pT3–T4) are contrasted to less advanced tumors (pT1–T2).

³The N category (defines the regional lymph node involvement) from the pathological cancer staging according to the 7th edition of TNM classification system (31); here, cases with nodal disease (N1) are contrasted to those without lymph node involvement (N0).

⁴The Cochran–Armitage test for trend.

⁵Adjusted for age.

⁶Adjusted for sex.

⁷The risk allele is specified in brackets.

Statistically significant associations are shown in bold.

equilibrium in the groups of PTC patients or healthy control subjects were found for rs6983267 ($P > 0.1$ for any exact two-sided test, $P > 0.1$ for any permutation test). Exact test for equality of allele frequencies in the subgroup of PTCs of pT1–pT2 category was negative ($P = 0.32$) and marginally significant in pT3–pT4 PTCs ($P = 0.07$).

DISCUSSION

In the present study we set out to determine the impact of genetic factors on PTC risk in the Kazakh population. We focused on several SNPs found to display confident association signals in the previous studies across different populations/ethnicities and also tested two SNPs that have been newly discovered in GWAS of thyroid cancer.

Our genotyping results unambiguously confirmed the associations of rs965513 (*FOXE1/PTCSC2*, 9q22.33), rs1867277 (*FOXE1* 5'UTR, 9q22.33), rs944289 (*PTCSC3/NKX2-1*, 14q13.3), rs2439302 (*NRG1* intron 1, 8q12) using canonical multivariate analysis essentially supplemented by rigorous statistical validation.

Functional roles of rs965513 and rs1867277 located in the *FOXE1* locus on chromosome 9q22.33 were linked to the transcriptional regulation of *FOXE1* and *PTCSC2*. rs965513 was shown to affect the expression of *FOXE1*, *PTCSC2* and *TSHR* (thyroid stimulating hormone receptor) in thyroid tissue (34), and rs1867277 regulates *FOXE1* expression through the recruitment of USF1/USF2 transcription factors (15), implicating these SNPs into thyroid homeostasis and development. Of note, transgenic mice overexpressing *FOXE1* in their thyroids displayed retardation in

the proliferation of follicular cells, suggestive of its tumor suppressor function (39). A meta-analysis that combined data from 23 studies in different countries and ethnicities evaluated that rs965513[A] risk allele had an OR = 1.58 (95% CI 1.32–1.90) in the pooled sample, and OR = 1.65 and 1.49 in Caucasian and Asian populations, respectively (40). Interestingly, in the Kazakh population, which is of Asian descent, we found an OR = 2.25 (95% CI 1.85–2.73), which is one of the strongest association signals ever reported for the *FOXE1* locus. Also of interest is the finding of age-related effect rs1867277 (*i.e.*, the higher risk in patients aged more than 55 years), which is reported for the first time. It should be noted that despite rs965513 and rs1867277 are located in the same genetic locus, their effect on PTC risk is independent (41). The age relatedness of rs1867277 effect could be addressed in independent or already available studies.

rs944289 located on chromosome 14q13.3 regulates expression of the *PTCSC3* lncRNA, which has tumor suppressor effect in thyroid cancer cell lines, through the recruitments of *C/EBPα* and *β* transcription factors (35). *PTCSC3* level was found to be significantly lower in PTC than in normal thyroid tissue (26), which corresponds well with its tumor suppressor function. Interestingly, rs944289 besides of PTC was also associated with follicular adenoma (26), indicating its broader function in thyroid tumorigenesis.

rs2439302 is located in intron 1 of *NRG1* on chromosome 8q12. *NRG1* encodes human epidermal growth factor receptor 3 (HER3) ligand whose dimers with HER2 can activate MAPK and AKT pathways known to play an important role in PTC (42). Similarly to *PTCSC3*, *NRG1* was also earlier associated with follicular adenoma (26).

rs10136427, whose association with PTC risk was confirmed in the Kazakh population for the first time, was previously detected on GWAS in the Italian, Polish, and Spanish population study providing strong evidence of association with DTC (12). rs10136427 is located in an intergenic region upstream *BATF*. *BATF* proteins are the “AP-1 inhibitors”; findings in mouse myeloid leukemia cells suggested they can act as tumor suppressors by promoting cell growth arrest and cell differentiation. Whether *BATF* could play a similar role in other tissues, such as the thyroid, remains unknown. Since this genetic variant was not immediately associated with *BATF* expression, a possibility was suggested that this genetic locus may act as a *trans*-regulatory region controlling the expression of distant genes that reside on the same or even different chromosome(s) (*trans*-eQTL) (12).

rs966423 located in the *DIRC3* intron on chromosome 2q35, displayed marginally significant association ($P = 0.07$) in the Kazakh population. This genetic variant was significantly associated with the risk for thyroid cancer in both European and Asian ethnicities with ORs from 1.28 to 1.34 (reviewed in (28)). In our study the OR = 1.18 (adjusted for age and sex) is lower than those previously described. It therefore is likely that our sample size (485 PTC patients and 1,008 healthy control subjects) did not provide sufficient statistical power (achieved power 44%). We interpret the association signal of this genetic variant as suggestive in the Kazakh population. The functional role of *DIRC3* lncRNA is likely to be that of tumor suppressor, and its relevance to thyroid cancer (8, 9) and other human malignancies such as, originally, familial renal cancer (43), melanoma (44), breast cancer (45) and laryngeal squamous cell carcinoma (46) has been reported.

The finding for rs7267944, which is located approximately 280 kB telomeric to *DHX35* on chromosome 20q12, was somewhat unexpected. While on the whole group association analysis the signal of rs7267944 was insignificant, we noticed a strong modifying effect of sex. Accordingly, we found significant association of rs7267944 with PTC in males but not in females. *DHX35* encodes a putative RNA helicase of DEAD/DEAH-box family, which are implicated in translation initiation, RNA splicing, and ribosome and spliceosome assembly. *DHX35* is relatively highly expressed in the endometrium, ovaries, prostate and testes possibly pointing at its relatedness to sex-specific biological function (47). In the thyroid, *DHX35* is also expressed, although its role in tissue homeostasis and carcinogenesis remains unestablished. Within our study we could not determine the reason for *DHX35* association with sex, which, besides the true association could be sampling bias, a phenomenon specific for the given ethnic group (and relevant environmental exposures) or occurring by chance. This could be clarified in an independent study in the Kazakh population and also in other ethnic groups by researcher with access to rs7267944 [or other SNP(s) in strong or perfect linkage disequilibrium with it] genotyping data and clinical/demographic information. It is also possible that rs7267944 may point on the genetic factor other than *DHX35* on chromosome 20q12 or elsewhere due to *trans*-eQTL effect.

A recent GWAS has identified rs6983267 (*POU5F1B/CCAT2*) as a key locus in the 8q24 region previously associated with DTC/

PTC. However, the association with thyroid cancer was somewhat controversial since the significant association was found in the Polish and UK populations, but no association was found in the Spanish, Italian, and Japanese groups (10). In the Kazakh population under study, we did not observe significant association signal on the whole group analysis, yet a correlation with the higher pT tumor stage was detected. When pT3–T4 tumors were tested, a significant association with PTC risk was confirmed. It is tempting to relegate controversies in the rs6983267 association with thyroid cancer in different populations not only to genetic heterogeneity but also to different distribution of clinicopathological characteristics of tumors in country-specific samples. rs6983267 resides in the intronic region of *POU5F1B*, which encodes a transcriptional activator implicated in multisite cancers (48–51). It is worth noting that this genetic variant is also localized inside the *CCAT2* lncRNA upregulated in colon cancer and implicated in other human malignancies (52–55). The exact roles of either *POU5F1B* or *CCAT2* in PTC remain to be established.

After confirming the associations of rs965513 (*FOXE1/PTCSC2*), rs944289 (*PTCSC3/NKX2-1*), rs1867277 (*FOXE1*), rs2439302 (*NRG1*), rs10136427 (*BATF*) and, suggestively, of rs966423 (*DIRC3*) with PTC in the whole group or on subgroup analysis for rs7267944 (*DHX35*) and rs6983267 (*POU5F1B/CCAT2*), we combined these genetic variants in a statistical model to evaluate their contribution to PTC risk as the predictive strength of the genetic variants can be improved by combining multiple SNPs in a model (27, 56). The final model, which included four SNPs, rs965513 (*FOXE1/PTCSC2*), rs944289 (*NKX2-1, PTCSC3*), rs2439302 (*NRG1*) and rs10136427 (*BATF*), was subjected to statistical validation to ensure its reliability. The model had good predictive strength as judged by the ROC analysis (AUC = 0.82). Using two different analogs of the coefficient of determination for logistic regression models, we considered it safe to claim that the four SNPs in the optimal model, adjusted for age and sex effects, could explain about 30–40% of the risk for PTC in the Kazakh population examined in the study with a retrospective case–control design.

Our study had certain advantages such as homogenous ethnicity of the participants, large sample size that provided sufficient statistical power to detect meaningful associations, and thorough selection of the genetic variants. On the other hand, the study was not devoid of limitations. We could not fully rule out sampling bias and acknowledge insufficient age and sex matching of cases and controls, which could affect the accuracy of some of the results obtained in the study. Also, clinicomorphological information was not detailed enough to analyze potentially clinically relevant correlations, and the lack of data on the participants' lifestyles and environmental exposures impeded the assessment of the impact of these factors on PTC risk.

In summary, our results unambiguously demonstrate the existence of genetic determinants of susceptibility to PTC among the SNPs analyzed in this work in the Kazakh population. We confirm the associations of rs965513 (*FOXE1/PTCSC2*), rs944289 (*PTCSC3/NKX2-1*), rs1867277 (*FOXE1*), rs2439302 (*NRG1*), and rs10136427 (*BATF*). The association of rs966423 (*DIRC3*) with PTC risk in the Kazakh population is

suggestive. The association signals in terms of ORs were generally comparable to those in typical Asian and European populations, and that of rs965513 (*FOXE1/PTCSC2*) was the highest so far reported. We also detected the age-related effect of rs1867277 (*FOXE1*) conferring the higher risk for PTC in patients older than 55 years and the association of rs7267944 (*DHX35*) with PTC risk in males and that of rs6983267 (*POU5F1B/CCAT2*) with more advanced tumor pT stage. We estimate the contribution of genetic factors to the susceptibility to PTC in the analyzed series from Kazakhstan to 30–40%, accounting for age and sex. To better understand the impact of different factors affecting PTC risk, further studies would be desirable to increase the number of potential genetic loci and to include the data on individual lifestyle and exposures to environmental agents.

DATA AVAILABILITY STATEMENT

Dataset used in this study may be made available upon request to Dr. Zhanna Mussazhanova (mussazhanova@nagasaki-u.ac.jp), subject to approval by the Semey Medical University Ethics Committee. Information on all genetic variants analyzed in this study is available in NCBI dbSNP database (<https://www.ncbi.nlm.nih.gov/snp/>).

ETHICS STATEMENT

The studies involving human participants were reviewed and approved by the Semey Medical University Ethics Committee

and Nagasaki University Human Genome Ethics Committee. Written informed consent to participate in this study was provided by the participants' legal guardian/next of kin.

AUTHOR CONTRIBUTIONS

ZM, VS, ME, ZKa, RI, SY, and MN conceived and designed the study. ZM, AK, ME, ZKa, RI, ZY, MM, AM, MS, ZKo, and SB collected and formalized the clinical information. ZM and TR performed the experiments, analyzed and formalized the raw data. VS and HK performed the statistical analyses. TR, SY, KM, and MN contributed comments to the paper. ZM and VS wrote the manuscript. All authors contributed to the article and approved the submitted version.

FUNDING

This work was supported in part by the Atomic Bomb Disease Institute of Nagasaki University, The Joint Hiroshima University, Nagasaki University, and Fukushima Medical University Research Base for Radiation Accidents and Medical Science, and by Takeda Science Foundation.

ACKNOWLEDGMENTS

The authors would like to thank all participants of this study for their collaboration.

REFERENCES

- International Agency for Research on Cancer. *Cancer Today (powered by GLOBOCAN)* (2019). Available at: <https://gco.iarc.fr/today/home> (Accessed March 12, 2020).
- Drozd VM, Saenko VA, Brenner AV, Drozdovitch V, Pashkevich VI, Kudelsky AV, et al. Major Factors Affecting Incidence of Childhood Thyroid Cancer in Belarus after the Chernobyl Accident: Do Nitrates in Drinking Water Play a Role? *PLoS One* (2015) 10:e0137226. doi: 10.1371/journal.pone.0137226
- Ward MH, Kilfoy BA, Weyer PJ, Anderson KE, Folsom AR, Cerhan JR. Nitrate intake and the risk of thyroid cancer and thyroid disease. *Epidemiology* (2010) 21:389–95. doi: 10.1097/EDE.0b013e3181d6201d
- Czene K, Lichtenstein P, Hemminki K. Environmental and heritable causes of cancer among 9.6 million individuals in the Swedish Family-Cancer Database. *Int J Cancer* (2002) 99:260–6. doi: 10.1002/ijc.10332
- Kerber RA, O'Brien E. A cohort study of cancer risk in relation to family histories of cancer in the Utah population database. *Cancer* (2005) 103:1906–15. doi: 10.1002/cncr.20989
- Gudmundsson J, Sulem P, Gudbjartsson DF, Jonasson JG, Sigurdsson A, Bergthorsson JT, et al. Common variants on 9q22.33 and 14q13.3 predispose to thyroid cancer in European populations. *Nat Genet* (2009) 41:460–4. doi: 10.1038/ng.339
- Takahashi M, Saenko VA, Rogounovitch TI, Kawaguchi T, Drozd VM, Takigawa-Imamura H, et al. The *FOXE1* locus is a major genetic determinant for radiation-related thyroid carcinoma in Chernobyl. *Hum Mol Genet* (2010) 19:2516–23. doi: 10.1093/hmg/ddq123
- Gudmundsson J, Sulem P, Gudbjartsson DF, Jonasson JG, Masson G, He H, et al. Discovery of common variants associated with low TSH levels and thyroid cancer risk. *Nat Genet* (2012) 44:319–22. doi: 10.1038/ng.1046
- Kohler A, Chen B, Gemignani F, Elisei R, Romei C, Figlioli G, et al. Genome-wide association study on differentiated thyroid cancer. *J Clin Endocrinol Metab* (2013) 98:E1674–81. doi: 10.1210/jc.2013-1941
- Figlioli G, Kohler A, Chen B, Elisei R, Romei C, Cipollini M, et al. Novel genome-wide association study-based candidate loci for differentiated thyroid cancer risk. *J Clin Endocrinol Metab* (2014) 99:E2084–92. doi: 10.1210/jc.2014-1734
- Mancikova V, Cruz R, Ingla-Perez L, Fernandez-Rozadilla C, Landa I, Cameselle-Teijeiro J, et al. Thyroid cancer GWAS identifies 10q26.12 and 6q14.1 as novel susceptibility loci and reveals genetic heterogeneity among populations. *Int J Cancer* (2015) 137:1870–8. doi: 10.1002/ijc.29557
- Figlioli G, Chen B, Elisei R, Romei C, Campo C, Cipollini M, et al. Novel genetic variants in differentiated thyroid cancer and assessment of the cumulative risk. *Sci Rep* (2015) 5:8922. doi: 10.1038/srep08922
- Gudmundsson J, Thorleifsson G, Sigurdsson JK, Stefansdottir L, Jonasson JG, Gudjonsson SA, et al. A genome-wide association study yields five novel thyroid cancer risk loci. *Nat Commun* (2017) 8:14517. doi: 10.1038/ncomms14517
- Son HY, Hwangbo Y, Yoo SK, Im SW, Yang SD, Kwak SJ, et al. Genome-wide association and expression quantitative trait loci studies identify multiple susceptibility loci for thyroid cancer. *Nat Commun* (2017) 8:15966. doi: 10.1038/ncomms15966
- Landa I, Ruiz-Llorente S, Montero-Conde C, Ingla-Perez L, Schiavi F, Leskela S, et al. The variant rs1867277 in *FOXE1* gene confers thyroid cancer susceptibility through the recruitment of USF1/USF2 transcription factors. *PLoS Genet* (2009) 5:e1000637. doi: 10.1371/journal.pgen.1000637
- Damiola F, Byrnes G, Moissonnier M, Pertesi M, Deltour I, Fillon A, et al. Contribution of ATM and *FOXE1* (TTF2) to risk of papillary thyroid carcinoma in Belarusian children exposed to radiation. *Int J Cancer* (2014) 134:1659–68. doi: 10.1002/ijc.28483

17. Penna-Martinez M, Epp F, Kahles H, Ramos-Lopez E, Hinsch N, Hansmann ML, et al. FOXE1 association with differentiated thyroid cancer and its progression. *Thyroid* (2014) 24:845–51. doi: 10.1089/thy.2013.0274
18. Maillard S, Damiola F, Clero E, Pertesi M, Robinot N, Rachedi F, et al. Common variants at 9q22.33, 14q13.3, and ATM loci, and risk of differentiated thyroid cancer in the French Polynesian population. *PLoS One* (2015) 10:e0123700. doi: 10.1371/journal.pone.0123700
19. Zhuang Y, Wu W, Liu H, Shen W. Common genetic variants on FOXE1 contributes to thyroid cancer susceptibility: evidence based on 16 studies. *Tumour Biol* (2014) 35:6159–66. doi: 10.1007/s13277-014-1896-y
20. Pereda CM, Lesueur F, Pertesi M, Robinot N, Lence-Anta JJ, Turcios S, et al. Common variants at the 9q22.33, 14q13.3 and ATM loci, and risk of differentiated thyroid cancer in the Cuban population. *BMC Genet* (2015) 16:22. doi: 10.1186/s12863-015-0180-5
21. Matsuse M, Takahashi M, Mitsutake N, Nishihara E, Hirokawa M, Kawaguchi T, et al. The FOXE1 and NKX2-1 loci are associated with susceptibility to papillary thyroid carcinoma in the Japanese population. *J Med Genet* (2011) 48:645–8. doi: 10.1136/jmedgenet-2011-100063
22. Tomaz RA, Sousa I, Silva JG, Santos C, Teixeira MR, Leite V, et al. FOXE1 polymorphisms are associated with familial and sporadic nonmedullary thyroid cancer susceptibility. *Clin Endocrinol (Oxf)* (2012) 77:926–33. doi: 10.1111/j.1365-2265.2012.04505.x
23. Jones AM, Howarth KM, Martin L, Gorman M, Mihai R, Moss L, et al. Thyroid cancer susceptibility polymorphisms: confirmation of loci on chromosomes 9q22 and 14q13, validation of a recessive 8q24 locus and failure to replicate a locus on 5q24. *J Med Genet* (2012) 49:158–63. doi: 10.1136/jmedgenet-2011-100586
24. Wang YL, Feng SH, Guo SC, Wei WJ, Li DS, Wang Y, et al. Confirmation of papillary thyroid cancer susceptibility loci identified by genome-wide association studies of chromosomes 14q13, 9q22, 2q35 and 8p12 in a Chinese population. *J Med Genet* (2013) 50:689–95. doi: 10.1136/jmedgenet-2013-101687
25. Bonora E, Rizzato C, Diquigiovanni C, Oudot-Mellakh T, Campa D, Vargiolu M, et al. The FOXE1 locus is a major genetic determinant for familial nonmedullary thyroid carcinoma. *Int J Cancer* (2014) 134:2098–107. doi: 10.1002/ijc.28543
26. Rogounovitch TI, Bychkov A, Takahashi M, Mitsutake N, Nakashima M, Nikitski AV, et al. The common genetic variant rs944289 on chromosome 14q13.3 associates with risk of both malignant and benign thyroid tumors in the Japanese population. *Thyroid* (2015) 25:333–40. doi: 10.1089/thy.2014.0431
27. Liyanarachchi S, Wojcik A, Li W, Czetwertynska M, Stachlewska E, Nagy R, et al. Cumulative risk impact of five genetic variants associated with papillary thyroid carcinoma. *Thyroid* (2013) 23:1532–40. doi: 10.1089/thy.2013.0102
28. Saenko VA, Rogounovitch TI. Genetic Polymorphism Predisposing to Differentiated Thyroid Cancer: A Review of Major Findings of the Genome-Wide Association Studies. *Endocrinol Metab (Seoul)* (2018) 33:164–74. doi: 10.3803/EnM.2018.33.2.164
29. Li J, Wang X, Dong J. Association of rs6983267 Polymorphism and Thyroid Cancer Susceptibility: A Systematic Review and Meta-Analysis. *Med Sci Monit* (2016) 22:1866–71. doi: 10.12659/msm.896507
30. RV Lloyd, RY Osamura, G Kloppel, J Rosai eds. *WHO classification of tumours of endocrine organs*. Lyon: IARC Press (2017).
31. Sobin LH, Gospodarowicz MK, Wittekind C. *International Union against Cancer. TNM classification of malignant tumours. 7th edition*. Chichester: Wiley-Blackwell (2010).
32. Chang CC, Chow CC, Tellier LCAM, Vattikuti S, Purcell SM, Lee JJ. Second-generation PLINK: rising to the challenge of larger and richer datasets. *GigaScience* (2015) 4:s13742-015-0047-8. doi: 10.1186/s13742-015-0047-8
33. Jendrzewski J, Liyanarachchi S, Nagy R, Senter L, Wakely PE, Thomas A, et al. Papillary Thyroid Carcinoma: Association Between Germline DNA Variant Markers and Clinical Parameters. *Thyroid* (2016) 26:1276–84. doi: 10.1089/thy.2015.0665
34. He H, Li W, Liyanarachchi S, Jendrzewski J, Srinivas M, Davuluri RV, et al. Genetic predisposition to papillary thyroid carcinoma: involvement of FOXE1, TSHR, and a novel lincRNA gene, PTCSC2. *J Clin Endocrinol Metab* (2015) 100:E164–72. doi: 10.1210/jc.2014-2147
35. Jendrzewski J, He H, Radomska HS, Li W, Tomsic J, Liyanarachchi S, et al. The polymorphism rs944289 predisposes to papillary thyroid carcinoma through a large intergenic noncoding RNA gene of tumor suppressor type. *Proc Natl Acad Sci U S A* (2012) 109:8646–51. doi: 10.1073/pnas.1205654109
36. He H, Li W, Liyanarachchi S, Wang Y, Yu L, Genutis LK, et al. The role of NRG1 in the predisposition to papillary thyroid carcinoma. *J Clin Endocrinol Metab* (2018) 103:1369–79. doi: 10.1210/jc.2017-01798
37. Graffelman J, Chang C, Puig X, Wigginton J. *Statistical Tests and Graphics for Hardy-Weinberg Equilibrium* (2019). Available at: <https://cran.r-project.org/web/packages/HardyWeinberg/HardyWeinberg.pdf> (Accessed March 12, 2020).
38. Cassell DL. *A Randomization-test Wrapper for SAS PROCs*. Available at: <https://support.sas.com/resources/papers/proceedings/proceedings/sugi27/p251-27.pdf> (Accessed March 12, 2020).
39. Nikitski A, Saenko V, Shimamura M, Nakashima M, Matsuse M, Suzuki K, et al. Targeted Foxe1 Overexpression in Mouse Thyroid Causes the Development of Multinodular Goiter But Does Not Promote Carcinogenesis. *Endocrinology* (2016) 157:2182–95. doi: 10.1210/en.2015-2066
40. Wang F, Yan D, Ji X, Han J, Chen M, Qiao H, et al. rs965513 polymorphism as a common risk marker is associated with papillary thyroid cancer. *Oncotarget* (2016) 7:41336–45. doi: 10.18632/oncotarget.9324
41. Nikitski AV, Rogounovitch TI, Bychkov A, Takahashi M, Yoshiura KI, Mitsutake N, et al. Genotype Analyses in the Japanese and Belarusian Populations Reveal Independent Effects of rs965513 and rs1867277 but Do Not Support the Role of FOXE1 Polyalanine Tract Length in Conferring Risk for Papillary Thyroid Carcinoma. *Thyroid* (2017) 27:224–35. doi: 10.1089/thy.2015.0541
42. Montero-Conde C, Ruiz-Llorente S, Dominguez JM, Knauf JA, Viale A, Sherman EJ, et al. Relief of feedback inhibition of HER3 transcription by RAF and MEK inhibitors attenuates their antitumor effects in BRAF-mutant thyroid carcinomas. *Cancer Discov* (2013) 3:520–33. doi: 10.1158/2159-8290.CD-12-0531
43. Bodmer D, Schepens M, Eleveld MJ, Schoenmakers EF, Geurts van Kessel A. Disruption of a novel gene, DIRC3, and expression of DIRC3-HSPBAP1 fusion transcripts in a case of familial renal cell cancer and t (q35;q21). *Genes Chromosomes Cancer* (2003) 38:107–16. doi: 10.1002/gcc.10243
44. Coe EA, Tan JY, Shapiro M, Louphrasitthiphol P, Bassett AR, Marques AC, et al. The MITF-SOX10 regulated long non-coding RNA DIRC3 is a melanoma tumour suppressor. *PLoS Genet* (2019) 15:e1008501. doi: 10.1371/journal.pgen.1008501
45. Michailidou K, Hall P, Gonzalez-Neira A, Ghoussaini M, Dennis J, Milne RL, et al. Large-scale genotyping identifies 41 new loci associated with breast cancer risk. *Nat Genet* (2013) 45:353–61. doi: 10.1038/ng.2563
46. Shen Z, Ren W, Bai Y, Chen Z, Li J, Li B, et al. DIRC3 and near NABP1 genetic polymorphisms are associated laryngeal squamous cell carcinoma patient survival. *Oncotarget* (2016) 7:79596–604. doi: 10.18632/oncotarget.12865
47. NCBI. *Gene database*. Available at: <https://www.ncbi.nlm.nih.gov/gene/60625#gene-expression> (Accessed March 12, 2020).
48. Yi J, Zhou LY, Yi YY, Zhu X, Su XY, Zhao Q, et al. Low Expression of Pseudogene POU5F1B Affects Diagnosis and Prognosis in Acute Myeloid Leukemia (AML). *Med Sci Monit* (2019) 25:4952–9. doi: 10.12659/MSM.914352
49. Pan Y, Zhan L, Chen L, Zhang H, Sun C, Xing C. POU5F1B promotes hepatocellular carcinoma proliferation by activating AKT. *Biomed Pharmacother* (2018) 100:374–80. doi: 10.1016/j.biopha.2018.02.023
50. Shen L, Du M, Wang C, Gu D, Wang M, Zhang Q, et al. Clinical significance of POU5F1P1 rs10505477 polymorphism in Chinese gastric cancer patients receiving cisplatin-based chemotherapy after surgical resection. *Int J Mol Sci* (2014) 15:12764–77. doi: 10.3390/ijms150712764
51. Hayashi H, Arai T, Togashi Y, Kato H, Fujita Y, De Velasco MA, et al. The OCT4 pseudogene POU5F1B is amplified and promotes an aggressive phenotype in gastric cancer. *Oncogene* (2015) 34:199–208. doi: 10.1038/nc.2013.547
52. Fu C, Xu X, Lu W, Nie L, Yin T, Wu D. Increased expression of long non-coding RNA CCAT2 predicts poorer prognosis in patients with hepatocellular carcinoma. *Med (Baltimore)* (2019) 98:e17412. doi: 10.1097/MD.00000000000017412
53. Shah MY, Ferracin M, Pilecki V, Chen B, Redis R, Fabris L, et al. Cancer-associated rs6983267 SNP and its accompanying long noncoding RNA

- CCAT2 induce myeloid malignancies via unique SNP-specific RNA mutations. *Genome Res* (2018) 28:432–47. doi: 10.1101/gr.225128.117
54. Yan L, Wu X, Yin X, Du F, Liu Y, Ding X. LncRNA CCAT2 promoted osteosarcoma cell proliferation and invasion. *J Cell Mol Med* (2018) 22:2592–9. doi: 10.1111/jcmm.13518
 55. Bai JG, Tang RF, Shang JF, Qi S, Yu GD, Sun C. Upregulation of long noncoding RNA CCAT2 indicates a poor prognosis and promotes proliferation and metastasis in intrahepatic cholangiocarcinoma. *Mol Med Rep* (2018) 17:5328–35. doi: 10.3892/mmr.2018.8518
 56. Van den Broeck T, Joniau S, Clinckemalie L, Helsen C, Prekovic S, Spans L, et al. The role of single nucleotide polymorphisms in predicting prostate cancer risk and therapeutic decision making. *Biomed Res Int* (2014) 2014:627510. doi: 10.1155/2014/627510

Conflict of Interest: The authors declare that the research was conducted in the absence of any commercial or financial relationships that could be construed as a potential conflict of interest.

Copyright © 2021 Mussazhanova, Rogounovitch, Saenko, Krykpayeva, Espenbetova, Azizov, Kondo, Matsuda, Kalmatayeva, Issayeva, Yeleubayeva, Madiyeva, Mukanova, Sandybayev, Bolsynbekova, Kozykenova, Yamashita and Nakashima. This is an open-access article distributed under the terms of the Creative Commons Attribution License (CC BY). The use, distribution or reproduction in other forums is permitted, provided the original author(s) and the copyright owner(s) are credited and that the original publication in this journal is cited, in accordance with accepted academic practice. No use, distribution or reproduction is permitted which does not comply with these terms.



Diagnostic Value of Sonographic Features in Distinguishing Malignant Partially Cystic Thyroid Nodules: A Systematic Review and Meta-Analysis

Xinlong Shi[†], Ruifeng Liu[†], Luying Gao, Yu Xia^{*} and Yuxin Jiang^{*}

Department of Ultrasound, Peking Union Medical College Hospital, Chinese Academy of Medical Science, Beijing, China

OPEN ACCESS

Edited by:

Valentina Drozd,
International Fund "Help for patients
with radiation induced thyroid cancer
'Arnica'", Belarus

Reviewed by:

Paolo Piero Limone,
Hospital Mauritian Turin, Italy
Takao Ando,
Nagasaki University Hospital, Japan

*Correspondence:

Yu Xia
xiayupumch@126.com
Yuxin Jiang
yuxinjiangxh@163.com

[†]These authors have contributed
equally to this work

Specialty section:

This article was submitted to
Thyroid Endocrinology,
a section of the journal
Frontiers in Endocrinology

Received: 31 October 2020

Accepted: 23 February 2021

Published: 19 March 2021

Citation:

Shi X, Liu R, Gao L, Xia Y and
Jiang Y (2021) Diagnostic Value
of Sonographic Features in
Distinguishing Malignant Partially
Cystic Thyroid Nodules: A Systematic
Review and Meta-Analysis.
Front. Endocrinol. 12:624409.
doi: 10.3389/fendo.2021.624409

Ultrasonography (US) is one of the most important methods for the management of thyroid nodules, which can be classified as solid, partially cystic, or cystic by composition. The various Thyroid Imaging Reporting and Data System classifications pay more attention to solid nodules and have reported pertinent US features associated with malignancy. However, the likelihood of malignancy of partially cystic thyroid nodules (PCTNs) is 3.3–17.6%, and few studies have systematically discussed the value of US in differentiating such entities. Therefore, we deemed it necessary to perform a systematic evaluation of US features in recognizing malignant PCTNs. Our systematic review and meta-analysis aimed to assess the value of US features in predicting malignant PCTNs. We searched the PubMed/MEDLINE, Web of Science, and Cochrane Library databases to find studies that researched US features of PCTNs and that were published before June 2020. Review Manager 5.3 was used to summarize suspicious US features and calculate the sensitivity, specificity, and likelihood ratios. MetaDiSc 1.4 was used to estimate receiver operating characteristic curves and calculate areas under the curves (AUCs). Our review included eight studies with a total of 2,004 PCTNs. Seven features were considered to be associated with malignancy. High specificity (>0.9) was found in nodules with a taller-than-wide shape, those that were spiculated/microlobulated or with an ill-defined margin, those with microcalcification, and a non-smooth rim. Among US features, eccentric configuration, microcalcification, and marked or mild hypoechogenicity were more reliable in predicting malignancy (AUC: 0.9592, 0.8504, and 0.8092, respectively). After meta-analysis, we recommend combining PCTN US features including an eccentric internal solid portion, marked or mild hypoechogenicity, and presence of microcalcification to better identify malignant nodules. More studies are needed to explore and improve the diagnostic value of US in PCTNs.

Keywords: meta-analysis, diagnostic values, sonographic features, partially cystic thyroid nodules, thyroid carcinoma

INTRODUCTION

Ultrasonography (US) is one of the most important methods for the management of thyroid nodules (TNs). In clinical practice, a nodule can be classified as solid, partially cystic, or cystic based on the internal cystic components (1). The various Thyroid Imaging Reporting and Data Systems (TI-RADS) classifications have paid more attention to solid nodules and have reported pertinent US features associated with malignancy (1–5). Several studies reported that nodules with microcalcification, hypoechogenicity (mild or marked), a taller-than-wide shape, or a spiculated/microlobulated margin are more likely to be carcinoma (6–9). However, the likelihood of malignancy of partially cystic thyroid nodules (PCTNs) is 3.3–17.6%, and few studies have systematically reported the US features associated with malignant PCTNs and discussed the value of US in differentiating such entities. As a matter of fact, malignant PCTNs can be easily missed due to their low prevalence (10–14). Therefore, we consider that more attention should be paid to the diagnosis of malignant PCTNs. Our systematic review and meta-analysis aimed to identify US risk factors indicative of malignant PCTNs and to assess the diagnostic performance of these features.

MATERIALS AND METHODS

Search Strategy

This meta-analysis was referred to Preferred Reporting Items for Systematic Review and Meta-analysis guideline (15). We searched the PubMed/MEDLINE and Web of Science databases to obtain relevant literature for this review. In the PubMed/MEDLINE database, the following search terms were conducted: (partially cystic thyroid nodules [MeSH Major Topic]) AND (ultrasonograph* OR sonograph* OR ultrasound OR US [MeSH Major Topic]). The advanced search terms “TS=[(partially cystic thyroid nodules) AND (ultrasoundgraph* OR sonograph* OR ultrasound OR US)]” were used in the Web of Science database. We also checked the Cochrane Library with “partially cystic thyroid” AND “ultraso*.” We did not screen according to language. From a search up to June 2020, 56 articles (31 in Web of Science and 25 in PubMed) in total were identified. There were no relevant studies registered in the Cochrane Library. All articles were managed with NoteExpress V3.0 and duplicated studies were manually deleted.

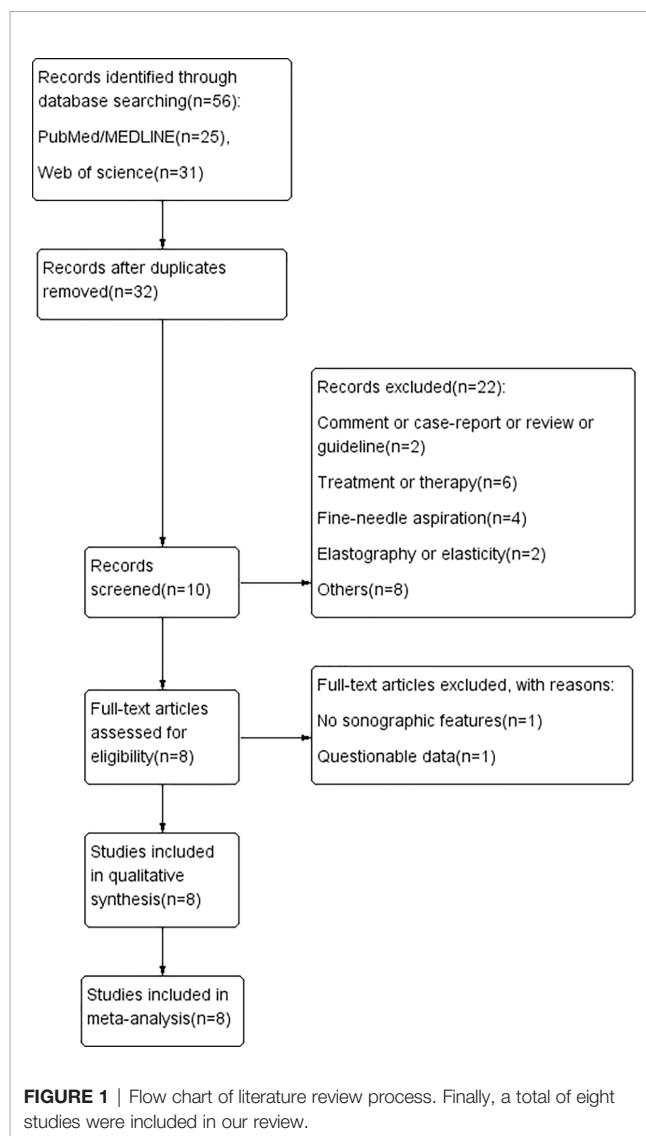
Inclusion and Exclusion Criteria

After searching the databases and deleting duplicated articles, we tab retained 56 studies for further analysis. Subsequent selection was performed by screening the titles and abstracts of all retrieved records. Comments, case reports, conference abstracts, letters, or reviews were filtered. The last round of selection was to apply strict and distinct inclusion and exclusion criteria by reviewing the full texts. Articles that met the following criteria were included in this study: (1) study on the sonographic features of PCTNs; (2) histopathologic results used as a reference standard; (3) research results available for evaluating the diagnostic value of sonographic features in

PCTNs; (4) retrospective or prospective study. The exclusion criteria were as follows: (1) studies on themes other than PCTNs; (2) diagnostic classification or no specific sonographic features about PCTNs; (3) insufficient or questionable data to finish a diagnostic 2-by-2 table; (4) improper deletion of studied cases. Finally, a total of eight studies (16–23) were retained according to the selection procedure in **Figure 1**.

Data Extraction

Two radiologists (XS and RL) individually reviewed the selected literature and extracted the data for systematic review and meta-analysis. We collected the following information from the selected articles: basic characteristics (name of first author, year of publication, country of origin, study design, number of TNs, number of included PCTNs, and scanner), sonographic performance of PCTNs, and diagnostic index of US features. According to several studies (1–5), some US features were excluded, such as vascularity. We regarded ovoid, ovoid-to-



round, flat and round, and regular and parallel nodules as being wider-than-tall (anteroposterior/transverse diameter [A/T] <1) and irregular-shaped nodules were classified as taller-than-wide (A/T ≥1). Any discrepant data were discussed by XS and RL and a specialist (YX) with over 20 years of experience to reach consensus.

Quality Assessment

QUADAS-2, a recommended tool for diagnostic accuracy studies (24, 25), was used by two reviewers to evaluate the quality of the eight included studies. Another reviewer was consulted for evaluation when any disagreement occurred.

Statistical Analysis

Our first step was to find the independent risk features for thyroid malignancy. An intervention review was created in Review Manager 5.3 to calculate odds ratios (ORs), 95% confidence intervals (CIs), and p-values and to evaluate the risk bias of the included articles. The I^2 inconsistency index was calculated to determine whether heterogeneity existed. If $I^2 \geq 50\%$, the heterogeneity could not be ignored, and therefore, a random-effects model would be recommended to replace the default model. Next, independent risk features were analyzed by MetaDiSc 1.4 software to evaluate the diagnostic performance for predicting malignancy. The relationship between sensitivity and 1-specificity determines whether a threshold effect exists. When $p > 0.05$, the threshold effect can be ignored when analyzing the source of heterogeneity. Without a threshold effect, we would directly calculate the pooled sensitivity (Se), specificity (Sp), positive and negative likelihood ratios (LR+ and LR-), diagnostic OR (DOR), and area under the curve (AUC). A hierarchical summary receiver operating characteristic curve (HSROC) should be used to calculate AUC when a threshold exists (26–29).

RESULTS

Table 1 demonstrates the basic information of the eight included studies. Half were performed in China (18, 21–23) and the other half were conducted in Korea (16, 17, 19, 20). **Figure 2** shows the outcomes of the QUADAS-2 questionnaire. All included studies had a low risk of bias and were of high quality. We noted that nodules were more prone to be malignant with internal solid content ≥50%, taller-than-wide shape, and when spiculated/

microlobulated or with an ill-defined margin. In terms of internal solid content of a PCTN, eccentric configuration, a non-smooth rim, marked or mild hypoechogenicity, and microcalcification were also potential malignant features for PCTNs. More details are shown in **Figure 3**. The overall ORs of the seven suspicious features ranged from 1.49 to 70.43. The p-values of all features were <0.01 except for nodules with a solid portion ≥50% ($p = 0.03$). Then, we combined RevMan 5.3 and MetaDiSc 1.4 software to evaluate the diagnostic accuracy. **Figure 4** and **Figure 5** show the pooled Se and Sp of diagnostic performance in the eight included studies. Except nodules with a solid portion ≥50%, the other six features revealed good specificity through a qualitative analysis. Four features (spiculated/microlobulated or ill-defined margin, eccentric configuration, microcalcification, and marked or mild hypoechogenicity) showed no threshold effect in this meta-analysis ($p = 0.337, 0.285, 0.955, 0.760$, respectively). Hence, we could obtain pooled diagnostic statistics from these four features. We only calculated the AUC from the HSROC for US features with an identified threshold effect. The pooled Se, Sp, LR+, LR-, DOR, 95% CIs, and AUCs are displayed in **Table 2**. From this table, we discovered that three features, except a non-smooth rim, of only the internal solid portion were more likely to predict the malignancy of PCTNs compared with features of the entire nodule (all AUCs >0.8). The AUC of the solid portion ≥50%, taller-than-wide shape, and spiculated/microlobulated or ill-defined margin were 0.6573, 0.7342, and 0.7138, respectively. Metaregression was conducted in MetaDiSc 1.4 to explore the source of heterogeneity. The variables were TP+FN (TP, True-positive; FN, False-negative), country of region, study design, and numbers of scanner used. We added year of publication to the metaregression of presence of microcalcification. We found that whether the study was conducted in China or South Korea was the main source of heterogeneity in terms of the presence of microcalcification ($p = 0.0482$, **Table S1**), while no other covariates could explain heterogeneity. We did not assess publication bias because our review included only eight studies, and the Cochrane Handbook recommends at least 10 studies when evaluating publication bias.

DISCUSSION

In our review, the incidence of malignant PCTNs varied from 5.0 to 45.8%. The diagnosis of malignant PCTNs is challenging, but worthy. It is of great importance to identify sonographic features

TABLE 1 | Basic characteristic of included studies.

First author	Year of publishing	Country of region	Study design	No. of TNs	No. of PCTNs	Rate of PCTNs (%)	Included PCTNs
Mi Jung Lee (16)	2009	South Korea	Prospective	1,056	392	37.1	335
Jang Mi Park (17)	2012	South Korea	Retrospective	NA	102	NA	102
Xiaoqing Wang (18)	2014	China	Retrospective	NA	265	NA	165
Eun Ju Ha (19)	2016	South Korea	Prospective	1,109	NA	NA	179
Dong Gyu Na (20)	2016	South Korea	Retrospective	2,000	449	22.5	449
Wenbo Li (21)	2017	China	Prospective	1,360	281	20.7	259
You Zhen Shi (22)	2019	China	Retrospective	NA	338	NA	338
Hai Na Zhao (23)	2020	China	Retrospective	NA	200	NA	177

NA, not available.

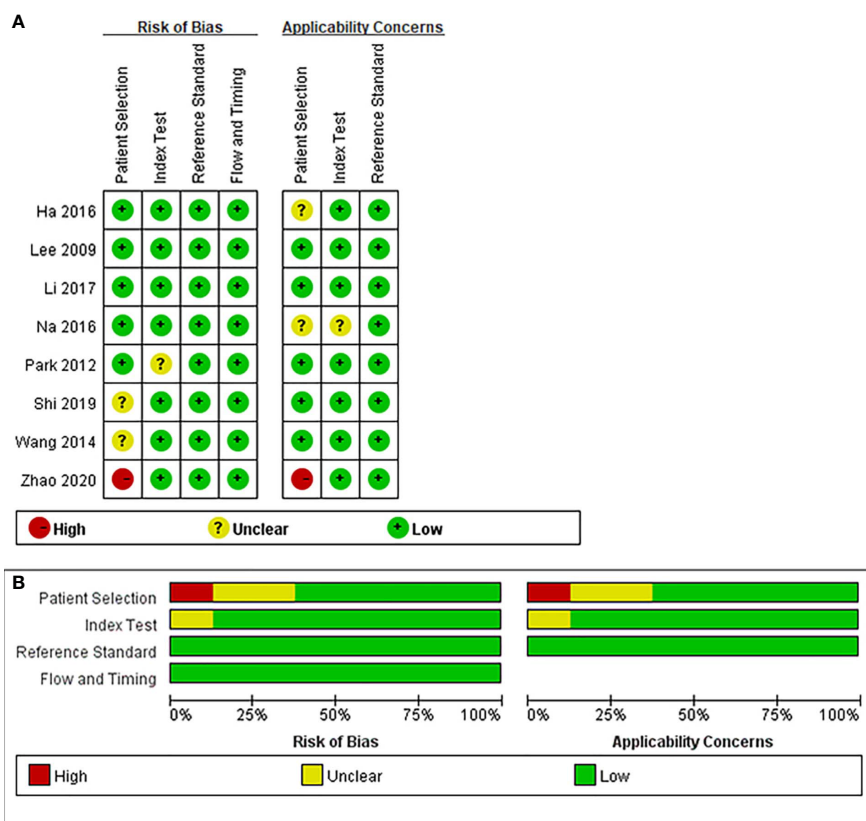


FIGURE 2 | Outcome of QUADAS-2 for included studies. **(A)** Risk-of-bias summary. **(B)** Risk-of-bias graph. Symbols: (+), low risk of bias; (?), unclear risk of bias; (-), high risk of bias.

that distinguish malignant PCTNs in clinical practice. Hence, we conducted this systematic review and meta-analysis to evaluate the value of US in predicting malignant PCTNs. After conducting an intervention review to determine independent risk factors for malignancy, we found PCTNs with seven US features had a higher risk of malignancy. Some of these features were in line with a previous meta-analysis regarding risky US features in all kinds of thyroid carcinoma (10). In our study, except non-smooth rim (AUC = 0.5), the AUCs of other six features were above 0.5. Notably, eccentric configuration, marked or mild hypoechoogenicity, or presence of microcalcification of internal solid portion had relatively high accuracy (0.85, 0.77, 0.90, respectively) in predicting malignancy among PCTNs.

A taller-than-wide (TTW) shape, defined as an anteroposterior/transverse diameter (A/T) ratio >1, would not be reliably correlated with malignant PCTNs in our review (AUC = 0.7342). Likewise, Kim reported that a taller than wide shape did not contribute to an increased risk of malignant PCTNs. The reason may lie in the noted inter- and even intraobserver variability of taller-than-wide shape (30, 31). Hypoechoogenicity showed fair diagnostic performance in our review (AUC = 0.8092). A previous study (32) that subdivided TNs based on their degree of hypoechoogenicity also found that TNs with marked or moderate hypoechoogenicity had significantly higher malignant risks than mild hypoechoogenicity ($p < 0.001$).

This feature related closely with malignancy from the perspective of pathology. Kim stated that the pathogenesis of marked hypoechoogenicity were associated with fibrotic regression following collapsed hemorrhagic component (31). The lack of follicular tissue arrangement may also lead to the hypoechoogenicity of malignant PCTNs (33). Microcalcification of internal solid portion was significantly associated with malignancy as well (AUC = 0.8504). The degeneration of tumor cells and additional collagen produced by tumor cells could lead to psammoma bodies, a histopathological marker of microcalcification (34). They are common in any kind of papillary thyroid carcinoma regardless of the internal content. To some extent, these could explain why PCTNs with hypoechoogenicity or microcalcification are prone to be malignant.

When compared to PCTNs with an eccentric configuration with a blunt angle, those with an eccentric configuration and an acute angle are more strongly associated with malignancy ($p < 0.001$) (18), which was also reported by Kim et al. (35). This phenomenon could be illustrated by the theory that malignant PCTNs usually develop from the wall of thyroid cysts, and the previous study has shown that the real tumor tissue is more likely to localize to the base of papillomatous lesions (36). A comment (37) reported that eccentric configuration harbors different meaning between nodules with a solid portion $\geq 50\%$ and solid

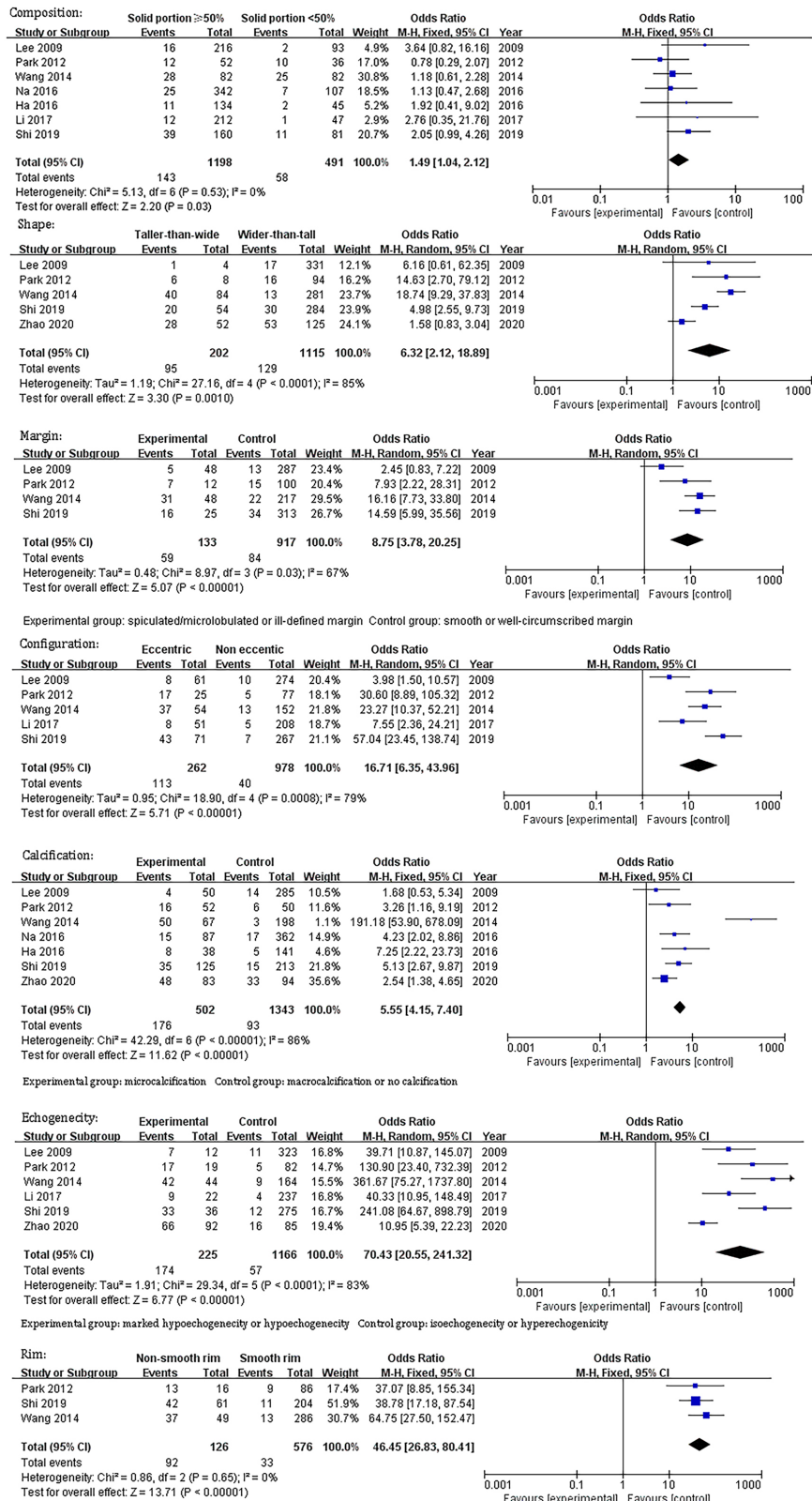


FIGURE 3 | Odds ratio and its 95% confidence intervals of seven sonographic features of partially cystic thyroid nodules.

solid composition $\geq 50\%$

Study	TP	FP	FN	TN	Sensitivity (95% CI)	Specificity (95% CI)	Sensitivity (95% CI)	Specificity (95% CI)
Ha 2016	11	45	2	134	0.85 [0.55, 0.98]	0.75 [0.68, 0.81]		
Lee 2009	16	200	2	113	0.89 [0.65, 0.99]	0.36 [0.31, 0.42]		
Li 2017	12	46	1	200	0.92 [0.64, 1.00]	0.81 [0.76, 0.86]		
Park 2012	12	40	10	40	0.55 [0.32, 0.76]	0.50 [0.39, 0.61]		
Shi 2019	39	167	11	121	0.78 [0.64, 0.88]	0.42 [0.36, 0.48]		
Wang 2014	28	158	25	54	0.53 [0.39, 0.67]	0.25 [0.20, 0.32]		

Taller-than-wide(A/T ≥ 1)

Study	TP	FP	FN	TN	Sensitivity (95% CI)	Specificity (95% CI)	Sensitivity (95% CI)	Specificity (95% CI)
Lee 2009	1	3	17	217	0.06 [0.00, 0.27]	0.99 [0.96, 1.00]		
Na 2016	6	2	16	78	0.27 [0.11, 0.50]	0.97 [0.91, 1.00]		
Park 2012	40	44	13	168	0.75 [0.62, 0.86]	0.79 [0.73, 0.84]		
Shi 2019	4	4	28	417	0.13 [0.04, 0.29]	0.99 [0.98, 1.00]		
Wang 2014	20	34	30	254	0.40 [0.26, 0.55]	0.88 [0.84, 0.92]		
Zhao 2020	28	24	53	72	0.35 [0.24, 0.46]	0.75 [0.65, 0.83]		

Spiculated/microlobulated or ill-defined margin

Study	TP	FP	FN	TN	Sensitivity (95% CI)	Specificity (95% CI)	Sensitivity (95% CI)	Specificity (95% CI)
Ha 2016	3	2	10	164	0.23 [0.05, 0.54]	0.99 [0.96, 1.00]		
Lee 2009	3	33	15	284	0.17 [0.04, 0.41]	0.90 [0.86, 0.93]		
Na 2016	6	0	26	417	0.19 [0.07, 0.36]	1.00 [0.99, 1.00]		
Park 2012	7	5	15	75	0.32 [0.14, 0.55]	0.94 [0.86, 0.98]		
Shi 2019	16	9	34	279	0.32 [0.20, 0.47]	0.97 [0.94, 0.99]		
Wang 2014	31	17	22	195	0.58 [0.44, 0.72]	0.92 [0.87, 0.95]		
Zhao 2020	50	17	31	79	0.62 [0.50, 0.72]	0.82 [0.73, 0.89]		

Eccentric solid position

Study	TP	FP	FN	TN	Sensitivity (95% CI)	Specificity (95% CI)	Sensitivity (95% CI)	Specificity (95% CI)
Lee 2009	8	53	10	264	0.44 [0.22, 0.69]	0.83 [0.79, 0.87]		
Li 2017	8	43	5	203	0.62 [0.32, 0.86]	0.83 [0.77, 0.87]		
Park 2012	17	8	5	72	0.77 [0.55, 0.92]	0.90 [0.81, 0.96]		
Shi 2019	43	28	7	260	0.86 [0.73, 0.94]	0.90 [0.86, 0.93]		
Wang 2014	37	17	16	195	0.70 [0.56, 0.82]	0.92 [0.87, 0.95]		

Microcalcifications

Study	TP	FP	FN	TN	Sensitivity (95% CI)	Specificity (95% CI)	Sensitivity (95% CI)	Specificity (95% CI)
Ha 2016	5	11	8	155	0.38 [0.14, 0.68]	0.93 [0.88, 0.97]		
Lee 2009	7	5	11	312	0.39 [0.17, 0.64]	0.98 [0.96, 0.99]		
Li 2017	9	13	4	233	0.69 [0.39, 0.91]	0.95 [0.91, 0.97]		
Na 2016	15	47	17	370	0.47 [0.29, 0.65]	0.89 [0.85, 0.92]		
Park 2012	17	2	5	78	0.77 [0.55, 0.92]	0.97 [0.91, 1.00]		
Shi 2019	33	3	17	285	0.66 [0.51, 0.79]	0.99 [0.97, 1.00]		
Wang 2014	42	2	11	210	0.79 [0.66, 0.89]	0.99 [0.97, 1.00]		
Zhao 2020	66	26	15	70	0.81 [0.71, 0.89]	0.73 [0.63, 0.81]		

Marked hypoechoogenicity or hypoechoogenicity

Study	TP	FP	FN	TN	Sensitivity (95% CI)	Specificity (95% CI)	Sensitivity (95% CI)	Specificity (95% CI)
Ha 2016	8	30	5	136	0.62 [0.32, 0.86]	0.82 [0.75, 0.87]		
Lee 2009	4	46	14	271	0.22 [0.06, 0.48]	0.85 [0.81, 0.89]		
Na 2016	15	72	17	345	0.47 [0.29, 0.65]	0.83 [0.79, 0.86]		
Park 2012	15	35	7	45	0.68 [0.45, 0.86]	0.56 [0.45, 0.67]		
Shi 2019	35	90	15	198	0.70 [0.55, 0.82]	0.69 [0.63, 0.74]		
Wang 2014	50	17	3	195	0.94 [0.84, 0.99]	0.92 [0.87, 0.95]		
Zhao 2020	48	35	33	61	0.59 [0.48, 0.70]	0.64 [0.53, 0.73]		

Non-smooth rim

Study	TP	FP	FN	TN	Sensitivity (95% CI)	Specificity (95% CI)	Sensitivity (95% CI)	Specificity (95% CI)
Park 2012	13	3	9	77	0.59 [0.36, 0.79]	0.96 [0.89, 0.99]		
Shi 2019	42	19	11	193	0.79 [0.66, 0.89]	0.91 [0.86, 0.95]		
Wang 2014	37	12	13	276	0.74 [0.60, 0.85]	0.96 [0.93, 0.98]		

FIGURE 4 | Forest plots of pooled sensitivity and specificity of US. Univariate analyses were performed for sensitivity and specificity, respectively. Except nodules with a solid portion $\geq 50\%$, the other six features revealed good specificity through a qualitative analysis.

portion $<50\%$ ($p = 0.001$). Only in predominant solid nodules, an eccentric position of solid component is a significantly malignant feature. This could explain why we did not find “solid portion $\geq 50\%$ ” as being a high-risk factor by itself for predicting malignancy

(AUC = 0.6573). Hence, we recommend integrating nodules with a solid portion $\geq 50\%$ with other potential US features in future studies. And we should be alert when a PCTN presented with predominant solid and eccentric configuration simultaneously.

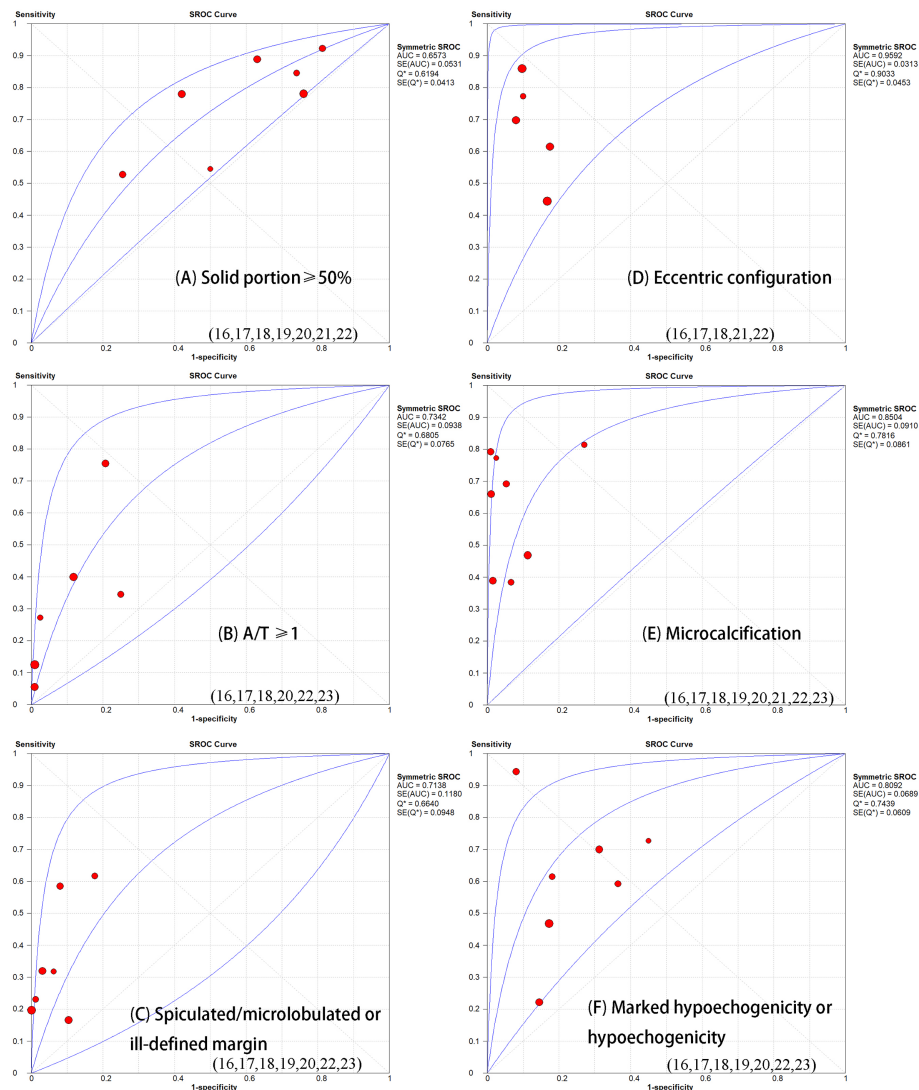


FIGURE 5 | Summary receiver operator characteristic curve (SROC) with area under the ROC curve (AUC) of six sonographic features in diagnosing partially thyroid cancer. The size of each study is indicated by the size of the solid circles. PCTNs with an eccentric configuration are more prone to malignancy (AUC=0.0952).

TABLE 2 | Diagnostic performance of each malignant feature.

Features	Se (95% CI)	Sp (95% CI)	PLR (95% CI)	NLR (95% CI)	DOR (95% CI)	AUC
Solid portion $\geq 50\%$	0.71 (0.64–0.77)	0.39 (0.37–0.41)	/	/	/	0.6573
A/T ≥ 1	0.39 (0.33–0.45)	0.92 (0.91–0.93)	/	/	/	0.7342
Spiculated/microlobulated or ill-defined margin	0.43 (0.37–0.49)	0.95 (0.94–0.96)	6.24 (3.39–11.47)	0.68 (0.56–0.84)	10.35 (5.21–20.54)	0.7138
Eccentric configuration	0.72 (0.65–0.80)	0.87 (0.85–0.89)	5.67 (3.42–9.38)	0.34 (0.20–0.59)	17.22 (6.53–45.41)	0.9592
Microcalcification	0.69 (0.63–0.74)	0.94 (0.93–0.95)	13.97 (6.10–31.97)	0.39 (0.27–0.55)	38.76 (6.10–31.97)	0.8504
Marked hypoechoogenicity/hypoechoogenicity	0.65 (0.59–0.71)	0.79 (0.77–0.81)	2.70 (1.66–4.38)	0.48 (0.30–0.77)	5.97 (2.47–14.43)	0.8092
Non-smooth rim	0.74 (0.65–0.81)	0.94 (0.92–0.96)	/	/	/	0.5

Se, sensitivity; Sp, specificity; PLR, positive likelihood ratio; NLR, negative likelihood ratio; DOR, diagnostic odds ratio; AUC, area under the curve.

In addition to univariate analysis, some studies combined multiple US features to evaluate the diagnostic performance of US for PCTNs (16, 19, 20). However, because the combination of US features in these studies were different, it was impossible for us to

evaluate the diagnostic accuracy of combined US features by meta-analysis. Lee et al. (16) found a high sensitivity and negative predictive value using combined US features to predict malignancy in PCTNs. Another two studies drew the same

conclusion that PCTNs would have an intermediate risk of malignancy if they presented more than one suspicious US feature (38, 39). The risk of malignancy increased as more suspicious US features were detected. Although different TI-RADS were put forward to evaluate the thyroid nodule, the attention paid to PCTNs were relatively less. Therefore, we suggest that clinicians focus on the following features: eccentric configuration, presence of calcification, and marked or mild hypoechogenicity. Overall, US has the ability to diagnose malignant PCTNs if high-risk features are appropriately recognized and interpreted.

Several limitations exist in our review. Firstly, only a small number of studies were used for this research, which rendered subgroup analysis ineffective when analyzing heterogeneity. Secondly, all included studies were performed in Asia, and so there may be population and race bias. Some features are closely associated and can exist simultaneously in malignant nodules (40); however the inherent relationship between suspicious US features could not be explored and we failed to evaluate the diagnostic value of combined US features. Then, more detailed classification of specific US feature could bring new insight, but we failed to do such research: for instance, included studies (19, 20, 29) in our review did not divide the degree of hypoechogenicity when exploring associated factors for malignancy, which limited our advanced analysis. Further study could be conducted to find the relationship between degree of hypoechogenicity and malignancy. Moreover, pooled data concerning the overall diagnostic value of US for PCTNs is not available.

CONCLUSION

Our review selected high-quality published studies to analyze the performance of US when diagnosing malignant PCTNs. After meta-analysis, we found that several US features were highly accurate when diagnosing malignant PCTNs. With the aim of improving the diagnostic accuracy of US, we suggest combining

several US features of the internal solid portion of PCTNs. More studies are needed to explore and improve the diagnostic value of US in PCTN.

DATA AVAILABILITY STATEMENT

The original contributions presented in the study are included in the article/**Supplementary Material**. Further inquiries can be directed to the corresponding authors.

AUTHOR CONTRIBUTIONS

XS and RL contributed equally to this review. RL conducted the work of search and collection of literature and helped XS to write the first draft of the manuscript. XS did the work of meta-analysis. LG contributed to the discussion. YX conceived and designed this review. YX and YJ revised the manuscript. All authors contributed to the article and approved the submitted version.

FUNDING

This study was supported by a grant from the Tibet Autonomous Region Science and Technology Project (XZ201901-GB-04) and the Tibet Autonomous Region Organization and Aiding Project [XZ2019ZR ZY05(Z)].

SUPPLEMENTARY MATERIAL

The Supplementary Material for this article can be found online at: <https://www.frontiersin.org/articles/10.3389/fendo.2021.624409/full#supplementary-material>

REFERENCES

- Shin JH, Baek JH, Chung J, Ha EJ, Kim JH, Lee YH, et al. Ultrasonography Diagnosis and Imaging-Based Management of Thyroid Nodules: Revised Korean Society of Thyroid Radiology Consensus Statement and Recommendations. *Korean J Radiol* (2016) 17:370–95. doi: 10.3348/kjr.2016.17.3.370
- Kwak JY, Han KH, Yoon JH, Moon HJ, Son EJ, Park SH, et al. Thyroid Imaging Reporting and Data System for US Features of Nodules: A Step in Establishing Better Stratification of Cancer Risk. *Radiology* (2011) 260:892–9. doi: 10.1148/radiol.11110206
- Russ G, Bonnema SJ, Erdogan MF, Durante C, Ngu R, Leenhardt L. European Thyroid Association Guidelines for Ultrasound Malignancy Risk Stratification of Thyroid Nodules in Adults: The EU-TIRADS. *Eur Thyroid J* (2017) 6:225–37. doi: 10.1159/000478927
- Haugen BR, Alexander EK, Bible KC, Doherty GM, Mandel SJ, Nikiforov YE, et al. 2015 American Thyroid Association Management Guidelines for Adult Patients with Thyroid Nodules and Differentiated Thyroid Cancer The American Thyroid Association Guidelines Task Force on Thyroid Nodules and Differentiated Thyroid Cancer. *Thyroid* (2016) 26:1–133. doi: 10.1089/thy.2015.0020
- Tessler FN, Middleton WD, Grant EG, Hoang JK, Berland LL, Teeffey SA, et al. ACR Thyroid Imaging, Reporting and Data System (TI-RADS): White Paper of the ACR TI-RADS Committee. *J Am Coll Radiol* (2017) 14:587–95. doi: 10.1016/j.jacr.2017.01.046
- Salmaslioglu A, Erbil Y, Dural C, Issever H, Kapran Y, Ozarmagan S, et al. Predictive value of sonographic features in preoperative evaluation of malignant thyroid nodules in a multinodular goiter. *World J Surg* (2008) 32:1948–54. doi: 10.1007/s00268-008-9600-2
- Popowicz B, Klencki M, Lewinski A, Slowinska-Klencka D. The usefulness of sonographic features in selection of thyroid nodules for biopsy in relation to the nodule's size. *Eur J Endocrinol* (2009) 161:103–11. doi: 10.1530/EJE-09-0022
- Hong YJ, Son EJ, Kim EK, Kwak JY, Hong SW, Chang HS. Positive predictive values of sonographic features of solid thyroid nodule. *Clin Imag* (2010) 34:127–33. doi: 10.1016/j.clinimag.2008.10.034
- Moon WJ, Jung SL, Lee JH, Na DG, Baek JH, Lee YH, et al. Benign and malignant thyroid nodules: US differentiation - Multicenter retrospective study. *Radiology* (2008) 247:762–70. doi: 10.1148/radiol.2473070944
- Remonti LR, Kramer CK, Leitao CB, Pinto LCF, Gross JL. Thyroid Ultrasound Features and Risk of Carcinoma: A Systematic Review and Meta-Analysis of Observational Studies. *Thyroid* (2015) 25:538–50. doi: 10.1089/thy.2014.0353
- Bellantone R, Lombardi CP, Raffaelli M, Traini E, De Crea C, Rossi ED, et al. Management of cystic or predominantly cystic thyroid nodules: the role of ultrasound-guided fine-needle aspiration biopsy. *Thyroid* (2004) 14:43–7. doi: 10.1089/105072504322783830

12. La Vecchia C, Malvezzi M, Bosetti C, Garavello W, Bertuccio P, Levi F, et al. Thyroid cancer mortality and incidence: a global overview. *Int J Cancer* (2015) 136:2187–95. doi: 10.1002/ijc.29251
13. Lin Y, Li P, Shi YP, Tang XY, Ding M, He Y, et al. Sequential treatment by polidocanol and radiofrequency ablation of large benign partially cystic thyroid nodules with solid components: Efficacy and safety. *Diagn Interv Imaging* (2020) 101:365–72. doi: 10.1016/j.diii.2019.11.005
14. Na DG, Kim JH, Kim DS, Kim SJ. Thyroid nodules with minimal cystic changes have a low risk of malignancy. *Ultrasonography* (2016) 35:153–8. doi: 10.14366/usg.15070
15. Moher D, Liberati A, Tetzlaff J, Altman DG, PRISMA Group. Preferred reporting items for systematic reviews and meta-analyses: the PRISMA statement. *BMJ* (2009) 339:b2535. doi: 10.1136/bmj.b2535
16. Lee MJ, Kim EK, Kwak JY, Kim MJ. Partially cystic thyroid nodules on ultrasound: probability of malignancy and sonographic differentiation. *Thyroid* (2009) 19:341–6. doi: 10.1089/thy.2008.0250
17. Park JM, Choi Y, Kwag HJ. Partially cystic thyroid nodules: ultrasound findings of malignancy. *Korean J Radiol* (2012) 13:530–5. doi: 10.3348/kjr.2012.13.530
18. Wang X, Wei X, Xu Y, Xin X, Zhang S. [Ultrasound characteristics of partially cystic thyroid nodules and their relationship with differential diagnosis of the lesions]. *Zhonghua Zhong Liu Za Zhi* (2014) 36(8):617–20. doi: 10.3760/cma.j.issn.0253-3766.2014.08.012
19. Ha EJ, Moon WJ, Na DG, Lee YH, Choi N, Kim SJ, et al. A Multicenter Prospective Validation Study for the Korean Thyroid Imaging Reporting and Data System in Patients with Thyroid Nodules. *Korean J Radiol* (2016) 17:811–21. doi: 10.3348/kjr.2016.17.5.811
20. Na DG, Baek JH, Sung JY, Kim JH, Kim JK, Choi YJ, et al. Thyroid Imaging Reporting and Data System Risk Stratification of Thyroid Nodules: Categorization Based on Solidity and Echogenicity. *Thyroid* (2016) 26:562–72. doi: 10.1089/thy.2015.0460
21. Li W, Zhu Q, Jiang Y, Zhang Q, Meng Z, Sun J, et al. Partially cystic thyroid nodules in ultrasound-guided fine needle aspiration: Prevalence of thyroid carcinoma and ultrasound features. *Med (Baltimore)* (2017) 96:e8689. doi: 10.1097/MD.0000000000000869
22. Shi YZ, Jin Y, Zheng L. Partially cystic thyroid nodules on ultrasound: The associated factors for malignancy. *Clin Hemorheol Microcirc* (2020) 74:373–81. doi: 10.3233/CH-190582
23. Whiting PF, Rutjes AW, Westwood ME, Mallett S, Deeks JN, Reitsma JB, et al. QUADAS-2: a revised tool for the quality assessment of diagnostic accuracy studies. *Ann Intern Med* (2011) 155:529–36. doi: 10.7326/0003-4819-155-8-201110180-00009
24. Zeng X, Zhang Y, Kwong JS, Zhang C, Li S, Sun F, et al. The methodological quality assessment tools for preclinical and clinical studies, systematic review and meta-analysis, and clinical practice guideline: a systematic review. *J Evid Based Med* (2015) 8:2–10. doi: 10.1111/jebm.12141
25. Zamora J, Abaira V, Muriel A, Khan K, Coomarasamy A. Meta-DiSc: a software for meta-analysis of test accuracy data. *BMC Med Res Methodol* (2006) 6:31. doi: 10.1186/1471-2288-6-31
26. Higgins JP, Thompson SG, Deeks JJ, Altman DG. Measuring inconsistency in meta-analyses. *BMJ* (2003) 327(7414):557–60. doi: 10.1136/bmj.327.7414.557
27. Cronin P, Kelly AM, Altae D, Foerster B, Petrou M, Dwamena BA. How to Perform a Systematic Review and Meta-analysis of Diagnostic Imaging Studies. *Acad Radiol* (2018) 25(5):573–93. doi: 10.1016/j.acra.2017.12.007
28. Lee J, Kim KW, Choi SH, Huh J, Park SH. Systematic Review and Meta-Analysis of Studies Evaluating Diagnostic Test Accuracy: A Practical Review for Clinical Researchers-Part II. Statistical Methods of Meta-Analysis. *Korean J Radiol* (2015) 16(6):1188–96. doi: 10.3348/kjr.2015.16.6.1188
29. Zhao HN, Liu JY, Lin QZ, He YS, Luo HH, Peng YL, et al. Partially cystic thyroid cancer on conventional and elastographic ultrasound: a retrospective study and a machine learning-assisted system. *Ann Transl Med* (2020) 8:495. doi: 10.21037/atm.2020.03.211
30. Grani G, Lamartina L, Ramundo V, Falcone R, Lomonaco C, Ciotti L, et al. Taller-Than-Wide Shape: A New Definition Improves the Specificity of TIRADS Systems. *Eur Thyroid J* (2020) 9(2):85–91. doi: 10.1159/000504219
31. Kim DW, Lee EJ, In HS, Kim SJ. Sonographic differentiation of partially cystic thyroid nodules: a prospective study. *AJNR Am J Neuroradiol* (2010) 31(10):1961–6. doi: 10.3174/ajnr.A2204
32. Lee JY, Na DG, Yoon SJ, Gwon HY, Paik W, Kim T, et al. Ultrasound malignancy risk stratification of thyroid nodules based on the degree of hypoechogenicity and echotexture. *Eur Radiol* (2020) 30(3):1653–63. doi: 10.1007/s00330-019-06527-8
33. Krátký J, Vítková H, Bartáková J, Telička Z, Antošová M, Límanová Z, et al. Thyroid nodules: pathophysiological insight on oncogenesis and novel diagnostic techniques. *Physiol Res* (2014) 63 Suppl 2(Suppl 2):S263–75. doi: 10.33549/physiolres.932818
34. Das DK. Psammoma body: a product of dystrophic calcification or of a biologically active process that aims at limiting the growth and spread of tumor? *Diagn Cytopathol* (2009) 37:534–41. doi: 10.1002/dc.21081
35. Kim DW, Park JS, In HS, Choo HJ, Ryu JH, Jung SJ. Ultrasound-based diagnostic classification for solid and partially cystic thyroid nodules. *AJNR Am J Neuroradiol* (2012) 33:1144–9. doi: 10.3174/ajnr.A2923
36. Yokozawa T, Miyauchi A, Kuma K, Sugawara M. Accurate and simple method of diagnosing thyroid nodules the modified technique of ultrasound-guided fine needle aspiration biopsy. *Thyroid* (1995) 5(2):141–5. doi: 10.1089/thy.1995.5.141
37. Zhang M, Fu C, Ma X, Li J, Cui K. Comment on “Partially Cystic Thyroid Nodules on Ultrasound: Probability of Malignancy and Sonographic Differentiation”. *Thyroid* (2016) 26:1645. doi: 10.1089/thy.2016.0389
38. Tessler FN, Middleton WD, Grant EG. Thyroid Imaging Reporting and Data System (TI-RADS): A User's Guide. *Radiology* (2018) 287:29–36. doi: 10.1148/radiol.2017171240
39. Horvath E, Majlis S, Rossi R, Franco C, Niedmann JP, Castro A, et al. An ultrasonogram reporting system for thyroid nodules stratifying cancer risk for clinical management. *J Clin Endocrinol Metab* (2009) 94:1748–51. doi: 10.1210/jc.2008-1724
40. Woliński K, Stangierski A, Szczepanek-Parulska E, Gurgul E, Ruchała M. Dependence of thyroid sonographic markers of malignancy and its influence on the diagnostic value of sonographic findings. *BioMed Res Int* (2015) 2015:693404. doi: 10.1155/2015/693404

Conflict of Interest: The authors declare that the research was conducted in the absence of any commercial or financial relationships that could be construed as a potential conflict of interest.

Copyright © 2021 Shi, Liu, Gao, Xia and Jiang. This is an open-access article distributed under the terms of the Creative Commons Attribution License (CC BY). The use, distribution or reproduction in other forums is permitted, provided the original author(s) and the copyright owner(s) are credited and that the original publication in this journal is cited, in accordance with accepted academic practice. No use, distribution or reproduction is permitted which does not comply with these terms.



Fine Needle Biopsy Versus Core Needle Biopsy Combined With/Without Thyroglobulin or BRAF 600E Mutation Assessment for Detecting Cervical Nodal Metastasis of Papillary Thyroid Carcinoma

OPEN ACCESS

Edited by:

Christoph Reiners,
University Hospital Würzburg,
Germany

Reviewed by:

Aime Franco,
Children's Hospital of Philadelphia,
United States
Akira Sugawara,
Tohoku University, Japan

*Correspondence:

Wei Du
duweitj@126.com
Hong Ge
gehong616@126.com

Specialty section:

This article was submitted to
Thyroid Endocrinology,
a section of the journal
Frontiers in Endocrinology

Received: 03 February 2021

Accepted: 10 March 2021

Published: 12 April 2021

Citation:

Zhang X, Zhang X, Du W, Dai L, Luo R,
Fang Q and Ge H (2021) Fine Needle
Biopsy Versus Core Needle Biopsy
Combined With/Without
Thyroglobulin or BRAF 600E
Mutation Assessment for Detecting
Cervical Nodal Metastasis of
Papillary Thyroid Carcinoma.
Front. Endocrinol. 12:663720.
doi: 10.3389/fendo.2021.663720

Xiaojun Zhang¹, Xu Zhang¹, Wei Du^{1*}, Liyuan Dai¹, Ruihua Luo¹, Qigen Fang¹
and Hong Ge^{2*}

¹ Department of Head Neck and Thyroid, Affiliated Cancer Hospital of Zhengzhou University, Henan Cancer Hospital, Zhengzhou, China, ² Department of Radiation Oncology, Affiliated Cancer Hospital of Zhengzhou University, Henan Cancer Hospital, Zhengzhou, China

Objectives: To analyze the diagnostic benefit of fine needle aspiration biopsy cytology (FNAB-C) and core needle biopsy tissue (CNB-T) with the addition of thyroglobulin (Tg) in the washout of the needle or BRAF V600E mutation assessment in assessing cervical lymph node metastasis (LNM) in papillary thyroid carcinoma.

Materials and Methods: A total of 186 lymph nodes were punctured by fine or core needle. The diagnostic performance of FNAB-C and CNB-T with Tg in the washout or BRAF V600E mutation assessment was compared.

Results: The optimal cutoff value of FNAB-Tg was 1.0 ng/ml, with an AUC of 0.976. The sensitivity and specificity of FNAB-C in predicting cervical LNM were 97.4% and 71.4%, respectively, and the addition of FNAB-Tg could contribute to a sensitivity of 100% and a specificity of 95%, but the introduction of BRAF V600E mutation assessment was associated with a decreased sensitivity of 96.3% and a decreased specificity of 50.0%. The FNAB-Tg level showed a comparable distribution in malignant lymph nodes with different TgAb statuses, serum TSH levels, and serum Tg levels. The sensitivity and specificity of CNB-T in predicting cervical LNM were 98.9% and 100%, respectively. The addition of CNB-Tg did not alter the diagnostic ability, but the introduction of BRAF V600E mutation assessment obtained the best performance, with a sensitivity of 100% and specificity of 100%.

Conclusion: The sensitivity and specificity of FNAB-C could be increased if combined with FNAB-Tg. CNB-T alone could provide satisfactory diagnostic reliability.

Keywords: papillary thyroid carcinoma, lymph node metastasis, FNAB-C, FNAB-Tg, BRAF V600E

INTRODUCTION

Papillary thyroid carcinoma (PTC) is the most common endocrine malignancy and accounts for more than 90% of all thyroid cancers (1). Unilateral or bilateral thyroidectomy combined with central neck dissection is the routine method of operation according to our guidelines (2). Lateral neck dissection is performed if cervical lymph node metastasis (LNM) is pathologically confirmed preoperatively or intraoperatively. Even if the operation is successful, a number of patients suffer from regional recurrence (3, 4); for these patients, it is important for the surgeon to accurately assess the lesion status preoperatively to avoid unnecessary surgery.

Ultrasound-guided fine needle aspiration biopsy cytology (FNAB-C) and core needle biopsy tissue (CNB-T) play an important role in evaluating cervical lymph node status in thyroid cancer and head and neck squamous cell carcinoma (SCC), respectively (5–21). However, the value of FNAB-C is greatly limited if the number of specimens is small or the specimens are obtained from cystic lymph nodes. Since it was first described by Pacini et al. (11), the measurement of thyroglobulin (Tg) in the washout of the needle (FNAB-Tg) has attracted increasing attention because of its higher reliability than FNAB-C (12–15). However, there is still great controversy regarding the best cutoff value of FNAB-Tg and whether serum thyroid stimulating hormone (TSH), thyroglobulin antibody (TgAb), serum Tg, and thyroid tissue interfere with the accuracy of FNAB-Tg (16, 17). Some researchers have reported that the clinical performance of FNAB-Tg was not affected by TgAb and TSH (10, 12), but others have asserted that the diagnostic value of FNAB-Tg could be greatly influenced by the presence of thyroid tissue, serum Tg, and TgAb (7, 14, 15, 18).

No researchers have yet analyzed the association between cervical LNM and CNB-T in thyroid cancer, so it remains unclear whether CNB-T is superior to FNAB-C in indicating LNM. In addition, the BRAF V600E mutation is the most common genetic alteration in thyroid cancer and occurs in nearly 80% of primary tumors and 50% of metastatic lymph nodes (22, 23). It therefore remains unknown whether the introduction of BRAF V600E mutation assessment could increase the diagnostic reliability of CNB-T and FNAB-C.

Thus, in the current study, we aimed to determine the answer to optimal value of Tg in the washout and compare the diagnostic performance between CNB-T and FNAB-C combined with/without Tg or BRAF 600E mutation assessment.

PATIENTS AND METHODS

Ethics Statement

The Our Hospital Institutional Research Committee approved our study, and all participants provided written informed consent. All methods were performed in accordance with the relevant guidelines and regulations. All procedures performed in studies involving human participants were in accordance with

the ethical standards of the institutional and/or national research committee and with the 1964 Declaration of Helsinki and its later amendments or comparable ethical standards.

Patient Selection

From January 2018 to October 2020, medical records of patients with surgically treated primary or recurrent/metastatic PTC were retrospectively reviewed. Enrolled patients must meet the following criteria: the patient underwent preoperative fine or core needle biopsy for suspicious lymph nodes and the punctured lymph nodes had been surgically excised. Then, 306 patients who had lymph node biopsy for suspicious metastasis from PTC were selected. A total of 143 patients had negative CNB-T or FNAB-C results and did not receive surgical treatment for the lymph nodes, and 8 patients had positive CNB-T or FNAB-C results but did not receive surgical treatment for the lymph nodes. These 151 patients were excluded, therefore, a total of 155 patients were enrolled for analysis.

Treatment Principles

Based on our guidelines for thyroid cancer (2), central neck dissection was routinely performed on patients treated for the first time, and lateral lymph node status was first assessed by ultrasound if there was suspicion of lateral LNM, FNAB-C or CNB-T combined with or without Tg in the washout or BRAF 600E mutation assessment.

For patients suspected of having regional recurrence, FNAB-C or CNB-T combined with or without Tg in the washout or BRAF 600E mutation assessment was performed for lateral neck lymph nodes, and FNAB-C or CNB-T combined with or without BRAF 600E mutation assessment was performed for central neck lymph nodes.

Cervical LNM was suggested if there were the following features, for ultrasound: absence of an echogenic hilum, round shape, microcalcification, peripheral blood flow on color Doppler images, or cystic changes (7–18); for CT: area with clear evidence of nonfat, low-density, or liquid components; largest diameter >15 mm at level II and >10 mm at other levels; and ratio of the longest to smallest diameter ≤ 2 .

The FNAB-C and CNB-T results were both classified into three groups: inadequate or nondiagnosis, negative, or positive for metastatic PTC. Immunohistochemistry was performed if there was a need for accurate diagnosis.

For patients treated for the first time, lateral neck dissection was performed if there was a positive FNAB-C or CNB-T result regardless of the value of Tg in the washout or BRAF 600E status; if there was a negative or nondiagnosis FNAB-C or CNB-T result but high Tg in the washout or BRAF 600E mutation assessment, frozen sectioning of the suspicious lymph nodes was also performed.

For patients suspected of having regional recurrence, an operation was performed if there was a positive FNAB-C or CNB-T result regardless of the Tg value in the washout or BRAF 600E status; if there was a negative or nondiagnosis FNAB-C or CNB-T result but high Tg in the washout or BRAF 600E mutation assessment, different procedures, including repeated

aspiration, close monitoring, direct surgery, etc., were selected accordingly.

Important Variable Definition

The normal ranges for serum TSH, Tg, and TgAb were from 0.27 mIU/L to 4.2 mIU/L, from 3.5 ng/ml to 77 ng/ml, and from 0 to 115 IU/ml, respectively. TgAb(+) was indicated if its value was higher than 115 IU/ml.

Fine and Core Needle Aspiration Technique and BRAF 600E Mutation Assessment

Fine needle aspiration biopsy was performed using a 22-gauge, and core needle biopsy was performed using an 18-gauge needle. Each aspiration was repeated at least three times to allow cytological or tissue examination and Tg in the washout determination or BRAF 600E mutation assessment. Immediately after aspiration, the needle and syringe were washed with 1 ml of normal saline and then sent to the laboratory if the Tg assay was required. A sufficient sample with an adequate number of tumor cells was used for real-time PCR analysis if BRAF 600E mutation assessment was required.

Statistical Analysis

The final outcome was confirmed by postoperative pathology, and the diagnostic abilities of FNAB-C and CNB-T were assessed with respect to their sensitivity, specificity, positive predictive value (PPV), and negative predictive value (NPV). The Mann-Whitney U test was used to compare the FNAB-Tg values between different groups. All statistical analyses were performed with SPSS 20.0, and $p < 0.05$ was considered to be significant.

RESULTS

Characteristics of the Patients and Lymph Nodes

Finally, 155 patients (50 male and 105 female) were enrolled, with a mean age of 43.7 (range: 19-78) years. Ninety-five (61.3%) patients had received no prior treatment, 49 (31.6%) patients had previously undergone total thyroidectomy, and 11 (7.1%) patients had previously received unilateral thyroid lobectomy (Table 1). A total of 186 solid lymph nodes were punctured and surgically treated;

TABLE 1 | Information of the enrolled 155 patients.

Variables	Patients (%)
Age	
<55	115 (74.2%)
≥55	40 (25.8%)
Sex	
Male	50 (32.3%)
Female	105 (67.7%)
Prior treatment	
None	95 (61.3%)
Total thyroidectomy	49 (31.6%)
Unilateral thyroid lobectomy	11 (7.1%)

among them, 88 (47.3%) lymph nodes underwent fine needle aspiration and 98 (52.7%) lymph nodes underwent core needle aspiration. Fifteen (8.1%) lymph nodes were located at level 6, and 171 (91.9%) lymph nodes were located at the lateral neck (levels 2-5). Postoperative pathology confirmed metastatic disease in 174 (92.6%) lymph nodes. BRAF 600E mutation assessment was performed in 88 lymph nodes, and a mutation was identified 41 (46.6%, 41/88) patients. Tg in the washout was evaluated in 98 lymph nodes, and its value was less than 1 ng/ml in 13 (13.3%, 10/98) patients and greater than 1 ng/ml in 85 (86.7%, 88/98) patients (Table 2).

ROC Curve of the Optimal Cutoff Value of FNAB-Tg

According to the ROC analysis (Figure 1), the optimal cutoff value of FNAB-Tg was 1.0 ng/ml, with an AUC of 0.976, and its sensitivity and specificity in predicting cervical LNM were 94.4% and 100%, respectively.

Diagnostic Performance Between FNAB-C and CNB-T

In 78 lymph nodes with positive FNAB-C results, 76 lymph nodes were confirmed to be metastatic by positive pathology; 7 lymph nodes had negative results, and 2 lymph nodes were confirmed to be metastatic by positive pathology. The sensitivity and specificity of FNAB-C in predicting cervical LNM were 97.4% and 71.4%, respectively (Table 3).

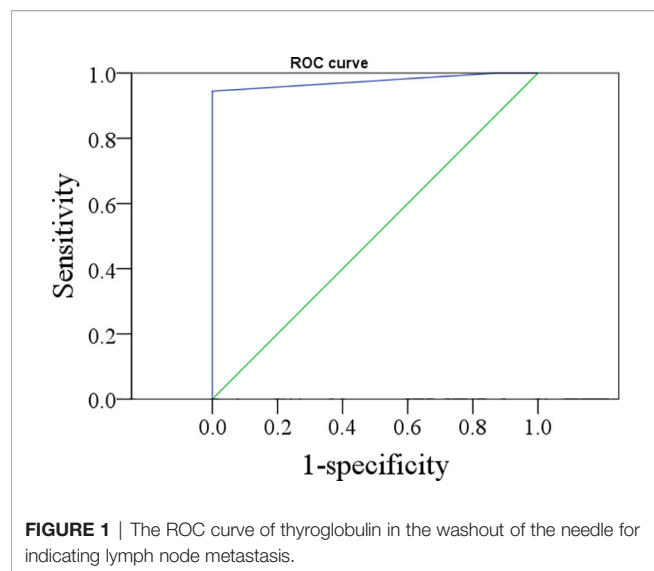
In 91 lymph nodes with positive CNB-T results, all lymph nodes were confirmed to be metastatic by positive pathology; in 7 lymph nodes had negative results, and 1 lymph node was confirmed to be metastatic by positive pathology. The sensitivity and specificity of CNB-T in predicting cervical LNM were 98.9% and 100%, respectively (Table 3).

Effect of BRAF 600E Mutation Assessment on the Diagnostic Performance of FNAB-C and CNB-T

In 32 lymph nodes, both FNAB-C and BRAF 600E mutation assessments were performed; in 28 lymph nodes with positive

TABLE 2 | Information of the 186 punctured lymph nodes.

Variables	Number (%)
Puncture type	
Fine needle	88 (47.3%)
Core needle	98 (52.7%)
Location	
Level 2-5	171 (91.9%)
Level 6	15 (8.1%)
Postoperative pathology	
Malignant	174 (93.5%)
Benign	12 (6.5%)
BRAF 600E mutation assessment	
Positive	41 (46.6%, 41/88)
Negative	47 (53.4%, 47/88)
Tg in the wash-out	
<1ng/ml	13 (13.3%, 10/98)
≥1ng/ml	85 (86.7%, 88/98)

**TABLE 3** | Diagnostic performance of between FNAB-C and CNB-T.

	Postoperative pathology	
	Malignant	Benign
FNAB-C		
Positive	76 (97.4%)	2 (28.6%)
Negative	2 (2.6%)	5 (71.4%)
CNB-T		
Positive	91 (98.9%)	0
Negative	1 (1.1%)	6 (100%)

FNAB-C results or BRAF 600E mutation assessments, 27 lymph nodes were found to be metastatic. The sensitivity and specificity of FNAB-C combined with BRAF 600E mutation assessment in predicting cervical LNM were 96.4% and 50%, respectively (**Table 4**).

In 56 lymph nodes, both CNB-T and BRAF 600E mutation assessments were performed; in 52 lymph nodes with positive CNB-T results or BRAF 600E mutation assessments, all lymph nodes were found to be metastatic. The sensitivity and specificity of CNB-T combined with BRAF 600E mutation assessment in predicting cervical LNM were 100% and 100%, respectively (**Table 4**).

TABLE 4 | Diagnostic performance in FNAB-C and CNB-T combined with or without Tg in the wash-out or BRAF 600E mutation assessment.

	Sensitivity	Specificity	PPV	NPV
FNAB-C	97.4%	71.4%	97.4%	71.4%
FNAB-C and FNAB-Tg	100%	95%	98%	100%
FNAB-C and BRAF 600E mutation	96.4%	50.0%	96.4%	50.0%
CNB-T	98.9%	100%	100%	85.7%
CNB-T and CNB-Tg	97.6%	100%	100%	66.7%
CNB-T and BRAF 600E mutation	100%	100%	100%	100%

Effect of Tg on the Diagnostic Performance of FNAB-C and CNB-T in the Washout

In 55 lymph nodes, both FNAB-Tg and FNAB-C were performed, and all 49 lymph nodes with positive FNAB-C results or high FNAB-Tg (≥ 1 ng/ml) were confirmed to be metastatic postoperatively. The sensitivity and specificity of FNAB-C combined with FNAB-Tg in predicting cervical LNM were 100% and 95%, respectively (**Table 4**).

In 43 lymph nodes, both CNB-Tg and CNB-T were performed, and all 40 lymph nodes with positive CNB-T results or high CNB-Tg (≥ 1 ng/ml) were confirmed to be metastatic postoperatively. The sensitivity and specificity of CNB-T combined with CNB-Tg in predicting cervical LNM were 97.6% and 100%, respectively (**Table 4**).

Association Between TgAb, Serum TSH, Serum Tg, Thyroid Tissue and FNAB-Tg

In 40 positive lymph nodes from TgAb(+) patients, the mean FNAB-Tg value was 228.1 ± 211.8 ng/ml, and in 58 positive lymph nodes from TgAb(-) patients, the mean FNAB-Tg value was 284.1 ± 211.8 ng/ml; the difference was not significant ($p=0.188$). (**Table 5**)

In 36 positive lymph nodes from low TSH patients, the mean FNAB-Tg value was 293.3 ± 211.6 ng/ml, in 35 lymph nodes from normal TSH patients, the mean FNAB-Tg value was 263.3 ± 214.1 ng/ml, and in 27 lymph nodes from high TSH patients, the mean FNAB-Tg value was 224.1 ± 184.9 ng/ml. However, this difference was not significant ($p=0.413$) (**Table 5**).

In 33 positive lymph nodes from low serum Tg patients, the mean FNAB-Tg value was 260.0 ± 207.6 ng/ml, in 35 lymph nodes from normal serum Tg patients, the mean FNAB-Tg value was 252.7 ± 204.9 ng/ml, and in 30 lymph nodes from high serum Tg patients, the mean FNAB-Tg value was 282.0 ± 210.0 ng/ml. However, this difference was not significant ($p=0.846$) (**Table 5**).

In 23 positive lymph nodes from patients without thyroid tissue presence, the mean FNAB-Tg value was 214.9 ± 194.0

TABLE 5 | Distribution of FNAB-Tg in positive lymph nodes with different characteristics.

Characteristic	FNAB-Tg (ng/ml)	p
TgAb		
Positive	228.1 ± 211.8	0.188
Negative	284.1 ± 211.8	
Serum TSH		
High	224.1 ± 184.9	0.413
Normal	263.3 ± 214.1	
Low	293.3 ± 211.6	
Serum Tg		
High	282.0 ± 210.0	0.846
Normal	252.7 ± 204.9	
Low	260.0 ± 207.6	
Thyroid tissue		
Yes	264.1 ± 207.2	0.331
No	214.9 ± 194.0	

ng/ml, and in 75 positive lymph nodes from patients with thyroid tissue presence, the mean FNAB-Tg value was 264.1 ± 207.2 ng/ml. However, this difference was not significant ($p=0.331$) (Table 5).

Association Between TgAb, Serum TSH, Serum Tg, Thyroid Tissue and the Diagnostic Performance of FNAB-Tg

As described in Table 6, both the sensitivity and NPV were 100% in positive lymph nodes with different characteristics, and both the specificity and PPV had a variation range of less than 5.0%.

DISCUSSION

The most important finding in the current study was that the optimal cutoff value of FNAB-Tg was 1.0 ng/ml, and its addition increased the sensitivity and specificity of FNAB-C. The diagnostic performance was not affected by TgAb, serum TSH, serum Tg, or thyroid tissue. CNB-T alone could provide satisfactory diagnostic reliability, and the additional benefit was greater with BRAF 600E mutation assessment than with FNAB-Tg. In all groups, CNB-T combined with BRAF 600E mutation assessment had the best diagnostic ability.

The optimal cutoff of FNAB-Tg value had been studied previously and reported to be in the range of 0.9 ng/ml to 50 ng/ml (17). A meta-analysis by Grani et al. (17) indicated a pooled sensitivity of 94.8% and a specificity of 91.2% with a cutoff of 0.9–1.1 ng/ml, a pooled sensitivity of 87.7% and a specificity of 94.2% with a cutoff of 10 ng/ml, and a pooled sensitivity of 97.3% and specificity of 94.9% with a cutoff of serum Tg in predicting cervical NLM. Uruno et al. (5) analyzed 129 fine needle punctured lymph nodes, of which 105 lymph nodes were positive by FNAB-Tg (range 6.2–8000 ng/ml) and 24 lymph nodes were negative (range 0.6–88.8 ng/ml). FNAB-Tg and FNAB-C can compensate for the loss of the other based on the

assumption that the lymph node is positive if the FNAB-Tg value is higher than the serum Tg level, taking blood contamination into consideration. However, in practice, the sample for FNAB-Tg is diluted with 1 ml normal saline, with a typical dilution between 50 and 200. In addition, Borel et al. (24) reported that the maximum blood contamination of the needle washout fluid in theory was approximately 20% and contamination was less than 5% in experiments evaluating albumin concentration in FNAB washout fluid; therefore, even if blood contamination did occur, the FNAB-Tg value was still lower in a negative lymph node than in a positive lymph node. This finding was supported by our ROC results. Pathology results are typically the gold standard for decision making in thyroid cancer; therefore, the main contribution of FNAB-Tg assessment is in determining the best balance between necessary and unnecessary surgery in metastatic patients with a negative or nondiagnostic pathological result. Konca Degertekin et al. (12) analyzed the diagnostic accuracy of FNAB-C and FNAB-Tg in 51 lymph nodes and found that FNAB-Tg ≥ 1 ng/ml was associated with similar accuracy and even a higher specificity and PPV compared to FNAB-C alone, and the authors concluded that the best cutoff value was 1.0 ng/ml. Moon et al. (25) reported that the median FNAB-Tg was 521.2 ng/ml in malignant lymph nodes, and the optimal cutoff value of FNAB-Tg was 1.0 ng/ml, with a sensitivity of 93.2% and a specificity of 95.9%. Combining FNAB-Tg and FNAB-C showed superior diagnostic power compared with the diagnostic strategy of using either FNAB-C or FNAB-Tg alone. The finding was consistent with our own results: a cutoff value of 1.0 ng/ml is related to high sensitivity and specificity.

However, factors that could affect FNAB-Tg need to be analyzed further. Li et al. (18) described 6 cases with very elevated FNAB-Tg levels that were confirmed to be normal thyroid tissue, in which 3 cases were labeled as metastatic lymph nodes at level 6. It has been accepted that residual thyroid tissue might be mistaken for suspicious lymph nodes in patients with a history of thyroid surgery, and this viewpoint was confirmed by Jeon et al. (7) and Tang et al. (15): some cases with high FNAB-Tg levels were ultimately explained by remnant thyroid tissue. Therefore, caution must be taken when a negative FNAB-C result but a high FNAB-Tg level is observed in samples collected from the central neck. However, the situation in lateral cervical lymph nodes is more difficult to discern. Usually, the needle path does not pass through the thyroid region during puncture for levels 2–5, and our results also confirmed that there was no thyroid tissue to be considered for a negative FNAB-C but positive FNAB-Tg.

The interference effect of TgAb is most frequently evaluated in the literature but remains unclear. Jo et al. (14) demonstrated that the FNAB-Tg level was significantly higher in TgAb- patients than in TgAb+ patients, and its sensitivity and PPV were increased by >10% in TgAb- patients compared to TgAb+ patients when using the same cutoff value. However, Konca Degertekin et al. (12) reported that TgAb+ and TgAb- patients had comparable FNAB-Tg levels in malignant lymph nodes, and the diagnostic performance of FNAB-Tg was independent of TgAb status. Similar findings were also published by Boi et al. (10)

TABLE 6 | Association between TgAb, serum TSH, serum Tg, thyroid tissue and the diagnostic performance of FNAB-C and FNAB-Tg in positive lymph nodes.

Characteristics	Diagnostic performance of FNAB-C and FNAB-Tg			
	Sensitivity	Specificity	PPV	NPV
TgAb				
Positive	100%	98.4%	100%	100%
Negative	100%	94.1%	96.9%	100%
Serum TSH				
High	100%	92.3%	100%	100%
Normal	100%	94.7%	96.7%	100%
Low	100%	97.8%	98.3%	100%
Serum Tg				
High	100%	93.7%	98.1%	100%
Normal	100%	95.2%	100%	100%
Low	100%	96.9%	97.2%	100%
Thyroid tissue				
Yes	100%	96.6%	99.0%	100%
No	100%	93.5%	97.2%	100%

and Duval et al. (26). There were at least two explanations for this finding: on the one hand, TgAb was negative in FNAB from patients with positive serum TgAb (27), and on the other hand, an elevated FNAB-Tg level can easily override the effect of TgAb caused by blood contamination.

The role of TSH and serum Tg has only been analyzed occasionally. One study commented that TSH increased the possibility of false-negative FNAB-Tg in malignant cases (7), but there was no strong evidence to support this viewpoint. In our opinion, blood contamination is a direct or indirect cause that could explain the effect of TSH and serum Tg. In the current study, FNAB-Tg was at the same level in patients with positive lymph nodes who had different TSH and serum Tg levels, and the diagnostic performance of FNAB-C had little relationship with TSH and serum Tg. This finding might be partially due to the abilities of our experienced thyroidologists and cytopathologists.

BRAF 600E mutation was the most common genetic change in PTC patients with geographical differences and occurred in most of the primary tumors and metastatic lymph nodes. Chen et al. (23) reported that 78% of positive lymph nodes had BRAF 600E gene changes, but the mutation was not associated with the number, extranodal extension, or stage of the positive lymph nodes. A slightly lower rate of 47.1% was reported by Kurtulmus et al. (22), but the authors found that the presence of the BRAF 600E mutation in lymph nodes was not affected by mutation in the primary tumor. This finding introduced the possibility of BRAF 600E mutation assessment in predicting cervical LNM. Li et al. (28) might be the only author to evaluate the utilization of BRAF 600E mutation assessment in diagnosing cervical LNM; in their study, 27 positive lymph nodes had a negative FNAB-C result, but 17 of the 27 cases were positive for BRAF 600E mutation. The authors concluded that BRAF 600E mutation assessment could provide diagnostic support in PTC patients, but the benefit extent was small. In our study, it was also noted that compared to FNAB-C alone, the diagnostic performance of FNAB-C combined with BRAF 600E mutation assessment was reduced. One possible explanation is that the samples collected from fine needle puncture ready for BRAF 600E mutation assessment were very limited, increasing the misdiagnosis rate.

Core needle biopsy is another method for disease diagnosis. Novoa et al. (21) confirmed its reliability based on a systemic analysis revealing that CNB provided a correct specific diagnosis in 87% of cases without major complications; however, no other authors have tried to evaluate the feasibility of CNB in predicting cervical LNM in PTC. We were the first to report the high sensitivity and specificity of CNB alone, which could be

explained by the fact that only clinically suspicious lymph nodes were punctured, and all the procedures were performed by experienced clinicians. It is interesting to note that the diagnostic ability of CNB-T is decreased when combined with CNB-Tg, and one possible explanation is that blood contamination is very frequent during CNB. However, the relationship between CNB-T and BRAF 600E mutation assessment can allow for the best diagnostic performance and prevent all unnecessary surgeries.

The current study has some limitations that must be acknowledged. First, our sample size was relatively small, which might have decreased our statistical power. Second, there is inherent bias in all retrospective studies. Third, we need to stay awake that the practicality of core biopsy on suspicious lymph nodes is limited in selective patients, especially the pediatric population, because core biopsy is more invasive than a fine needle aspiration.

In summary, the sensitivity and specificity of FNAB-C could be increased when combined with FNAB-Tg, with an optimal cutoff value of 1.0 ng/ml. CNB-T alone can provide satisfactory diagnostic reliability, and the additional benefit is greater with BRAF 600E mutation assessment than with FNAB-Tg.

DATA AVAILABILITY STATEMENT

The original contributions presented in the study are included in the article. Further inquiries can be directed to the corresponding authors.

ETHICS STATEMENT

The studies involving human participants were reviewed and approved by The Our Hospital Institutional Research Committee, and all participants provided written informed consent. The patients/participants provided their written informed consent to participate in this study.

AUTHOR CONTRIBUTIONS

All the authors made the contribution in study design, manuscript writing, studies selecting, data analysis, study quality evaluating, and manuscript revising. All authors contributed to the article and approved the submitted version.

REFERENCES

- Cabanillas ME, McFadden DG, Durante C. Thyroid cancer. *Lancet* (2016) 388:2783–95. doi: 10.1016/S0140-6736(16)30172-6
- Liu ST, Zhang X. [Epidemiology and management guidelines of thyroid cancer]. *Zhonghua Er Bi Yan Hou Tou Jing Wai Ke Za Zhi* (2016) 51:146–9.
- Filetti S, Durante C, Hartl D, Leboulleux S, Locati LD, Newbold K, et al. ESMO Guidelines Committee. Thyroid cancer: ESMO Clinical Practice Guidelines for diagnosis, treatment and follow-up. *Ann Oncol* (2019) 30:1856–83. doi: 10.1093/annonc/mdz400
- Brito JP, Hay ID. Management of Papillary Thyroid Microcarcinoma. *Endocrinol Metab Clin North Am* (2019) 48:199–213. doi: 10.1016/j.jec.2018.10.006
- Uruno T, Miyauchi A, Shimizu K, Tomoda C, Takamura Y, Ito Y, et al. Usefulness of thyroglobulin measurement in fine-needle aspiration biopsy specimens for diagnosing cervical lymph node metastasis in patients with

- papillary thyroid cancer. *World J Surg* (2005) 29:483–5. doi: 10.1007/s00268-004-7701-0
6. Achille G, Garrisi VM, Russo S, Guastamacchia E, Giagulli VA, Schirosi L, et al. Thyroglobulin Determination in Fine Needle Aspiration Biopsy Washout of Suspicious Lymph Nodes in Thyroid Carcinoma Follow up. *Endocr Metab Immune Disord Drug Targets* (2017) 17:213–8. doi: 10.2174/1871530317666170531092501
 7. Jeon SJ, Kim E, Park JS, Son KR, Baek JH, Kim YS, et al. Diagnostic benefit of thyroglobulin measurement in fine-needle aspirates of cervical lymph nodes for diagnosing metastatic cervical lymph nodes from papillary thyroid cancer: correlations with US features. *Korean J Radiol* (2009) 10:106–11. doi: 10.3348/kjr.2009.10.2.106
 8. Cunha N, Rodrigues F, Curado F, Ilhéu O, Cruz C, Naidenov P, et al. Thyroglobulin detection in fine-needle aspirates of cervical lymph nodes: a technique for the diagnosis of metastatic differentiated thyroid cancer. *Eur J Endocrinol* (2007) 157:101–7. doi: 10.1530/EJE-07-0088
 9. Frasoldati A, Toschi E, Zini M, Flora M, Caroggio A, Dotti C, et al. Role of thyroglobulin measurement in fine-needle aspiration biopsies of cervical lymph nodes in patients with differentiated thyroid cancer. *Thyroid* (1999) 9:105–11. doi: 10.1089/thy.1999.9.105
 10. Boi F, Baghino G, Atzeni F, Lai ML, Faa G, Mariotti S. The diagnostic value for differentiated thyroid carcinoma metastases of thyroglobulin (Tg) measurement in washout fluid from fine-needle aspiration biopsy of neck lymph nodes is maintained in the presence of circulating anti-Tg antibodies. *J Clin Endocrinol Metab* (2006) 91:1364–9. doi: 10.1210/jc.2005-1705
 11. Pacini F, Fugazzola L, Lippi F, Ceccarelli C, Centoni R, Miccoli P, et al. Detection of thyroglobulin in fine needle aspirates of nonthyroidal neck masses: a clue to the diagnosis of metastatic differentiated thyroid cancer. *J Clin Endocrinol Metab* (1992) 74:1401–4. doi: 10.1210/jcem.74.6.1592886
 12. Konca Degertekin C, Yalcin MM, Cerit T, Ozkan C, Kalan I, Iyidir OT, et al. Lymph node fine-needle aspiration washout thyroglobulin in papillary thyroid cancer: Diagnostic value and the effect of thyroglobulin antibodies. *Endocr Res* (2016) 41:281–9. doi: 10.3109/07435800.2016.1141936
 13. Al-Hilli Z, Strajina V, McKenzie TJ, Thompson GB, Farley DR, Regina Castro M, et al. Thyroglobulin Measurement in Fine-Needle Aspiration Improves the Diagnosis of Cervical Lymph Node Metastases in Papillary Thyroid Carcinoma. *Ann Surg Oncol* (2017) 24:739–44. doi: 10.1245/s10434-016-5625-1
 14. Jo K, Kim MH, Lim Y, Jung SL, Bae JS, Jung CK, et al. Lowered cutoff of lymph node fine-needle aspiration thyroglobulin in thyroid cancer patients with serum anti-thyroglobulin antibody. *Eur J Endocrinol* (2015) 173:489–97. doi: 10.1530/EJE-15-0344
 15. Tang S, Buck A, Jones C, Sara Jiang X. The utility of thyroglobulin washout studies in predicting cervical lymph node metastases: One academic medical center's experience. *Diagn Cytopathol* (2016) 44:964–8. doi: 10.1002/dc.23554
 16. Zhu XH, Zhou JN, Qian YY, Yang K, Wen QL, Zhang QH, et al. Diagnostic values of thyroglobulin in lymph node fine-needle aspiration washout: a systematic review and meta-analysis diagnostic values of FNA-Tg. *Endocr J* (2020) 67:113–23. doi: 10.1507/endocrj.EJ18-0558
 17. Grani G, Fumarola A. Thyroglobulin in lymph node fine-needle aspiration washout: a systematic review and meta-analysis of diagnostic accuracy. *J Clin Endocrinol Metab* (2014) 99:1970–82. doi: 10.1210/jc.2014-1098
 18. Li QK, Nugent SL, Straseski J, Cooper D, Riedel S, Askin FB, et al. Thyroglobulin measurements in fine-needle aspiration cytology of lymph nodes for the detection of metastatic papillary thyroid carcinoma. *Cancer Cytopathol* (2013) 121:440–8. doi: 10.1002/cncy.21285
 19. Ryu KH, Lee JH, Jang SW, Kim HJ, Lee JY, Chung SR, et al. US-guided core-needle biopsy versus US-guided fine-needle aspiration of suspicious cervical lymph nodes for staging workup of non-head and neck malignancies: A propensity score matching study. *J Surg Oncol* (2017) 116:870–6. doi: 10.1002/jso.24747
 20. Wagner JM, Monfore N, McCullough AJ, Zhao L, Conrad RD, Krempel GA, et al. Ultrasound-Guided Fine-Needle Aspiration With Optional Core Needle Biopsy of Head and Neck Lymph Nodes and Masses: Comparison of Diagnostic Performance in Treated Squamous Cell Cancer Versus All Other Lesions. *J Ultrasound Med* (2019) 38:2275–84. doi: 10.1002/jum.14918
 21. Nova E, Gürtler N, Arnoux A, Kraft M. Role of ultrasound-guided core-needle biopsy in the assessment of head and neck lesions: a meta-analysis and systematic review of the literature. *Head Neck* (2012) 34:1497–503. doi: 10.1002/hed.21821
 22. Kurtulmus N, Ertas B, Saglican Y, Kaya H, Ince U, Duren M. BRAFV600E Mutation: Has It a Role in Cervical Lymph Node Metastasis of Papillary Thyroid Cancer? *Eur Thyroid J* (2016) 5:195–200. doi: 10.1159/000448112
 23. Chen P, Pan L, Huang W, Feng H, Ouyang W, Wu J, et al. BRAF V600E and lymph node metastases in papillary thyroid cancer. *Endocr Connect* (2020) 9:999–1008. doi: 10.1530/EC-20-0420
 24. Borel AL, Boizel R, Faure P, Barbe G, Boutonnat J, Sturm N, et al. Significance of low levels of thyroglobulin in fine needle aspirates from cervical lymph nodes of patients with a history of differentiated thyroid cancer. *Eur J Endocrinol* (2008) 158:691–8. doi: 10.1530/EJE-07-0749
 25. Moon JH, Kim YI, Lim JA, Choi HS, Cho SW, Kim KW, et al. Thyroglobulin in washout fluid from lymph node fine-needle aspiration biopsy in papillary thyroid cancer: large-scale validation of the cutoff value to determine malignancy and evaluation of discrepant results. *J Clin Endocrinol Metab* (2013) 98:1061–8. doi: 10.1210/jc.2012-3291
 26. Duval MADS, Zanella AB, Cristo AP, Faccin CS, Graudenz MS, Maia AL. Impact of Serum TSH and Anti-Thyroglobulin Antibody Levels on Lymph Node Fine-Needle Aspiration Thyroglobulin Measurements in Differentiated Thyroid Cancer Patients. *Eur Thyroid J* (2017) 6:292–7. doi: 10.1159/000479682
 27. Sigstad E, Heilo A, Paus E, Holgersen K, Grøholt KK, Jørgensen LH, et al. The usefulness of detecting thyroglobulin in fine-needle aspirates from patients with neck lesions using a sensitive thyroglobulin assay. *Diagn Cytopathol* (2007) 35:761–7. doi: 10.1002/dc.20726
 28. Li J, Liu J, Yu X, Bao X, Qian L. BRAFv600e mutation combined with thyroglobulin and fine-needle aspiration in diagnosis of lymph node metastasis of papillary thyroid carcinoma. *Pathol Res Pract* (2018) 214:1892–7. doi: 10.1016/j.prp.2018.09.003

Conflict of Interest: The authors declare that the research was conducted in the absence of any commercial or financial relationships that could be construed as a potential conflict of interest.

Copyright © 2021 Zhang, Zhang, Du, Dai, Luo, Fang and Ge. This is an open-access article distributed under the terms of the Creative Commons Attribution License (CC BY). The use, distribution or reproduction in other forums is permitted, provided the original author(s) and the copyright owner(s) are credited and that the original publication in this journal is cited, in accordance with accepted academic practice. No use, distribution or reproduction is permitted which does not comply with these terms.



Risk Stratification in Patients With Follicular Neoplasm on Cytology: Use of Quantitative Characteristics and Sonographic Patterns

Ming-Hsun Wu¹, Kuen-Yuan Chen¹, Min-Shu Hsieh², Argon Chen^{3*} and Chiung-Nien Chen¹

¹ Department of Surgery, National Taiwan University Hospital, Taipei, Taiwan, ² Department of Pathology, National Taiwan University Hospital, Taipei, Taiwan, ³ Graduate Institute of Industrial Engineering, National Taiwan University, Taipei, Taiwan

OPEN ACCESS

Edited by:

Christoph Reiners,
University Hospital Würzburg,
Germany

Reviewed by:

Paolo Miccoli,
University of Pisa, Italy
Hernan Tala,
Universidad del Desarrollo, Chile

*Correspondence:

Argon Chen
achen@ntu.edu.tw

Specialty section:

This article was submitted to
Thyroid Endocrinology,
a section of the journal
Frontiers in Endocrinology

Received: 06 October 2020

Accepted: 22 March 2021

Published: 30 April 2021

Citation:

Wu M-H, Chen K-Y, Hsieh M-S,
Chen A and Chen C-N (2021) Risk
Stratification in Patients With Follicular
Neoplasm on Cytology: Use of
Quantitative Characteristics and
Sonographic Patterns.
Front. Endocrinol. 12:614630.
doi: 10.3389/fendo.2021.614630

Objectives: Differentiating thyroid nodules with a cytological diagnosis of follicular neoplasm remains an issue. The goal of this study was to determine whether ultrasonographic (US) findings obtained preoperatively from the computer-aided detection (CAD) system are sufficient to further stratify the risk of malignancy for this diagnostic cytological category.

Methods: From September 2016 to September 2018 in our hospital, patients diagnosed with Bethesda category IV (follicular neoplasm or suspicion of follicular neoplasm) thyroid nodules and underwent surgical excisions were included in the study. Quantification and analysis of tumor features were performed using CAD software. The US findings of the region of interest, including index of composition, margin, echogenicity, texture, echogenic dots indicative of calcifications, tall and wide orientation, and margin were calculated into computerized values. The nodules were further classified into American Thyroid Association (ATA) and American College of Radiology Thyroid Imaging Reporting & Data System (TI-RADS) categories.

Results: 92 (10.1%) of 913 patients were diagnosed with Bethesda category IV thyroid nodules. In 65 patients, the histological type of the nodule was identified. The quantitative features between patients with benign and malignant conditions differed significantly. The presence of heterogeneous echotexture, blurred margins, or irregular margins was shown to have the highest diagnostic value. The risks of malignancy for nodules classified as having very low to intermediate suspicion ATA, non-ATA, and high suspicion ATA patterns were 9%, 35.7%, and 51.7%, respectively. Meanwhile, the risks of malignancy were 12.5%, 26.1%, and 53.8% for nodules classified as TIRADS 3, 4, and 5, respectively. When compared to human observers, among whom poor agreement was noticeable, the CAD software has shown a higher average accuracy.

Conclusions: For patients with nodules diagnosed as Bethesda category IV, the software-based characterizations of US features, along with the associated ATA patterns and TIRADS system, were shown helpful in the risk stratification of malignancy.

Keywords: follicular neoplasm, ultrasonography, thyroid gland, thyroid cancer (TC), follicular thyroid carcinoma (FTC)

INTRODUCTION

Thyroid nodular disease is one of the most common endocrine disorders. The preoperative diagnosis of thyroid nodule is commonly based on fine-needle aspiration cytology (FNAC) results (1). However, follicular cell-derived thyroid nodules have overlapping cytomorphological features (2–4); thus, 15%–30% of aspirations are indeterminate (5). The Bethesda system of thyroid cytopathology defines follicular neoplasm (FN) or suspicion of follicular neoplasm (SFN) as Bethesda category IV, with the goal of increasing the probability of detecting follicular thyroid cancers (6). It reports a 10% to 40% association with malignancy risk, and diagnostic thyroidectomy is often recommended for making a diagnosis (7–9). Moreover, up to 85% of thyroidectomy procedures are performed for benign lesions in this category (10). The ATA guidelines suggest consider using assessment methods for molecular markers, such as mutational testing using next-generation sequencing or special immunohistochemical staining, rather than the operative approach for diagnosis. However, these methods are expensive and currently are not widely available.

High-resolution ultrasonography (US) is the initial imaging technique used to evaluate the gross morphologic characteristics of thyroid nodules. Most studies of the US features of thyroid nodules have focused on how to select patients for further cytological examinations, while few studies have reported the predictive value of US for malignant nodules in Bethesda category IV. In addition, the results of these studies were not conclusive (1, 11, 12). Our previous study showed that certain gray-scale US features may help differentiate pathologically confirmed follicular thyroid cancer (FTC) from follicular adenoma (FA) (13). However, tumors with Bethesda category IV cytology do not always result in a histologic diagnosis of FTC and FA, and it remains uncertain whether they can be used to differentiate this category preoperatively. In addition, algorithms that can identify patients at high risk of malignancy may allow surgeons to perform a single definitive operation (usually lobectomy or total thyroidectomy if needed), thereby saving time, reducing patient morbidity, and reducing costs.

The major limitations of thyroid US are inter-observer and intra-observer variability (14–19). Computerized quantification methods that can characterize the sonographic features to make the diagnosis more objective are available, and have shown acceptable agreement with experienced clinicians (20–26). A computer-aided detection (CAD) system (K180006) had been developed based on these methods and validated following the guidelines of the United States Food and Drug Administration (FDA) for clinical use.

Because further differentiation of Bethesda category IV lesions is challenging, we aimed to examine whether the information provided by commercial CAD to surgeons is sufficient to predict thyroid cancer. Moreover, we examined the usefulness of the current ATA and TIRADS systems in surgical planning for these patients.

MATERIALS AND METHODS

Participants

The institutional review board of the National Taiwan University Hospital approved the data collection and analyses in this study. Based on thyroid FNACs performed during the study period from September 2016 to September 2018 in the National Taiwan University Hospital, 92 (10.1%) of 913 patients were diagnosed with Bethesda category IV thyroid nodules. Because molecular testing is not widely available in Taiwan, physicians recommended surgical excision to these patients for the removal and definitive diagnosis of an FN/SFN thyroid nodule. Sixty-five patients who underwent thyroidectomy were recruited in this study. The diagnoses were based on the histopathological findings of surgical specimens that were assessed by pathologists. The other 27 patients refused to undergo an operation.

Equipment and Ultrasonographic Procedures

All sonograms were performed using commercial ultrasonography devices with multi-frequency (4–12 megahertz) linear probes set to the highest frequency available, including HDI 5000 (Philips Medical Systems, Bothell, WA, the USA), Voluson 730 (GE Medical Systems, Milwaukee, WI, the USA), and ALOKA ProSound 2 (Hitachi Medical Systems Europe, Steinhilfen, Switzerland). The procedure was performed while the participant was in a supine position with the neck hyperextended. Images were captured using the maximum nodule diameter. Image analysis was conducted offline using the DICOM format of images on a separate computer. Quantification of tumor features was performed using a commercial software (AmCAD-UT, AmCad BioMed, Taiwan).

Briefly, the operators provided the four endpoints of the axes on the thyroid nodule margins. The CAD software was used to calculate the contour of the mass, to distinguish it from normal thyroid tissues. In the image analysis session, the US findings of the region of interest (ROI), including index of composition (CoI), index of margin (MI), index of echogenicity (EI), index of texture (TI), index of echogenic dots indicative of calcifications (CaI), index of tall and wide orientation (TWI), and index of margin irregularity (MII), were calculated into computerized values.

CoI calculated the percentage of the cystic component consisting of the anechoic pixels. The anechoic pixels were those pixels with the gray-scale intensity readings below a certain pre-defined threshold inside the ROI (20). CaI was the proportion of the echogenic foci in the solid component of ROI. The solid component was defined to be the area of the ROI excluding the cystic area. Echogenic foci were then represented by those hyperechoic pixels with the gray-scale intensity readings higher than a pre-defined threshold (20). EI was the difference between the average gray-scale intensities of the ROI area and the surrounding reference area outside the ROI (21). TI was to compute the texture heterogeneity of the solid component by calculating the texture variation among small areas within the ROI (22). The higher TI value indicated a greater composition difference of the nodule tissue. TWI calculated the height to width ratio with the nodule height measured along the sound-beam direction and the nodule width in the direction perpendicular to the height as defined by ACR. MI was an indicator of the ill-defined margin that calculated the proportion of the indistinctive border between the nodule and the thyroid parenchyma (27). MII was computed to describe how irregular the nodule margin was by comparing the radius variation of the ROI margin to that of a smooth margin defined by the nodule long and short axes and a corresponding Bezier curve.

These index values were then quantified to represent features that described the thyroid nodule, including factors such as solid or cystic; well-defined or ill-defined; hyperechoic/isoechoic or hypoechoic/markedly hypoechoic; heterogeneous or homogeneous; presence of calcification; presence of taller-than-wide orientation; and presence of irregular margin (20–23).

CAD software was used to classify nodules according to the 2015 ATA sonographic patterns (CAD-ATA), using the referral description of the sonographic features (28). Scenarios not described in the 2015 ATA classification were classified into a separate category referred to as non-ATA patterns. These scenarios included heterogeneous nodules with or without other suspicious features, and iso- or hyperechoic nodules with at least one suspicious feature.

CAD software was also utilized to calculate the total risk score of each thyroid nodule by summing the scores of each US feature and classifying them into TIRADS categories (CAD-TIRAD) (29).

Recorded images of thyroid ultrasound were also independently reviewed by three human observers (MH Wu, KY Chen, and MF Wang), all with more than 10 years' experience in thyroid ultrasound. They interpreted each nodule with 2015 ATA sonographic patterns (Observer-ATA) and TIRADS categories (Observer-TIRAD). If there are discordance in their results, the final interpretation was determined by consensus of two or more observers. When there was no consensus through the independent assessment, the image was reviewed jointly to reach a consensus.

The malignancy rate of each of the ATA and TIRADS category was calculated based on the final histological outcomes of the nodules.

Pathological Evaluation

The decision to biopsy thyroid nodules in our institute was based on 2015 ATA recommendations according to sonographic patterns and sizes. Cytological diagnoses were made using the Bethesda System for Reporting Thyroid Cytopathology by board-certified cytologists, and were retrieved from the cytology reports (6, 30). In our thyroid FNAC practice, cases with inconsistent diagnoses were reviewed and agreement was achieved by discussion.

Statistical Analysis

Data were summarized using descriptive statistics. Categorical variables were presented as numbers and percentages, while continuous variables were presented as means and standard deviations or medians and ranges for those tested significantly not conforming to normal distributions. Data on patient characteristics were analyzed with Student's *t*-test or analysis of variance for continuous variables, Mann-Whitney test for non-normal continuous variables and chi-square test or Fisher's exact test for categorical variables. Diagnostic performance was estimated by Positive Predictive Value (PPV), Negative Predictive Value (NPV), Sensitivity, and Specificity, all calculated with 95% Confidence Intervals (95% CI). Statistical analyses were performed using SAS 9.4 (Cary, NC, USA). All *p*-values were two-sided, and the significance level was set at 5%.

RESULTS

Based on thyroid FNACs performed during the study period, 92 (10.1%) of 913 patients were diagnosed with Bethesda category IV thyroid nodules. Among them, 27 patients refused to undergo an operation. There were no significant age, sex, and nodule size differences in those with and without surgeries in this study. In total, 65 patients who underwent surgery were included for further analysis. Of these, 22 had cancer in the thyroid nodule, based on histopathological examination, i.e., a malignancy rate of 33.8% (22/65).

The demographic characteristics of the 65 patients with 65 thyroid nodules are summarized in **Table 1**. Histopathology results revealed that 19 nodules were nodular goiter; 24 were FA; 15 were papillary thyroid cancer (PTC), including four follicular variant subtypes; and 7 were FTC. None of the patients in this study had Noninvasive follicular thyroid neoplasm with papillary-like nuclear features (NIFTP). The average width, height, and length of the nodules were 2.2 ± 1.3 , 1.6 ± 0.8 , and 3.3 ± 1.5 cm, respectively.

The quantitative values of the features between benign and malignant nodules are shown in **Figure 1**. Significant differences were observed in the feature indices of CaI, EI, TI, TWI, and MII.

The demographic and sonographic characteristics of patients with benign and malignant nodules are presented in **Table 2**. No significant differences were observed in terms of age and sex distribution ($p = 0.64$ and 0.076 , respectively). A higher number of malignant tumors had heterogeneous echotexture (15/22, 68.2% versus 14/43, 32.6%, $p = 0.0067$) and taller-than-wide orientation (6/22, 27.3% versus 3/43, 7.0%, $p = 0.0261$).

TABLE 1 | Demographic characteristics of patients diagnosed with follicular neoplasm on cytology.

Characteristics	Number (%) or mean \pm SD (range)
Gender	
Male	10 (15.4)
Female	55 (84.6)
Age	46.8 \pm 14.1 (18–73)
Histological diagnosis	
Nodular goiter	19(29.2)
Follicular/Hurthle cell adenoma	24(36.9)
Papillary carcinoma	15(23.1)
Follicular/Hurthle cell carcinoma	7(10.8)
Location of nodules	
Left	22 (33.8)
Right	41 (63.1)
Isthmus	2 (3.1)
Size of nodules (cm)	
Length	2.38 \pm 1.28 (0.72–7.28)
Width	2.18 \pm 1.26 (0.56–7.19)
Height	1.62 \pm 0.82 (0.35–4.72)

To learn the preoperative diagnostic value of the US features determined by CAD in differentiating benign from malignant nodules, we calculated the positive and negative predictive values and the sensitivity, specificity, and average accuracy (average sensitivity and specificity), as shown in **Table 3**. Using a combination of three features, namely, heterogeneous echotexture, irregular margin, and blurred margin, was found to have the highest average accuracy (0.735). 47% of benign Bethesda category IV nodules were with none of these features and 100% of malignant nodules were accurately diagnosed by having at least one of the features present.

The nodules were classified into the 2015 ATA sonographic patterns and TIRADS categories based on the sonographic characteristics by both CAD and human observers. For CAD, none of the nodules had an ATA benign pattern. Twenty-two nodules were classified as very low to intermediate suspicion

TABLE 2 | Comparison of the demographic characteristics of the participants and sonographic characteristics between thyroid nodules with benign and malignant histology.

	Benign (n = 43)	Malignant (n = 22)	p value
Gender			0.076 ^F
Male/female	4/39	6/16	
Age	47 \pm 13.9, 18–73	46.4 \pm 14.7, 23–72	0.64 ^t
Location of nodule			0.63 ^F
Left/right/isthmus	16/26/1	6/15/1	
Size of the nodule (cm)			
Length	2.3 (0.92–7.28)	1.55 (0.72–5.12)	0.03*
Width	2.07 (0.64–7.19)	1.41 (0.56–5.20)	0.05*
Height	1.54 (0.35–3.87)	1.2 (0.45–4.72)	0.27*
Sonographic characteristics			
Taller-than-wide Morphology	3 (7.0%)	6 (27.3%)	0.0261[†]
Component			0.17 ^F
Solid/mixed	30/13 (69.8%)	11/11 (50.0%)	
Calcification			0.86 ^F
Macro/eggshell/micro	2/4/13	1/2/12	
Hypo-echogenicity	20 (46.5%)	15 (68.2%)	0.10 [†]
Heterogeneous echotexture	14 (32.6%)	15 (68.2%)	0.0067[†]
Blurred margins	11 (25.6%)	9 (40.9%)	0.2087 [†]
Irregular margins	11 (25.6%)	9 (40.9%)	0.2087 [†]

^FThese variable were compared using the Fisher's exact test.

[†]These variable were compared using the chi-square test.

^tThese variable were compared using the Student's t-test.

*These variable were compared using the Mann-Whitney U test.

Bold denotes statistically significant results.

patterns, 29 as high suspicion patterns, and 14 as non-ATA patterns. The risk of finding malignant nodules with very low to intermediate suspicion patterns, non-ATA patterns, and high suspicion patterns were 9%, 35.7%, and 51.7%, respectively. None of the nodules were classified as TIRADS 1 and 2 in our study. Meanwhile, 16, 23, and 26 nodules were classified as TIRADS 3, 4, and 5, respectively. The risk of developing malignant nodules in each TIRADS category increased with

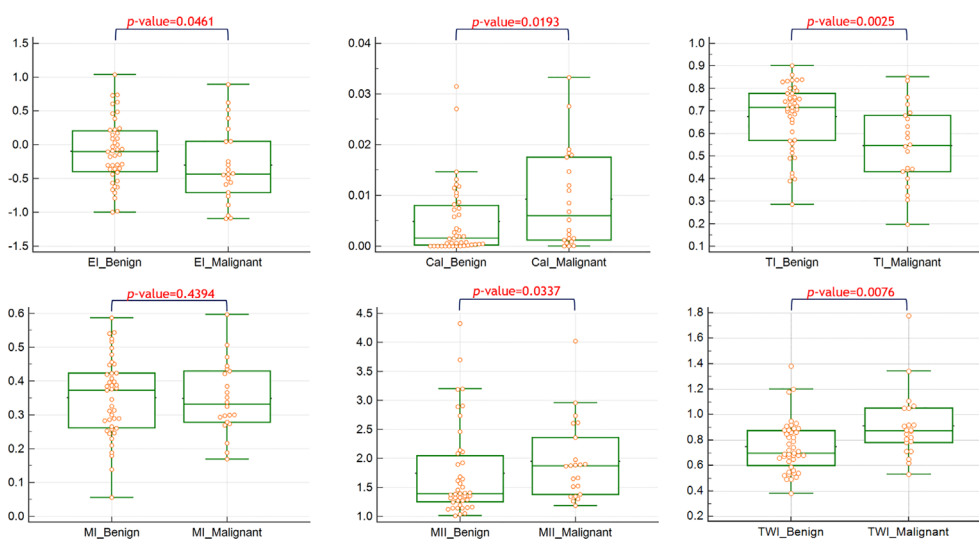
**FIGURE 1 |** The quantitative values of the features between benign and malignant nodules.

TABLE 3 | Sonographic features used in differentiating benign from malignant conditions in 65 patients with follicular neoplasms.

	PPV (95% CI)	NPV (95% CI)	Sensitivity (95% CI)	Specificity (95% CI)	Average*
Sonographic characteristics					
Hypo-echogenicity	0.44 (33.7-55.1)	0.77 (63.8-87.0)	0.68 (45.1-86.1)	0.56 (39.9-70.9)	0.62
Calcification	0.48 (33.8-62.6)	0.75 (64.6-83.2)	0.55 (32.2-75.6)	0.70 (53.9-82.8)	0.625
Heterogeneous echotexture	0.52 (39.0-64.2)	0.81 (68.5-88.8)	0.68 (45.1-86.1)	0.67 (51.5-80.9)	0.675
Blurred margin	0.45 (28.6-62.6)	0.71 (62.5-78.4)	0.41 (20.7-63.6)	0.74 (58.8-86.5)	0.575
Irregular margin	0.45 (28.6-62.6)	0.71 (62.5-78.4)	0.41 (20.7-63.6)	0.74 (58.8-86.5)	0.575
Taller-than-wide morphology	0.67 (35.6-87.9)	0.71 (65.6-76.6)	0.27 (10.7-50.2)	0.93 (80.9-98.5)	0.6
Combination of heterogeneous, irregular margin, and blurred margin	0.49 (42.0-55.8)	1.0 (-)	1.0 (84.6-100.0)	0.47 (31.2-62.3)	0.735

*Average sensitivity and specificity.

increasing TIRADS score: TIRADS 3, 12.5%; TIRADS 4, 26.1%; and TIRADS 5, 53.8% (**Table 4**).

For human observers, the intraclass correlation coefficients (ICC) for absolute agreements of the distributions of the 2015 ATA sonographic patterns and TIRADS categories among observers were poor to fair with $r = 0.24$ [CI 0.09–0.40] and $r = 0.44$ [CI 0.29–0.58], respectively (**Supplementary Table 1**). The risk of finding malignant nodules by observer-consensus with benign to intermediate suspicion patterns, non-ATA patterns, and high suspicion patterns were 16.7%, 0%, and 43.2%, respectively. The malignant rate by observer-consensus was 25% for TIRADS 1-3, 21.2% for TIRADS 4, and 50% TIRADS 5 (**Table 4**).

The diagnostic values of the ATA/TIRADS determined by CAD and observers are shown in **Table 5**. The CAD software appeared to have higher average accuracies than the observers (0.675/0.68 and 0.64/0.655, respectively).

DISCUSSION

Follicular thyroid neoplasms have numerous clinical and cytological characteristics, and it is difficult to achieve a precise diagnosis preoperatively. The use of clinical manifestations, imaging study results, and even findings of fine-needle aspiration/biopsy of thyroid nodules is not optimal. Resected

surgical specimens are important in obtaining an accurate diagnosis of thyroid follicular neoplasms. The ATA guidelines recommend removal and definitive diagnosis of an FN/SFN thyroid nodule, if molecular testing is not performed or inconclusive. However, only 10%-40% of nodules in this category are found to be malignant based on histopathology examination (28, 31). The management of these thyroid nodules, prevention of unnecessary thyroidectomy, and determination of the extent of resection are extremely important in this clinical setting (32). The fact that most patients in the current study have benign diseases based on postoperative histology examination, which is consistent with previous studies (28, 31), justifies the effort to improve the selection of surgery candidates.

Studies have shown that the clinical predictive factors for malignancy in Bethesda category IV nodules include sex and age at diagnosis (5, 33, 34). In this study, we found no difference in terms of sex and age between patients with benign and malignant nodules. Some studies have shown that a larger nodule size is indicative of malignancy. However, the current study and other studies have shown that nodule size is not a predictive factor of malignancy in patients with Bethesda category IV nodules (1, 35–37). Moreover, nodules that were found to be Bethesda category IV by FNAC and were subsequently surgically resected had been previously reported to be larger than those that were not resected (38). However, no significant size differences between nodules with and without surgeries were

TABLE 4 | Malignancy rate based on the ATA and TIRADS category in 65 patients diagnosed with follicular neoplasm on cytology.

	CAD	No. of cases (n=65)	Benign (n=43)	Malignant (n=22)	Risk of Malignancy, %	Observers	No of cases (n=65)	Benign (n=43)	Malignant (n=22)	Risk of Malignancy, %
ATA category	Benign to Intermediate	22	20	2	9.1	Benign to Intermediate	18	15	3	16.7
	Non-ATA	14	9	5	35.7	Non-ATA	3	3	0	0
	High	29	14	15	51.7	High	44	25	19	43.2
TIRADS category	2–3	16	14	2	12.5	2–3	4	3	1	25.0
	4	23	17	6	26.1	4	33	26	7	21.2
	5	26	12	14	53.8	5	28	14	14	50.0

TABLE 5 | Comparison between CAD and Observers.

		PPV (95% CI)	NPV (95% CI)	Sensitivity (95% CI)	Specificity (95% CI)	Average*
CAD Performance	ATA category of high suspicion	0.52 (39.0-64.2)	0.81 (68.5-88.8)	0.68 (45.1-86.1)	0.67 (51.5-80.9)	0.675
	TIRADS category of highly suspicious	0.54 (39.6-67.5)	0.80 (68.4-87.4)	0.64 (40.7-82.8)	0.72 (56.3-84.7)	0.68
Observers Performance	ATA category of high suspicion	0.43 (35.9-50.7)	0.86 (66.4-94.8)	0.86 (65.1-97.1)	0.42 (27.0-57.9)	0.64
	TIRADS category of highly suspicious	0.50 (37.0-63.0)	0.78 (66.8-86.7)	0.64 (40.7-82.8)	0.67 (51.5-80.9)	0.655

*Average sensitivity and specificity.

observed in this study (data not shown). Regarding the pathology distribution, 22 of 62 (33.8%) Bethesda IV nodules were cancers with 15 papillary thyroid cancers being the most common type of cancers and 7 follicular and Hurthle cell carcinomas accounting for about 10% of cases. The distribution appears to be consistent with previous studies (4, 39, 40), where 13~22% of Bethesda IV nodules were PTC or follicular variant PTC and about 9% were follicular or Hurthle cell carcinoma. Although a significant proportion of patients with malignant nodules presented with papillary thyroid cancers, four of them had follicular variants of papillary thyroid cancers.

US is widely used for the screening of thyroid nodules. The presence of US features indicates a malignancy potential for thyroid nodules (41–44). Based on these findings, the nodule can be categorized, and decisions can be made as to whether FNAC or follow-up is required (5, 11, 29, 38). Studies about post-FNAC stratification are limited, and few studies have explored the US features of follicular neoplasm (45, 46). In the current study, the presence of heterogeneous echotexture and taller-than-wide features was higher in malignant than benign follicular neoplasms. In the past, heterogeneity echotexture was found to be not as important as other sonographic features, and was not listed in the current ATA and TIRADS category system. However, in the current study and in our previous work, heterogeneous echotexture is associated with an increased risk of malignancy, particularly for follicular neoplasms (13, 22). Studies have shown that a taller-than-wide feature is extremely specific for malignant thyroid nodules. However, information about such features in follicular neoplasms is limited (28, 43, 47, 48).

Because US is a relatively subjective diagnostic method, observers may have different opinions when describing and interpreting lesions (14, 49), leading to poor reliability for some features (14, 16, 17, 19, 50–56). Several studies have shown that inconsistencies in the interpretation of ultrasonographic features occur in up to 70% of cases (17, 19, 56). This low reproducibility, that may cause uncertainty in clinical management of thyroid nodules, emphasizes the need for an objective quantification method, such as a software device to computerize these features (54). The sensitivity and specificity of US findings vary in the literature (44, 57). The diagnostic performance of thyroid US in Bethesda category IV nodules has a lower sensitivity (50%) and positive predictive value (PPV) (50%) than that in other Bethesda categories. Thus, the

importance of the current US morphological guidelines for this category is limited (58). The CAD software system, as used in this study, can reduce the difference in feature interpretation, and the reader experiences a gap while increasing reading accuracy, which may be used as an accompaniment in imaging diagnosis (20–23, 59).

We showed a difference in the quantitative index of echogenicity, calcification, echotexture, margin and tall-wide orientation in a malignant tumor with Bethesda category IV, which is different from a 'yes' or 'no' binary feature presentation. Quantitative indices provide detailed comparisons and can establish more precise predictive models in future studies.

The role of sonographic features or patterns should not only be used in selecting nodules that must be biopsied, but also in determining the management after cytological diagnosis (60). Recently, it was determined that the rate of malignancy in these types of nodules can be stratified according to sonographic patterns (60, 61). In this study, the features were used to classify using the ATA and ACR TIRADS, which are the most popular category systems to differentiate the risk of malignancy. This showed that both systems can help stratify those who may benefit from or who should have a pathological diagnosis. However, this study also showed that a relatively high percentage (21.5%, 14 of 65) of tumors had non-ATA patterns, and that there was a large gap in the malignancy rate (9.1%–51.7%) from ATA very low, low, intermediate to ATA high suspicion. In this study, the ACR TIRADS system included more feature information, and the malignant rate increased (12.5%–53.8%) with advancing CAD TIRADS scores as indicated in **Table 4**. This suggests that this approach may result in better stratification for Bethesda category IV tumors. Compared with the risk of malignancy of Bethesda category IV, which is highly uncertain with a range from 10% to 40%, the additional risk stratification by CAD TIRADS will further help the surgery decision. Once more studies with greater sample sizes are conducted to confirm the findings, nodules categorized with Bethesda IV and TIRADS 3 or below would be considered low risk of malignancy and may undergo continuous follow-up. Bethesda IV nodules categorized with TIRADS 4 would be considered moderate risk of malignancy and lobectomy could be suggested. A high risk of malignancy is seen in nodules categorized with Bethesda IV and TIRADS 5, and at least lobectomy or total thyroidectomy for larger nodules is

suggested. Numerous variations in TIRADS have been proposed, and some of them included additional US features, such as elastography and vascularity criteria (47). The ACR TIRADS used in our study is simple, convenient, and accurate and can be used to stratify the risk of malignancy. Furthermore, we showed that 30.8% of follicular neoplasms do not present features such as heterogeneity, blurred margin, and irregular margin; their malignancy rate is 0%. These patients could be spared from surgery and monitoring. However, further large-scale studies would need to confirm the findings of the current study.

However, we found in the study that there were differences between the human observers and the CAD in ATA/TIRAD interpretation. Even among the human observers, the consistence of interpretation was also shown to be poor or fair. Thus, further large-scale studies must be conducted to confirm the findings of the current study.

This study had several limitations: first, we only included patients who underwent surgery and therefore potential selection bias may have affected the study results. Nevertheless, this bias was inevitable because histopathology was necessary to provide a reliable diagnosis in patients with Bethesda category IV nodules. Second, in order to acquire dicom-format images for software analysis, all patients enrolled in this study were arranged for additional ultrasound scans. Therefore, collecting an extremely large number of cases within a short period of time is impossible. Studies with a larger number of cases should be conducted when the CAD software can be applied more widely to routine clinical examination with a standard workflow. Third, the applicability of this study should be limited to those nodules pre-selected for FNAC based on ATA guidelines and diagnosed as Bethesda IV category. Fourth, instead of real-time images during ultrasonography, only static images selected and recorded by the US examiners were analyzed in this study. Thus, the advantage of dynamic US examination was not considered in the current study. In addition, because of the nature of this study, elastography or vascularization was not available in our workflow.

CONCLUSION

For patients with nodules pre-selected for FNAC based on ATA guidelines and diagnosed as Bethesda category IV, the software-based characterizations of US features, along with the associated ATA patterns and TIRADS system, were shown helpful in the risk stratification of malignancy.

REFERENCES

1. Raber W, Kaserer K, Niederle B, Vierhapper H. Risk factors for malignancy of thyroid nodules initially identified as follicular neoplasia by fine-needle aspiration: results of a prospective study of one hundred twenty patients. *Thyroid* (2000) 10:709–12. doi: 10.1089/10507250050137806
2. Baloch Z, LiVolsi VA, Jain P, Jain R, Aljada I, Mandel S, et al. Role of repeat fine-needle aspiration biopsy (FNAB) in the management of thyroid nodules. *Diagn Cytopathol* (2003) 29:203–6. doi: 10.1002/dc.10361
3. Suster S. Thyroid tumors with a follicular growth pattern: problems in differential diagnosis. *Arch Pathol Lab Med* (2006) 130:984–8. doi: 10.5858/2006-130-984-TTWAFG
4. Goldstein RE, Nettekville JL, Burkey B, Johnson JE. Implications of follicular neoplasms, atypia, and lesions suspicious for malignancy diagnosed by fine-needle aspiration of thyroid nodules. *Ann Surg* (2002) 235:656–662; discussion 662–654. doi: 10.1097/0000658-200205000-00007
5. Baloch ZW, Fleisher S, LiVolsi VA, Gupta PK. Diagnosis of “follicular neoplasm”: a gray zone in thyroid fine-needle aspiration cytology. *Diagn Cytopathol* (2002) 26:41–4. doi: 10.1002/dc.10043

DATA AVAILABILITY STATEMENT

The raw data supporting the conclusions of this article will be made available by the authors, without undue reservation.

ETHICS STATEMENT

The studies involving human participants were reviewed and approved by the institutional review board of the National Taiwan University Hospital approved the data collection and analyses in this study. The patients/participants provided their written informed consent to participate in this study.

AUTHOR CONTRIBUTIONS

M-HW, C-NC, K-YC, AC and M-SH proposed the study. M-HW, C-NC, K-YC and AC performed research, analyzed the data and wrote the first draft. M-SH collected the data. M-HW, C-NC, K-YC and AC analyzed the data. All authors contributed to the design and interpretation of the study and to further drafts. All authors contributed to the article and approved the submitted version.

FUNDING

The AmCad BioMed Corporation, Taipei, Taiwan, sponsored this study in terms of technical assistance and financial support.

ACKNOWLEDGMENTS

The authors would like to thank the Department of Medical Research at the National Taiwan University Hospital for providing assistance with statistical analysis.

SUPPLEMENTARY MATERIAL

The Supplementary Material for this article can be found online at: <https://www.frontiersin.org/articles/10.3389/fendo.2021.614630/full#supplementary-material>

6. Cibas ES, Ali SZ. Conference NCITFSotS. The Bethesda System For Reporting Thyroid Cytopathology. *Am J Clin Pathol* (2009) 132:658–65. doi: 10.1309/AJCPHLWMI3JV4LA
7. American Thyroid Association Guidelines Taskforce on Thyroid N and Differentiated Thyroid C, Cooper DS, Doherty GM, Haugen BR, Kloos RT, et al. Revised American Thyroid Association management guidelines for patients with thyroid nodules and differentiated thyroid cancer. *Thyroid* (2009) 19:1167–214. doi: 10.1089/thy.2009.0110
8. Perros P. Thyroid Cancer Guidelines Update G. Introduction to the updated guidelines on the management of thyroid cancer. *Clin Med (Lond)* (2007) 7:321–2. doi: 10.7861/clinmedicine.7-4-321
9. Musholt TJ, Clerici T, Dralle H, Frilling A, Goretzki PE, Hermann MM, et al. German Association of Endocrine Surgeons practice guidelines for the surgical treatment of benign thyroid disease. *Langenbecks Arch Surg* (2011) 396:639–49. doi: 10.1007/s00423-011-0774-y
10. Pacini F, Burroni L, Ciuoli C, Di Cairano G, Guarino E. Management of thyroid nodules: a clinicopathological, evidence-based approach. *Eur J Nucl Med Mol Imaging* (2004) 31:1443–9. doi: 10.1007/s00259-004-1680-0
11. Gulcelik NE, Gulcelik MA, Kuru B. Risk of malignancy in patients with follicular neoplasm: predictive value of clinical and ultrasonographic features. *Arch Otolaryngol Head Neck Surg* (2008) 134:1312–5. doi: 10.1001/archotol.134.12.1312
12. Miyakawa M, Onoda N, Etoh M, Fukuda I, Takano K, Okamoto T, et al. Diagnosis of thyroid follicular carcinoma by the vascular pattern and velocimetric parameters using high resolution pulsed and power Doppler ultrasonography. *Endocr J* (2005) 52:207–12. doi: 10.1507/endocrj.52.207
13. Kuo TC, Wu MH, Chen KY, Hsieh MS, Chen A, Chen CN. Ultrasonographic features for differentiating follicular thyroid carcinoma and follicular adenoma. *Asian J Surg* (2019) 43(1):339–46. doi: 10.1016/j.asjsur.2019.04.016
14. Wienke JR, Chong WK, Fielding JR, Zou KH, Mittelstaedt CA. Sonographic features of benign thyroid nodules: interobserver reliability and overlap with malignancy. *J Ultrasound Med* (2003) 22:1027–31. doi: 10.7863/jum.2003.22.10.1027
15. Hegedus L. Thyroid size determined by ultrasound. Influence of physiological factors and non-thyroidal disease. *Dan Med Bull* (1990) 37:249–63.
16. Lyshchik A, Drozd V, Schloegl S, Reiners C. Three-dimensional ultrasonography for volume measurement of thyroid nodules in children. *J Ultrasound Med* (2004) 23:247–54. doi: 10.7863/jum.2004.23.2.247
17. Brauer VF, Eder P, Miehle K, Wiesner TD, Hasenclever H, Paschke R. Interobserver variation for ultrasound determination of thyroid nodule volumes. *Thyroid* (2005) 15:1169–75. doi: 10.1089/thy.2005.15.1169
18. Jarlov AE, Nygard B, Hegedus L, Karstrup S, Hansen JM. Observer variation in ultrasound assessment of the thyroid gland. *Br J Radiol* (1993) 66:625–7. doi: 10.1259/0007-1285-66-787-625
19. Choi SH, Kim EK, Kwak JY, Kim MJ, Son EJ. Interobserver and intraobserver variations in ultrasound assessment of thyroid nodules. *Thyroid* (2010) 20:167–72. doi: 10.1089/thy.2008.0354
20. Chen KY, Chen CN, Wu MH, Ho MC, Tai HC, Huang WC, et al. Computerized detection and quantification of microcalcifications in thyroid nodules. *Ultrasound Med Biol* (2011) 37:870–8. doi: 10.1016/j.ultrasmedbio.2011.03.002
21. Wu MH, Chen CN, Chen KY, Ho MC, Tai HC, Chung YC, et al. Quantitative analysis of dynamic power Doppler sonograms for patients with thyroid nodules. *Ultrasound Med Biol* (2013) 39:1543–51. doi: 10.1016/j.ultrasmedbio.2013.03.009
22. Chen KY, Chen CN, Wu MH, Ho MC, Tai HC, Kuo WH, et al. Computerized quantification of ultrasonic heterogeneity in thyroid nodules. *Ultrasound Med Biol* (2014) 40:2581–9. doi: 10.1016/j.ultrasmedbio.2014.06.009
23. Wu MH, Chen CN, Chen KY, Ho MC, Tai HC, Wang YH, et al. Quantitative analysis of echogenicity for patients with thyroid nodules. *Sci Rep* (2016) 6:35632. doi: 10.1038/srep35632
24. Choi YJ, Baek JH, Park HS, Shim WH, Kim TY, Shong YK, et al. A Computer-Aided Diagnosis System Using Artificial Intelligence for the Diagnosis and Characterization of Thyroid Nodules on Ultrasound: Initial Clinical Assessment. *Thyroid* (2017) 27:546–52. doi: 10.1089/thy.2016.0372
25. Jeong EY, Kim HL, Ha EJ, Park SY, Cho YJ, Han M. Computer-aided diagnosis system for thyroid nodules on ultrasonography: diagnostic performance and reproducibility based on the experience level of operators. *Eur Radiol* (2019) 29:1978–85. doi: 10.1007/s00330-018-5772-9
26. Yoo YJ, Ha EJ, Cho YJ, Kim HL, Han M, Kang SY. Computer-Aided Diagnosis of Thyroid Nodules via Ultrasonography: Initial Clinical Experience. *Korean J Radiol* (2018) 19:665–72. doi: 10.3348/kjr.2018.19.4.665
27. Wu MH, Chen KY, Shih SR, Ho MC, Tai HC, Chang KJ, et al. Multi-Reader Multi-Case Study for Performance Evaluation of High-Risk Thyroid Ultrasound with Computer-Aided Detection. *Cancers (Basel)* (2020) 12(2):373. doi: 10.3390/cancers12020373
28. Haugen BR, Alexander EK, Bible KC, Doherty GM, Mandel SJ, Nikiforov YE, et al. 2015 American Thyroid Association Management Guidelines for Adult Patients with Thyroid Nodules and Differentiated Thyroid Cancer: The American Thyroid Association Guidelines Task Force on Thyroid Nodules and Differentiated Thyroid Cancer. *Thyroid* (2016) 26:1–133. doi: 10.1089/thy.2015.0020
29. Tessler FN, Middleton WD, Grant EG, Hoang JK, Berland LL, Teefey SA, et al. ACR Thyroid Imaging, Reporting and Data System (TI-RADS): White Paper of the ACR TI-RADS Committee. *J Am Coll Radiol* (2017) 14:587–95. doi: 10.1016/j.jacr.2017.01.046
30. Cibas ES, Ali SZ. The 2017 Bethesda System for Reporting Thyroid Cytopathology. *Thyroid* (2017) 27:1341–6. doi: 10.1089/thy.2017.0500
31. Cibas ES, Ali SZ. The Bethesda System for Reporting Thyroid Cytopathology. *Thyroid* (2009) 19:1159–65. doi: 10.1089/thy.2009.0274
32. Kuru B, Atmaca A, Tarim IA, Kefeli M, Topgul K, Yoruker S, et al. Risk factors associated with malignancy and with triage to surgery in thyroid nodules classified as Bethesda category III (AUS/FLUS). *Eur J Surg Oncol* (2016) 42:87–93. doi: 10.1016/j.ejso.2015.09.026
33. Macias CA, Arumugam D, Arlow RL, Eng OS, Lu SE, Javidian P, et al. A risk model to determine surgical treatment in patients with thyroid nodules with indeterminate cytology. *Ann Surg Oncol* (2015) 22:1527–32. doi: 10.1245/s10434-014-4190-8
34. Kuru B, Kefeli M. Risk factors associated with malignancy and with triage to surgery in thyroid nodules classified as Bethesda category IV (FN/SFN). *Diagn Cytopathol* (2018) 46:489–94. doi: 10.1002/dc.23923
35. Lubitz CC, Faquin WC, Yang J, Mekel M, Gaz RD, Parangi S, et al. Clinical and cytological features predictive of malignancy in thyroid follicular neoplasms. *Thyroid* (2010) 20:25–31. doi: 10.1089/thy.2009.0208
36. Miller B, Burkey S, Lindberg G, Snyder WH, Nwariaku FE. Prevalence of malignancy within cytologically indeterminate thyroid nodules. *Am J Surg* (2004) 188:459–62. doi: 10.1016/j.amjsurg.2004.07.006
37. Kiernan CM, Solorzano CC. Bethesda Category III, IV, and V Thyroid Nodules: Can Nodule Size Help Predict Malignancy? *J Am Coll Surg* (2017) 225:77–82. doi: 10.1016/j.jamcollsurg.2017.02.002
38. Lee SH, Baek JS, Lee JY, Lim JA, Cho SY, Lee TH, et al. Predictive factors of malignancy in thyroid nodules with a cytological diagnosis of follicular neoplasm. *Endocr Pathol* (2013) 24:177–83. doi: 10.1007/s12022-013-9263-x
39. Krane JF, Vanderlaan PA, Faquin WC, Renshaw AA. The atypia of undetermined significance/follicular lesion of undetermined significance: malignant ratio: a proposed performance measure for reporting in The Bethesda System for thyroid cytopathology. *Cancer Cytopathol* (2012) 120:111–6. doi: 10.1002/cncy.20192
40. Liu FH, Liou MJ, Hsueh C, Chao TC, Lin JD. Thyroid follicular neoplasm: analysis by fine needle aspiration cytology, frozen section, and histopathology. *Diagn Cytopathol* (2010) 38:801–5. doi: 10.1002/dc.21294
41. Papini E, Guglielmi R, Bianchini A, Crescenzi A, Taccogna S, Nardi F, et al. Risk of malignancy in nonpalpable thyroid nodules: predictive value of ultrasound and color-Doppler features. *J Clin Endocrinol Metab* (2002) 87:1941–6. doi: 10.1210/jcem.87.5.8504
42. Brito JP, Gionfriddo MR, Al Nofal A, Boehmer KR, Leppin AL, Reading C, et al. The accuracy of thyroid nodule ultrasound to predict thyroid cancer: systematic review and meta-analysis. *J Clin Endocrinol Metab* (2014) 99:1253–63. doi: 10.1210/jc.2013-2928
43. Alexander EK, Marqusee E, Orcutt J, Benson CB, Frates MC, Doubilet PM, et al. Thyroid nodule shape and prediction of malignancy. *Thyroid* (2004) 14:953–8. doi: 10.1089/thy.2004.14.953
44. Khoo ML, Asa SL, Witterick IJ, Freeman JL. Thyroid calcification and its association with thyroid carcinoma. *Head Neck* (2002) 24:651–5. doi: 10.1002/hed.10115

45. Mazzaferri EL. Management of a solitary thyroid nodule. *N Engl J Med* (1993) 328:553–9. doi: 10.1056/NEJM199302253280807
46. McHenry CR, Phitayakorn R. Follicular adenoma and carcinoma of the thyroid gland. *Oncologist* (2011) 16:585–93. doi: 10.1634/theoncologist.2010-0405
47. Kwak JY, Han KH, Yoon JH, Moon HJ, Son EJ, Park SH, et al. Thyroid imaging reporting and data system for US features of nodules: a step in establishing better stratification of cancer risk. *Radiology* (2011) 260:892–9. doi: 10.1148/radiol.11110206
48. Kim EK, Park CS, Chung WY, Oh KK, Kim DI, Lee JT, et al. New sonographic criteria for recommending fine-needle aspiration biopsy of nonpalpable solid nodules of the thyroid. *AJR Am J Roentgenol* (2002) 178:687–91. doi: 10.2214/ajr.178.3.1780687
49. Cronan JJ. Thyroid nodules: is it time to turn off the US machines? *Radiology* (2008) 247:602–4. doi: 10.1148/radiol.2473072233
50. Park SH, Kim SJ, Kim EK, Kim MJ, Son EJ, Kwak JY. Interobserver agreement in assessing the sonographic and elastographic features of malignant thyroid nodules. *AJR Am J Roentgenol* (2009) 193:W416–423. doi: 10.2214/AJR.09.2541
51. Moon WJ, Jung SL, Lee JH, Na DG, Baek JH, Lee YH, et al. Benign and malignant thyroid nodules: US differentiation—multicenter retrospective study. *Radiology* (2008) 247:762–70. doi: 10.1148/radiol.2473070944
52. Park CS, Kim SH, Jung SL, Kang BJ, Kim JY, Choi JJ, et al. Observer variability in the sonographic evaluation of thyroid nodules. *J Clin Ultrasound* (2010) 38:287–93. doi: 10.1002/jcu.20689
53. Valderrabano P, Klippenstein DL, Tourtelot JB, Ma Z, Thompson ZJ, Lilienfeld HS, et al. New American Thyroid Association Sonographic Patterns for Thyroid Nodules Perform Well in Medullary Thyroid Carcinoma: Institutional Experience, Systematic Review, and Meta-Analysis. *Thyroid* (2016) 26:1093–100. doi: 10.1089/thy.2016.0196
54. Lam CA, McGettigan MJ, Thompson ZJ, Khazai L, Chung CH, Centeno BA, et al. Ultrasound characterization for thyroid nodules with indeterminate cytology: inter-observer agreement and impact of combining pattern-based and scoring-based classifications in risk stratification. *Endocrine* (2019) 66(2):278–87. doi: 10.1007/s12020-019-02000-0
55. Slapa RZ, Slowinska-Srzednicka J, Szopinski KT, Jakubowski W. Gray-scale three-dimensional sonography of thyroid nodules: feasibility of the method and preliminary studies. *Eur Radiol* (2006) 16:428–36. doi: 10.1007/s00330-005-2903-x
56. Hoang JK, Middleton WD, Farjat AE, Teeffey SA, Abinanti N, Boschini FJ, et al. Interobserver Variability of Sonographic Features Used in the American College of Radiology Thyroid Imaging Reporting and Data System. *AJR Am J Roentgenol* (2018) 211:162–7. doi: 10.2214/AJR.17.19192
57. Frates MC, Benson CB, Charboneau JW, Cibas ES, Clark OH, Coleman BG, et al. Management of thyroid nodules detected at US: Society of Radiologists in Ultrasound consensus conference statement. *Radiology* (2005) 237:794–800. doi: 10.1148/radiol.2373050220
58. Park SY, Hahn SY, Shin JH, Ko EY, Oh YL. The Diagnostic Performance of Thyroid US in Each Category of the Bethesda System for Reporting Thyroid Cytopathology. *PLoS One* (2016) 11:e0155898. doi: 10.1371/journal.pone.0155898
59. Jeong EY, Kim HL, Ha EJ, Park SY, Cho YJ, Han M. Computer-aided diagnosis system for thyroid nodules on ultrasonography: diagnostic performance and reproducibility based on the experience level of operators. *Eur Radiol* (2018) 29(4):1978–85. doi: 10.1007/s00330-018-5772-9
60. Valderrabano P, McGettigan MJ, Lam CA, Khazai L, Thompson ZJ, Chung CH, et al. Thyroid Nodules with Indeterminate Cytology: Utility of the American Thyroid Association Sonographic Patterns for Cancer Risk Stratification. *Thyroid* (2018) 28:1004–12. doi: 10.1089/thy.2018.0085
61. Chng CL, Kurzawinski TR, Beale T. Value of sonographic features in predicting malignancy in thyroid nodules diagnosed as follicular neoplasm on cytology. *Clin Endocrinol (Oxf)* (2015) 83:711–6. doi: 10.1111/cen.12692

Conflict of Interest: M-HW, K-YC, AC and C-NC received research grant support from AmCad BioMed.

The remaining author declares that the research was conducted in the absence of any commercial or financial relationships that could be construed as a potential conflict of interest.

Copyright © 2021 Wu, Chen, Hsieh, Chen and Chen. This is an open-access article distributed under the terms of the Creative Commons Attribution License (CC BY). The use, distribution or reproduction in other forums is permitted, provided the original author(s) and the copyright owner(s) are credited and that the original publication in this journal is cited, in accordance with accepted academic practice. No use, distribution or reproduction is permitted which does not comply with these terms.



Predictive Value of Thyroglobulin Changes for the Curative Effect of Radioiodine Therapy in Patients With Metastatic Differentiated Thyroid Carcinoma

Congcong Wang, Ruiguo Zhang, Renfei Wang*, Zhaowei Meng, Guizhi Zhang, Feng Dong, Yajing He and Jian Tan

OPEN ACCESS

Edited by:

Christoph Reiners,
University Hospital Würzburg,
Germany

Reviewed by:

James Nagarajah,
Radboud University Nijmegen
Medical Centre, Netherlands
Eleonora Molinaro,
University of Pisa, Italy

*Correspondence:

Renfei Wang
roslyn_en@163.com

Specialty section:

This article was submitted to
Thyroid Endocrinology,
a section of the journal
Frontiers in Endocrinology

Received: 13 February 2021

Accepted: 14 April 2021

Published: 10 May 2021

Citation:

Wang C, Zhang R, Wang R,
Meng Z, Zhang G, Dong F,
He Y and Tan J (2021) Predictive
Value of Thyroglobulin Changes
for the Curative Effect of Radioiodine
Therapy in Patients With Metastatic
Differentiated Thyroid Carcinoma.
Front. Endocrinol. 12:667544.
doi: 10.3389/fendo.2021.667544

Department of Nuclear Medicine, Tianjin Medical University General Hospital, Tianjin, China

Background: Serum thyroglobulin (Tg) serves as a sensitive and easily available tumor marker for patients with metastatic differentiated thyroid carcinoma (m-DTC). The aim of the present study was to evaluate the predictive value of suppressed Tg changes ($\Delta\text{sup-Tg}$) and/or stimulated Tg changes ($\Delta\text{sti-Tg}$) to evaluate the efficacy of radioiodine therapy (RT).

Methods: We studied 117 patients with m-DTC who received RT. $\Delta\text{sup-Tg}$ and $\Delta\text{sti-Tg}$ were compared after the first RT in different therapeutic response groups and a receiver-operating characteristic (ROC) curve was used to determine the cut-off values to predict non-remission. Univariate and multivariate analyses were used to investigate the effects of 17 observed factors on the efficacy of RT.

Results: A total of 218 RT events in 117 patients with m-DTC were analyzed. After the last RT, the remission rate was 70.94% (83/117), and the proportion of remission events accounted for 74.77% (163/218). ROC curve analysis showed that the cut-off values for $\Delta\text{sup-Tg}$ and $\Delta\text{sti-Tg}$ after the first RT to predict the non-remission of RT were 21.54% and 27.63%, respectively. Age, the size of the metastasis, the maximum count of target metastatic lesions and the average count of contralateral non-target tissue on tomographic imaging ($T_{\text{max}}/\text{NT}_{\text{mean}}$) of the first RT, and $\Delta\text{sup-Tg}$ after the first RT were identified as independent factors associated with RT efficacy.

Conclusions: Tg response was valuable to predict RT efficacy for patients with m-DTC. Age, the size of the metastasis, $T_{\text{max}}/\text{NT}_{\text{mean}}$, and $\Delta\text{sup-Tg}$ after the first RT were verified as independent predictive factors of RT efficacy.

Keywords: differentiated thyroid carcinoma, radioiodine therapy, iodine radioisotope, curative effect, metastatic lesion, thyroglobulin change

INTRODUCTION

Differentiated thyroid carcinoma (DTC) accounts for approximately 90% of all thyroid carcinomas, and has a relatively good prognosis; however, 5–25% of patients with DTC develop distant metastasis (1–5). The 10-year survival rate of patients with metastatic differentiated thyroid carcinoma (m-DTC) is significantly reduced compared with patients with non-metastatic DTC (6). Radioiodine therapy (RT) has been recognized as a conventional therapeutic strategy for patients with ^{131}I -avid m-DTC for nearly 80 years (6, 7). Studies have confirmed that RT can significantly reduce the tumor-related mortality of patients with m-DTC and improve their overall survival significantly (8, 9).

The 2015 American Thyroid Association (ATA) management guidelines pointed out that ^{131}I -avid metastatic lesions can be treated with ^{131}I , and the response to the previous RT and real-time disease status should be combined to assess whether the patient should undergo repeated RT (3, 4). Unfortunately, the guidelines failed to provide detailed indications for repeated RT. Therefore, how to evaluate the efficacy of RT on patients with m-DTC and how to determine the decision and timing of repeated RT have caused a considerable controversy, becoming important issues in current clinical work (1, 3, 4, 10).

A series of studies confirmed that multiple interrelated factors might change the uptake of ^{131}I by metastatic lesions positively or negatively, and may ultimately change the RT outcome (1, 4, 10–12). Thyroglobulin (Tg) is an important and easily measured tumor marker for DTC, which reflects the patient's tumor burden and is influenced by the levels of thyroglobulin antibody (TgAb) and thyroid stimulating hormone (TSH) (3, 4, 13). Meanwhile, Tg also has value to predict the response or resistance to RT.

Therefore, this retrospective clinical study aimed to evaluate the curative effect of RT by analyzing the clinical data of 117 patients with ^{131}I -avid m-DTC, aiming to explore the value of Tg change in predicting the efficacy of RT, to identify relevant factors that affect RT efficacy, and provide a basis for clinical decision-making.

MATERIALS AND METHODS

Study Conduct

The study protocol was approved by the Medical Ethics Committee of Tianjin Medical University General Hospital. All the patients who participated in this study provided written informed consent form before the start of the research. The authors performed anonymous analysis on all clinical data used in this study and fully guaranteed the accuracy and completeness of the data and analysis.

Study Populations

We screened retrospectively 1821 patients with DTC who had received a total thyroidectomy and RT at our hospital from January 2013 to June 2019 using our institutional radionuclide

therapy information system. Among these 1821 patients, we identified 117 patients with ^{131}I -avid m-DTC with no thyroid tissue residue, as demonstrated using post-therapeutic ^{131}I whole-body scanning (Rx-WBS) (78 female, 39 male, sex ratio (F:M) 2:1; age range: 11–74 years). Data comprising the clinicopathological characteristics of the patients at the time of diagnosis with DTC, the time of diagnosis of metastasis, lesion location and size, the changes in suppressed thyroglobulin (sup-Tg) and stimulated thyroglobulin (sti-Tg) before and after each RT, and the efficacy evaluation, were collected.

Inclusion and Exclusion Criteria for This Study

The inclusion criteria of this study were as follows: (1) The patients underwent total or near total thyroidectomy. (2) The histopathological type was diagnosed as DTC. (3) The patient had undergone radioiodine residual ablation and no residual thyroid tissue was found upon Rx-WBS. (4) Focal or diffuse ^{131}I -avid metastatic lesions were observed on Rx-WBS after excluding the physiological ^{131}I uptake and contamination, with or without positive findings on other diagnostic/functional imaging modalities (computed tomography, CT; magnetic resonance imaging, MRI; ultrasonography, whole body bone static imaging, WBI; and Rx-WBS). (5) Negative TgAb. (6) Follow-up for more than six months after the last RT. The exclusion criteria comprised any of the following: (1) The patient did not undergo standard RT and efficacy evaluation. (2) Periodical follow-up data were incomplete. (3) The patient suffered from other malignant diseases.

RT Procedures

The preparation and protocol of RT for patients with m-DTC were carried out according to the recommendations of the 2015 ATA guidelines (4). All the subjects strictly withdrew from levothyroxine and followed a low-iodine diet for 2–4 weeks before RT (TSH > 30 mIU/L) (1). Oral ^{131}I at a dose of 5.55–7.40 GBq was given for each round of RT, and the interval between rounds of RT varied from 6 to 12 months (4, 14). The patients underwent Rx-WBS and tomographic image fusion was performed using a single photon emission computed tomography/computed tomography instrument (SPECT/CT, GE Discovery NM/CT 670; GE healthcare, Chicago, IL, USA) 3–7 days after RT (15). The region-of-interest (ROI) technique was used to analyze the uptake of ^{131}I of the metastatic lesion on tomographic imaging semi-quantitatively (16). Briefly, the regions of each target metastatic lesion (T) and contralateral non-target tissue (NT) were delineated separately, and the maximum T count (T_{\max}) and the average count of NT (NT_{mean}) were recorded. Consequently, $T_{\max}/NT_{\text{mean}}$ was used as an index to evaluate the ability of the metastatic lesion to uptake ^{131}I .

Tg Assessment Profile

In this study, we performed separate quantitative analysis of sup-Tg and sti-Tg during RT. Sup-Tg was measured 3–4 months before and 2–3 months after RT, which was denoted as sup-Tg₁

(TSH < 0.1mIU/L) and sup-Tg₂ (TSH < 0.1mIU/L), respectively. The sti-Tg and TSH (TSH > 30mIU/L) on the day or within 3 days before RT (sti-Tg₁, TSH₁) and at the next (sti-Tg₂, TSH₂) time of RT were measured and recorded. Δ sup-Tg, the change in the value of sup-Tg, was defined as follows: $[(\text{sup-Tg}_1 - \text{sup-Tg}_2) / \text{sup-Tg}_1 \times 100\%]$. To eliminate the influence of TSH, we defined the change in the value of sti-Tg as follows: Δ sti-Tg = $[(\text{sti-Tg}_1 / \text{TSH}_1 - \text{sti-Tg}_2 / \text{TSH}_2) / (\text{sti-Tg}_1 / \text{TSH}_1) \times 100\%]$.

Evaluation for the Efficacy of RT

According to the relevant literature (4, 6, 10, 11, 17), we combined the changes in serology and diagnostic imaging (Rx-WBS and ultrasound, CT, MRI, and WBI) to divide the efficacy of RT into a complete response (CR), partial response (PR), stable disease (SD), and progressive disease (PD). Then, patients with CR and PR were included in the remission group, while those with SD and PD were included in the non-remission group.

1. CR: No abnormal ¹³¹I uptake and the disappearance of all detectable metastatic lesions upon Rx-WBS and/or other imaging modalities, sti-Tg < 1ng/mL and/or sup-Tg < 0.2ng/mL.
2. PR: Decreased ¹³¹I uptake or reduced numbers of metastatic lesions upon Rx-WBS and/or other imaging modalities, with decreased sti-Tg and/or sup-Tg levels.
3. SD: No obvious change in the size of the metastatic lesions or ¹³¹I uptake upon Rx-WBS and/or other imaging modalities, with any change in sti-Tg and/or sup-Tg.
4. PD: Increased size or number of metastases, or higher ¹³¹I uptake upon Rx-WBS and/or other imaging modalities, with increased sti-Tg and/or sup-Tg levels.

Statistical Analysis

IBM SPSS 26.0 software (IBM Corp, Armonk, NY, USA) was used to perform the statistical analysis of the data. Data are presented as means \pm standard deviations, medians with ranges, numbers with percentages, or proportions. The Mann-Whitney U test was used to compare the Δ sup-Tg and Δ sti-Tg values in the different efficacy groups. Receiver-operating characteristic (ROC) curves were established to predict non-remission of RT for patients with m-DTC. The Mann-Whitney U test, chi-squared tests, or two-sample t test were performed for univariate analyses according to needs, and significant factors were then included in the logistic regression analysis to identify the independent risk factors that affect the efficacy of RT. $P < 0.05$ was considered statistically significant.

RESULTS

Therapeutic Efficacy of RT

The 117 patients with m-DTC included in this study were followed-up regularly after receiving RT. The rates of CR, PR, SD, and PD were 19.66% (23 cases), 51.28% (60 cases), 16.24% (19 cases) and 12.82% (15 cases), respectively. The remission group (CR+PR) comprised 83 cases (70.94%), while the non-remission group (SD+PD) included 34 cases (29.06%). The enrolled patients with m-DTC received RT for one to five times, and a total of 218 RT events were finally recorded. Among them, the events of CR, PR, SD, and PD accounted for 10.55% (23/218), 64.22% (140/218), 18.35% (40/218), and 6.88% (15/218), respectively. The proportions of remission events (CR+PR) and non-remission events (SD+PD) were 74.77% (163/218) and 25.23% (55/218), respectively.

Comparison of the Δ sup-Tg and Δ sti-Tg After The First/Single RT in Different Therapeutic Outcomes

The median Δ sup-Tg after the first RT in the patients in the remission group was 31.68%, while that in the non-remission group was only 12.02%. There was a statistical difference between the two groups ($z = -6.801$, $P < 0.001$). Meanwhile, the median Δ sti-Tg after the first RT in the patients in the remission group was 39.72%, which was also significantly higher than the 21.63% in the non-remission group ($z = -5.961$, $P < 0.001$) (Table 1).

Out of 218 RT events, remission RT was obtained for 163 events, while 55 yielded non-remission events. In the remission events, the median Δ sup-Tg and Δ sti-Tg after a single RT event were 29.06% and 34.24%, respectively, while they were only 5.99% and 12.54% in the non-remission events, which were statistically significantly different between the two types of therapeutic efficacy events ($z = -10.298$ and -9.005 , both $P < 0.001$) (Table 1).

ROC Curve Analysis of Δ sup-Tg and Δ sti-Tg After the First/Single RT to Predict the Curative Effect

The ROC curve showed that the Δ sup-Tg and Δ sti-Tg values after the first RT showed a good performance to predict non-remission (Figure 1A). A cut-off value of Δ sup-Tg after the first RT at 21.54% was achieved to detect patients that did not achieve remission, with a sensitivity of 86.7% and specificity of 88.2%, and area under the curve (AUC) of 0.901. Meanwhile, a cut-off value of Δ sti-Tg after the first RT at 27.63% was obtained, with a sensitivity of 88.0%, a specificity of 73.5%, and the corresponding

TABLE 1 | Comparison of the Δ sup-Tg and Δ sti-Tg values after the first or single RT for different therapeutic outcomes.

Efficacy	the first RT(n=117)		Efficacy of the event	single RT event(n=218)	
	Δ sup-Tg (%)	Δ sti-Tg (%)		Δ sup-Tg (%)	Δ sti-Tg (%)
Remission group	31.68(25.31,37.82)	39.72(31.82,53.63)	Remission event	29.06(22.10,35.10)	34.24(26.41,42.41)
Non-remission group	12.02(2.69,18.11)	21.63(3.08,30.45)	Non-remission event	5.99(-6.98,11.96)	12.54(-29.63,21.93)
Z	-6.801	-5.961	Z	-10.298	-9.005
P-value	<0.001	<0.001	P-value	<0.001	<0.001

RT, radioiodine therapy.

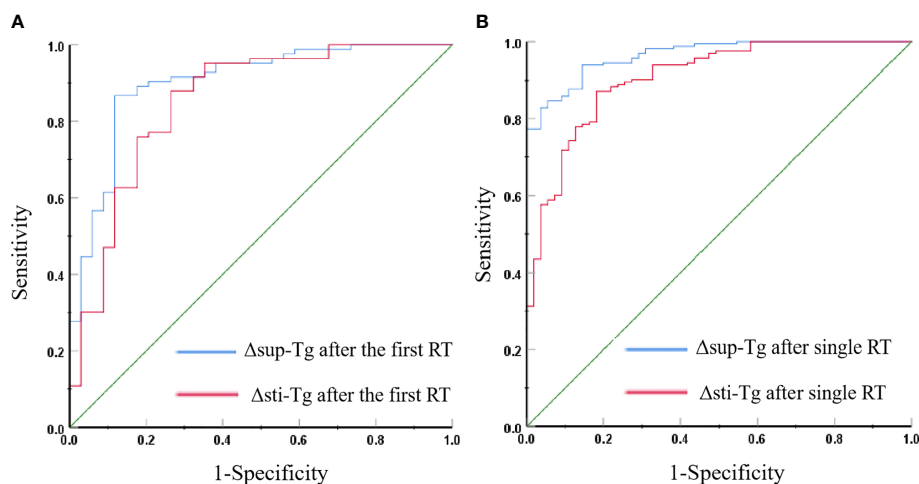


FIGURE 1 | (A) Receiver operating characteristic (ROC) curves for Δ sup-Tg and Δ sti-Tg after the first RT to predict non-remission. **(B)** ROC curves for Δ sup-Tg and Δ sti-Tg after a single RT to predict non-remission.

AUC of 0.852, respectively. Thus, if the Δ sup-Tg was lower than 21.54% and/or Δ sti-Tg was lower than 27.63% after the first RT, the curative effect was more likely to be non-remission.

The cut-off value of Δ sup-Tg after a single RT at 12.90% and Δ sti-Tg after single RT at 22.69% were obtained by ROC curve analyses to best distinguish remission and non-remission events, with corresponding specificities of Δ sup-Tg and Δ sti-Tg after single RT separately of 85.5% and 81.8%, and sensitivities of 93.9% and 87.1%, and AUCs of 0.965 and 0.906, respectively (**Figure 1B**). That is, after single RT, a Δ sup-Tg was less than 12.90%, and/or Δ sti-Tg of less than 22.69% indicated that the single RT has poor efficacy.

Univariate Analyses of the Efficacy of RT for m-DTC Patients

Upon analyzing the relationship between clinicopathological features and the therapeutic efficacy of ^{131}I , a total of 17 factors were involved in the univariate analysis (**Tables 2, 3**). We found that older patients, subjects with a bigger primary tumor, higher T stage, extrathyroidal invasion, BRAF^{V600E} mutation positive, metastatic lesions > 1cm, extrapulmonary distant metastases, higher sti-Tg levels at diagnosis, lower $T_{\text{max}}/\text{NT}_{\text{mean}}$ after the first RT, and those with lower Δ sup-Tg and Δ sti-Tg after the first RT had a higher probability of non-remission ($P = 0.000, 0.000, 0.017, 0.027, 0.006, 0.000, 0.022, 0.003, 0.000, 0.000, \text{ and } 0.000$, respectively). However,

we found no statistically significant differences in sex ($P = 0.249$), histological type ($P = 0.208$), N stage ($P = 0.283$), primary tumor multifocal ($P = 0.587$), diagnosis time of metastases ($P = 0.105$), and the first RT dose ($P = 0.306$).

Multivariate Analyses of the Efficacy of RT for Patients With m-DTC

Multivariate logistic regression analysis was performed on efficacy-related factors from the univariate analysis. Multivariate logistic regression (**Table 4**) revealed that only the age, the size of the metastases, the $T_{\text{max}}/\text{NT}_{\text{mean}}$ of the first RT, and the Δ sup-Tg after the first RT were verified as independent factors that predicted non-remission after RT. In summary, older patients with m-DTC (odds ratio [OR]: 1.180; 95% confidence interval [CI]: 1.063-1.308; $P = 0.002$), subjects with larger metastases (OR: 31.890, 95%CI: 2.832-359.162; $P = 0.005$), lower $T_{\text{max}}/\text{NT}_{\text{mean}}$ of the first RT (OR: 0.719, 95%CI: 0.568-0.910; $P = 0.006$), and lower Δ sup-Tg after the first RT (OR: 0.832, 95%CI: 0.746-0.927; $P = 0.001$) had a higher probability of non-remission.

DISCUSSION

Lungs, bones, and lymph nodes are the most common sites of DTC metastasis. The existence of metastatic lesions is the main

TABLE 2 | Univariate analyses for the continuous variables.

Characteristics	Remission group	Non-remission group	t or z	P-value
Age (year)	40.83 \pm 12.61	55.03 \pm 9.562	-5.902	<0.001
Primary tumor size (cm)	1.9(1.2,2.7)	2.8(1.9,3.6)	-3.501	<0.001
sti-Tg levels at diagnosis ($\mu\text{g/L}$)	63.60(15.32,159.00)	146.50(67.53,275.48)	-2.952	0.003
The first RT dose (GBq)	5.72 \pm 1.25	5.97 \pm 1.15	-1.028	0.306
$T_{\text{max}}/\text{NT}_{\text{mean}}$ of the first RT ^a	17.50(9.58,28.51)	8.14(4.63,14.26)	-4.824	<0.001
Δ sup-Tg after the first RT (%)	31.68(25.31,37.82)	12.02(2.69,18.11)	-6.801	<0.001
Δ sti-Tg after the first RT (%)	39.72(31.82,53.63)	21.63(3.08,30.45)	-5.961	<0.001

^aThe median $T_{\text{max}}/\text{NT}_{\text{mean}}$ is included in the study when the patient has multiple metastatic lesions. RT, radioiodine therapy.

TABLE 3 | Univariate analyses for the categorical variables.

Characteristics	n	Remission group (%)	Non-remission group (%)	χ^2	P-value
Sex				1.327	0.249
Male	39	25(64.10)	14(35.90)		
Female	78	58(74.36)	20(25.64)		
Histological type				1.584	0.208
Papillary	110	80(72.73)	30(27.27)		
Follicular	7	3(42.86)	4(57.14)		
T stage				10.146	0.017
T1	43	35(81.40)	8(18.60)		
T2	21	18(85.71)	3(14.29)		
T3	23	14(60.87)	9(39.13)		
T4	30	16(53.33)	14(46.67)		
N stage				2.525	0.283
N0	25	19(76.00)	6(24.00)		
N1a	18	10(55.56)	8(44.44)		
N1b	74	54(72.97)	20(27.03)		
Primary tumor multifocal				0.294	0.587
Yes	89	62(69.66)	27(30.34)		
No	28	21(75.00)	7(25.00)		
Extrathyroidal invasion				4.882	0.027
Yes	64	40(62.50)	24(37.50)		
No	53	43(81.13)	10(18.87)		
BRAF ^{V600E} mutation				7.526	0.006
Positive	74	46(62.16)	28(37.84)		
Negative	43	37(86.05)	6(13.95)		
Diagnosis time of metastases				2.630	0.105
After RT	25	21(84.00)	4(16.00)		
Before RT	92	62(67.39)	30(32.61)		
The diameter of metastatic lesions				26.358	0.000
≤1cm	73	64(87.67)	9(12.33)		
>1cm	44	19(43.18)	25(56.82)		
Metastases sites				7.627	0.022
Only lung metastases	64	52(81.25)	12(18.75)		
Only lymphatic metastasis	24	15(62.50)	9(37.50)		
Multi-site metastasis	29	16(55.17)	13(44.83)		

T, tumor; N, lymph node. RT, radioiodine therapy.

TABLE 4 | Logistic regression analyses of the variables affecting non-remission after RT in 117 patients with m-DTC.

Characteristics	β	Standard error	Wald	P-value	OR	95%CI
Age	0.165	0.053	9.733	0.002	1.180	1.063-1.308
The diameter of metastatic lesions	3.462	1.235	7.853	0.005	31.890	2.832-359.162
T_{max}/NT_{mean} of the first RT ^a	-0.330	0.120	7.539	0.006	0.719	0.568-0.910
Δ sup-Tg after the first RT (%)	-0.184	0.055	11.070	0.001	0.832	0.746-0.927
Constant	-6.202	2.462	6.346	0.012	0.002	

^aThe median T_{max}/NT_{mean} is included in the study when the patient has multiple metastatic lesions; β , regression coefficient; OR, odds ratio; CI, confidence interval; RT, radioiodine therapy.

cause of the decline in the quality of life and death of patients with m-DTC (6, 11, 18). If an early diagnosis and effective treatment are not undertaken, the 5-year mortality rate can be as high as 50% (19). ¹³¹I is one of the main methods of postoperative adjuvant treatment for patients with intermediate or high-risk DTC, which can significantly improve the overall survival rate and reduce the risk of recurrence, metastasis, and death (17, 20).

However, the conventional response evaluation criteria in solid tumors (RECIST) are usually imperfect to assess the RT response of patients with m-DTC, because un-measurable lesions are often found. In addition, because of the indolence and well differentiation of ¹³¹I-avid m-DTC, it is difficult to detect the morphological changes of the lesions in the early stage

upon anatomical imaging (1, 6, 21). Although the response to therapy classification modified by the 2015 ATA guidelines can dynamically assess the patient's disease status in real time (4), the effectiveness of RT cannot be adequately reflected because patients with ¹³¹I-avid m-DTC have been in a state of "structural incomplete response" under imaging evaluation for a long time.

Tg, an important biochemical marker for DTC, reflects the tumor burden of patients with DTC with total thyroidectomy accurately (4). The presence of TgAb will interfere with the determination of Tg and affect the accuracy of disease monitoring; therefore, the levels of Tg and TgAb were monitored simultaneously in this study and those subjects with TgAb positivity were excluded. Regular monitoring of Tg can be

used to assist the evaluation of the efficacy of RT for patients with ^{131}I -avid m-DTC, and a decrease in Tg is one of the important signs of effective treatment (13, 22, 23).

Therefore, the combined use of serological and imaging indicators has been established an indispensable tool to evaluate the efficacy of RT. Our previous study (17) showed that the sti-Tg value at diagnosis was an independent and significant predictor of RT efficacy in patients with DTC with pulmonary metastasis. The ROC curve analysis took a sti-Tg value of 55.50 ng/mL as the cut-off value, and the sensitivity and specificity of predicting non-remission was 78.7% and 73.1%, respectively. However, this was a static cut-off method to predict efficacy and judge prognosis, which did not consider the influence of the magnitude of ΔTg on prognosis during the treatment. Miyauchi et al. (24) proposed that the Tg doubling time could predict the recurrence and overall survival of patients with DTC. Barres et al. (25) reported that in patients with DTC treated using repeated RT, the reduction in sti-Tg after the first RT was related to prognosis. Patients with a 60% decrease in sti-Tg after the first RT were more likely to achieve CR upon subsequent RT. In this retrospective study, we found that patients with a decrease in sup-Tg of less than 21.54% and/or a decrease in sti-Tg of less than 27.63% after the first RT would have a higher probability of non-remission.

The uptake of ^{131}I determines the dose of radiation absorbed by metastatic lesions, which directly affects the efficacy of RT (12). A prospective study of 77 patients with ^{131}I -avid m-DTC in China showed that the maximum target/background ratio (T/B_{max}) upon Rx-WBS and the change in the value of the sup-Tg level ($\Delta\text{Tg}_{\text{on}}\%$) after previous RT were associated independently with the outcome of the next RT (1). In the present study, for patients with m-DTC with multiple ^{131}I -avid metastatic lesions, we took the median $\text{T}_{\text{max}}/\text{NT}_{\text{mean}}$ at the first RT as an index to evaluate the ^{131}I uptake ability of the lesions. We found that the median $\text{T}_{\text{max}}/\text{NT}_{\text{mean}}$ of the first RT in the remission group (17.50) was significantly higher than that of the non-remission group (8.14).

The efficacy of RT toward m-DTC is affected by many factors. Studies have shown that in older patients, DTC accompanied by distant metastasis (lung and bone metastasis), large tumor size, and high sti-Tg before the first RT have poor therapeutic effects (10, 11, 17). The univariate and multivariate analysis in the present study showed that age, the size of the metastases, the $\text{T}_{\text{max}}/\text{NT}_{\text{mean}}$ of the first RT, and the $\Delta\text{sup-Tg}$ after the first RT were related independently to the efficacy of RT. Notably, in predicting non-remission, the sensitivity and specificity of the $\Delta\text{sup-Tg}$ value after the first RT at a cut-off value of 21.54% were 86.7% and 88.2%, respectively. This means that a lower decrease in sup-Tg after the first RT is directly associated with non-remission. The reason might be that older patients have a relatively long disease course and poor sensitivity to radiation. The poor uptake of ^{131}I by the lesions would result in an insufficient absorbed dose of radiation in the lesions, thus affecting the efficacy of RT (2, 12). Therefore, the results allowed us to hypothesize that young patients with m-DTC with small metastatic lesions, good iodine uptake ability, and a $\Delta\text{sup-Tg}$ after the first RT greater than 21.54% could benefit from repeated RT.

In this study, patients with extrathyroidal invasion had no abnormal neck uptake after successful radioiodine remnant ablation. The reasons may be as follows: Extrathyroidal

invasion was discovered in the patients during surgery. After a standardized total or near total thyroidectomy, the tumor tissue was basically removed. After the patient was treated with radioiodine remnant ablation, the hidden tumor tissue was completely eliminated.

In terms of efficacy, patients with radioiodine refractory lesions (both with and without ^{131}I -avid lesions) were classified into the non-remission group. For patients judged to have radioiodine refractory differentiated thyroid carcinoma (RAIR-DTC), especially those who did not absorb iodine or whose disease progressed despite absorbing iodine, RT termination may be considered. We should formulate an appropriate individualized follow-up treatment plan based on the patient's condition (4). For some patients with RAIR-DTC with stable or slow progress, inoperable resection, and low tumor burden, the strategy of follow-up monitoring under TSH suppression therapy (TSH should be less than 0.1 mU/L) could be adopted. Local treatments (including surgical resection, external irradiation, and ablation) could be adopted for RAIR-DTC lesions with single occurrence, local clinical symptoms, and invasion of surrounding important organs and tissue structures. If the disease progresses rapidly, therapeutic strategies, such as targeted therapy, might be considered.

In RT decision-making and follow-up management for recurrent or metastatic DTC, sup-Tg and sti-Tg are important reference indicators to evaluate the response to RT, and a decrease in Tg often indicates a response to previous RT (4, 26). Our study further confirmed that not only can the trend of Tg be used to evaluate efficacy, but also the quantitative Tg change displayed a robust prediction of the outcome of RT. In brief, a decrease in sup-Tg less than 21.54% after the first RT indicated that patients had a higher probability of non-remission after RT.

Nevertheless, some limitations existed in this study. First, the presumed influence of the ^{131}I remnant thyroid ablation on the effect of RT in the next course could not be determined definitively nor completely ruled out. Second, this retrospective single-center study did not include a large enough number of cases. Third, although we followed the inclusion criteria and exclusion criteria strictly to select the samples, selection bias might still exist because of the small number of cases eventually included in this study. Finally, the follow-up time was short, and thus the evaluation of long-term clinical outcome was lacking. Therefore, for the scalability of this study, we should seek multi-center institutions to establish a cut-off value of ΔTg to predict the efficacy of RT.

CONCLUSION

In summary, the present study demonstrated that most patients with m-DTC could benefit from RT. Older subjects with metastases > 1 cm, lower $\text{T}_{\text{max}}/\text{NT}_{\text{mean}}$ and lower $\Delta\text{sup-Tg}$ after the first RT were less likely to experience remission. The optimal cut-off value for $\Delta\text{sup-Tg}$ after the first RT to predict RT efficacy for m-DTC was 21.54%. These findings have important guiding significance for the optimization of treatment strategies and the evaluation of prognosis of patients with m-DTC.

DATA AVAILABILITY STATEMENT

The datasets used during the present study are available from the corresponding author upon reasonable request.

ETHICS STATEMENT

The studies involving human participants were reviewed and approved by Ethical Committee of Tianjin Medical University General Hospital. Written informed consent to participate in this study was provided by the participants' legal guardian/next of kin.

AUTHOR CONTRIBUTIONS

CW and RW contributed to the conception and design of the study. CW, RZ, and FD assisted with data acquisition. CW, RZ, and RW conducted the statistical analyses and drafted the manuscript. JT, ZM, YH, GZ, and FD critically revised the

manuscript. All authors contributed to the article and approved the submitted version.

FUNDING

This study was sponsored by the National Natural Science Foundation of China (Grant No. 81801732 and 81501510).

ACKNOWLEDGMENTS

We acknowledge the substantial contributions of the physicians and staff members of the Nuclear Medicine Department at Tianjin Medical University who participated in these patients' management and follow-up. We thank Dr. Renfei Wang for her careful guidance. Finally, we acknowledge the numerous physicians' and scientists' efforts whose contributions were critical in the registry's early years.

REFERENCES

- Sa R, Cheng L, Jin YC, Fu H, Shen Y, Chen LB. Distinguishing Patients With Distant Metastatic Differentiated Thyroid Cancer Who Biochemically Benefit From Next Radioiodine Treatment. *Front Endocrinol (Lausanne)* (2020) 11:587315. doi: 10.3389/fendo.2020.587315
- Sampson E, Brierley JD, Le LW, Rotstein L, Tsang RW. Clinical Management and Outcome of Papillary and Follicular (Differentiated) Thyroid Cancer Presenting With Distant Metastasis At Diagnosis. *Cancer* (2007) 7:1451–6. doi: 10.1002/cncr.22956
- Albano D, Bertagna F, Bonacina M, Durmo R, Cerudelli E, Gazzilli M, et al. Possible Delayed Diagnosis and Treatment of Metastatic Differentiated Thyroid Cancer by Adopting the 2015 ATA Guidelines. *Eur J Endocrinol* (2018) 3:143–51. doi: 10.1530/EJE-18-0253
- Haugen BR, Alexander EK, Bible KC, Doherty GM, Mandel SJ, Nikiforov YE, et al. 2015 American Thyroid Association Management Guidelines for Adult Patients With Thyroid Nodules and Differentiated Thyroid Cancer: The American Thyroid Association Guidelines Task Force on Thyroid Nodules and Differentiated Thyroid Cancer. *Thyroid* (2016) 1:1–133. doi: 10.1089/thy.2015.0020
- Furuya-Kanamori L, Sedrakyan A, Onitilo AA, Bagheri N, Glasziou P, Doi SAR. Differentiated Thyroid Cancer: Millions Spent With No Tangible Gain? *Endocr Relat Cancer* (2018) 1:51–7. doi: 10.1530/ERC-17-0397
- Qiu ZL, Song HJ, Xu YH, Luo QY. Efficacy and Survival Analysis of 131I Therapy for Bone Metastases From Differentiated Thyroid Cancer. *J Clin Endocrinol Metab* (2011) 10:3078–86. doi: 10.1210/jc.2011-0093
- McCormack KR. Bone Metastases From Thyroid Carcinoma. *Cancer* (1966) 2:181–4. doi: 10.1002/1097-0142(196602)19:2<181::aid-cncr2820190207>3.0.co;2-2
- Podnos YD, Smith DD, Wagman LD, Ellenhorn JDI. Survival in Patients With Papillary Thyroid Cancer is Not Affected by the Use of Radioactive Isotope. *J Surg Oncol* (2007) 1:3–7. doi: 10.1002/jso.20656
- Verburg FA. Advantages of Dosimetry in 131I Therapy of Differentiated Thyroid Carcinoma. *Q J Nucl Med Mol Imaging* (2019) 3:253–7. doi: 10.23736/S1824-4785.19.03196-0
- Song HJ, Qiu ZL, Shen CT, Wei WJ, Luo QY. Pulmonary Metastases in Differentiated Thyroid Cancer: Efficacy of Radioiodine Therapy and Prognostic Factors. *Eur J Endocrinol* (2015) 3:399–408. doi: 10.1530/EJE-15-0296
- Xu L, Liu Q, Liu Y, Pang H. Parameters Influencing Curative Effect of 131I Therapy on Pediatric Differentiated Thyroid Carcinoma: A Retrospective Study. *Med Sci Monit* (2016) 22:3079–85. doi: 10.12659/msm.896876
- Wierst R, Brans B, Havekes B, Kemerink GJ, Halders SG, Schaper NN, et al. Dose-Response Relationship in Differentiated Thyroid Cancer Patients Undergoing Radioiodine Treatment Assessed by Means of 124I PET/CT. *J Nucl Med* (2016) 7:1027–32. doi: 10.2967/jnumed.115.168799
- Holsinger FC, Ramaswamy U, Cabanillas ME, Lang J, Lin HY, Busaidy NL, et al. Measuring the Extent of Total Thyroidectomy for Differentiated Thyroid Carcinoma Using Radioactive Iodine Imaging: Relationship With Serum Thyroglobulin and Clinical Outcomes. *JAMA Otolaryngol Head Neck Surg* (2014) 5:410–5. doi: 10.1001/jamaoto.2014.264
- Cooper DS, Doherty GM, Haugen BR, Kloos RT, Lee SL, Mandel SJ, et al. Revised American Thyroid Association Management Guidelines for Patients With Thyroid Nodules and Differentiated Thyroid Cancer. *Thyroid* (2009) 11:1167–214. doi: 10.1089/thy.2009.0110
- Chen LB, Luo QY, Shen Y, Yu YL, Yuan ZB, Lu HK, et al. Incremental Value of 131I SPECT/CT in the Management of Patients With Differentiated Thyroid Carcinoma. *J Nucl Med* (2008) 12:1952–7. doi: 10.2967/jnumed.108.052399
- Yang X, Li J, Li XY, Liang ZY, Gao W, Liang J, et al. Tert Promoter Mutation Predicts Radioiodine-Refractory Character in Distant Metastatic Differentiated Thyroid Cancer. *J Nucl Med* (2017) 2:258–65. doi: 10.2967/jnumed.116.180240
- Wang RF, Zhang YQ, Tan J, Zhang GZ, Zhang RG, Zheng W, et al. Analysis of Radioiodine Therapy and Prognostic Factors of Differentiated Thyroid Cancer Patients With Pulmonary Metastasis: An 8-Year Retrospective Study. *Med (Baltimore)* (2017) 19:e6809. doi: 10.1097/MD.00000000000006809
- Haq M, Harmer C. Differentiated Thyroid Carcinoma With Distant Metastases At Presentation: Prognostic Factors and Outcome. *Clin Endocrinol (Oxf)* (2005) 1:87–93. doi: 10.1111/j.1365-2265.2005.02304.x
- Nixon LJ, Whitcher MM, Palmer FL, Tuttle RM, Shaha AR, Shah JP, et al. The Impact of Distant Metastases At Presentation on Prognosis in Patients With Differentiated Carcinoma of the Thyroid Gland. *Thyroid* (2012) 9:884–9. doi: 10.1089/thy.2011.0535
- Jonklaas J, Sarlis NJ, Litofsky D, Ain KB, Bigos ST, Brierley JD, et al. Outcomes of Patients With Differentiated Thyroid Carcinoma Following Initial Therapy. *Thyroid* (2006) 12:1229–42. doi: 10.1089/thy.2006.16.1229
- Kwon SY, Lee SW, Kong EJ, Kim KY, Kim BL, Kim J, et al. Clinicopathologic Risk Factors of Radioactive Iodine Therapy Based on Response Assessment in Patients With Differentiated Thyroid Cancer: A Multicenter Retrospective Cohort Study. *Eur J Nucl Med Mol Imaging* (2020) 3:561–71. doi: 10.1007/s00259-019-04634-8
- He Y, Pan MZ, Huang JM, Xie P, Zhang F, Wei LG. Iodine-131: An Effective Method for Treating Lymph Node Metastases of Differentiated Thyroid Cancer. *Med Sci Monit* (2016) 22:4924–8. doi: 10.12659/msm.899028

23. Yang X, Liang J, Li TJ, Yang K, Liang DQ, Yu Z, et al. Postoperative Stimulated Thyroglobulin Level and Recurrence Risk Stratification in Differentiated Thyroid Cancer. *Chin Med J (Engl)* (2015) 8:1058–64. doi: 10.4103/0366-6999.155086
24. Miyauchi A, Kudo T, Miya A, Kobayashi K, Ito Y, Takamura Y, et al. Prognostic Impact of Serum Thyroglobulin Doubling-Time Under Thyrotropin Suppression in Patients With Papillary Thyroid Carcinoma Who Underwent Total Thyroidectomy. *Thyroid* (2011) 7:707–16. doi: 10.1089/thy.2010.0355
25. Barres B, Kelly A, Kwiatkowski F, Batisse-Lignier M, Fouilhoux G, Aubert B, et al. Stimulated Thyroglobulin and Thyroglobulin Reduction Index Predict Excellent Response in Differentiated Thyroid Cancers. *J Clin Endocrinol Metab* (2019) 8:3462–72. doi: 10.1210/je.2018-02680
26. Thyroid cancer working group C. Chinese Society of Clinical Oncology (CSCO) Diagnosis and Treatment Guidelines for Persistent/Recurrent and

Metastatic Differentiated Thyroid Cancer 2018 (English Version). *Chin J Cancer Res* (2019) 31(1):99–116. doi: 10.21147/j.issn.1000-9604.2019.01.06

Conflict of Interest: The authors declare that the research was conducted in the absence of any commercial or financial relationships that could be construed as a potential conflict of interest.

Copyright © 2021 Wang, Zhang, Wang, Meng, Zhang, Dong, He and Tan. This is an open-access article distributed under the terms of the Creative Commons Attribution License (CC BY). The use, distribution or reproduction in other forums is permitted, provided the original author(s) and the copyright owner(s) are credited and that the original publication in this journal is cited, in accordance with accepted academic practice. No use, distribution or reproduction is permitted which does not comply with these terms.

Advantages of publishing in Frontiers



OPEN ACCESS

Articles are free to read
for greatest visibility
and readership



FAST PUBLICATION

Around 90 days
from submission
to decision



HIGH QUALITY PEER-REVIEW

Rigorous, collaborative,
and constructive
peer-review



TRANSPARENT PEER-REVIEW

Editors and reviewers
acknowledged by name
on published articles

Frontiers

Avenue du Tribunal-Fédéral 34
1005 Lausanne | Switzerland

Visit us: www.frontiersin.org

Contact us: frontiersin.org/about/contact



REPRODUCIBILITY OF RESEARCH

Support open data
and methods to enhance
research reproducibility



DIGITAL PUBLISHING

Articles designed
for optimal readership
across devices



FOLLOW US

@frontiersin



IMPACT METRICS

Advanced article metrics
track visibility across
digital media



EXTENSIVE PROMOTION

Marketing
and promotion
of impactful research



LOOP RESEARCH NETWORK

Our network
increases your
article's readership